

Proceedings of

GSM 2024

7th Grid Service Market Symposium

1 - 2 July, Lucerne, Switzerland

Edited by:

Davor Bošnjak
Thomas Kudela
Dr. Ivana Kockar

Prof. Christoph Imboden (Chair)

Dr. Michael Moser
Prof. Carlo Alberto Nucci
Sebastian Ziegler

Prof. Nikos Hatziaargyriou
Dr. Bastian Schwark
Andreas Svendstrup-Bjerre

Co-Edited by:

Emre Avici Fiona Moore

Dr. Michael Spirig



Copyright © Hochschule Luzern + European Fuel Cell Forum AG

These proceedings must not be made available for sharing through any other open electronic means.

DOI 10.5281/zenodo.15023007

ISBN 978-3-905592-83-2

Sessions:

G01 Opening & Welcome

G02 Future of Grid Service Markets I

G03 Advanced Technologies Providing Flexibility I

G04 Enabling Technologies I

G05 International Projects for the Energy Transition

G06 Advanced Technologies Providing Flexibility II

**G07 Enabling Technologies II &
Operation & Regional Conditions**

G08 Grid Service Operation

G09 Future of Grid Service Markets II

Copyright © 2024 HSLU + EFCF

Published on:

www.GridServiceMarket.com/DOI

LORY Lucerne Open Repository
Universität Luzern
Hochschule Luzern
Pädagogische Hochschule Luzern
Historisches Museum Luzern

by
Hochschule Luzern
Werftstrasse 4
6002 Luzern
Switzerland

Tel. +41 - 41 - 228 4242
Info@HSLU.ch, www.HSLU.ch

www.GridServiceMarket.com/LIBRARY

GSM-Library

by
European Fuel Cell Forum AG
Obgardihalde 2
6043 Luzern-Adligenswil
Switzerland

Tel. +41 - 44 - 586-5644
Forum@EFCF.com, www.EFCF.com

Foreword

Between 2000 and 2021, total electricity generation in Europe increased by 13%. In the same period, the share from hydropower, tidal, biofuels, wind, solar and geothermal sources have risen from 19% to 39%, reflecting the massive transformation that the electricity industry has undergone in recent years. The political will to continue the transition is evident, as competitive energy prices, reducing dependencies on third parties - especially Russian fossil gas supplies - and decarbonizing the energy system are among the top priorities of European Commission President Ursula von der Leyen for the years 2024 to 2029.¹⁾

However, the transition to decarbonized energy sources requires not only the large-scale deployment of renewable energy, but also the development of sophisticated techno-economic mechanisms to ensure energy security, economic efficiency, and environmental sustainability in the future. Grid services play a central role in this transition as they provide the necessary flexibility. As the share of intermittent renewable energy sources such as wind and solar increases, grid services enable electricity to be available at the right time, in the right place, and in the right amount, optimizing costs and reliability. They also open up new market opportunities and enable both established players and new entrants to contribute to a more resilient energy system.

The 7th Grid Service Market Symposium (GSM), which took place on July 1 and 2, 2024 in Lucerne, Switzerland, brought together 69 experts from 16 European countries to share knowledge and discuss the latest developments in this important field. Participants included professionals from academia, industry, associations, and policy organizations, all addressing the challenges and opportunities of the ongoing energy transition. The event offered a rich program with a wide range of topics including advanced technologies for grid flexibility, market developments, regulations, operational challenges, international collaborations, and case studies showcasing successful implementations. Keynote speakers provided insights into the future of grid services and addressed critical topics such as the looming flexibility gap and the importance of a robust transmission infrastructure. In addition to the presentations, the symposium facilitated in-depth discussions on market harmonization in Europe and international projects. The GSM continues to serve as an important platform for thought leaders, researchers, and industry experts to shape the future of grid services. The knowledge shared at this event will play a crucial role in the development of sustainable, reliable, and economically viable electricity systems in the years to come.

We are very grateful to all participants, speakers, and organizers for their contribution to the success of the symposium. Their commitment to innovation and collaboration is instrumental to the progress needed to meet the energy challenges of tomorrow.

We hope you enjoy the proceedings of GSM 2024, and we look to welcoming you to future events.

Sincerely
Prof. Christoph Imboden & Dr. Michael Spirig
HSLU EFCF

A specially formed **International Advisory Board (IAB)** assured constant high quality and a strong focus on industry challenges. The members of the IAB 2024 are:

- Davor Bošnjak, HEP, Croatia
- Prof. Nikos Hatziaargyriou, National Technical University of Athens, Greece
- Prof. Christoph Imboden, Lucerne University, Switzerland
- Dr. Ivana Kockar, University of Strathclyde, UK
- Thomas Kudela, Ørsted A/S, Denmark
- Prof. Carlo Alberto Nucci, Uni Bologna, Italy
- Dr. Bastian Schwark, Swissgrid AG, Switzerland
- Andreas Svendstrup-Bjerre, BattMan Energy ApS, Denmark
- Sebastian Ziegler, 50 Hertz, Germany
- Dr. Michael Moser, SFOE, Switzerland

The following pages contain the paper contributions accepted by the IAB.

The GSM 2024 was supported by:

- The Lucerne University of Applied Sciences and Arts UAS HSLU, www.HSLU.ch
- European Fuel Cell Forum AG, www.EFCF.com
- 24/7 ZEN, www.24-7zenproject.eu
- SwissGrid, www.swissgrid.ch

Table of Content

Foreword	3
Table of Content	5
G03 (G06)	8
Advanced Technologies Providing Flexibility	
G0303	9
Water electrolysis powered by renewables: Optimising the cost of green hydrogen production across Europe	
Paolo Marocco, Marta Gandiglio, Massimo Santarelli <i>Department of Energy, Politecnico di Torino – C.so Duca degli Abruzzi 24, 10129 Turin/IT;</i>	
G0310	16
Analysing charging processes of electric vehicles to reduce grid load and emissions	
Enrique Romano, André Egli, Claas Wagner <i>Hochschule Luzern CC Energy Economics, Horw/Switzerland;</i>	
G0311	26
Optimal V2X operation of EV fleets with PV-battery charging station for demand-side flexibility provision	
Federica Bellizio, Philipp Heer <i>Urban Energy Systems Laboratory, Swiss Federal Laboratories for Materials Science and Technology, Empa, Dübendorf/Switzerland;</i>	
G0312	38
Relief of the power grid through cost-effective hydrogen generation	
Gabriele Humbert*, Hanmin Cai, Binod Prasad Koirala, Philipp Heer <i>Urban Energy System Laboratory, Empa, Ueberlandstrasse 129, 8600 Dübendorf/CH;</i>	
G04	48
Enabling Technologies I	
G0401	49
Intraday solar irradiance forecasting using public cameras	
Roy Sarkis (1), Ilker Oguz (1), Demetri Psaltis (1), Mario Paolone (1), Christophe Moser (1), Luisa Lambertini (1,2) <i>(1) EPFL, Lausanne/Switzerland</i> <i>(2) Università della Svizzera Italiana (USI), Ticino/Switzerland;</i>	
G0410	61
The influence of the World and European championships on the electricity consumption diagram (load curve) of the Republic Croatia	
Petar Ribarić, Davor Bošnjak <i>HEP Trgovina Ltd., Zagreb/Croatia;</i>	
G0411	71
Exploring the Potential of Quantum Computing for Electrical Power System Optimization	
Zlatko Ofak (1), Dino Mileta (1), Tin Bobetko (1), Dario Jukić (2), Karlo Lelas (3), Hrvoje Buljan (4) <i>(1) Uprise d.o.o., Zagreb/Croatia;</i> <i>(2) Faculty of Civil Engineering, University of Zagreb, Zagreb/Croatia;</i> <i>(3) Faculty of Textile Technology, University of Zagreb, Zagreb/Croatia;</i> <i>(4) Faculty of Science, University of Zagreb, Zagreb/Croatia;</i>	
G05	81
International Projects for the Energy Transition	
G0503	82

Market-based procurement of grid-friendly flexibility – the ENFLATE project

André S. Eggli (1), Sébastien Rolland (2), Christoph Imboden (1), Davide Orifici (2)

(1) *Lucerne University of Applied Sciences and Arts, Lucerne/Switzerland;*

(2) *European Power Exchange EPEX SPOT, Paris/France;*

G0504 87

A Case Study for Unveiling Flexibility Options in Achieving Swiss National Energy Goals

Olena Levon (1), André Eggli (2), Christoph Imboden (2)

(1) *HSLU, Institute of Electrical Engineering, CC Digital Energy and Electric Power;*

(2) *HSLU, Institute of Innovation and Technology Management, FT Energy Economics, Horw/Switzerland;*

G0505 98

Flexibility provision from local energy communities exemplified by the SUSTENANCE and SERENE H2020 projects

Birgitte Bak-Jensen (1), Rakesh Sinha (1), Sanjay Chaudhary (1), Hessam Golmohamadi (1), Gerwin Hoogsteen (2), Aditya Pappu (2), Bahman Ahmadi (2), Richard van Leeuwen (3), Javier F. Gonzales (3); Patryk Chaja (4), Weronika Radziszewska (4), Zakir Rather (5)

(1) *Aalborg University, Denmark;* (2) *University of Twente, The Netherlands;* (3) *Saxion university of applied science, The Netherlands;* (4) *Institute of Fluid-Flow machinery, Poland;* (5) *Indian Institute of Technology Bombay/India;*

G0507 108

VPP implementations: different types of services developed, experiences and platforms

Gary Howorth, Ivana Kockar

University of Strathclyde, Glasgow/UK;

G0508 119

Empowering Prosumers in the Energy Transition: The REEFLEX Approach to Flexibility Markets and Improved Grid Management

Gregorio Fernández (1), Asier Rueda (1), Lorena Elorza-Urriarte (1), Marcos Remiro-Cinca (1), Georgios Skaltsis (2)

(1) *CIRCE Technology Centre, Zaragoza/Spain;* (2) *CERTH ITI, Thessaloniki/Greece;*

G07 Enabling Technologies II & 128

Operation & Regional Conditions

G0701 129

Sector Coupling for Renewable Energy Sources Integration – A Case Study for the German Gas Transmission Network

Luisa Di Francesco (1), Marco Cavana (1), Yifei Lu (2,3), Pierluigi Leone (1), Andrea Benigni (2,3,4)

(1) *Department of Energy “Galileo Ferraris”, Politecnico di Torino, Torino/Italy;*

(2) *IEK-10: Energy Systems Engineering, Forschungszentrum Jülich, 52428 Jülich/Germany;*

(3) *RWTH Aachen University, 52056 Aachen/Germany;*

(4) *JARA-Energy, 52425 Jülich/Germany;*

G0702 140

UrbanTwin: Development of a Local Energy Strategy and Grid Infrastructure 2050

Pål Forr Austnes (1), Riccardo Saporiti (2), Catarina G. Braz (3), Bingqian Liu (3), Luc Girardin (3), Mario Paolone (1), Fabio Nobile (2), François Maréchal (3), Max Chevron (4)

(1) *Distributed Electrical Systems Laboratory, EPFL Lausanne, ELL 136 Station 11, 1015 Lausanne/Switzerland;*

(2) *Scientific Computing and Uncertainty Quantification – CSQI Chair, EPFL Lausanne, Bâtiment MA, Station 8, 1015 Lausanne/Switzerland;*

(3) *Industrial Process and Energy Systems Engineering Group, EPFL Valais Wallis, Rue de l'Industrie 17, 1951 Sion/Switzerland;*

(4) *Services Industriels de Lausanne, Lausanne/Switzerland;*

G0703	151
Managing and Optimizing a Set of PV Installations at the Low-Voltage Grid Level: A Data-Driven Concept through Machine Learning Techniques	
Thibaud Alt (1), Beat Wolf (2), Jean-Philippe Bacher (3), Frédéric Montet (4)	
(1) Groupe E SA, Route de Morat 135, 1763 Granges-Paccot/Switzerland;	
(2,4) iCoSys institute, HEIA-FR, HES-SO University of Applied Sciences and Arts, Western Switzerland, Bld de Pérolles 80, 1700 Fribourg/Switzerland;	
(3) ENERGY institute, HEIA-FR, HES-SO University of Applied Sciences and Arts, Western Switzerland, Bld de Pérolles 80, 1700 Fribourg/Switzerland;	
G0704	162
Interoperability by Sovereign and Secure Data Exchange in Trustworthy Data Spaces	
Andreas Rumsch, Eugen Rodel, Christoph Imboden	
Lucerne University of Applied Sciences and Arts, Horw/Switzerland;	
G08	175
Enabling Technologies	
G0802	176
Data-driven predictive control for demand side management: Theoretical and experimental results	
Mingzhou Yin (1), Hanmin Cai (2), Andrea Gattiglio (2), Fazel Khayatian (2), Roy S. Smith (1), Philipp Heer (2)	
(1) Automatic Control Laboratory, Swiss Federal Institute of Technology in Zürich, Zürich/Switzerland;	
(2) Urban Energy Systems Laboratory, Swiss Federal Laboratories for Material Science and Technology (Empa), Dübendorf/Switzerland;	
G0803	183
Assessment of Economic Surplus of the European Balancing Platforms	
Ulf Kasper (1), Andreas Kindsmüller (1), David Steber (1), Simon Remppis (2), Dominik Schlipf (2), Alexander Warsewa (2)	
(1) Amprion GmbH, System Operation, Pulheim/Germany;	
(2) Transnet BW GmbH, System Operation, Wendlingen/Germany;	

G03 (G06)

Advanced Technologies Providing Flexibility

G0303

Water electrolysis powered by renewables: Optimising the cost of green hydrogen production across Europe

Paolo Marocco, Marta Gandiglio, Massimo Santarelli

Department of Energy, Politecnico di Torino – C.so Duca degli Abruzzi 24, 10129 Turin/IT;
Tel.: +39 0110904432
paolo.marocco@polito.it

Abstract

Depending on the end-use application, electrification may not always be technically feasible or the most cost-effective option. In particular, industries with substantial challenges in decarbonisation, such as hard-to-abate sectors (e.g., steel, cement, fertilizer) and heavy-duty transport (e.g. trucks, maritime, aviation) necessitate alternative solutions. In this context, hydrogen or hydrogen-derived fuels play a crucial role in the transition away from fossil fuels.

At present, the most promising way to produce low-carbon hydrogen is water electrolysis powered by renewable energy sources. Achieving a cost-optimal design of the power-to-hydrogen (PtH) system, encompassing both renewable energy generators and electrolyzers, is essential for delivering green hydrogen at the lowest possible cost. In this work, renewable-based PtH systems are designed with the aim of reliably fulfilling a specified hydrogen demand profile, while concurrently minimising the cost of hydrogen production. The optimal design problem is solved utilising the mixed integer linear programming technique. Specifically, both the sizes of the PtH components (i.e., renewable generators, electrolyser and hydrogen storage) and their operation over time are set as decision variables. Special attention is also given to accurately modelling the electrolyser behaviour, by implementing a real partial-load performance curve for the electrochemical device, constrained within an appropriate modulation range.

A European-scale assessment is conducted with the ultimate goal of investigating how wind and solar resources influence the optimal design of the PtH system. The levelised cost of hydrogen (LCOH) is found to vary across a wide range, spanning from 5 €/kg to more than 20 €/kg, depending on the PtH configuration and geographical location. The study highlights the importance of hybridising renewable production in limiting the oversizing of the PtH components, thereby ensuring favourable LCOH values.

Introduction

Hydrogen is currently gaining unprecedented momentum, marked by a rapid increase in the number of hydrogen-related policies and projects worldwide [1]. Presently, hydrogen serves various essential roles: as a feedstock for chemical production (such as ammonia and methanol), as a reducing agent in steelmaking, and for the purification and upgrading of heavy oil fractions in refineries. Moreover, it is expected to play a pivotal role in expediting the transition towards a carbon-neutral future. Indeed, in a decarbonised society, hydrogen and its derivatives will fulfil a wide range of applications, including heavy-duty transport such as shipping and aviation [2], the chemical industry [3], high-grade heat generation [4], and long-term energy storage [5].

In this context, it becomes essential to provide low-carbon hydrogen at the lowest possible cost, making it competitive with fossil fuel-based routes (i.e., natural gas and coal), which currently dominate the global hydrogen production [6]. However, because of the fluctuating behaviour of solar and wind energy, new challenges emerge in guaranteeing a reliable and cost-effective supply of green hydrogen.

In this work, an optimisation framework is developed to address the cost-optimal design of hydrogen production systems powered by renewable energy sources. In contrast to the existing literature on this topic, which typically focuses on specific case studies, the present work extends the analysis to several European countries. The goal is to assess how wind and solar resources influence the optimal design of the power-to-hydrogen (PtH) system and the hydrogen cost. In order to identify the most cost-effective solution for each country, the European-scale assessment also covers various system configurations based on the type of renewable generator: photovoltaic (PV)-only, wind turbine (WT)-only and hybrid (i.e., both PV and WT).

1. Materials and methods

Figure 1 shows the layout of the PtH system analysed in this work. The electricity that powers the electrolyser comes from a photovoltaic and/or wind system. A hydrogen storage system is also included to provide flexibility and reliably cover the hydrogen demand of the end-user.

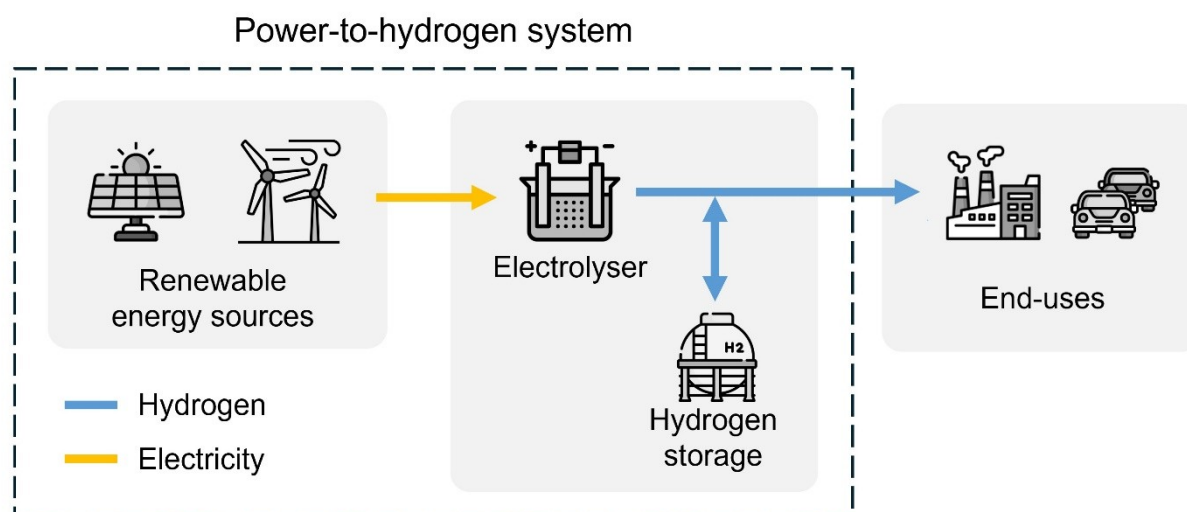


Figure 1. Layout of the power-to-hydrogen system.

An optimisation framework – based on the mixed integer linear programming (MILP) technique – was developed to address the optimal design of renewable-based hydrogen production systems. The levelised cost of hydrogen (LCOH) was used as objective function of the optimisation problem. Specifically, the aim is to cover the hydrogen demand of the end-user for each time step (t) of the time horizon (T), while simultaneously minimising the LCOH. The simulation was carried out over a year-long time horizon with hourly resolution.

As schematised in Figure 2, the primary inputs to the MILP-based optimisation process are as follows:

1. The techno-economic data (e.g., investment costs, operation & maintenance costs, modulation range, efficiency curve) associated with all components of the PtH system.
2. The hydrogen demand profile $\forall t \in T$.
3. The meteorological data, in terms of capacity factor (CF) profiles, of the photovoltaic and wind systems $\forall t \in T$.

The following decision variables are provided:

1. The optimal sizes of all components of the PtH system, i.e., photovoltaic, wind turbine, electrolyser and hydrogen storage.
2. The electrical power supplied to the electrolyser (input) and the hydrogen power generated by the electrolyser (output) $\forall t \in T$.
3. The surplus renewable power not supplied to the electrolyser $\forall t \in T$.
4. The charging and discharging power of the hydrogen storage $\forall t \in T$.
5. The quantity of energy stored in the hydrogen storage $\forall t \in T$.

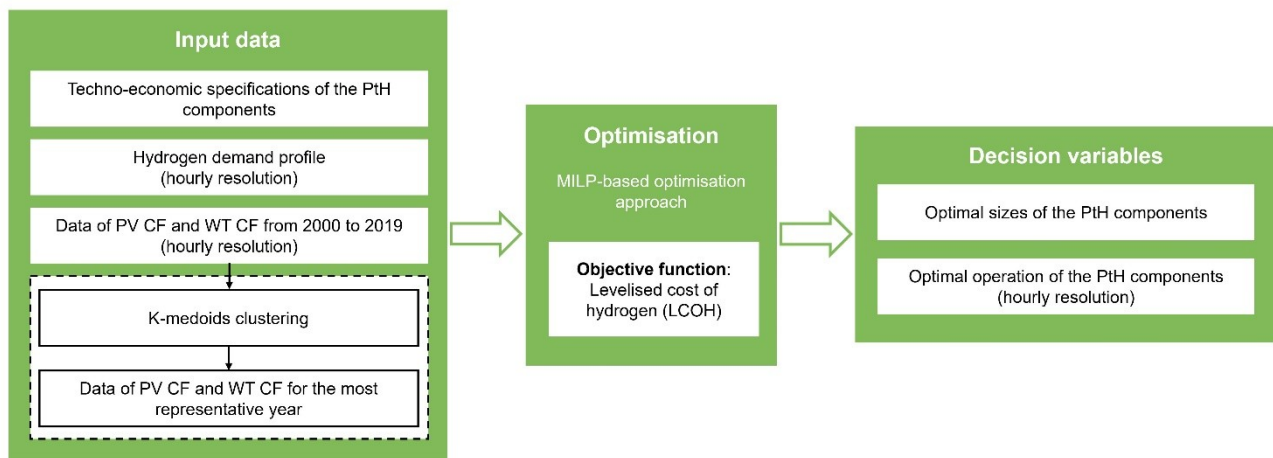


Figure 2. Optimisation framework for the optimal design of power-to-hydrogen (PtH) systems.

A detailed description of the optimal design methodology can be found in [7]. In the present study, it is further expanded to improve the robustness in estimating the electricity production from renewable energy sources. Specifically, country-aggregated time series of PV and WT capacity factors from the year 2000 to 2019 were taken from [8]. As shown in Figure 2, the k-medoids clustering technique was then applied to pinpoint the most representative year, which was then used as input to the optimisation framework. This process was repeated for all European countries with the goal of evaluating the optimal LCOH as solar and wind availability varies.

The LCOH was computed according to the following expression (in €/kg):

$$LCOH = \frac{CAPEX_0 + \sum_{j=1}^N \frac{OPEX_j + REP_j}{(1+d)^j}}{\sum_{j=1}^N \frac{M_{H_2}}{(1+d)^j}} \quad (1)$$

where $CAPEX_0$ are the total capital expenditures occurring at the beginning of the analysis period (i.e., $j=0$), $OPEX_j$ are the total operation and maintenance costs of the PtH system during the j -th year, REP_j are the total replacement costs of the PtH system during the j -th year (for a given component, replacement costs are null if it does not need to be replaced in that year), M_{H_2} is the amount of hydrogen produced annually by the PtH system, d is the discount rate, and N is the project lifetime.

For an accurate representation of the partial-load performance of the electrolyser, a real efficiency curve was also implemented within the MILP framework. In particular, a proton-exchange membrane (PEM) electrolyser was considered, given its good compatibility with variable renewable energy sources. The list of all techno-economic assumptions, along with the electrolyser efficiency curve, is reported in [7].

In this work, the hydrogen demand profile was set constant to reflect a typical industrial process. Indeed, the demand for hydrogen in heavy industrial applications, such as the steelmaking process and ammonia production, typically remains steady over time [9].

2. Results and discussion

The average annual capacity factors of PV and WT are shown in Figure 3. For each European country, they refer to the most representative year, which was computed according to a clustering procedure of country-aggregated CF time series from 2000 to 2019. The average PV capacity factor spans from 10% (Finland) to 19% (Cyprus); whereas a broader range is found for wind farms, from 7% (Slovenia) to 30% (Finland).

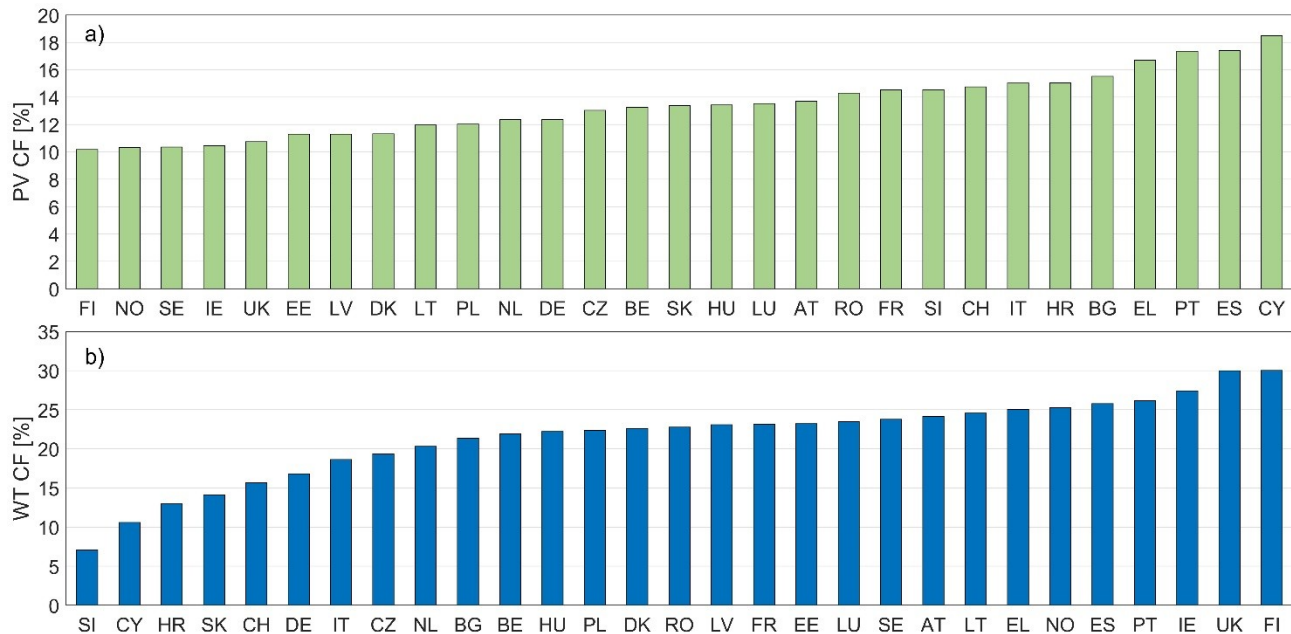


Figure 3. a) Average annual capacity factor of photovoltaic (PV CF) and wind turbine (WT CF) for different European countries. Acronyms of the European countries are provided in the Nomenclature section.

Based on the identified hourly profiles of PV and WT capacity factors, the optimal design of the PtH system was conducted for different European countries, considering a steady hydrogen demand profile over the year. Figure 4 shows the resulting LCOH values for the various PtH configurations (i.e., PV-only, WT-only and hybrid).

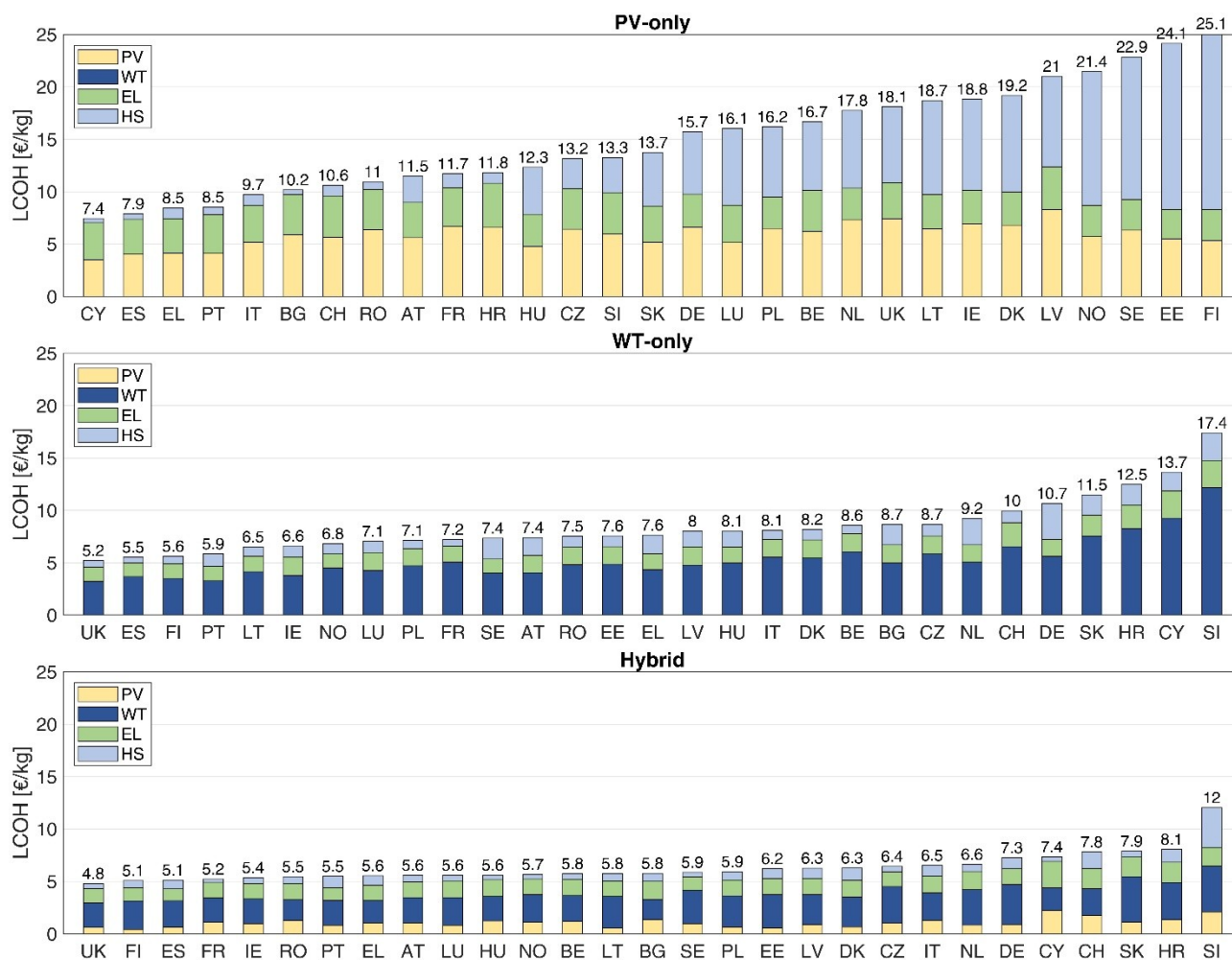


Figure 4. LCOH breakdown of the PV-only, WT-only and hybrid configurations for different European countries.

Examining the results of the PV-only scenario, the LCOH is in the range of 7.4 to 25.1 €/kg, depending on the PV capacity factor. It is worth noting that, moving to countries with lower PV availability, the cost of hydrogen increases mainly due to a sharp rise in the contribution associated with the hydrogen storage system. Specifically, geographical locations with an average PV CF below approximately 13% necessitate large-scale hydrogen storage systems (approximately 500 to 2000 hours of autonomy), which significantly impacts the final cost of hydrogen. For instance, in regions with limited availability of solar resource – such as Norway, Sweden, Estonia and Finland – over half of the LCOH is attributed to the hydrogen storage section.

Despite the higher specific cost of wind turbines (1120 €/kW) compared to PV (650 €/kW), the LCOH for WT-only systems, which ranges from 5.2 to 17.4 €/kg, is lower than that of PV-only systems (except for Croatia, Cyprus and Slovenia). Indeed, WT-only configurations generally require less oversizing of the electrolyser and hydrogen storage (with respect to the average hydrogen demand to be covered), and also enable better exploitation of the local renewable resource.

Finally, hybridising the renewable production is highly effective in limiting the oversizing of PtH components (i.e., renewable generators, electrolyser and hydrogen storage). As can be seen from

Figure 4, for all European countries, deploying both PV and WT emerges as the most favourable solution, with an LCOH that spans from 4.8 to 12 €/kg. The hybrid solution achieves an average LCOH reduction of 52% compared to the PV-only configuration and 23% compared to the WT-only configuration.

3. Conclusion

A European-scale assessment was conducted to investigate the influence of renewable energy sources on the optimal design of hydrogen production systems. To this aim, an optimisation framework, based on the mixed integer linear programming technique, was developed. In addition, a clustering procedure was implemented to pinpoint the most representative year from a multi-year time series.

Depending on the European country, the LCOH varies across a wind range, spanning from about 5 to over 20 €/kg. In PV-only systems (7.4-25.1 €/kg), the hydrogen storage emerges as a significant cost contributor (above 30%) when the average annual PV capacity factor falls below approximately 13%. Compared to PV-only systems, WT-only configurations typically necessitate less oversizing of the electrolyser and hydrogen storage, resulting in lower LCOH values (5.2-17.4 €/kg). Finally, for all European countries, hybridising the renewable production emerges as the optimal solution for delivering green hydrogen at the lowest cost (4.8-17.4 €/kg). Future works will further delve into this assessment for evaluating size and cost correlations as a function of the geographical location.

Acknowledgment

This publication is part of the project NODES which has received funding from the MUR – M4C2 1.5 of PNRR funded by the European Union - NextGenerationEU (Grant agreement no. ECS00000036).

Nomenclature

AT	Austria	LCOH	Levelised cost of hydrogen
BE	Belgium	LT	Lithuania
BG	Bulgaria	LU	Luxemburg
CF	Capacity factor	LV	Latvia
CH	Switzerland	NL	Netherlands
CY	Cyprus	NO	Norway
CZ	Czechia	PEM	Proton exchange membrane
DE	Germany	PL	Poland
DK	Denmark	PT	Portugal
EE	Estonia	PtH	Power-to-Hydrogen
EL	Greece	PV	Photovoltaic
ES	Spain	RO	Romania
FI	Finland	SE	Sweden
FR	France	SI	Slovenia
HR	Croatia	SK	Slovakia
HU	Hungary	UK	United Kingdom
IE	Ireland	WT	Wind turbine
IT	Italy		

References

- [1] P.M. Falcone, M. Hiete, A. Sapio, Hydrogen economy and sustainable development goals: Review and policy insights, *Curr. Opin. Green Sustain. Chem.* 31 (2021) 100506. <https://doi.org/10.1016/j.cogsc.2021.100506>.
- [2] M.C. Massaro, R. Biga, A. Kolisnichenko, P. Marocco, A.H.A. Monteverde, M. Santarelli, Potential and technical challenges of on-board hydrogen storage technologies coupled with fuel cell systems for aircraft electrification, *J. Power Sources*. 555 (2023) 232397. <https://doi.org/10.1016/j.jpowsour.2022.232397>.
- [3] M. Mersch, N. Sunny, R. Dejan, A.Y. Ku, G. Wilson, S. O'Reilly, G. Soloveichik, J. Wyatt, N. Mac Dowell, A comparative techno-economic assessment of blue, green, and hybrid ammonia production in the United States, *Sustain. Energy Fuels*. (2024) 1495–1508. <https://doi.org/10.1039/d3se01421e>.
- [4] P. Marocco, M. Gandiglio, D. Audisio, M. Santarelli, Assessment of the role of hydrogen to produce high-temperature heat in the steel industry, *J. Clean. Prod.* 388 (2023) 135969. <https://doi.org/10.1016/j.jclepro.2023.135969>.
- [5] P. Marocco, D. Ferrero, A. Lanzini, M. Santarelli, The role of hydrogen in the optimal design of off-grid hybrid renewable energy systems, *J. Energy Storage*. 46 (2022) 103893. <https://doi.org/10.1016/J.EST.2021.103893>.
- [6] International Energy Agency, Global Hydrogen Review 2023, 2023. <https://www.iea.org/reports/global-hydrogen-review-2023> (accessed May 28, 2024).
- [7] P. Marocco, M. Gandiglio, M. Santarelli, Optimal design of PV-based grid-connected hydrogen production systems, *J. Clean. Prod.* (2023) 140007. <https://doi.org/https://doi.org/10.1016/j.jclepro.2023.140007>.
- [8] S. Pfenninger, I. Staffell, Long-term patterns of European PV output using 30 years of validated hourly reanalysis and satellite data, *Energy*. 114 (2016) 1251–1265. <https://doi.org/10.1016/j.energy.2016.08.060>.
- [9] International Energy Agency, Ammonia Technology Roadmap: Towards more sustainable nitrogen fertiliser production, Paris, 2021. <https://www.iea.org/reports/ammonia-technology-roadmap> (accessed October 31, 2023).

G0310

Analysing charging processes of electric vehicles to reduce grid load and emissions

Enrique Romano, André Eggli, Claas Wagner
Hochschule Luzern CC Energy Economics, Horw/Switzerland;
enrique.romano@hslu.ch

Abstract

Private electricity production and consumption are expected to increase in the forthcoming years due to the growing number of electric cars, the replacement of oil-based heating systems with heat pumps, and the rise of locally produced energy from solar panels. This poses a challenge to the existing grid as well as the entire energy sector of Switzerland, particularly during peak load periods and when surplus photovoltaic energy is lost unused. This thesis investigates the flexibility of electric car owners in relation to charging sessions and proposes a data-driven optimised charging management system that minimises grid load and emissions.

A combination of data from charging sessions, transformer stations, emissions from electricity production and weather is used to assess the flexibility of charging sessions and define the framework of such a system. The analysis focuses on a demonstration site in St. Gallen, providing predictions and visualisations to measure the impact of electric cars on a local scale. The results contribute to the goals of the ENFLATE project and Switzerland's climate neutrality targets.

The findings reveal that electric vehicle owners exhibit heterogeneous but long-term regular charging behaviours. Peak load occurs when individuals return from work and start charging immediately, although low energy tariffs can shift the charging start time. The proposed system allows electric car owners to book a timeslot when the car is plugged in and needs charging. The charging management system selects the optimal charging time based on the availability of surplus energy and low emission times. To effectively shift charging, the system must incorporate dynamic pricing linked to emissions. This approach ensures optimal use of renewable energy and increases grid stability, supporting Switzerland's transition to a user friendly and sustainable energy future.

Introduction

The consumption of electricity in private households has increased in the last few years and is expected to rise further in the future. This is due to the replacement of oil heating with heat pumps and the shift towards cars driven by electricity instead of fossil fuel. Furthermore, the amount of electricity generated by photovoltaic systems is also increasing [1]. These factors pose a challenge to the power grid in the upcoming years, as the consumption and the input continue to rise and put additional pressure on the transformer. Especially on cold winter or sunny summer days, it may come to temporary bottlenecks on the local transformer.

The ENFLATE project aims to address these challenges by the shifting electricity flows resulting from the growth of local renewable energy sources and battery electric vehicles (BEV). The current grid was not designed to handle these changes and requires flexibility, particularly during peak load periods. Expanding the existing grid is too expensive and would have to be paid by private individuals, further increasing the already rising electricity prices.

Peak load is reached in two ways. Excessive electricity consumption or strong feed-in from photovoltaic systems on sunny days can potentially overload the transformer. The trading platform used in the project allows individuals to sell their flexibility, such as not charging their electric cars at a certain time when maximum load could be reached [2]. In general, fixed appliances such as electric boilers and heat pumps are better suited to dissipate excess energy than electric vehicles. This is because BEVs need to be plugged in to receive electricity and have a battery that is not yet fully charged. Implementation of efficient and flexible charging infrastructure for BEVs is crucial in decreasing the load on the grid and achieving carbon neutrality by 2050.

The EKZ has provided charging infrastructure data of Zurich. This data is used to understand the current behaviour of charging processes. With knowledge of the behaviour, the flexibility potential of charging sessions is investigated. In addition to analysing historical emission and energy consumption data, various visualisations are created to present the data objectively and build a charging management system in a way that minimises the impact on the grid and environment. Overall, the ideas aim to reduce the impact of BEVs on the grid, which will be a topic of great interest in the next years with increasing inflow of electricity from solar panels and growth in BEVs.

1. Planned analysis and discussions

The first step is to explore all the data. The central objective is to model the charging behaviours of electric cars based on charging infrastructure data from Zurich. Possible patterns are researched using visualisations to identify differences or coherences among various types of electric car owners. These results are considered as the basis for modelling the behaviour, assessing flexibility, and defining the framework of the charging management system to solve the problems.

After getting an overview on how currently BEVs are charged, a search to limiting factors on basis of the greenhouse gas (GHG) emissions per kWh and future grid limits is conducted. Modelling the charging behaviour and finding limits in emission and the grid is fundamental to creating appropriate and realistic charging implementation ideas. These findings are then discussed in the chapter after the results, to determine how well they work and how much capacity can be reserved for BEVs in the upcoming future. They are essential for the adoption of their energy management technology. A short overview of the whole process from data preparation to the final product is shown in figure 1.

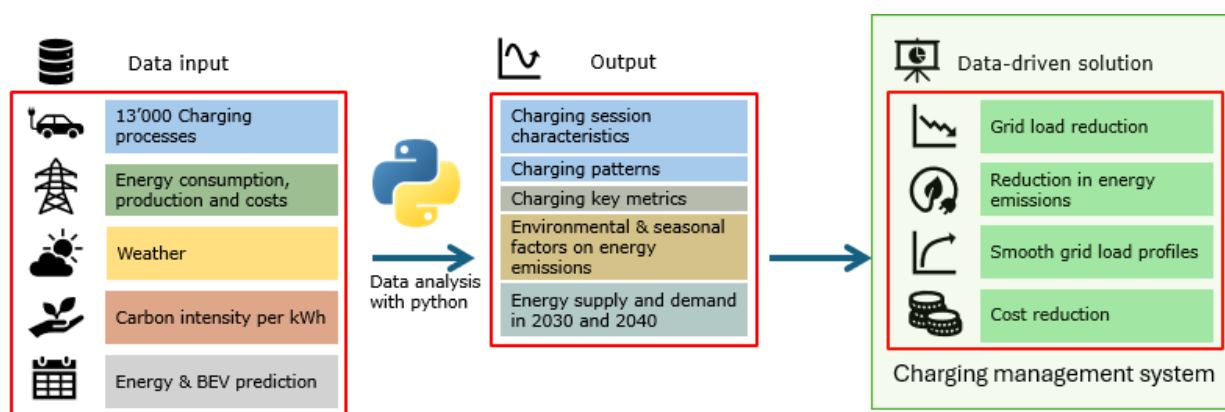
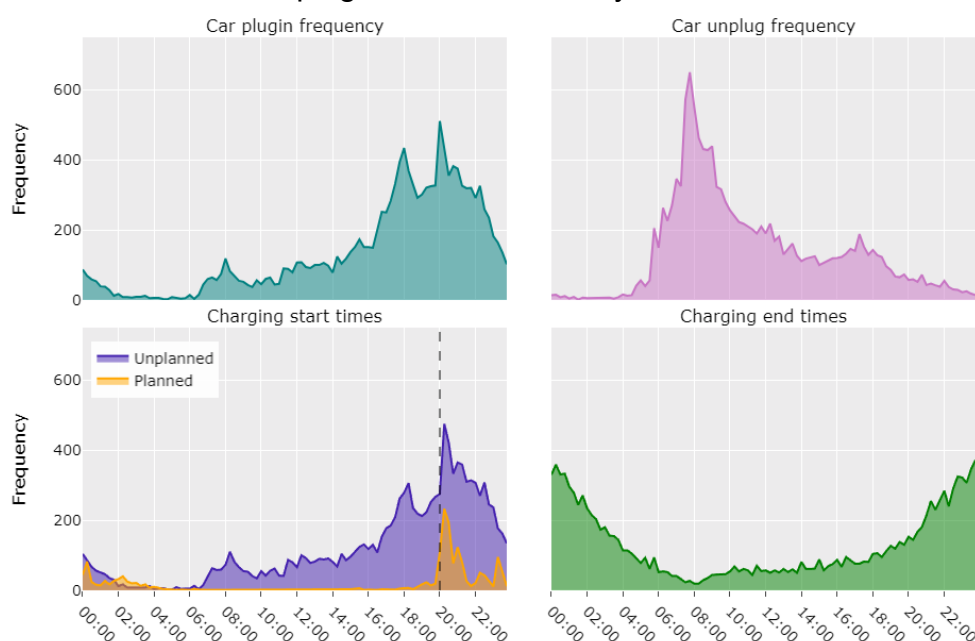


Figure 1 - Data-driven process roadmap

2. Characteristics of charging sessions and energy mix emissions

An in-depth analysis of the data has yielded valuable insights into the characteristics of charging processes. The data received from the EKZ revealed additional insights beyond those initially anticipated.

The majority of BEVs are connected to a wall box and begin charging immediately following the end of a workday. This peak happens twice: once at 18:00 and again at 20:00. It is notable that 86.4% of users employ a dumb charging approach, whereby the car is charged immediately after the cable is connected. The remaining charging sessions are planned, with users scheduling the start time to occur after 20:00 in order to take advantage of the lower electricity tariff offered by the EKZ. Some users even schedule charging at the middle of the night. Most cars are unplugged at 7:45 in the morning. However, some car owners unplug their cars as early as 6:00. The aforementioned facts

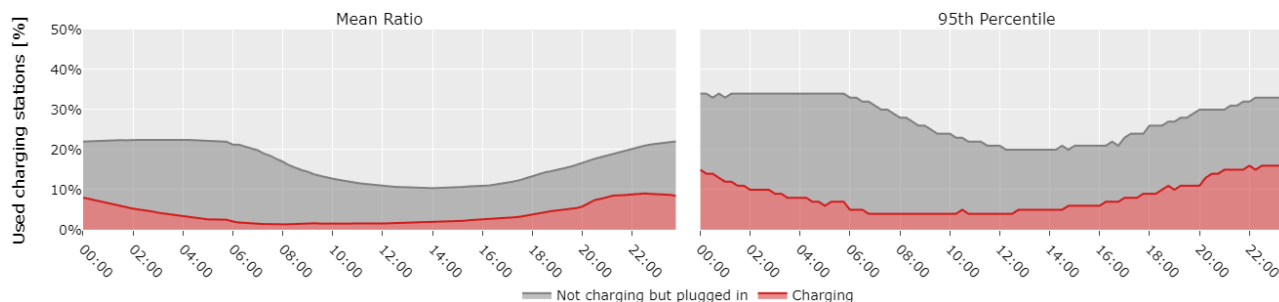


are derived from figure 2.

Figure 2 - Daily trends in BEV charging behaviour

Figure 3 illustrates the connection probability between charging stations and BEV divided into charging and not charging but plugged in events. It is observed that there is a notable increase in the number of cars charging during evening times at 17:00, which coincides with the period when many users return from work. The number of cars charging increases

until it peaks at 21:00, after which it remains stable until midnight. Following midnight, the number of cars charging decline as a lower necessity for charging is required given that the cars are then fully charged. Between 6:00 and 17:00, the number of cars charging remains constant. 23.2% of the total charging session is spent charging the car, with the remainder spent in a plugged-in state without charging. Charging sessions derived from the data exhibit a distinct character. Once the vehicle has reached a fully charged state, it



remains connected to the power source until the car is required for use again.

Figure 3 - Connection probability of BEVs in a 24-hour cycle

The connection probability between charging times and the number of available stations was also measured in order to ascertain the number of charging stations in use for each hour of the day. At the highest peak, from midnight to 5:00, 20% of all charging stations are in a plugged-in state. Over the course of this period, the proportion of cars that are charging decreases from 9% to 2%. This connection probability is very similar to that from the evaluations from the university of Stuttgart, where the ratio fluctuates daily between 19% and 9% [3].

In addition to the graphical analysis of charging times, statistical evaluations were conducted to extract numerical values from the data. Table 1 displays the distributions of selected metrics, which provide an overall understanding of certain distributions in charging processes. The data presented includes the first quartile (Q1), median, mean (μ), and third quartile (Q3) for each metric.

Table 1 - Summary of key metrics from 13'000 charging processes

	Q1	median	μ	Q3
Charging sessions per week	0.62	1.23	1.43	1.85
Energy flown per charging session [kWh]	13.03	26.5	28.24	39.86
Charging duration [h:m]	1:45	3	3:10	4
Plugged in time [h:m]	10	13	13:46	17
GHG emissions per charging session (gCO ₂ /kWh)	1'117	2'511	3'379	4'651
Costs per charging session [CHF]	2.19	4.97	5.33	7.73
Time in between charging sessions [days]	0.58	2.22	3.12	4.53

When the average energy input for each charging session is scaled down to the energy needed for each day, this equates to 29.5 km driven by each BEV, if each car consumes 19 kWh per 100 km. The observed variation in GHG emissions per charging session is attributed to the differing emission profiles observed at different times of the day and year.

A study of 45'000 charging processes from 480 households in Germany revealed that an electric car is charged on average 2.2 times a week. The average time spent plugged in is 11.4 hours. The frequency of charging is significantly higher, and the plug-in time is shorter than the results presented in this thesis [4]. One possible reason for these large deviations can be explained by the difference in car-dependency, geography and daily driving distance between Switzerland and Germany [5][6].

It is not possible to extract and cluster charging patterns with a times series clustering algorithm due to the vast differences between all charging stations, which prevent the algorithm from identifying similarities. The patterns are not in similar shapes that could be meaningfully divided into groups by an algorithm. Therefore, a manual approach is applied. Upon manual inspection of the data, as shown in figure 4, it becomes clear that each station shows a regular charging pattern over time, but the charging patterns varies between each charging station. The upcoming figure presents a visual representation of the charging sessions from nine stations over a three-month period.

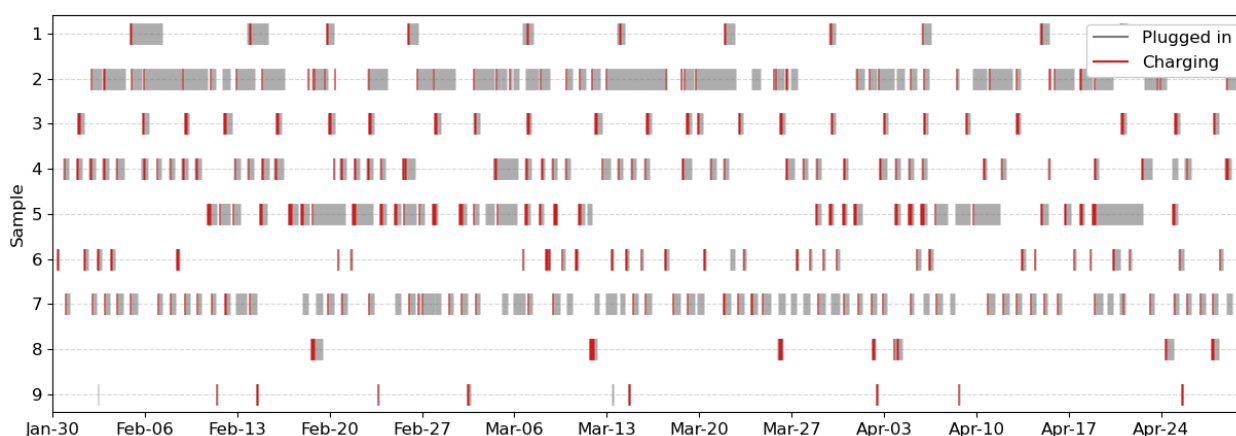


Figure 4 - Charging sessions of a sample of charging stations

Some individuals regularly plug in and charge their BEVs after work. Others always leave their car plugged in, even when it does not need to be charged. Some only charge it when it is necessary. There is no relationship between weather or season and charging behaviour. Holidays and weekends result in the same amount of charging processes and postponed unplugging times. Furthermore, it has been demonstrated that the frequency of charging has a direct impact on the consistency of the charging process over time. This implies that the predictability of subsequent charging process increases with the frequency of charging events, as opposed to longer periods in between charging events.

The average GHG emissions per kilowatt-hour in Switzerland is 85 gCO₂eq/kWh. Figure 5 illustrates the change in gCO₂eq/kWh emissions during a day, also incorporating the life cycle of the energy generators. The differences within the seasons were labelled with confidence bands, which demonstrate the variation from the 1st quantile to the 3rd quantile. During spring and autumn, there is minimal variation in emissions throughout the day. The emissions of the energy mix are stable at 64 gCO₂eq/kWh during the summer and at 71 gCO₂eq/kWh during spring and autumn. However, during winter, there is a notable discrepancy in emissions, with fluctuations occurring throughout the day and reaching elevated levels of over 200 gCO₂eq/kWh during the night.

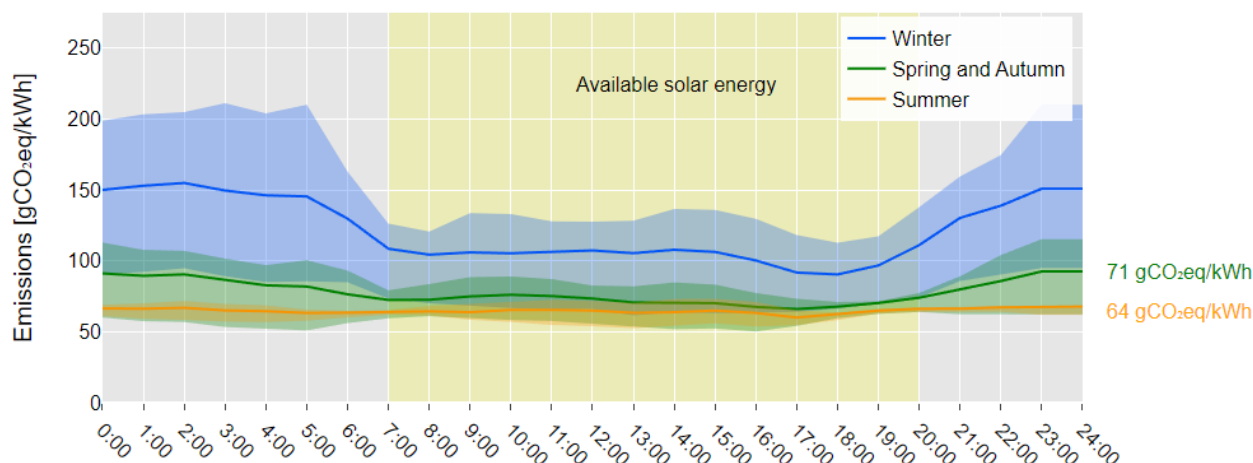


Figure 5 - Seasonal gCO₂eq/kWh emissions throughout the day

The generation of local energy from solar panels results in an emission of 30-50 gCO₂eq/kWh, a figure that is dependent upon the photovoltaic panel technology employed and the consideration of the entire lifecycle of the photovoltaic panel [7][8][9]. Using only energy from locally produced sources results in a reduction of 22% to 58% of CO₂ equivalent emissions per kWh. However, this reduction is contingent upon the availability of sufficient global solar radiation during specific hours on sunny days.

Figure 6 illustrates that Switzerland relied on German electricity during the night on a period of low temperatures between the 23rd and 27th of January 2023. It is also notable that, on such winter nights, there is a high jump from 70 gCO₂eq/kWh to over 300 gCO₂eq/kWh after 20:00. This presents a significant challenge when postponing the charging of large quantities of batteries into winter nights, particularly in the context of the change to the low tariff. It is also noteworthy that on such days, there is not enough available sunlight to even charge a car by a household plug. The temperature on these days was at -2.9°C in St. Gallen. It is therefore imperative to closely predict such situations throughout the year and to exercise control over the charging of BEVs during such periods.

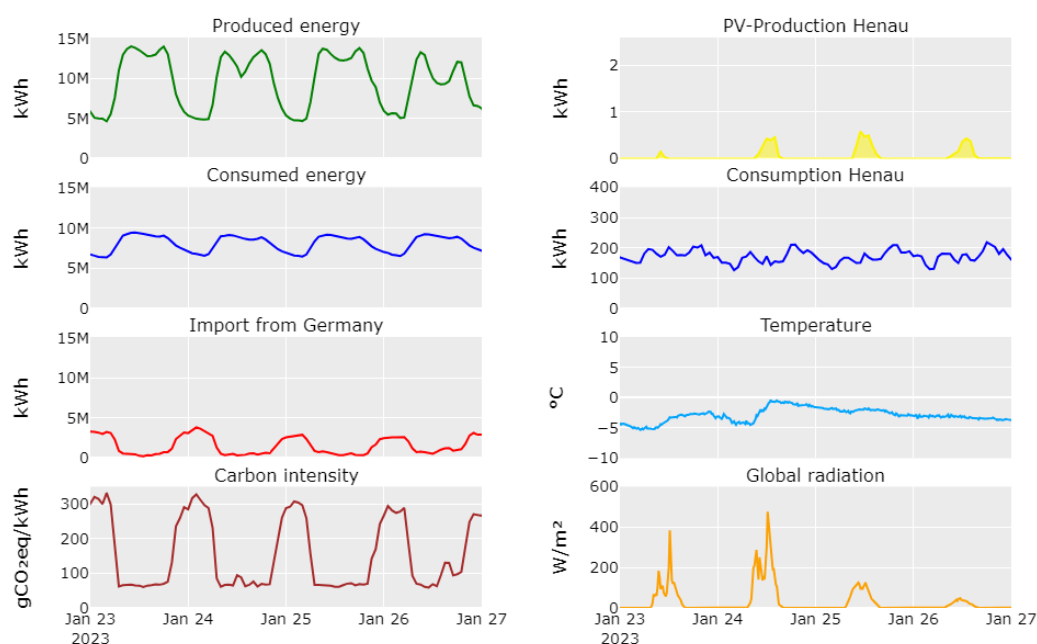


Figure 6 - Energy, weather, and emission metrics over four days

In the most unfavourable circumstances, the charging of a BEV results in the emission of 18kg of CO₂, compared to 64 kg for a diesel car over the same period. This means BEVs have running emissions more than 3.55 times lower than comparable gasoline cars. This aligns closely with the ICCT's life cycle emissions estimates, which show BEVs having 2.94 to 3.23 times lower emissions over their lifetime compared to internal combustion engine cars [10].

3. Added Values/Conclusion

The daily routines, charging needs and the electricity pricing of BEVs are the main factors influencing the charging behaviour. It is discovered that there are no similar charging patterns decipherable across BEV owners, which can be generalised in behaviour groups. However, it is encouraging to note that each user appears to remain consistent in their behaviour over a long period of time. The more frequently a BEV owner charges their vehicle, the more consistent and predictable upcoming charging processes become. The analyses have enabled a more comprehensive understanding of the charging demand of electric vehicles. This, in turn, enables the development of ideas for more effective energy infrastructure and energy management strategies.

In general, there is a high availability of surplus solar power from March to October during the day after 7:30 until 20:00. In winter, there is not enough solar power to get an excessive amount. Therefore, solutions must avoid charging during high emissions times in winter, which occur mainly during very cold nights. The availability of plugged-in electric cars is unfortunately better at nighttime based on the analyses. The charging capacity at early mornings and evenings can be increased by turning off boilers and heat pumps for a few hours until the excess energy accumulated exceeds reheat energy needs. The additional electricity generated is insufficient to charge multiple vehicles and is therefore in this case not a viable solution.

Optimising charging of BEVs means optimising GHG emissions and energy costs. These need to be linked together in the solution. When locally produced solar power is available, there are no costs associated with electricity procurement, and the GHG are lower than those resulting from the use of the electricity mix from Switzerland at these times. However, the costs due to the low tariff in the winter months play against the GHG emissions. The electricity costs decrease at 20:00 and at the same time, the GHG emissions explode on cold nights. This is due to the fact that the missing electricity is imported from Germany, where 24% of energy is still produced with coal [11]. The results of the study indicate that small cost incentives, such as the switch to a low-tariff rate, have a significant impact on the charging start time. The price per kWh decreased by 18%, and 13.6% of all BEV owners changed their charging start time to after 20:00. The findings of the study suggest that cost adjustments in the electricity price could be a useful lever to influence charging behaviour.

As soon as the production of solar energy is greater than the local electricity consumption, an electric car can be used to absorb the otherwise lost energy. Controlling the charging infrastructure of electric vehicles is more complex than that of a heating pump or boiler. An intervention into vehicle charging would be noticed by the user, in contrast to the heat generators. The time flexibility of a BEV is low. This is because it is linked to the plugged-in time, the individual driving behaviour, and the current situation of the owner. Additionally, available battery storage is required to charge flexibly. Plugged-in and fully charged cars cannot be used to dissipate energy anymore. Once they are charged, only V2G solutions are effective. V2G solutions could also increase the local flexibility. They can be charged at a place with high solar energy input, for example at work, and at home this electricity can be fed for the operation of household appliances during low sunlight.

It is also crucial to highlight the significant potential for solar energy generation at the workplace. During typical working hours, solar radiation levels are high, which translates to a correspondingly high energy generation potential.

In order to enhance the flexibility of charging processes, it is essential to address the cost approaches and to grant vehicle owners the autonomy to organise their charging processes according to their preferences. This also encompasses the option of not having the charging process entirely controlled by a management system, as this may not always be the optimal solution due to the multitude of behaviours.

To promote the flexibility of BEVs, a solution is proposed for integration into the ENFLATE Strompilot energy management system. This solution involves a local management system capable of controlling boilers, heat pumps, and charging stations. It also requires a flexible electricity pricing structure to accommodate the diverse lifestyles of BEV owners, allowing them complete freedom to choose their charging times.

BEV owners can schedule a charging window of when their vehicle is at home and plugged in but not fully charged. The management system identifies the most optimal charging times, initially prioritising excess solar power to eliminate costs and then focusing on charging BEVs during periods of minimal GHG emissions.

To motivate BEV owners to adapt their charging behaviour, pricing incentives are crucial. Charging during high-emission periods or predicted high grid loads should be priced higher, encouraging users to charge during off-peak times for price benefits. Additionally, a system could be introduced, rewarding users with a lower energy tariff for charging during periods of lesser GHG emissions per kWh. Charging when excessive energy from solar panels is available remains free. The height of the tariff would depend on factors such as time of charging, the size of the entered charging window, the use of excess energy, and avoided GHG emissions. Early planning and reservation of charging times would yield higher returns, while last-minute changes would incur higher costs.

The charging management system maintains considerable flexibility in managing electric vehicle charging schedules based on entered time slots. Initially, the system monitors the electrical grid to prevent overload, which occurs from charging multiple vehicles simultaneously. Additionally, the system prioritises charging based on the cost of electricity. Charging during periods when excess solar power is available is highly prioritised, as this reduces the cost of electricity to zero and also relieves the grid load as a side effect. This further reduces the risk of sudden load peaks and power interruptions. The system then prioritises charging during times of lower carbon dioxide emissions when there is no excess solar energy available, as higher emissions correlate with higher electricity costs in the pricing strategy. Users are notified about the expected charging times for their vehicles, the predicted price, and saved costs. By the end of each individually defined time slot, the vehicle is fully charged.

This approach not only provides flexibility but also minimises the impact of BEVs on the local and national energy grids by better distributing the use of energy across the day. This could reduce the need for costly grid capacity expansions and significantly lower GHG emissions.

The solution's most significant strength lies in its scalability. It can be introduced on a single home scale, or it can be expanded to encompass a wider area, making it versatile for managing large fleets. Additionally, it supports a wide range of BEVs, from small-scale personal vehicles to large fleet vehicles or even trucks, ensuring broad applicability.

The solution addresses three key challenges of today simultaneously. High, rising energy prices, smoothing grid load, and reducing emissions in line with the climate neutrality goals of Switzerland. It promotes self-produced solar energy and prevents the transformer from

reaching its technical limits, preventing potential fires and heavy wear. This results in reduced infrastructure costs and enhanced safety.

With this solution, the BEV owner is always focussed and takes the full responsibility of their car, preserving their autonomy without intrusive system interference. A user has always the option to charge the car spontaneously at the standard energy price without an intervention from the management system. However, this charging behaviour would always be strategically priced higher, to encourage using the management system. Otherwise, users would revert to their previous habits of charging their vehicles on the spot.

BEVs that are not plugged in or are already fully charged when the user reserves a timeslot do not present a challenge to the infrastructure and therefore do not require any solutions to this potential issue.

This solution also has drawbacks. It is important to consider direct, indirect, and macroeconomic rebound effects that could result from behaviour changes due to the lower electricity costs. The system's reliance on solar energy also introduces vulnerability to sudden weather changes, such as overcast conditions that reduce solar panel efficiency. Legal compliance is another essential factor, including ensuring that there is no discrimination in access based on human or regional differences, and meeting data protection and other relevant laws.

Moreover, the effectiveness of this concept must be tested on a large scale, which involves significant costs. Infrastructure updates are necessary, including the installation of smart meters to support the management system. Ultimately, the benefits derived from the management system must justify these expenditures.

The charging management system should create a situation in which a lesser number of vehicles charge at a fewer daily frequency, rather than many BEVs charging a small amount of energy at the same time. The latter places a much greater load on the grid than the former. To address this problem the system should therefore know the number of remaining battery charge of each BEV.

This paper presents an abridged version of a bachelor's thesis written at the Lucerne University of Applied Sciences and Arts for the degree programme in mobility, data science and economics. The complete version is available upon request from the authors.

References

- [1] swissgrid. (2023). Netz der Zukunft. Swissgrid. <https://www.swissgrid.ch/de/home/projects/future-grid.html>
- [2] ENFLATE: ENabling FLexibility provision by all Actors and sectors through markets and digital TEchnologies. (2023). Hochschule-Luzern. <https://www.hslu.ch/de-ch/hochschule-luzern/forschung/projekte/detail/?pid=6216>
- [3,4] Wagner, C. (2024, March 20). Vehicle-to-Home vs. Heimspeicher—Welche Option bietet mehr Potential für Privathaushalte? Netzimpuls, Universität Stuttgart IEH. https://esuich.sharepoint.com/:b:/r/sites/ESMSETIT-Event/Freigegebene%20Dokumente/General/2024/NetzImpuls/Unterlagen%20f%C3%BCr%20Teilnehmende/Pr%C3%A4sentationen/0905_Wagner_Universit%C3%A4t%20Stuttgart_Vehicle-to-home%20vs.%20Heimspeicher.pdf?csf=1&web=1&e=C8obck
- [5] ARE, B. für R. (2015). Mikrozensus Mobilität und Verkehr. Mikrozensus Mobilität und Verkehr. <https://www.are.admin.ch/are/de/home/verkehr-und-infrastruktur/grundlagen-und-daten/verkehrsverhalten.html>

- [6] Bundesministerium für Verkehr und digitale Infrastruktur. (2018). *Ergebnisbericht— Mobilität in Deutschland – MiD*. https://bmdv.bund.de/SharedDocs/DE/Anlage/G/mid-ergebnisbericht.pdf?__blob=publicationFile#:~:text=„Im%20Durchschnitt%20werden%20pro,als%20Menschen%20in%20ländlichen%20Gebieten.“
- [7] Wirth, H. & Fraunhofer ISE. (2024). *Aktuelle Fakten zur Photovoltaik in Deutschland*. <https://www.ise.fraunhofer.de/de/veroeffentlichungen/studien/aktuelle-fakten-zur-photovoltaik-in-deutschland.html>
- [8] IPCC. (2014). *Climate change 2014: Mitigation of climate change Working Group III contribution to the fifth assessment report of the Intergovernmental Panel on Climate Change*. Cambridge university press.
- [9] Kim, H. C., Fthenakis, V., Choi, J., & Turney, D. E. (2012). Life Cycle Greenhouse Gas Emissions of Thin-film Photovoltaic Electricity Generation: Systematic Review and Harmonization. *Journal of Industrial Ecology*, 16(s1). <https://doi.org/10.1111/j.1530-9290.2011.00423.x>
- [10] Bieker, G. (2021, July 20). A global comparison of the life-cycle greenhouse gas emissions of combustion engine and electric passenger cars. *International Council on Clean Transportation*. <https://theicct.org/publication/a-global-comparison-of-the-life-cycle-greenhouse-gas-emissions-of-combustion-engine-and-electric-passenger-cars/>
- [11] Electricity Maps. (2023). *Live 24/7 CO₂ emissions of electricity consumption*. <http://electricitymap.tmrow.co>

Acknowledgement of funding

This project has received funding from the European Union's Horizon Europe program under the Grant Agreement No 101075783.

This work was supported by the Swiss State Secretariat for Education, Research and Innovation (SERI) under contract number 22.00283.

G0311

Optimal V2X operation of EV fleets with PV-battery charging station for demand-side flexibility provision

Federica Bellizio, Philipp Heer

Urban Energy Systems Laboratory, Swiss Federal Laboratories for Materials Science and Technology, Empa, Dübendorf/Switzerland;
Tel.: +41-58-765-3931
federica.bellizio@empa.ch

Abstract

The increasing number of electric vehicles (EVs) expected on the road in the coming years poses new threats to the reliability of the power system. However, it can also play a key role as a source of demand-side flexibility to support the system in managing uncertainty resulting from the integration of renewable and distributed energy resources. However, for flexibility provision in new emerging demand-response (DR) markets, there are participation requirements on minimum bid sizes that could be challenging to meet for EV fleets. The onsite coupling between photovoltaics (PVs), battery energy storage systems (BESS) and EV fleets with vehicle-to-grid (V2G) technology has shown extremely promising performance in terms of demand-side flexibility provision. To avoid overbidding in DR markets, aggregators need new operational tools: i) to quantify the available flexible energy in advance for accurate flexibility market bidding and, ii) to operate the charging station cost-efficiently while reserving flexible energy in case of accepted bids.

This paper proposes a novel operational tool for EV aggregators with PV-battery charging station aiming at reducing their energy costs and generating new revenues from the provision of demand-side flexibility. The contribution of this paper is twofold:

- A chance-constrained intraday optimization of the BESS and EV fleet charging scheduling for flexibility quantification and robust flexibility bidding in DR markets;
- A flexibility-aware real-time controller to account for operational uncertainty while reserving the flexible energy to provide in case of accepted bids.

A case study on the NEST and move demonstrators at Empa, in Switzerland, was used to investigate the aggregator's cost-benefits of adopting the proposed tool in real-time operations. The test system representing the PV-battery charging station included a 168 kWh battery, 110 kWp PV systems, and 4 charge points (CPs). A fleet of 4 EVs with V2G technology moving between the charging station and the service site was sampled from real charging data provided by TotalEnergies. Results showed that the revenues stemming from the provision of flexibility in the form of availability significantly exceeded the energy costs of the charging station. We also showed that V2G technology and a more interactive involvement of EV users in the provision schemes can significantly enhance the overall cost-benefits. This highlights the need for implementing new incentives for the installation of V2G chargers and reshaping the regulatory framework to incentivize active participation of EV users, either by staying within the boundaries of their comfort or by appropriately compensating for their discomfort.

Introduction

The current regulatory policies aimed at promoting the transition from fossil fuel to low emission transportation have incentivized significant technological advancements, leading to reduced EV cost, increased EV range and denser charging infrastructure. Consequently, EVs are becoming more popular, with the global EV fleet projected to reach 145 million units by 2030 [1]. On the one hand, the added energy demand from the growing EV supply equipment required for charging poses new threats to the reliability of the power system [2]. On the other hand, the increasing number of EVs on the road can play a key role as a source of flexibility for a more reliable system operation if their charging scheduling is properly optimised. The additional storage capacity offered by EVs can support the system to deal with the operational uncertainty resulting from the integration of renewable and distributed energy resources. This would allow for an improved utilization of the existing grid assets and a consequent reduction of the investment costs to reinforce the network equipment [3], [4]. However, for flexibility provision in new emerging DR markets, there are participation requirements on minimum bid sizes that could be challenging to meet for EV fleets [5].

The onsite coupling between PVs, BESS and EV fleets with V2G technology has shown extremely promising performance in terms of demand-side flexibility provision [6]–[8]. In a V2X operation, EV fleets can be used for site self-consumption maximization by storing electricity surplus produced by PVs and releasing it during peak hours [9], for load peak shifting in grid congestion occurrences or for voltage and frequency regulation by consuming or injecting power when the grid constraints are violated [10]. By aggregating the EV fleet and BESS capacity, the requirement of minimum bid size can be easily met, enabling the participation of EVs in DR markets, and hence the generation of new revenue streams for aggregators [11]. Several approaches have been proposed for demand/side flexibility quantification, most of them distinguishable into direct and indirect quantification [12], [13]. Direct approaches aim to quantify the flexibility directly at the level of individual technologies in a bottom-up manner. Conversely, indirect approaches assume a specific market and control strategy and evaluate the impact of energy flexibility according to standardized metrics [14], e.g. operational cost savings, peak power, or carbon emission reductions. In particular, model predictive control (MPC) has been widely used to indirectly quantify the flexibility [15], [16]. However, most studies have observed that uncertainties arising from generation and load forecasts, EV user behaviors, and the electricity market can significantly impact the V2X setting in terms of profitability, comfort and grid constraint violations [17], [18]. To overcome the challenge of considering uncertainty when quantifying energy flexibility, sampling-based approaches or stochastic MPC-based schemes have been investigated extensively. In [19], a stochastic optimization model was used to maximize the expected profits of an EV aggregator through optimal day-ahead bidding strategies. Similarly, in [20], [21], mixed-integer linear programming frameworks were proposed, incorporating Machine Learning (ML) forecasting algorithms and Monte Carlo (MC) simulations to cope with the uncertainties, respectively. While the studies listed above address various challenges, to the best of the authors' knowledge, there remains a deficiency in comprehensive tools for multi-site V2X operation of EV fleets providing demand-side flexibility while ensuring users' comfort.

1. Requirements for Grid Services - Technical & Market Conditions

To avoid overbidding in DR markets, aggregators need new operational tools: i) to quantify the available flexible energy in advance for accurate flexibility market bidding and, ii) to operate the charging station cost-efficiently while reserving flexible energy in case of accepted bids. This paper proposes a novel operational tool for EV aggregators with PV-battery charging station aiming at reducing their energy costs and generating new revenues from the provision of demand-side flexibility. The flowchart of the proposed approach is shown in Fig. 1. The first step is the time-ahead prediction of the available flexibility based on forecasts of the charging station generation and load, as well as EV arrival and departure times and energy demand [22]. Subsequently, such forecasts are fed as input to a multisite optimizer that provides 15-hour ahead optimal charging/ discharging schedules for an onsite BESS and an EV fleet moving between different sites during the day, thus being able to provide flexibility services at different locations. An example of the EV daily trip is shown in Fig. 2. The EV fleet moves between the charging station and another site for daily services, which is also equipped with CPs. The available flexible energy capacity resulting from the optimization can then be bid in intraday DR markets. Finally, in real-time operation, a controller adjusts the BESS and EV schedules based on real-time measurements and acceptance of the market bids. The flexibility market framework shown in Fig. 3 was assumed [24], [25]. In such a framework, transmission and distribution operators can procure flexibility in two respective and competitive DR markets, i.e. a local market for congestion management and a national market for frequency response services. The flexibility providers participate in the most profitable market, i.e. higher availability (or reservation) prices per MWh of provided energy flexibility.

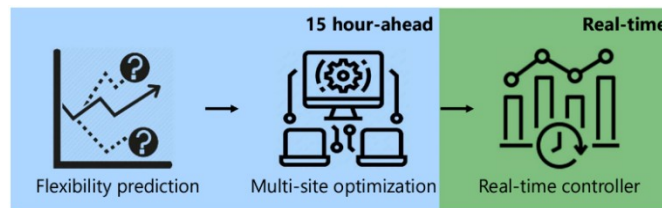


Fig.1 The proposed operational tool for demand-side flexibility provision.

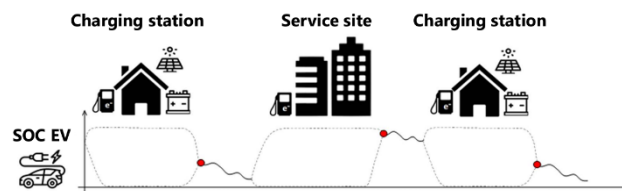


Fig.2 An example of daily EV trip.

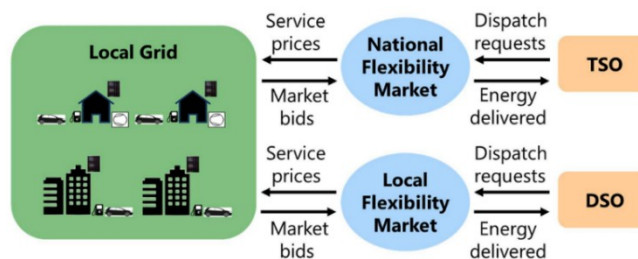


Fig. 3. The assumed market framework.

2. Approach towards Flexibility

This section first describes the deterministic intraday charging schedule optimization with the operating constraints related to all the assets available at the charging station and the EV fleet moving between the station and the service site. Subsequently, the chance-

constrained formulation is provided to account for forecast errors and quantify the flexibility in terms of an envelope for robust DR intraday market bids [26], [27]. The flexibility envelope provides the aggregators with the maximum, hourly flexible energy that is available to bid at 9am every morning for the next 15 hours. The aggregators can decide whether to bid the maximum available flexible energy or less according to their risk management strategies.

A. Multi-site optimization

In this section, the schedules for a charging station equipped with a battery, PV generation and a fleet of K EVs over a finite time horizon with hourly time step is provided. Let $\mathcal{T} = \{0, \dots, T-1\}$ where T is the length of the horizon considered with a time discretization t . The EV $k \in [1, K]$ can charge (C_t^k) and discharge (D_t^k), acquiring energy needed for each trip ($E_t^{k,tr}$), as well as providing an upward service by reducing charging ($A_t^{k,c,n}, A_t^{k,c,l}$ for national and local service, respectively) or increasing discharging ($A_t^{k,d,n}, A_t^{k,d,l}$ for national and local service, respectively) in the form of availability, whenever it is connected to the grid, at the charging station ($T_t^{k,sta}$) or at the service site ($T_t^{k,ser}$) [28]. The charging/discharging power of the EV can be regulated between 0 and a maximum power level allowed by the charger (P_{max}^k). Similarly, the state of charge (SoC) of each EV at each timestep SoC_t^k is limited between 10% – 90% of the maximum EV energy capacity E_{cap}^{EV} . The same input and control variables are considered for the onsite battery. The battery can charge (C_t^B) and discharge (D_t^B), as well as providing an upward balancing service by reducing charging ($A_t^{B,c,n}, A_t^{B,c,l}$ for national and local service, respectively) or increasing discharging ($A_t^{B,d,n}, A_t^{B,d,l}$ for national and local service, respectively) in the form of availability. The charging/discharging power of the battery can be regulated between 0 and a maximum allowed power level (P_{max}^B). Finally, the battery SoC at each timestep SoC_t^B is limited between 10% – 90% of the maximum battery energy capacity E_{cap}^B . The electricity prices π_t^{el} , the national and local flexibility service prices for availability, $\pi_t^{A,n}$ and $\pi_t^{A,l}$, are known ahead of the time horizon. The trips that the EVs need to take, including the length of the trip in hours and the energy required, the onsite generation and load of the station are forecasted for the whole time horizon, thus they are considered as given in the deterministic formulation.

The objective function maximizes revenues from flexibility service provision, while meeting the station energy and EV energy trip requirements and maximizing the station self-consumption (i.e. minimizing the energy imported from the grid E_t^{imp}), as shown below:

$$\max \sum_{t \in \mathcal{T}} \left(\sum_{k=1}^K \left((A_t^{k,c,n} + A_t^{k,d,n} + A_t^{B,c,n} + A_t^{B,d,n}) \cdot \pi_t^{A,n} + (A_t^{k,c,l} + A_t^{k,d,l} + A_t^{B,c,l} + A_t^{B,d,l}) \cdot \pi_t^{A,l} - C_t^k \cdot \pi_t^{el} \cdot T_t^{k,ser} - \epsilon^p \cdot D_t^k \right) - E_t^{imp} \cdot \pi_t^{el} - \epsilon^p \cdot D_t^B \right), \quad (1)$$

where $T_t^{k,ser}, T_t^{k,sta} = 1$ if the EV is connected to a CP at the service site or at the charging station, respectively, otherwise $T_t^{k,ser}, T_t^{k,sta} = 0$. ϵ^p is a penalty factor that penalizes onsite battery and EV discharging, thus minimizing battery cycling, while only minimally affecting revenues from providing availability as a service. A zero feed-in tariff is assumed, indicating that no revenues are generated for selling energy E_t^{exp} back to the grid [29].

The operating models of the station, battery, and EVs include several constraints. The energy balance of the entire charging station is given by:

(2)

with E_t^l and E_t^{PV} being the onsite load and generation, respectively.

The constraint seen in Eq. (3) describes the EV battery's energy balance, taking into account the energy needed for mobility purposes as well as the losses caused by charging and discharging efficiencies, η_c^{EV} and η_d^{EV} .

$$\text{SoC}_t^k = \text{SoC}_{t-1}^k + \eta_c^{EV} \cdot C_t^k - \frac{D_t^k}{\eta_d^{EV}} - E_t^{k,tr}, \quad \forall t \in \mathcal{T}, k \in [1, K]. \quad (3)$$

When the EVs are not connected to the grid, the charging, discharging and availability for services are zero:

$$C_t^k = D_t^k = A_t^{k,c,l} = A_t^{k,d,l} = A_t^{k,c,n} = A_t^{k,d,n} = 0, \quad \forall t \in \{T_t^{k,sta}, T_t^{k,ser} = 1\}, k \in [1, K]. \quad (4)$$

The constraint seen in Eq. (5) limits the SoC of each EV between the lower and upper bounds of the battery's energy content, which is assumed to be the same for each EV:

$$0.1 \cdot E_{cap}^{EV} \leq \text{SoC}_t^k \leq 0.9 \cdot E_{cap}^{EV}, \quad \forall t \in \mathcal{T}, k \in [1, K]. \quad (5)$$

Moreover, each EV battery cannot charge and discharge at the same time:

$$C_t^k \cdot D_t^k = 0, \quad \forall t \in \mathcal{T}, k \in [1, K]. \quad (6)$$

When an EV commits to service availability, the maximum power allowed by its charger P_{max}^k , as well as whether the EV is charging or discharging, need to be taken into account

$$\begin{cases} A_t^{k,d,n} + A_t^{k,d,l} + D_t^k \leq P_{max}^k \cdot \Delta t \\ A_t^{k,c,n} + A_t^{k,c,l} \leq C_t^k \\ (D_t^k - C_t^k) + (A_t^{k,d,n} + A_t^{k,d,l} + A_t^{k,c,n} + A_t^{k,c,l}) \leq P_{max}^k \cdot \Delta t \end{cases} \quad \forall t \in \mathcal{T}, k \in [1, K], \quad (7)$$

where Δt denotes the time interval. Simultaneously, when the bid is accepted, it is important to ensure that the committed energy is available for the service to be sustained for the required time t_s :

$$\begin{cases} x_t^k + C_t^k \cdot \eta_c^{EV} - \frac{(D_t^k + A_t^{k,d,n} + A_t^{k,d,l}) \cdot t_s}{\eta_d^{EV}} \geq 0.1 \cdot E_{cap}^{EV} \\ x_t^k \leq \text{SoC}_t^k \\ x_t^k \leq \text{SoC}_{t-1}^k \end{cases} \quad \forall t \in \mathcal{T}, k \in [1, K], \quad (8)$$

where x_t^k is an auxiliary decision variable introduced for linearisation. The flexibility service provision only considers availability, rather than utilization, which occurs infrequently [30]. Finally, the EV battery's energy level is at the required level E_{req}^{EV} set by aggregator at the end of each day:

$$E_t^{exp} - E_t^{imp} = E_t^l - E_t^{PV} - D_t^B + C_t^B + \sum_{k=1}^K (C_t^k - D_t^k) \cdot T_t^{k,sta}, \quad \forall t \in \mathcal{T},$$

$$\text{SoC}_{T-1}^k = E_{req}^{EV}.$$

(9)

Similarly, all the constraints in Eqs. (3)-(9) are imposed for the battery $\forall t \in \mathcal{T}$.

B. Accounting for uncertainty

In order to mitigate the effect of uncertainty on the market bidding strategy, an intraday chance-constrained optimization is formulated [31]. The uncertainty derives from the forecasts of onsite load and PV generation, and EV charging sessions (i.e. arrival and departure times, and charging energy demand). Chance-constraints are probabilistic constraints that ensure that the limits will hold with a pre-described probability $1 - \epsilon$, where ϵ is the acceptable violation probability. This is done by replacing the original constraints with tightened constraints, where tightenings represent security margins against uncertainty and are evaluated using MC simulations. To enforce a chance constraint with $1 - \epsilon$ probability, we need to ensure that the $1 - \epsilon$ quantile of the distribution remains within the bounds. Thus, the tightening corresponds to the difference between the value with zero forecast error (indicated with superscript 0) and $1 - \epsilon$ quantile value evaluated based on the empirical distribution resulting from the MC simulations.

The optimization is solved using an iterative algorithm. It alternates between solving a deterministic optimization with tightened constraints, and evaluating the following tightenings at each iteration m : If the maximum changes in the tightenings between two subsequent iterations are below a certain threshold η^Ω , the algorithm has converged and a feasible solution has been found. The solution represents the maximum, hourly flexible energy that is available to bid while ensuring the station operational constraints and the user comfort boundaries.

C. Real-time Controller

A finite horizon MPC-based controller to account for real-time operational uncertainty while reserving the flexible energy to provide in case of accepted bids is formulated in this section. The new objective function is given by:

$$\min \sum_{t \in \mathcal{T}} \left(\sum_{k=1}^K \left(C_t^k \cdot \pi_t^{el} \cdot T_t^{k,ser} + \epsilon^p \cdot D_t^k \right) + E_t^{imp} \cdot \pi_t^{el} + \epsilon^p \cdot D_t^B \right) \quad (10)$$

The constraints in Eqs. (2)-(9) and the battery constraints are imposed. However, the EV battery energy balance constraint in Eq. (3) is modified to provide flexible energy when the bids are accepted:

$$SoC_t^k = SoC_{t-1}^k + \eta_c^{EV} \cdot C_t^k - \frac{D_t^k}{\eta_d^{EV}} - E_t^{k,tr} - E_t^{k,bid} \cdot T_t^{k,bid}, \forall t \in \mathcal{T}, k \in [1, K], \quad (11)$$

with $E_t^{k,bid}$ representing the flexible energy from EVs and battery, respectively, bid in the intraday DR markets, $T_t^{k,bid} = 1$ in case of accepted bids, otherwise $T_t^{k,bid} = 0$. No revenues are assumed for flexibility provision in the form of utilization. A similar modification is applied to the battery energy constraint.

At each time step t , the optimization in Eq. (10) takes the real-time measurement and the acceptance of market bids as inputs, and determines the optimal charging/discharging schedules for the EV fleet and onsite battery for the full horizon $\mathcal{T} = \{t, \dots, t + T - 1\}$ using the updated forecasts of onsite load and PV generation, and EV charging sessions. However, only the optimal schedules at time step t are applied.

3. Added Values/Conclusion

This section provides an overview of the performance of the proposed tool in terms of energy cost reduction and generation of new revenues from demand-side flexibility provision.

A. Test system and assumptions

A case study was conducted on the NEST and move demonstrators at Empa, in Switzerland [23]. This test system representing the PV-battery charging station included a 168 kWh battery, 110 kWp PV systems, and 4 CPs. Historical data for PV generation and load for August 2022 were used to test the proposed tool. Charging data for a fleet of 4 EVs with V2G technology and 40 kWh battery each, moving between the charging station and the service site, was sampled from real data provided by TotalEnergies with over 2 million charging sessions and 5317 CPs across the Netherlands [22]. The V2X operation of the EV fleet was considered exclusively at the charging station, as described in Eq. (2). A maximum allowed power level $P_{max}^k = 15$ kW and $P_{max}^B = 80$ kW were assumed for the EVs and onsite battery, respectively. The required battery level set by the aggregator at the end of each day was $E_{req}^{EV} = 0.9 \cdot E_{cap}^{EV}$ and $E_{req}^B = 0.9 \cdot E_{cap}^B$. Electricity and national flexibility service prices for availability, π_t^{el} and $\pi_t^{A,n}$, were taken from for August 2022. In such a price modeling, the prices for national flexibility services reflect the need for inertia of transmission operators following the integration of renewable sources. Higher prices are modeled when the hourly share of renewable integration is higher, thus corresponding to lower system's inertia and a higher need for the system operator [32]. The same price variation of national flexibility services was assumed for local flexibility services, as the congestion risk increases when the hourly share of renewable integration is higher, similar to the inertia need in national flexibility price modeling. However, for local services, different mean values were considered based on the locations of the charging station or service site, i.e. higher mean values for locations with a higher congestion risk. In this work, the service site, which is located in urban areas, has a higher congestion risk than the charging station, resulting in higher local service prices. The assumed prices are shown in Fig. 5 for one week. Dynamic containment [33] and congestion management [34] were considered as national and local flexibility services, respectively. A finite time horizon of 15 hours with time step $\Delta t = 1$ h was used for both the multi-site optimization and real-time controller. The electricity and flexibility prices were assumed to be known ahead of this horizon, which is in line with the current intraday energy and balancing service market arrangements. The required time for the flexibility service to be sustained when called on was $t_s = 1$ h. The multi-site optimization was performed once every day for the horizon 9am-11pm to calculate the intraday market bids, with $\epsilon^p = 0.05$ to minimize battery cycling. Conversely, the real-time MPC controller was run hourly with a 15 hour horizon. However, the aggregator becomes aware of accepted bids only after the intraday market clearing at 9am every day. The forecasts of onsite load and PV generation, and EV charging sessions are fed as inputs to both the multi-site optimization and the real-time controller. Long short-term memory (LSTM) neural networks with 3 layers and 15 neurons per layer were used for these forecasts. The input and output rolling windows of the LSTM models were one week and 15 hours, respectively. In order to capture the seasonal trend, historical data from June to July 2022 was used to train and test the LSTM models for onsite load and PV generation. Synthetic data from January to July 2022 was used for the prediction of EV charging sessions. The training and testing split was 80%/20%, while the data from August was used for the validation of all predictive models. Weather data were used as additional features to improve the predictive performance. More specifically, for the EV charging sessions, new features were created to capture the charging behaviour of each EV in the fleet [22]. Subsequently, a causality-based feature selection approach was used to select the most relevant features for training, thus enhancing the performance. The error

distributions of onsite load and PV generation, charging session duration and energy demand, were used for the MC simulations to account for uncertainty, enforcing the chance constraints with an $\epsilon = 5\%$ violation probability.

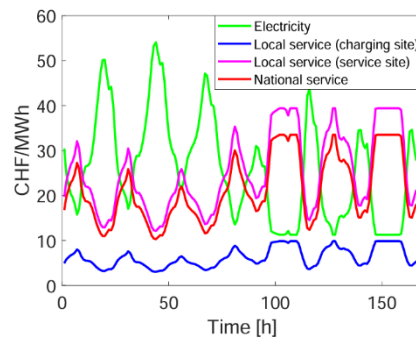


Fig. 5. The assumed weekly prices for electricity, availability for local (charging station and service site) and national flexibility services.

B. The flexibility envelope

This section focuses on evaluating the flexibility envelope through which aggregators can make flexibility bids in intraday DR markets according to their risk management strategies. The optimal charging schedule resulting from the chance-constrained, multi-site optimization for a single EV over the time horizon 9am-11pm is shown in Fig. 6. The EV was at the charging station (indicated in the grey box area), on a trip and at the service site (in the red and light blue box area), respectively. Following the trips, the battery SoC decreased due to the energy consumed for travelling. When the EV charges, it gets paid for offering availability to reduce its charging and increase its discharging. As a result, the EV charged at the service site when the price for local service provision was significantly higher. Subsequently, the EV charged again upon returning to the charging station in the evening, as constrained by Eq. (9). The optimization resulted in a similar charging schedule for the onsite battery, which provided only national service availability, as the prices for such services were always higher than the local ones at the charging station. Simultaneously, the chance-constrained optimization aimed at reducing the overall electricity costs of the charging station. No electricity was imported from the grid when the PV generation was sufficient to satisfy the load. Subsequently, when no PV generation was available in the evening, the battery was first discharged to meet the load as the electricity price was high. Finally, when the electricity price decreased, the battery was charged.

The chance-constrained, multi-site optimization resulted in a net revenue (i.e. revenues net of electricity costs) of CHF 3'142 for August 2022. The available flexible energy from EVs and the onsite battery to bid in DR markets is aggregated and shown in Fig. 7 in the form of a flexibility envelope for the whole considered month. Here, the envelope resulting from the proposed chance-constrained optimization, indicated as approach i), was compared against: ii) the naive forecast-based approach in which the forecasts are assumed to be perfectly accurate and considered in the deterministic optimization, iii) the deterministic approach in which real measurements are used as inputs to the optimization, providing the true flexibility potential.

The proposed approach i) resulted in more conservative estimates of the available flexible energy, preventing overbidding in DR markets, thus avoiding penalties. In terms of net revenues, the proposed approach i) decreased the revenues only by CHF 11 compared to the true revenues resulting from approach iii). Conversely, approach ii) increased the revenues by CHF 114, but this increase needs to be offset by overbidding penalties, resulting in a significantly lower net revenue.

Additional studies were conducted to investigate the best technology, i.e. unidirectional smart charging (V1G) and V2G, to fully exploit the demand-side flexibility and quantify the

cost-benefits of a more interactive involvement of EV users in flexibility provision schemes. Using the proposed multi-site, chance-constrained optimization, different settings were compared in terms of net revenues against the described baseline approach with V2G technology in Table 1: i) only V1G was available, ii) the EVs were flexible on arrival and departure times by 1 hour, iii) EVs were flexible on arrival and departure times by 2 hours. The results highlighted that with a small fleet of 4 EVs the net revenues over a month could be increased by up-to 14% when considering V2G technology and by up-to 5% by asking the EV users in advance if they would be flexible with their parking times. This resulted in a single user's revenue increasing by-up to CHF 40 in a month, significantly incentivizing their participation in flexibility provision. Such revenue increase could be interpreted as the minimum discomfort price of EV users, i.e. the minimum price at which individual EV users would be willing to reschedule their trips in exchange for higher revenues.

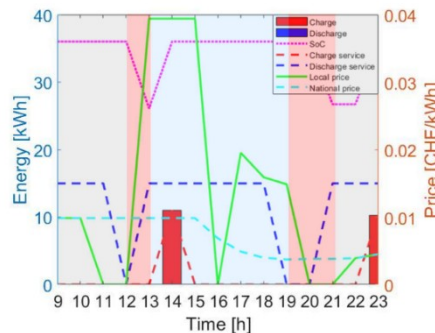


Fig. 6. The optimal charging schedule for a single EV over the time horizon 9am-11pm.

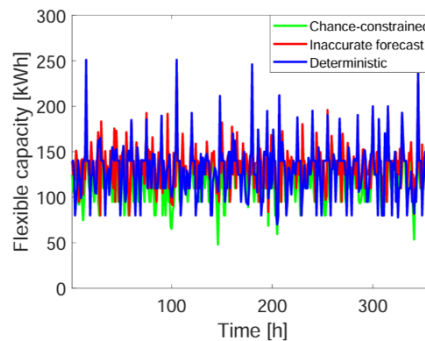


Fig. 7. The flexibility envelope for August 2022 according to three different approaches.

TABLE I
COMPARISON OF NET REVENUES WITH DIFFERENT TECHNICAL AND SOCIAL SETTINGS

	Settings			
	Baseline	V1G	1h Flex User	2h Flex User
<i>Net revenue</i> [CHF]	3'142	2'692	3'207	3'300
	—	(−14%)	(+2%)	(+5%)

C. The real-time performance

In this section, the performance of the MPC controller in responding to real-time measurements and acceptance of the intraday market bids was analyzed. In Fig. 8, the changes in the aggregated SoC of the EVs and onsite battery following the acceptance of the bids are shown over a week. It was assumed that one bid was accepted per day. It is worth noting the main discrepancies relate to the provision of the bid flexible energy and the following recharging of the batteries. This resulted in an energy cost increase of CHF 516 as no revenues for flexibility utilization were considered. However, such an increase was significantly lower than the net revenue resulting from providing availability as a

service in intraday DR markets, highlighting the cost-benefits of providing flexibility services for the aggregators.

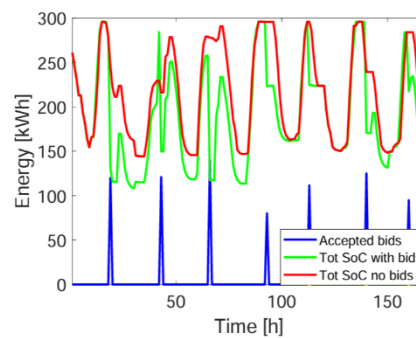


Fig. 8. The aggregated SoC of the EVs and onsite battery over a week with and without accepted intraday market bids.

D. Discussion

The proposed approach still has a few limitations that need to be considered. The resulting net revenues strictly depend on the assumed market framework, electricity, and flexibility service prices. While flexibility markets show promise in managing local congestion or supporting the transmission grids, only a few pilot projects currently exist, and it is challenging to foresee their development in the coming years. With the integration of more renewable generation sources into future power systems, leading to higher operational uncertainty, the prices of ancillary services, and consequently the revenues from flexibility provision, are likely to rise [32]. Nevertheless, the proposed tool can adapt to various market frameworks and prices, technical and social settings, consistently leading to reduced energy costs and new revenue generation. The case study only showed the benefits of using a fleet of 4 EVs, but the tool can easily scale to larger fleets as the approach iteratively solves a deterministic optimization with tightened constraints and the resolution of a deterministic optimization generally requires only a few seconds, specifically less than 60s in this work using a standard machine with 12 CPU cores and 64 GB RAM. A constant charging power per hour was assumed for both the EVs and onsite battery. However, in practice, the charging power is higher initially and gradually decreases as the battery approaches the maximum SoC. In all our studies, a zero sell price for energy was assumed. Making energy arbitrage profitable could further increase the net revenues, albeit with higher battery cycling. Similarly, the aggregator's net revenues could be significantly enhanced if the flexibility provision in the form of utilization is remunerated. Finally, the study overlooked the temporal-spatial analysis of flexibility provision, focusing on availability remunerations while disregarding the potential risk of insufficient flexible capacity for future time slots. Nonetheless, diversifying the assets in the bidding pool and implementing a risk management strategy could help mitigate this risk.

E. Conclusion

The electrification of urban mobility can support grid decarbonization through the provision of demand-side flexibility. However, there is a need for novel operational tools for EV aggregators to facilitate such provision while reducing their energy costs. This paper proposes leveraging data-driven techniques and physics models in a novel tool for optimal V2X operation of EV fleets with a PV-battery charging station. The tool is designed to minimize aggregator's energy costs and maximize new revenues from the provision of flexibility, by providing risk-aware flexibility quantification, market bids, and real-time control decisions. Using a case study on the NEST and move demonstrators at Empa, in Switzerland, we showed that the revenues stemming from the provision of flexibility in the

form of availability significantly exceeded the energy costs of the charging station, even when the market bids were accepted in real-time operation with no revenues from utilization as a service. Results also showed that V2G technology and a more interactive involvement of EV users in the provision schemes can significantly enhance the overall cost-benefits. This highlights the need for implementing new incentives for the installation of V2G chargers and reshaping the regulatory framework to incentivize active participation of EV users, either by staying within the boundaries of their comfort or by appropriately compensating for their discomfort. Future work will focus on sector coupling by equipping the charging station with both electrical and thermal resources, enabling a more comprehensive cost-benefit and feasibility analysis of V2X operations for demand-side flexibility provision.

References

- [1] International Energy Agency, "Global EV Outlook 2021," Tech. Rep., 2021. [Online].
- [2] D. Božič and M. Pantoš, "Impact of electric-drive vehicles on power system reliability," *Energy*, vol. 83, pp. 511–520, 2015.
- [3] C. Loschan, D. Schwabeneder, G. Lettner, and H. Auer, "Flexibility potential of aggregated electric vehicle fleets to reduce transmission congestions and redispatch needs: A case study in Austria," *International Journal of Electrical Power & Energy Systems*, vol. 146, p. 108802, 2023.
- [4] G. Strbac, D. Pudjianto, M. Aunedi, P. Djapic, F. Teng, X. Zhang, H. Ameli, R. Moreira, and N. Brandon, "Role and value of flexibility in facilitating cost-effective energy system decarbonisation," *Progress in Energy*, vol. 2, no. 4, p. 042001, 2020.
- [5] V. Rasouli, Á. Gomes, and C. H. Antunes, "Characterization of aggregated demand-side flexibility of small consumers," in *2020 International Conference on Smart Energy Systems and Technologies (SEST)*. IEEE, 2020, pp. 1–6.
- [6] S. M. Ahsan, H. A. Khan *et al.*, "Optimized power dispatch for smart building (s) and electric vehicles with V2X operation," *Energy Reports*, vol. 8, pp. 10849–10867, 2022.
- [7] M. S. Islam, N. Mithulananthan, and K. Y. Lee, "Suitability of PV and battery storage in EV charging at business premises," *IEEE Transactions on Power Systems*, vol. 33, no. 4, pp. 4382–4396, 2017.
- [8] S. S. Ravi and M. Aziz, "Utilization of electric vehicles for vehicle-to-grid services: Progress and perspectives," *Energies*, vol. 15, no. 2, p. 589, 2022.
- [9] D. Dallinger, S. Gerda, and M. Wietschel, "Integration of intermittent renewable power supply using grid-connected vehicles—A 2030 case study for California and Germany," *Applied Energy*, vol. 104, pp. 666–682, 2013.
- [10] D. B. Richardson, "Electric vehicles and the electric grid: A review of modeling approaches, impacts, and renewable energy integration," *Renewable and Sustainable Energy Reviews*, vol. 19, pp. 247–254, 2013.
- [11] F. Gonzalez Venegas, M. Petit, and Y. Perez, "Participation of electric vehicle fleets in local flexibility tenders: Analyzing barriers to entry and workable solutions," *Robert Schuman Centre for Advanced Studies Research Paper No. RSCAS*, vol. 12, 2021.
- [12] G. Reynders, R. A. Lopes, A. Marszal-Pomianowska, D. Aelenei, J. Martins, and D. Saelens, "Energy flexible buildings: An evaluation of definitions and quantification methodologies applied to thermal storage," *Energy and Buildings*, vol. 166, pp. 372–390, 2018.
- [13] A. Amadeh, Z. E. Lee, and K. M. Zhang, "Quantifying demand flexibility of building energy systems under uncertainty," *Energy*, vol. 246, p. 123291, 2022.
- [14] A. Kathirgamanathan, T. Péan, K. Zhang, M. De Rosa, J. Salom, M. Kummert, and D. P. Finn, "Towards standardising market-independent indicators for quantifying energy flexibility in buildings," *Energy and Buildings*, vol. 220, p. 110027, 2020.
- [15] R. De Coninck and L. Helsen, "Quantification of flexibility in buildings by cost curves—Methodology and application," *Applied Energy*, vol. 162, pp. 653–665, 2016.
- [16] F. Oldewurtel, D. Sturzenegger, G. Andersson, M. Morari, and R. S. Smith, "Towards a standardized building assessment for demand response," in *52nd IEEE Conference on Decision and Control*. IEEE, 2013, pp. 7083–7088.
- [17] P. Dossow and T. Kern, "Profitability of v2x under uncertainty: Relevant influencing factors and implications for future business models," *Energy Reports*, vol. 8, pp. 449–455, 2022.
- [18] U. Langenmayr, W. Wang, and P. Jochem, "Unit commitment of photovoltaic-battery systems: An advanced approach considering uncertainties from load, electric vehicles, and photovoltaic," *Applied Energy*, vol. 280, p. 115972, 2020.
- [19] Y. Zheng, H. Yu, Z. Shao, and L. Jian, "Day-ahead bidding strategy for electric vehicle aggregator enabling multiple agent modes in uncertain electricity markets," *Applied Energy*, vol. 280, p. 115977, 2020.
- [20] H. C. Güldorum, I. Şengör, and O. Erdinc, "Management strategy for V2X equipped EV parking lot considering uncertainties with LSTM Model," *Electric Power Systems Research*, vol. 212, p. 108248, 2022.
- [21] D. Thomas, O. Deblecker, and C. S. Ioakimidis, "Optimal operation of an energy management system for a grid-connected smart building considering photovoltaics' uncertainty and stochastic electric vehicles' driving schedule," *Applied Energy*, vol. 210, pp. 1188–1206, 2018.
- [22] F. Bellizio, B. Dijkstra, A. Fertig, J. V. Dijk, and P. Heer, "Machine Learning Approaches for the Prediction of Public EV Charge Point Flexibility," *International Journal of Electrical Power & Energy Systems*, 2024, in review. [Online].
- [23] P. Richner, P. Heer, R. Largo, E. Marchesi, and M. Zimmermann, "NEST—una plataforma para acelerar la innovación en edificios," *Informes de la Construcción*, vol. 69, no. 548, pp. e222–e222, 2017.
- [24] J. Villar, R. Bessa, and M. Matos, "Flexibility products and markets: Literature review," *Electric Power Systems Research*, vol. 154, pp. 329–340, 2018.
- [25] T. Schittekatte and L. Meeus, "Flexibility markets: Q&A with project pioneers," *Utilities policy*, vol. 63, p. 101017, 2020.

- [26] J. Gasser, H. Cai, S. Karagiannopoulos, P. Heer, and G. Hug, "Predictive energy management of residential buildings while self-reporting flexibility envelope," *Applied Energy*, vol. 288, p. 116653, 2021.
- [27] H. Cai and P. Heer, "Experimental implementation of a context-aware prosumer," in *Journal of Physics: Conference Series*, vol. 2042, no. 1. IOP Publishing, 2021, p. 012068.
- [28] A. Blatiak, F. Bellizio, L. Badesa, and G. Strbac, "Value of optimal trip and charging scheduling of commercial electric vehicle fleets with vehicle-to-grid in future low inertia systems," *Sustainable Energy, Grids and Networks*, vol. 31, p. 100738, 2022.
- [29] J. D. Bishop, C. J. Axon, D. Bonilla, M. Tran, D. Banister, and M. D. McCulloch, "Evaluating the impact of V2G services on the degradation of batteries in PHEV and EV," *Applied energy*, vol. 111, pp. 206–218, 2013.
- [30] M. Aunedi and G. Strbac, "Whole-system Benefits of Vehicle-to-Grid Services from Electric Vehicle Fleets," in *2020 Fifteenth International Conference on Ecological Vehicles and Renewable Energies (EVER)*. IEEE, 2020, pp. 1–9.
- [31] S. Karagiannopoulos, L. Roald, P. Aristidou, and G. Hug, "Operational Planning of Active Distribution Grids under Uncertainty," in *IREP 2017, X Bulk Power Systems Dynamics and Control Symposium*, 2017.
- [32] L. Badesa, G. Strbac, M. Magill, and B. Stojkovska, "Ancillary services in Great Britain during the COVID-19 lockdown: A glimpse of the carbon-free future," *Applied Energy*, vol. 285, p. 116500, 2021.
- [33] National Grid ESO, "Markets Roadmap to 2025," Tech. Rep., 2021. [Online].
- [34] GOPACS, "Product Conditions," Tech. Rep. [Online].

G0312

Relief of the power grid through cost-effective hydrogen generation

Gabriele Humbert^{*}, Hanmin Cai, Binod Prasad Koirala, Philipp Heer

Urban Energy System Laboratory, Empa,
Ueberlandstrasse 129, 8600 Dübendorf/CH;
gabriele.humbert@empa.ch

Abstract

Hydrogen generation sites convert electricity from renewable energy sources (RES) or the grid to satisfy targeted hydrogen production. The design and operation of hydrogen generation sites are conventionally treated as two separate silos. However, due to the intermittent and seasonal behaviour of renewable energy sources, the system design needs to facilitate cost-effective and flexible operation.

This work targets the optimal design of a hydrogen generation site producing 100 kg_{H2}/day. In contrast to the vast majority of the literature, dynamic boundary conditions with a 1-hour resolution are adopted to accurately account for the specificity of the considered case studies. A PEM electrolyzer powered by both a PV-battery couple and the grid is accounted for, and the deployment of the heat generated from the hydrogen conversion is considered. Different objective functions are associated with both the cost of the generated hydrogen and the flexibility services provided to the grid. The key aim is to understand how the optimal design of the system varies depending on the targeted objective.

The results demonstrate significant variations in optimal sizes and performance metrics based on different optimization objectives. For cost minimization, the solution excludes battery components and maximizes PV usage, resulting in a value-adjusted levelized cost of hydrogen of 10.9 CHF/kg. Conversely, flexibility-focused optimizations favour larger electrolyzers and significant battery capacity. Multi-objective optimization targeting both cost and peak power minimization provides instead a balanced solution, significantly reducing the peak power metric by 40.5% compared to the cost minimization problem, while achieving lower costs than the peak power minimization problem.

Ultimately, this work highlights the critical interplay between design and operational aspects in hydrogen generation sites. It offers practical design guidelines for the optimal design and operation of hydrogen generation sites to both researcher and practitioner, as well as contributes to methodological advancements in optimizing such energy systems.

Introduction

In the context of energy systems, flexibility refers to the ability to adjust generation and consumption patterns in response to variability and uncertainty in demand and supply [1]. This capability is essential for maintaining grid stability, especially with the growing penetration of intermittent renewable energy sources (RES). In this regard, hydrogen is envisioned to play a critical role in future energy systems due to its ability to store energy and potential to decarbonize sectors considered hard to abate [2]. Hydrogen generation can significantly contribute to grid stability by absorbing excess electricity during periods of high RES availability and producing energy during low production periods, thereby balancing supply and demand. Traditionally, hydrogen generation sites the design and operation of hydrogen generation sites are treated as separate silos, with little consideration for their mutual influence. Conventional approaches often rely on approximated boundary conditions which fail to capture the variability of RES and grid conditions [3,4].

This work builds upon one of our previous study [5] and adopts a numerical tool targeting the simultaneous optimization of sizing and operation, namely a single-layer approach [6,7], of a hydrogen generation site. Unlike traditional methodologies, this study employs dynamic boundary conditions with a 1-hour resolution, accurately reflecting the intermittent nature of renewable energy sources. The system under consideration includes a PEM electrolyzer powered by both a PV-battery couple and the grid, incorporating the utilization of heat generated from hydrogen conversion. Further, by considering multiple objectives, such as the cost of generated hydrogen and the flexibility services provided to the grid, this work aims to understand how the optimal design varies depending on the targeted objectives.

1. Requirements for Grid Services - Technical & Market Conditions

This work adopts a mixed integer linear programming (MILP) model to concurrently optimize the sizing and operation of a hydrogen generation site. The full description of the adopted model is reported in [5]. The specific hydrogen generation site under consideration is depicted in Figure 1. A Proton Exchange Membrane (PEM) electrolyzer was considered, with size S_e , which was sourced by a PV-battery couple and by the grid. The size of the PV field, S_{PV} , indicates the peak of produced power, while the battery storage capacity is indicated with the symbol K_b . Waste heat recovery (WHR) solutions were also considered, with the recovered heat injected in a district heating networks (DHN) at 65 °C. Such temperature level was selected in agreement with the Empa campus in Dubendorf, Switzerland [8], and it is suitable for domestic hot water supply. It is worth nothing that, to inject heat into the high-temperature DHN, a heat pump is required, with the heat pump size referred to as S_{HP} .

The adopted optimization approach targets the objective functions described in section 2.1. It is important to note that, while Figure 1 depicts all the possible technology candidates considered in the work, the developed optimization model is allowed to select null size for each of these technologies. That is, the optimal design might not encompass all the components depicted in Figure 1, but rather a subset of these. The specific technical conditions for the considered energy systems are included in the constraints implemented. Specifically, the energy and mass balances need to be satisfied at each time step, t . Further, exclusivity constraints were imposed for the imported and exported electrical energy from the grid, as well as for the charging and discharging operation of the battery. A piecewise-affine (PWA) approximations for cost terms and for the PEM electrolyzer conversion efficiency was implemented. Finally, penalization terms were also

added to discourage on/off operation of the electrolyzer and to, therefore, ensure a long component's lifespan [9,10].

Concerning the considered market conditions, day-ahead prices for the electricity were considered for the electricity imports [11], while the export costs were calculated as per the import plus an additional cost for distribution and transmission costs. The revenues for exporting heat were calculated as a fraction of the electricity cost, in agreement to [12].

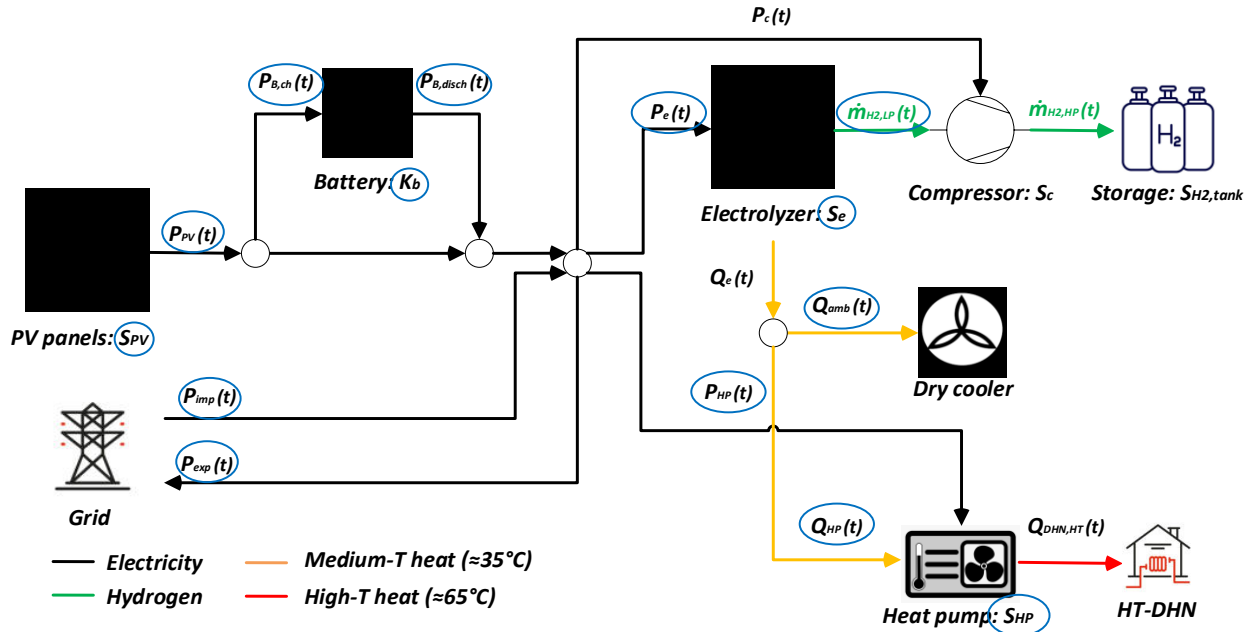


Figure 1 Schematic of the hydrogen generation site under investigation. The decision variables of the optimization problem are circled in blu.

1.1 Adopted input parameters

The adopted model requires techno-economic parameters to characterize the considered technology asset. Such techno-economic parameters consider the technology efficiency, unit price, lifetime, and maintenance cost [9,13]. Additionally, boundary conditions with a one-hour resolution and one-year horizon were imposed. Such boundary conditions refer to the considered heat price [12], an hydrogen demand of 100 kg/day [3], the solar irradiance [14], the ambient temperature, and the electricity cost [11]. No heat demand was considered, as the DHN is assumed to accept all the heat recovered from the site. As a case study, the year 2022 was considered and the site was assumed to be located in Dubendorf, Switzerland. Figure 2 reports the boundary conditions used for the analysis.

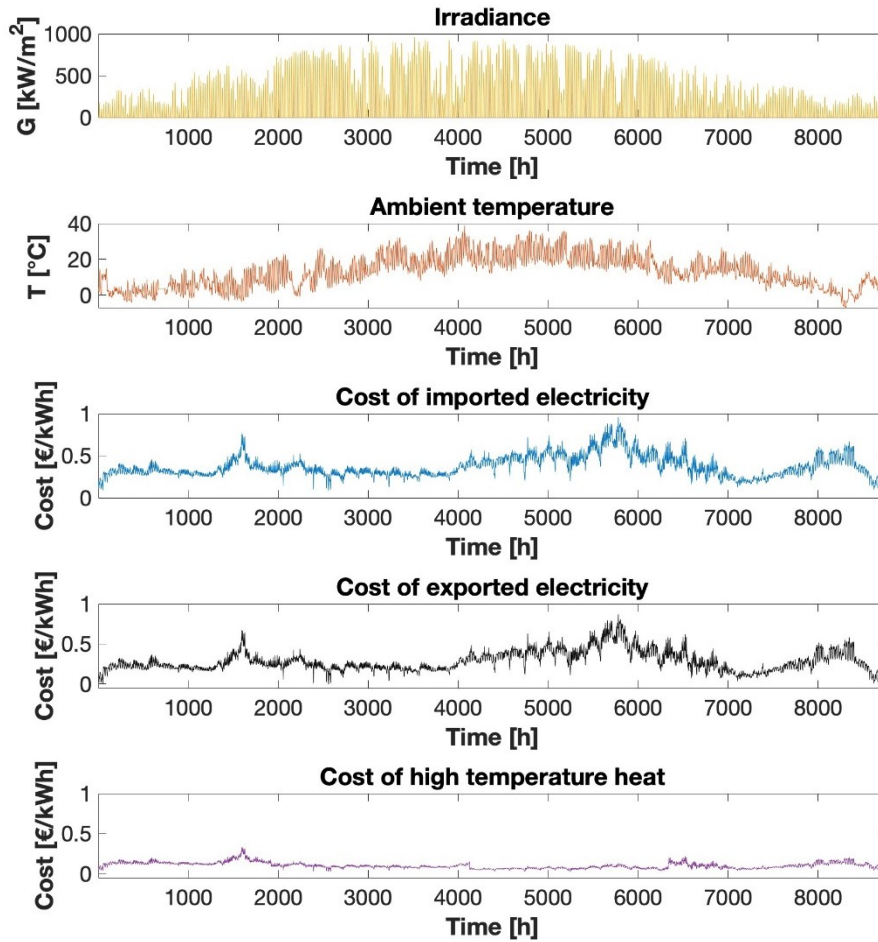


Figure 2 Boundary conditions for the considered case study in Dubendorf, Switzerland, and year 2022.

2. Approach towards Flexibility

The optimization approach presented in section 1 was adopted to explore the impact of objective functions linked to hydrogen production cost and flexibility services on the optimal design. Conventionally, hydrogen generation sites are designed to minimize the value-adjusted levelised cost of hydrogen [3,15], VALCOH, defined as:

$$VALCOH = \frac{cost_{tot}}{m_{H2,year}} = \frac{cost_{inst,a} + cost_{op,year} + cost_{maint,a} + rev_{year}}{m_{H2,year}} \quad (1)$$

Where $cost_{inst,a}$ is the annualized investment cost linked to all the technologies selected by the optimizer, $cost_{op}$ is the operational cost linked to the purchased electricity over the year, $cost_{maint,a}$ is the annualized maintenance cost calculated as a percentage of the investment costs for each technology, while the term rev_{year} indicates the sum of the revenues over the year from the export of electricity and heat.

2.1. Flexibility metrics

This work considers three flexibility metrics among the most adopted ones in the literature [16], namely peak power, self-sufficiency, and flexibility factor. The definition of these metrics is provided in Table 1.

TABLE I. **Definition and description of the flexibility metrics considered in this work.**

<i>Flexibility metric</i>	<i>Definition</i>	<i>Description</i>
<u><i>Peak Power</i></u>	$PP = \max (P_{imp}(t))$	Peak power during the considered period of time (one year)
<u><i>Self-sufficiency</i></u>	$SS = 1 - \sum_{t=1}^{8760} \frac{P_{imp}(t)}{P_e(t) + P_c(t) + P_{HP}(t)}$	Indicator for the imported energy during high load hours versus during low load hours. The FF ranges between – 1 (energy imported only during high load hours) and 1 (energy imported only during low load hours).
<u><i>Flexibility Factor</i></u>	$FF = \frac{P_{imp,low\ load}(t) - P_{imp,high\ load}(t)}{P_{imp,low\ load}(t) + P_{imp,high\ load}(t)}$	Degree to which the on-site generation is sufficient to satisfy the energy needs of the site.

The low and high load times adopted in the definition of the flexibility factor were selected in agreement with typical energy tariffs from Swiss DSOs [17]: low load from 21.00 to 7.00, high load otherwise.

2.2. Objective functions

In agreement with the metrics introduced in Table I, four different objective functions were implemented:

- *Cost minimization: $\min (cost_{tot} + cost_{pen})$*
The minimization of the total costs associated with investment, operation and maintenance is targeted. Additionally, a penalization term was considered, in agreement with [9], to penalize undesirable operations of the electrolyzers.
- *Peak power minimization: $\min (P_{imp,max})$*
An additional scalar design variable, $P_{imp,max}$, was defined within the optimization problem which constraints the maximum value of the imported power over the year, $P_{imp}(t) \leq P_{imp,max}$.
- *Self-sufficiency maximization: $\min (\sum_{k=1}^{8760} P_{imp}(t))$*
Accounting for the self-sufficiency definition provided in Table 1 within the optimization problem would result in nonlinearities. Therefore, the implemented optimization problem only targets the minimization of the imported electricity from the grid to maximize the site's self-sufficiency. Please note that the proposed implementation does not consider the reduction of the site energy consumption as viable way to increase the SS metric.
- *Flexibility Factor minimization: $\min \sum_{k=1}^{8760} (P_{imp, lowhour}(t) - P_{imp, highhour}(t))$*
Directly considering the FF within the objective function of the optimization problem would cause nonlinearities. Therefore, only the numerator of the FF expression is

minimized. Nonetheless, the identified optimal solution is the same as for the minimization of the FF term.

3. Key Results and Conclusion

Table II summarizes the key results for the single-objective optimization problems. The single objective optimization results reveal significant variations in optimal sizes and performance metrics depending on the targeted objective. For the cost minimization approach, battery solutions were excluded due to their high investment costs. Instead, the PV field size was maximized at 1500 kW, and a relatively large electrolyzer size of 397.1 kW was selected. This configuration allowed efficient use of daytime PV electricity and low-cost electricity imports.

In the peak power minimization scenario, the sizes of the PV field, battery, and electrolyzer were all maximized. This allows to reduce peak power by better exploiting the locally produced energy from PV and thus minimizing the amount of electricity required from the grid. Similarly, the self-sufficiency maximization scenario also selected maximum sizes for all key components. However, different operational strategies led to higher self-sufficiency (0.7) but also higher peak power (521.0 kW).

Finally, concerning the flexibility factor minimization problem, the optimal configuration included a 24 MWh battery and a 500 kW electrolyzer, but no PV field. This resulted in large imports during the night and low imports during the day to achieve the desired daily hydrogen production.

TABLE II. **Key results of the single-objective optimization.**

		Sizes				Metrics			
		C_b	S_e	S_{PV}	S_{HP}	VALCOH	PP	SS	FF
		[MWh]	[kW]	[kW]	[kW _e]	[CHF/kg]	[kW]	[-]	[-]
Objective function	VALCOH	0.0	397.1	1500.0 (max)	12.2	10.9	426.0	0.5	0.4
	PP	24.0 (max)	500.0 (max)	1500.0 (max)	21.2 (max)	63.6	212.5	0.5	-0.1
	SS	24.0 (max)	500.0 (max)	1500.0 (max)	21.2 (max)	62.5	521.0	0.7	0.0
	FF	0.0	500.0 (max)	0.0	21.2 (max)	28.3	537.0	0.0	-1.0

The optimal operational trends are depicted in Figure 2 for a selected week in February. For the cost minimization problem, Figure 2 (a), electricity from the grid is only imported at night to exploit lower purchasing costs. During this period, the electrolyzer remains continuously operational to avoid penalization costs included in the objective function. In the peak power minimization scenario, Figure 2 (b), the amount of imported electricity is significantly reduced. The electrolyzer exhibits an on/off behavior, as no penalization costs were considered for this type of operation. This on/off operation is also affected by the minimum workload imposed (20%).

The operational trends for the self-sufficiency maximization problem, Figure 2(c), are similar to those for cost minimization. However, no electricity exports occur, and due to the larger size of the electrolyzer, more PV power is directly used to generate hydrogen during the day to meet the demand. Lastly, for the flexibility factor minimization problem, Figure 2(d), a straightforward trend is observed. Electricity is imported during the night (low load

periods), while no imports occur during the day. To meet the hydrogen demand, battery storage is utilized to extend the operational hours of the electrolyzer.

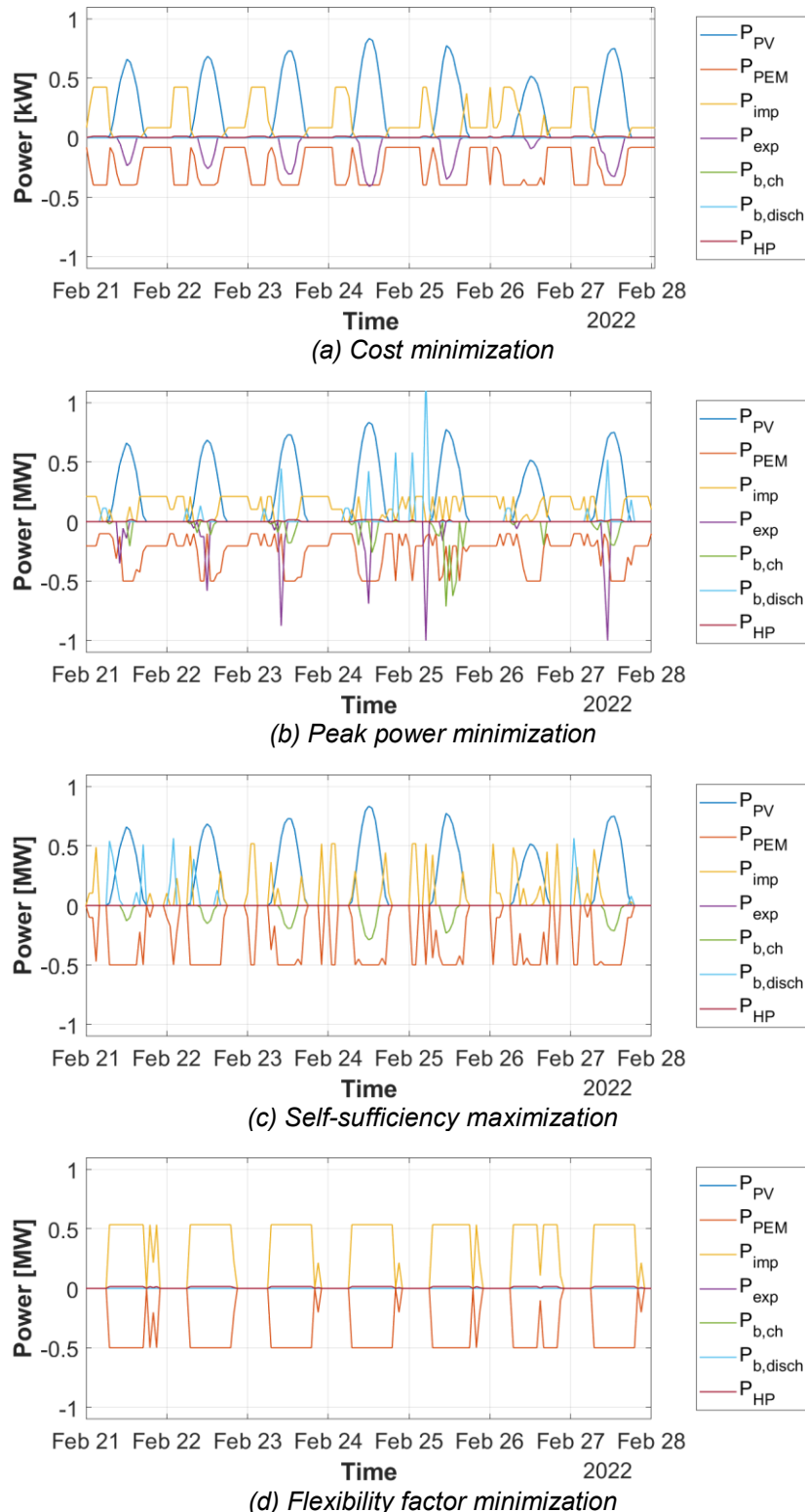


Figure 3 Operational behaviours for a selected week in February for the four optimization problems under consideration.

3.2. Multi-objective optimization

A multi-objective optimization approach was tested, considering both cost and peak power minimization problems with a 0.5 weight coefficient. The resulting metrics are depicted in Figure 4. A sharp decrease in both VALCOH and PP metrics is observed compared to the single-objective optimization problems. Compared to the pure peak power minimization problem, the multi-objective optimization results in a VALCOH reduction of up to 81.4%. Similarly, the PP metric is reduced by 40.5% when compared to the cost minimization problem.

Regarding the selected technology sizes, a relatively large electrolyzer size of 357.2 kW is chosen, which is similar to the one selected for the cost minimization approach. Additionally, no battery component is selected, while the PV field size is maximized within the considered solution space. Overall, the selected sizes resemble those for the cost minimization approach. However, the peak power metric is significantly reduced by adopting operation strategies that target a smoother import of electricity throughout the year.

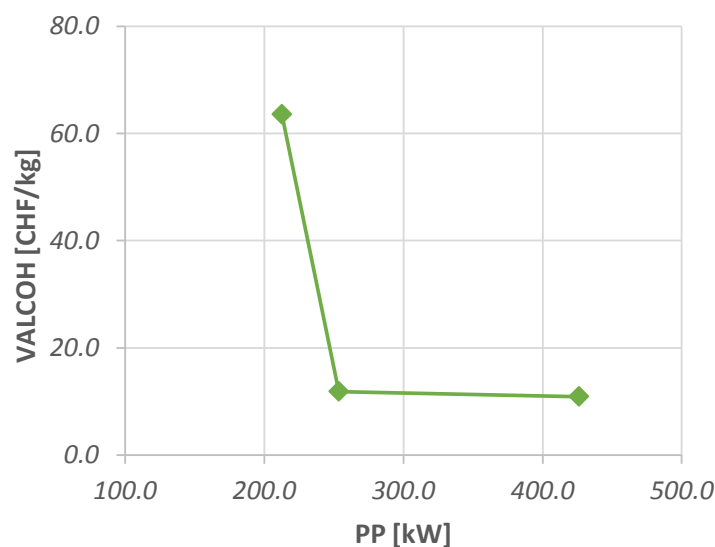


Figure 4 Pareto front for the value-adjusted levelised cost of hydrogen and the peak power.

3.2. Conclusion

Automation will change the way we operate systems and consequently also the way we design them. This study proposes a MILP optimization approach to concurrently optimize sizing and operation of a hydrogen generation site. Furthermore, given the increasing need for enhanced flexibility from energy systems, various optimization targets were considered. Together with the conventional cost minimization approach, flexibility-focused optimizations were studied. The key findings from the study are summarized as follows:

- **Concurrent optimization of sizing and operation:** the MILP optimization approach adopted in this work is proved beneficial to capture the specificity of a design case and is proved to embed flexibility metrics from the literature within the optimization framework. Overall, in the spirit of increase energy system automation, the adoption of design tools that considers the mutual influence of design and operational aspects is key;

- *Design differences by objective*: Designs targeting optimal flexibility differ significantly from the most cost-effective ones. For cost minimization, batteries are not selected, whereas for enhanced flexibility, batteries are always included. Higher flexibility is achieved with larger electrolyzer sizes. Local electricity production from renewable energy sources (RES) is always advantageous, except in designs targeting the maximal flexibility factor, where large imports during the night are beneficial;
- *Multi-Objective Optimization*: A multi-objective optimization approach, targeting both cost and peak power minimization, provides a balanced solution by significantly reducing the peak power metric compared to the cost minimization problem, and achieving lower costs compared to the peak power minimization problem. Although the cost is higher than the single-objective cost minimization, this approach effectively balances and reduces both metrics, resulting in a more robust overall design.

These conclusions highlight the impact of considering multiple objectives on the optimal design of hydrogen generation sites and the role of advanced optimization tools in developing effective and efficient energy systems. By understanding and leveraging these trade-offs, it is possible to design systems that better meet the diverse needs of modern energy grids.

References

- [1] Reynders G, Amaral Lopes R, Marszal-Pomianowska A, Aelenei D, Martins J, Saelens D. Energy flexible buildings: An evaluation of definitions and quantification methodologies applied to thermal storage. *Energy Build* 2018;166:372–90. <https://doi.org/10.1016/j.enbuild.2018.02.040>.
- [2] Vilbergsson K V., Dillman K, Emami N, Ásbjörnsson EJ, Heinonen J, Finger DC. Can remote green hydrogen production play a key role in decarbonizing Europe in the future? A cradle-to-gate LCA of hydrogen production in Austria, Belgium, and Iceland. *Int J Hydrogen Energy* 2023;48:17711–28. <https://doi.org/10.1016/J.IJHYDENE.2023.01.081>.
- [3] Minutillo M, Perna A, Forcina A, Di Micco S, Jannelli E. Analyzing the levelized cost of hydrogen in refueling stations with on-site hydrogen production via water electrolysis in the Italian scenario. *Int J Hydrogen Energy* 2021;46:13667–77. <https://doi.org/10.1016/j.ijhydene.2020.11.110>.
- [4] Perna A, Jannelli E, Di Micco S, Romano F, Minutillo M. Designing, sizing and economic feasibility of a green hydrogen supply chain for maritime transportation. *Energy Convers Manag* 2023;278:116702. <https://doi.org/10.1016/j.enconman.2023.116702>.
- [5] Vandenberghe R, Humbert G, Cai H, Prasad B. Optimal sizing and operation of hydrogen generation sites accounting for waste heat recovery. *Submitt to Appl Energy* 2024:1–39.
- [6] Marocco P, Ferrero D, Martelli E, Santarelli M, Lanzini A. An MILP approach for the optimal design of renewable battery-hydrogen energy systems for off-grid insular communities. *Energy Convers Manag* 2021;245:114564. <https://doi.org/10.1016/j.enconman.2021.114564>.
- [7] Gabrielli P, Gazzani M, Martelli E, Mazzotti M. Optimal design of multi-energy systems with seasonal storage. *Appl Energy* 2018;219:408–24. <https://doi.org/10.1016/j.apenergy.2017.07.142>.
- [8] Empa - NEST - Homepage n.d. <https://www.empa.ch/web/nest/> (accessed June 28, 2023).

- [9] Ibáñez-Rioja A, Puranen P, Järvinen L, Kosonen A, Ruuskanen V, Ahola J, et al. Simulation methodology for an off-grid solar–battery–water electrolyzer plant: Simultaneous optimization of component capacities and system control. *Appl Energy* 2022;307:118157. <https://doi.org/10.1016/j.apenergy.2021.118157>.
- [10] Norazahar N, Khan F, Rahmani N, Ahmad A. Degradation modelling and reliability analysis of PEM electrolyzer. *Int J Hydrogen Energy* 2024;50:842–56. <https://doi.org/10.1016/J.IJHYDENE.2023.07.153>.
- [11] ENTSOE. EU electricity market n.d. <https://www.entsoe.eu/> (accessed May 1, 2023).
- [12] Baldini L. Dynamic energy weighting factors to promote the integration of renewables into buildings. *Sustain Built Environ Reg Conf Zurich 2016* 2016:234–9. <https://doi.org/10.3218/3774-6>.
- [13] Gabrielli P, Flamm B, Eichler A, Gazzani M, Lygeros J, Mazzotti M. Modeling for optimal operation of PEM fuel cells and electrolyzers. *EEEIC 2016 - Int Conf Environ Electr Eng 2016*. <https://doi.org/10.1109/EEEIC.2016.7555707>.
- [14] Richner P, Heer P, Largo R, Marchesi E, Zimmermann M. NEST - A platform for the acceleration of innovation in buildings. *Inf La Constr* 2017;69:1–8. <https://doi.org/10.3989/id.55380>.
- [15] Perna A, Minutillo M, Di Micco S, Jannelli E. Design and Costs Analysis of Hydrogen Refuelling Stations Based on Different Hydrogen Sources and Plant Configurations. *Energies* 2022;15. <https://doi.org/10.3390/en15020541>.
- [16] Li H, Wang Z, Hong T, Piette MA. Energy flexibility of residential buildings: A systematic review of characterization and quantification methods and applications. *Adv Appl Energy* 2021;3:100054. <https://doi.org/10.1016/j.adapen.2021.100054>.
- [17] BKW: Wir machen Lebensräume lebenswert. n.d. <https://www.bkw.ch/de> (accessed May 30, 2024).

G04

Enabling Technologies I

G0401

Intraday solar irradiance forecasting using public cameras

**Roy Sarkis (1), Ilker Oguz (1), Demetri Psaltis (1), Mario Paolone (1),
Christophe Moser (1), Luisa Lambertini (1,2)**

(1) EPFL, Lausanne/Switzerland

(2) Universita' della Svizzera Italiana (USI), Ticino/Switzerland;

roy.sarkis@epfl.ch

Abstract

With the significant increase in photovoltaic (PV) electricity generation, more attention has been given to PV power forecasting. Indeed, accurate forecasting allows power grid operators to better schedule and dispatch their assets, such as energy storage systems and reserve. In this paper, we propose a hybrid deep learning model and a convolutional neural network with memory, to provide intraday (2 hours) solar irradiance forecasts using sequentially-collected images from public webcams. The images are collected from two webcams available on EPFL's campus and capture a 360° view of the surroundings (sky and ground). The proposed neural network is trained on a year worth of data.

The performance of the proposed model is compared to those of a standard time-series forecast models, a linear regression as well as state-of-the-art neural networks trained on the same data set. We find that the proposed methodology outperforms all other models and matches the state-of-the-art methodology implemented by a global solar irradiance data modelling company while providing simplicity of implementation and efficient computation. We attribute this result to the information content present in the side view images of the sky and clouds unlike the top view of a satellite image. We expect that by adding more webcams and by combining information from satellite and weather models, we will further increase the solar irradiance prediction accuracy. This is attributed to our results showing that the use of two webcams instead of one decreases our root mean squared error.

The proposed methodology is very simple, computationally inexpensive and proves to perform very well to provide GHI forecasts for PV generation prediction. Improving GHI forecasting at the local level can be aggregated up to a regional or even national level and can help predict a country's imbalances in the transmission grid leading to optimal use of energy sources. With better intraday predictions, the dispatch plan (set a day in advance) could be followed more accurately and hence avoid imbalances that incur penalties and require use of non-renewable sources.

1. Introduction

In the last decade, the global usage of photovoltaics (PV) was the fastest developing renewable energy source with more than 1000 gigawatts of additional generation capacity installed [1]. This growth is mainly attributed to the decreasing costs of installations and smaller carbon footprint. However, the ongoing shift from traditional power sources in favor of renewables, like PV, requires the availability of an adequate and reliable capacity of regulating power. This challenge is addressed by achieving controllability over all the distribution networks so as not to deviate from their dispatch. This objective is achieved through the integration of decentralized generation and energy storage systems. This is evident in various frameworks including virtual power plants¹, active distribution networks² (ADNs) and grid-tied microgrids³ which aim to provide local energy balance and ancillary services to the upper grid layer by using diverse resources [2]. Storage systems in ADNs have been used to offset the effect of stochastic and uncontrollable resources. This concept refers to the capability of the ADN to track a day-ahead power schedule, henceforth called *dispatch plan*. The optimal computation of the day-ahead dispatch plan and its intraday tracking, rely on the availability of PV forecasting tools along with the exploitation of energy storage systems operating at different time horizons [3].

As a matter of fact, the enhancement of ADN dispatch relies on the availability of high-performance forecasting tools of both electricity consumption and local power generation at both day-ahead and intraday time horizons along with storage systems of different energy reservoirs sizes and power regulation capabilities.

As known, the solar irradiance is quantified using the global horizontal irradiance (GHI) which represents the total solar radiation (including both the direct and diffuse radiation) incident on a horizontal surface. GHI is affected by many factors such as the time of the year, time of the day, weather, and, most importantly, cloud coverage.

GHI forecasting can be achieved using different techniques. The choice of the optimal method depends on the forecast horizon as well as the geographical scale [4]. These techniques are statistical methods, numerical weather predictions, sky images and satellite images. The use of sky cameras has shown to be a promising method for intrahour GHI forecasting [5, 6]. With the developments in deep learning, current machine learning (ML) models are able to extract information from such images and establish dependencies within sequential data. We propose a new hybrid deep learning model, composed by a convolutional neural network combined with long short-term memory (CNN-LSTM) layers, for intraday GHI forecasting. This paper mainly focuses on the 2-hour time horizon. However, different time horizons are also tested; 10, 20, 30, 60 and 180 minutes. This focus on intraday forecasting horizons is of interest for management of ADNs and microgrid energy storage systems and intraday electricity market trades.

A key innovative element of this paper is the use of images from publicly available webcams as well as combining images from different locations. Webcams typically present a side view of the sky, which brings cloud height information not present in all sky cameras

¹ A set of grid-tied controllable or partially-controllable energy conversion devices (e.g., solar panels, batteries and electric vehicles) that collectively provide ancillary services to the local and/or the bulk power grid.

² ADNs are distribution networks that have systems in place to control a combination of generators, loads and energy storage (collectively termed as distributed energy resources – DERs).

³ A localized electricity network that can operate independently while still being connected to the main power grid, enabling it to generate, store, and distribute electricity as needed.

and satellite images. The neural network is trained on a dataset of public webcam images collected on EPFL campus and surrounding areas. Figure 1 shows two sample images taken at the same time from the webcams located on EPFL's campus. The two annotations, the green arrow and the blue rectangle, show the locations of two buildings on campus, building TCV and Rolex Learning Center. Figure 2 shows the location and the field of view (not limited by the red circle in terms of distance) of both cameras on EPFL's campus. The webcams used in this work are Roundshot's "livecam gen 3" webcams. The coordinates of camera "livecam EPFL BC" are 46.518391°N, 6.561931°E and those for camera "EPFL Place Maurice Cosandey" are 46.51776°N, 6.56662°E.



Fig. 1: Sample images from the webcams on the EPFL campus.



Fig. 2: Cameras' locations on the EPFL campus.

Table 1 shows a quick comparison between the livecam gen 3 and a "Basler" USB 1.8 megapixel camera (acA1300-200uc). The livecam gen 3 cameras were only used since they are preinstalled on campus. Using data fusion ML methods, multiple camera feeds are combined to train a neural network. Figure 3 shows the proposed deep neural network (DNN) architecture, which is described in more details in section 4. The methodology presented in this paper is scalable beyond EPFL because of the ever-increasing coverage of weather webcams.

Table 1: Cameras' Comparison

	Webcam	All-sky camera
--	--------	----------------

Cost (\$)	7400 - 8000	550 - 630
Spatial Resolution (pixels)	10752 × 2048	1280 × 1024
Temporal Resolution	1 panorama every 10 minutes	1 image every 1 minute
Field of View	panoramas up to 360°	up to 180° × 180°

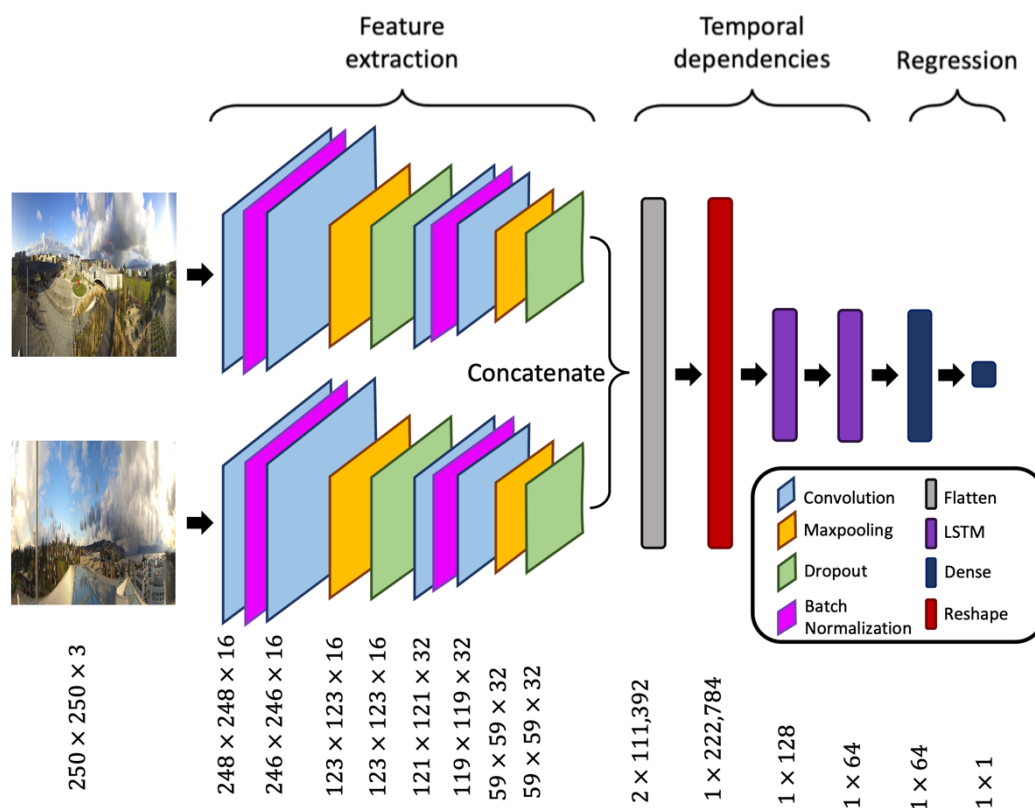


Fig. 3: Proposed CNN-LSTM network.

2. Data and methodology

This section presents the data collection process as well as the specifics related to the methodology of the CNN-LSTM network.

2.1 Data

The images used in this study are downloaded from Roundshot's [website](http://www.roundshot.com). They are 360° images with different resolutions. Two sample images are provided in Figure 1. Figure 2 shows the location of the two cameras on EPFL's campus. As previously mentioned, the main reason these cameras were used is due to the fact that they were preinstalled on campus. An alternative in case such cameras did not exist is to install outdoor 4K (3840 × 2160 pixels) security webcams that is a fraction of Roundshot's webcam price and provide images at a higher rate.

A python code downloads the images from the two different cameras from the public website, at a 10-minute frequency (as described on the webpage). All the timestamps of the downloaded images are used although some are missing for unknown reasons. Additionally, corrupted images were manually removed. Such images had distorted colors, i.e. very high contrast or very dark colors, or part of the image was missing. Only images taken between sunrise and sunset are used to make sure sunlight time is considered. As the images from both locations are different in width and height, they are scaled down

using the “Pillow” python image library before being used as input to the neural network. Finally, an Apogee SP-230 all-seasons pyranometer collects local GHI measurements which are re-sampled at a 10-minute frequency to match the images.

Once all the images are collected, cleaned and scaled, we cross-check the timestamps at which the images are collected to match that of the pyranometer’s measurements. The final dataset is then comprised of two images from two different cameras (collected at the same time “ t ”) and a corresponding GHI measurement (representing the GHI at “ $t + 2$ hours”). The data used in this study spans from end of December 2021 until the end of January 2023.

2.2 Methodology

The proposed CNN-LSTM network has two 3-dimensional input layers (as the images are RGB) followed by a time-distributed CNN block implemented to extract spatial features from each image separately. The CNN block is comprised of the following:

- A BatchNormalization layer between two Convolutional layers (Conv2D) with 16 filters and rectified linear (Relu) activation function
- A MaxPooling2D layer
- A Dropout layer with a dropout rate of 0.3
- A BatchNormalization layer between two Conv2D layers with 32 filters and Relu activation function
- A MaxPooling2D layer
- A Dropout layer with a dropout rate of 0.1.

The outputs of the CNN blocks are then concatenated together, flattened, reshaped and used as input to two consecutive LSTM layers. The two LSTM layers consist of 128 and 64 units respectively. Finally, a fully connected layers with 64 neurons is used leading to the output layer with a single neuron. The network is then trained with the scaled images and an early stopping criteria of 10 epochs is added. It should be noted that the ‘*restore best weight*’ parameter is set to ‘*True*’ to make sure to restore the model weights from the epoch with the lowest error. It is worth mentioning that the hyperparameter tuning of the network was done via a grid search using the *sklearn* library in python. This was performed on the number of filters in the CNN block, the number of neurons in the LSTM and Dense layers as well as the rate of the Dropout layer. The architecture of the network is presented in Figure 3.

2.3 Evaluation metrics

The performance of the deep neural network is assessed using the following metrics: RMSE, normalized RMSE (nRMSE) and per unit RMSE (puRMSE) defined as:

$$RMSE = \sqrt{\sum_{t=1}^N \frac{(\widehat{GHI}_t - GHI_t)^2}{N}}$$

$$puRMSE = \frac{RMSE}{GHI_{max}}$$

$$nRMSE = \frac{RMSE}{GHI_{mean}}$$

where N denotes the total number of testing timestamps, \widehat{GHI}_t denotes the predicted value of GHI, GHI_{max} and GHI_{mean} denote the maximum and average value of GHI, respectively.

We also compare the RMSE against the persistence model, in particular the smart persistence, which is treated as a benchmark. Both the simple and smart persistence models are commonly used benchmarks for irradiance forecasting. The simple persistence model is a very basic approach for predicting GHI. That assumes that the GHI will remain constant over time, i.e., $GHI_{t+n} = GHI_t$ where $n = 1, 2, \dots$ is an index to the next time measurement. Usually, such model is used as benchmark for short-term predictions (<30 minutes). In contrast, the smart persistence (SP) model improves on the simple version by assuming that the relative GHI remains constant over the forecasting horizon. This is presented as such:

$$SP_{t+n} = \frac{GHI_t}{GHI_{t,cs}} GHI_{t+n,cs}$$

where the subscript *cs* represents clear sky conditions. It should be noted that the different models reported in Figure 4 outperform the smart persistent model except the CNN and ARIMA_{cam} models.

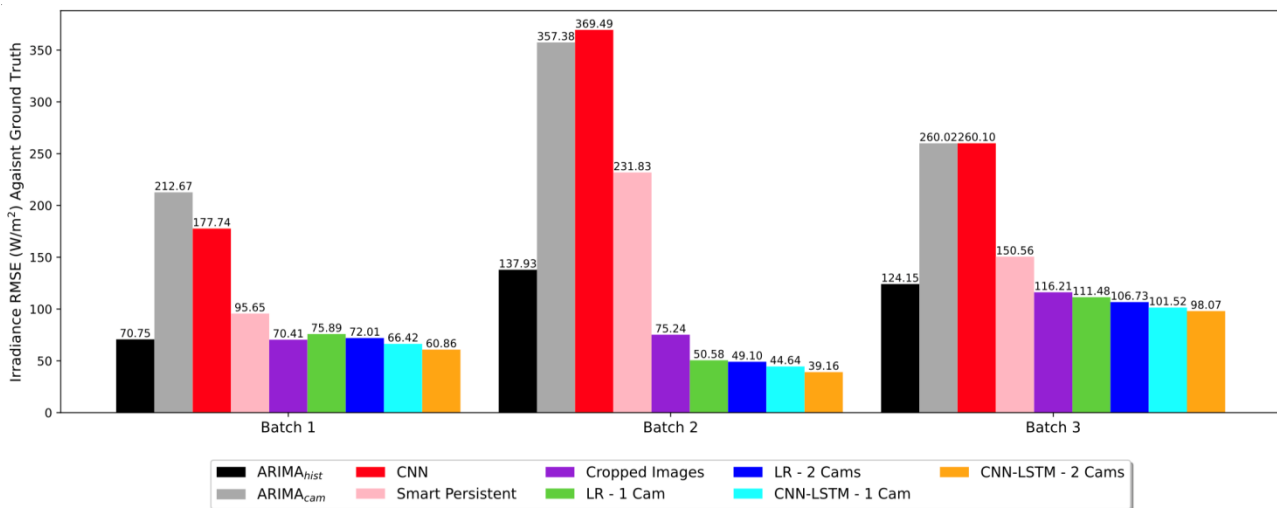


Fig. 4: Forecasts' RMSE comparison by model.

These metrics are used to compare different forecasting models such as an ARIMA time series model, a linear regression model and the proposed deep neural network with and without an LSTM layer. This research also compares the results of the proposed model, when using images from one camera only against adding the images from both cameras. Additionally, we test whether using the full images is better than using a cropped version that only captures the sky and clouds. Figure 5 illustrates a cropped version of Figure 1. Finally, the best model is benchmarked against Solcast's forecasts.

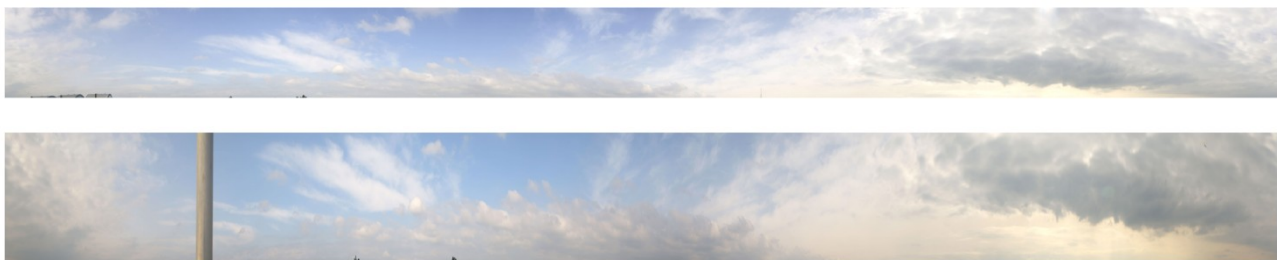


Fig. 5: Cropped sample images from both EPFL cameras.

3. Results and discussion

Figure 4 summarizes the aforementioned metrics for different models and data batches. As only one year worth of data is available, three different batches of images were from the full dataset to be used as out-of-sample testing samples. These batches cover a few days from different times of the year. Batch 1 includes images from January 27th, 2022, until February 10th, 2022, with four missing days due to the unavailability of data from the cameras. Batch 2 covers the data collected from July 7th to 19th 2022 with four missing days. Batch 3 covers eight consecutive days from September 18th to 25th 2022. As already mentioned before, once the data was cleaned and the images timestamps were cross-checked from the two cameras, some timestamps were lost. This results in having a different number of images for different days.

With regard to the time series approach, the ARIMA model was chosen independently for each batch by analyzing the autocorrelation and partial autocorrelation of the training data. The training data represents historical GHI measurements prior to the dates of the respective batches, i.e. for batch 1, the ARIMA model would be fit on historical GHI data from December 2021 until January 26, 2023. Additionally, for each batch, we test two different ARIMA models: one fitted on historical GHI collected at a 10-minute frequency (including GHI during the night) and one fitted on historical GHI collected only at timestamps where images are available. The first model is denoted as ARIMA_{hist} and the second as ARIMA_{cam}. It should be noted that both models are seasonal ARIMAs. The fit was done using the “*Statsmodel*” library in python. This package provides the “*STLForecast*” function that decomposes the time series into a seasonal trend using locally estimated scatterplot smoothing (LOESS) to extract the seasonal, trend and low pass components.

Once the model is fitted, the autocorrelation and partial autocorrelation functions are used to identify the optimal lag order of the autoregressive and moving average components. These functions serve as a guide for selecting the dominant model. We further test and compare different models (i.e. different lag orders) using the Akaike information criterion (AIC) [7] and Bayesian information criterion (BIC) to choose the best model. The two measures provide a measure of goodness of fit for each model and by balancing between model complexity and model fit. The AIC value of a model is computed as $AIC = 2k - 2 \ln(\hat{L})$ where k and \hat{L} represent respectively the number of parameters and the maximized log-likelihood function of the model. The BIC is given by $BIC = \log(N) \times k - 2 \ln(\hat{L})$ where N is the sample size. For batch 1, both ARIMA models had the same order of (5,1,3). In the case of batch 2, ARIMA_{hist} had an order of (4,1,4) whereas ARIMA_{cam} had an order of (6,1,4). Finally, for batch 3, both models shared the same order of (3,1,3).

As shown in Figure 4, both time series models perform worse than the proposed CNN-LSTM network for all three batches with a RMSE of up to 9 times in case of batch 2. The results were in line with our expectations as we know time series model perform poorly for intraday GHI predictions. An interesting result is the large difference in RMSE between the two ARIMA models in each batch as the ARIMA_{hist} model, fitted on historical GHI with no missing timestamps, is able to better predict future GHI. It is also expected that this could be the case when it comes to images as having an uninterrupted sequence of images might improve the network’s performance. To test the effect of the LSTM layer in the proposed architecture, the two LSTM layers are removed, and the new network (labeled CNN) is tested on the same three batches. The impact that the LSTM layers have on the predictions’ accuracy is clear as the RMSE increases by a factor of up to 9.5 in the case of

batch 2. This increase in RMSE was expected as the images have a temporal aspect that cannot be handled properly by the CNN layers alone.

To test whether using images from two separate cameras provide a prediction improvement, we report the lowest error obtained by using images from one camera only. This is done for the linear regression as well as for the proposed DNN. In other words, given that there are two sets of images (one from each camera), we fit the linear regression and the DNN on each set alone and report the lowest error which is reported in Figure 4. The models are labeled LR - 1 Cam and LR - 2 Cams for the linear regression with one and 2 cameras respectively, and CNN-LSTM - 1 Cam and CNN-LSTM - 2 Cams for the proposed network. The results of these tests show that including the two sets of images as input always improves the RMSE of the proposed DNN by more than 10% in the case of batch 2. Figure 5 shows the DNN's prediction and the ground truth of batch 2. From the previous experiments, we can conclude that including an LSTM layer along with two images yield the lowest RMSE error as depicted by model CNN-LSTM - 2 Cams in Figure 4. Additionally, a different model with "ConvLSTM" layers was tested. The RMSE was on par or worse than the proposed CNN-LSTM architecture. In batch 2 for example, the RMSE was around 10% higher. Additionally, it takes twice as long per epoch to train a network comprised of 3 ConvLSTM layers followed by two dense (fully connected) layers. The training time per epoch was 44 seconds compared to 19 seconds for our proposed network. It also requires more epochs for the ConvLSTM to converge compared to the CNN-LSTM.

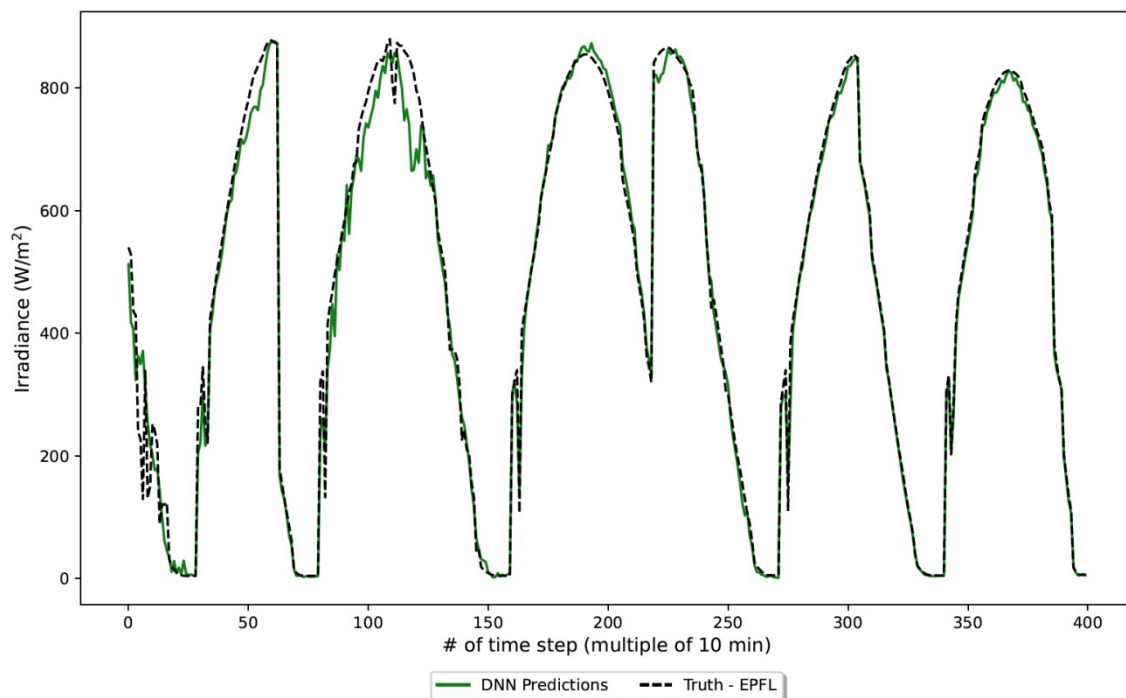


Fig. 6: DNN predictions (batch 2) and ground truth.

This research also explores whether using the full uncropped images (showing both the sky and surrounding areas) provides more information (and hence improved GHI prediction) compared to the cropped images. As expected, using the cropped images provides less accurate forecasts with a RMSE three times higher in case of batch 3. This is mainly due to the information that is being lost once the images are cropped. Such information could represent but is not limited to shadows and reflections. As the collected images could potentially show people, one use case of the cropped images is privacy

protection as the image would be limited to the sky and clouds. This is specially the case for the first sample image in figure 1. To mitigate this problem without cropping the images, OpenCV's YOLO v3 (You Only Look Once) model for object detection was used. This is a pre-trained model that is optimized for object detection for 80 different categories. YOLO v3 was used to detect people in the raw images of the camera that might have privacy concerns. The detected people are then blurred with a gaussian blur from OpenCV. Finally, the proposed neural network is trained on the down sampled blurred images. The performance of the network is not affected for the three batches.

Additionally, using the same DNN architecture, we benchmark the accuracy of the forecasts against that of Solcast. For this, we first collect the forecasts of Solcast for the location of interest, EPFL (Lat: 46.5191, Long: 6.5668) in this case. Using Solcast's API, we can collect their GHI predictions 2 hours in advance at a 10-minute frequency which matches the frequency of the image collection. The data is collected for 12 days starting from March 28, 2023, till April 11, 2023 (March 30th and 31st are missing) while simultaneously downloading the images corresponding to those timestamps. This constitutes the testing dataset which includes 673 couples of images (673 images from each camera) and Solcast's predictions. Consequently, at every time step " t ", two images and Solcast's forecast for " $t + 2 \text{ hours}$ " are collected. Once all the data was collected and the timestamps are cross-checked to match each other, the DNN is trained on all the data available (end of December 2021 till end of January 2023). The trained network is then used to predict the testing set. The RMSE between Solcast's prediction and the true measurements is computed as well as the RMSE of our predictions. The training process is repeated 10 times; in each iteration, the DNN is re-initialized with a new set of random weights. Figure 7 shows the daily RMSE of Solcast's predictions and the average (of the 10 runs) daily RMSE of the DNN's predictions.

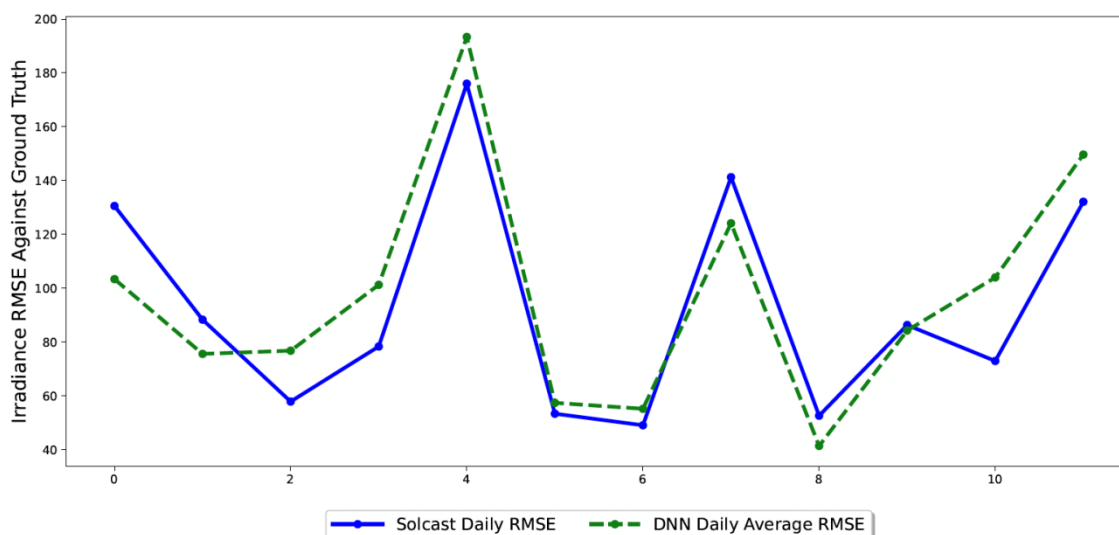


Fig. 7: Daily RMSE comparison between Solcast and the proposed CNN-LSTM.

From figure 7, we can clearly see that the GHI prediction of the proposed network based only on information from two webcams matches that of Solcast which uses satellite images and weather models. As noted on their website, their method for estimating GHI consists of multiple steps summarized as follows:

- Combining raw geostationary satellite images with atmospheric forecasts. This generates the "Solcast cloud model" that is the determinant
- Combining atmospheric pressure and water vapor, aerosols and ozone, and albedo (surface reflectivity) to form the "clear sky GHI".

- Combining the “cloud opacity” model with the “clear sky GHI” to predict GHI.

Our proposed method consists of simply using downsampled raw images from webcams without any additional information. The proposed DNN is also tested for different horizons. Results are shown in figure 8.

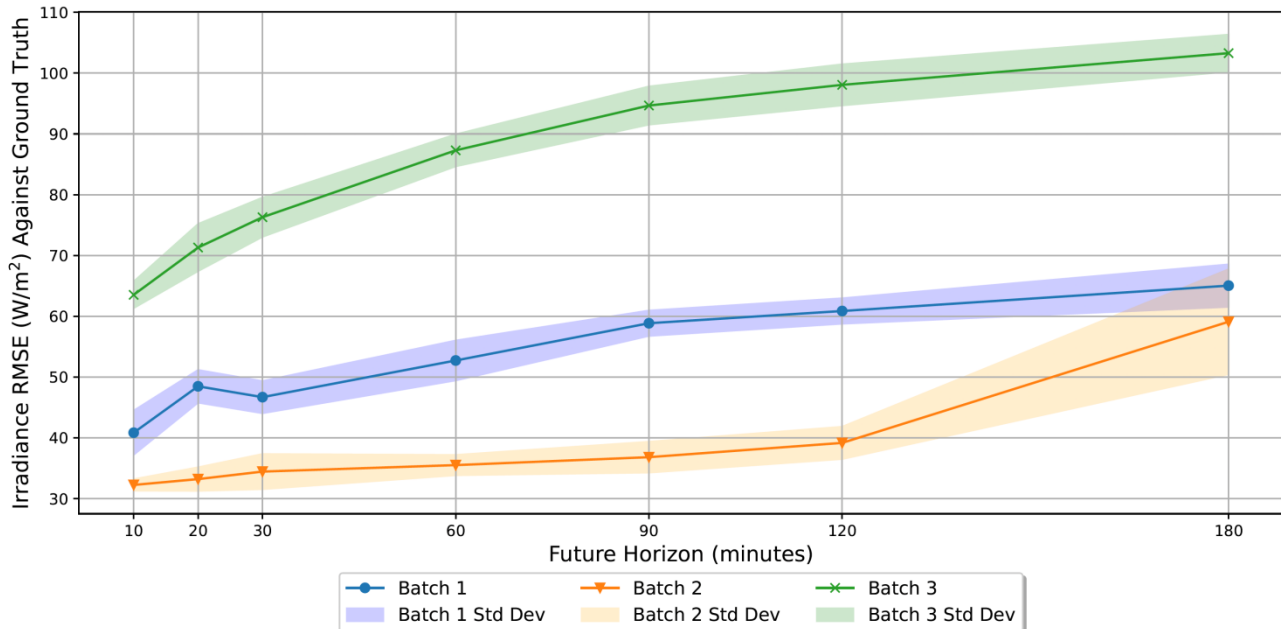


Fig. 8: RMSE by time horizon for the three testing sets.

The findings of this study are attributed to the characteristics of the webcam images. While these webcams may not capture the entire sky (as an all-sky camera would), especially at higher elevations, the wide field of view covered especially along the horizon allows them to capture cloud's movements across consecutive images. This can provide valuable information about cloud cover dynamics, which is the most significant factor in solar irradiance forecasting. This depth perception can help in identifying cloud layers and understanding atmospheric dynamics. For example, cumulus clouds are typically associated with fair weather, while nimbostratus clouds often indicate precipitation. The images, as depicted in figure 1, show distant clouds across a few kilometers. Additionally, webcams offer scalability, allowing to deploy multiple cameras to cover larger areas or multiple locations. This scalability makes them suitable for expanding monitoring networks or upgrading existing systems as needed. Roundshot already has a network of more than 400 active live webcams around Switzerland. There also exists many other public webcams that can be queried.

Another important attribute are shadows cast by objects in the webcam's field of view that can serve as useful features for the network. The presence and movement of shadows across the images can indicate the position and intensity of sunlight, as well as the shape and orientation of objects. By analyzing shadow patterns over time, the CNN layers can learn to infer cloud cover, cloud shadows, and other atmospheric phenomena. These features can enhance the accuracy of GHI forecasts by providing additional context about the local weather conditions.

One potential limitation of this study is that the training process was done using local images and GHI measurement, i.e. both the cameras and the GHI measurements are located within a radius of 150-200 meters. A possible solution is to use estimates of GHI

as reported by meteorological forecasting companies or data from nearby weather stations. With this in mind, transfer learning could be also a possible future direction. Transfer learning is a machine learning method where a model trained for a certain task (on a certain dataset) is used for a different but similar task. In our case, one could leverage this by training the proposed network with enough local images and GHI measurements and then using the pre-trained network with images from another locations to predict GHI measurements. Other directions that can be explored are adding more images, include meteorological data, or combine the existing network with a time series model. Additionally, a comparative analysis between the proposed webcam-based methodology and an all-sky camera shall be conducted. Such a comparison could offer valuable insights into the efficacy and potential advantages of our methodology in real-world solar irradiance forecasting applications.

4. Conclusion

In this paper, we present a method for intraday GHI forecasting focusing on the 2-hour time horizon. To the best of the authors' knowledge, we are the first to use images from public webcams instead of all-sky cameras. We also use the raw collected images with no pre-processing except for downsampling the images.

The research in this study shows that the proposed DNN outperforms other models (ARIMA, linear regression and CNN). The forecasts of the proposed network are compared with the predictions provided by Solcast - a global solar forecasting and solar irradiance data modeling company. It is shown that with information only from two public webcams, we are able to match their predictions. Additionally, this research highlights the importance of LSTM layers in handling time-series data even when it comes to images as removing it would drastically increases the RMSE. We attribute this result to the information content present in the side view images of the sky and clouds. We expect that by adding more webcams and by combining information from satellite and weather models, we will be able to further increase the GHI prediction accuracy.

The proposed methodology is very simple, computationally inexpensive and proves to perform very well to provide GHI forecasts for PV generation prediction. Improving GHI forecasting at the local level can be aggregated up to a regional or even national level and can help predict a country's imbalances in the transmission grid leading to optimal use of energy sources. With better intraday predictions, the dispatch plan (set a day in advance) could be followed more accurately and hence avoid imbalances that incur penalties and require use of non-renewable sources.

References

- [1] [Irenastat online data query tool](#) (2023).
- [2] F. Sossan, E. Namor, R. Cherkaoui, M. Paolone, Achieving the dispatch- ability of distribution feeders through prosumers data driven forecasting and model predictive control of electrochemical storage, IEEE Transac- tions on Industrial Electronics 7 (4) (2016) 1762–1777.
- [3] J. H. Yi, R. Cherkaoui, M. Paolone, Dispatch-aware planning of energy storage systems in active distribution network, Electric Power Systems Research 190 (2021).

- [4] R. H. Inman, H. T. C. Pedro, C. F. M. Coimbra, Solar forecasting methods for renewable energy integration, *Progress in Energy and Combustion Science* 39 (6) (2013) 535–576.
- [5] C. W. Chow, B. Urquhart, M. Lave, A. Dominguez, J. Kleissl, J. Shields, B. Washom, Intra-hour forecasting with a total sky imager at the UC San Diego solar energy testbed, *Solar Energy* 85 (11) (2011) 2881–2893.
- [6] J. Calbo, J. Sabburg, Feature extraction from whole-sky ground-based images for cloud-type recognition, *Journal of Atmospheric and Oceanic Technology* 25 (1) (2008) 3–14.
- [7] P. J. Brockwell, R. A. Davis, *Introduction to Time Series and Forecasting*, 2nd Edition, Springer-Verlag, 2002.

G0410

The influence of the World and European championships on the electricity consumption diagram (load curve) of the Republic Croatia

Petar Ribarić, Davor Bošnjak
HEP Trgovina Ltd., Zagreb/Croatia;
Tel.: +385-1-6321-563, +385-1-6322-626
petar.ribaric@hep.hr, davor.bosnjak.hep.hr

Abstract

This paper shows how employees of HEP Trgovina Ltd. forecast an electricity consumption diagram (load curve) of the Republic of Croatia and which challenges they face during their operational work. It is known that the consumption diagram is the most influenced by: temperature, cloud cover/insolation, fog, precipitation, wind speed and direction, and air humidity (dew point). Depending on the season, the same mentioned factors can lower or raise the consumption diagram. The paper also describes how sports competitions also affect such a diagram. It is shown how two World championships and one European football championship affected the consumption of electricity in the Republic of Croatia. Special attention is focused on individual historical matches of Croatian football players and their impact on consumption in the Republic of Croatia and how they are included in the electricity consumption forecast. A resolution of the specified days, in addition to an hourly resolution, also contains a 15-minute resolution where there could be seen with more details an influence of the start, half-time, end and extra time of the match on the consumption diagram. The aim of the paper is to show the extent to which such historical sport moments, in addition to the aforementioned meteorological influences, further challenge the process of planning and managing not only the portfolio of the HEP Group, but to a large extent the power system of the Republic of Croatia as a whole.

Introduction

Today, the electric power industry is a very important factor for the growth and development of society, economic stability and the functioning of the state. The increasing demand for energy, the security of supply, and recently the rise in energy prices and climate change have caused energy efficiency to have an increasingly significant impact in the field of energy. As a result, the impact of energy efficiency is gaining more and more attention and significance in the world every day. This is why the forecasting of electricity consumption and production is an increasingly common phenomenon among large industrial customers, but also among all others who strive to optimize their daily energy needs. If the customer adequately predicts price movements on the electricity market, and makes a diagram of his consumption plan and optimizes it with a diagram of his own production plan, he can achieve significant savings and reduce the harmful impact on the environment. As is well known, it is impossible to store electricity in large quantities, so every supplier or manager of the balancing group on the market is obliged to make detailed consumption plans for all their customers in order to reduce their own balancing energy costs and at the same time increase the safety of power systems, and thus and security of supply to all customers.

The head of the balance group is obliged to balance all its customers on an intra-day basis, or in the event of outages and deviations of a power plant, he is obliged to compensate for the difference at other power plants or to balance himself by buying and selling surpluses or deficits on the electricity exchange (CROPEX). If it is not able to reduce its deviations to zero, its deviations must be balanced by the transmission system operator (HOPS) and that amount of energy must be charged to the cause of the deviation. The transmission system operator is responsible for keeping the transmission system safe, reliable and efficient. In order to keep the transmission system in balance, the transmission system operator will, through auxiliary services, ask the other balance group leader to, if possible, balance the power system. Such a balance group leader, who provides an auxiliary service, performs this balancing by increasing or decreasing production at his power plants, or he can ask customers, with whom a balancing agreement for the provision of auxiliary services has been concluded, to decrease or increase their electricity consumption. Customers with their own production have additional options for providing balancing energy, especially those with built-in energy storage. In addition to balancing the power system through auxiliary services involving other balance group managers, the transmission system operator can balance the power system by trading on the electricity exchange (CROPEX) or by using other available mechanisms (exchange of auxiliary services with other transmission system operators, etc.) .

Therefore, the need to predict electricity consumption diagrams is becoming an increasingly common and important activity today. Forecasting consumption is a challenging task, and more and more time is invested in the development and progress of this area. In the beginning, electricity consumption forecasting was done on the basis of the experience of experts who were engaged in this work on a daily basis. Today, there are various computer tools that work on the principle of neural networks and use databases, meteorological factors and take into account the influence of holidays and other specific days in the calendar, and based on them make predictions of electricity consumption. There are currently three ways of predicting electricity consumption, namely:

- short-term prediction of electricity consumption - represents a period from one hour to a week
- medium-term forecast of electricity consumption – represents a period from one week to one month

- long-term forecasting of electricity consumption - represents a period from one month to one year and longer

1. Short-term method of forecasting electrical energy

This paper presents an exclusively short-term method of forecasting electricity consumption and a way of creating a load diagram at the day-ahead level (D-1). Then, the way in which certain historical sports successes were included in the diagram of the spending plan and how they were achieved was shown.

Short-term forecasting refers to a period from one hour to one week in advance. Short-term forecast forecasts up to 24 hours in advance are presented, because such a forecasting method is necessary for creating a load diagram for the next day, or in this case for a day ahead (D-1).

A key role in planning the operation of reliable, safe and economical power systems is played by the short-term method of planning electricity consumption. Therefore, it is necessary to create the most accurate load diagram in order to use all the advantages of the production units and provide the greatest social benefit (eng. "social welfare"). Creating a day-ahead load diagram (D-1) is a complex and demanding process that is influenced by many meteorological factors. It is known that the load diagram is most affected by: temperature, rain, fog, cloudiness/insolation, and wind speed and direction. Depending on the season, the same listed factors can lower or raise the load diagram. For example, an increase in cloud cover in summer lowers the load diagram, while in winter it raises it. Temperature has the opposite effect on the load diagram. The increase in temperature in summer affects the increase of the load diagram, and in winter its influence is reflected by the lowering of the load diagram. Therefore, it is very important to recognize which meteorological factor will have a dominant influence because it will have the most influence on the shape of the load diagram. Also, when planning the load diagram, it often happens that several of the mentioned factors change during the day and that they act in parallel. Then we get unusual forms of the load diagram, which are quite different from the normal ones, when we have the influence of only one factor, and the others can be considered unchanging (lat. "ceteris paribus"). With all the advanced meteorology, it is very difficult to predict at what time and at what exact location a change in weather will occur, and in what proportion meteorological factors will affect the change in the load diagram. Therefore, the work of the planner is very challenging and requires years of learning and improvement, which are necessary in order to be able to determine as precisely and in detail as possible the moment of the weather change and its impact on the load diagram. Even more challenging and complex is the job of the dispatcher who, on the day of execution of the planned diagram, tries to predict all necessary corrections, especially in real time when estimating the amount and duration of deviations from the plan, as well as the duration of such deviations. Any deviation must be compensated in real time from available sources (power plants) that are technically capable of providing such additional balancing service. This complex process includes the entire chain of duty personnel in:

- HOPS d.d. (duty dispatchers of the National Dispatch Center in cooperation with duty dispatchers of network centers and dispatchers of all neighboring power systems networked into a single network),
- HEP-Trgovini d.o.o. in which the dispatcher on duty acts as the head of the balance group for the entire HEP group and performs the necessary corrections in cooperation with HEP-Production and other parts of the HEP group
- HEP-Proizvodnji d.o.o. in which the duty dispatchers of the production centers Dalmatia, West and North, in cooperation with crews in all power plants, carry out the necessary orders to increase or decrease production depending on the needs of the power system.

2. Influence of sports competitions on the load diagram

In this paper, we will show how the successes of our football players influenced the diagram of electricity consumption in the Republic of Croatia. For each major competition in which they participated in the period from 2018 to 2022, plans of the consumption diagram, realization of the consumption diagram, and 15-minute presentations of their matches, where you can clearly see how the beginning, half-time, end, overtime and penalties will be shown influenced the movement of the electricity consumption diagram. In addition to the electricity consumption plan, which was created by the employees of HEP-Trgovina d.o.o., a presentation of the plan of neural networks and their prediction of extraordinary events was presented. On the graphs, you can clearly see their accuracy or deviation in this case.

2.1. World Cup 2018

The first major sports competition we will show is the 2018 World Cup in Russia. The pictures will show the load diagrams for the matches when the Croatian national team played in the elimination phase, which means against Denmark, Russia, England and the final against France.

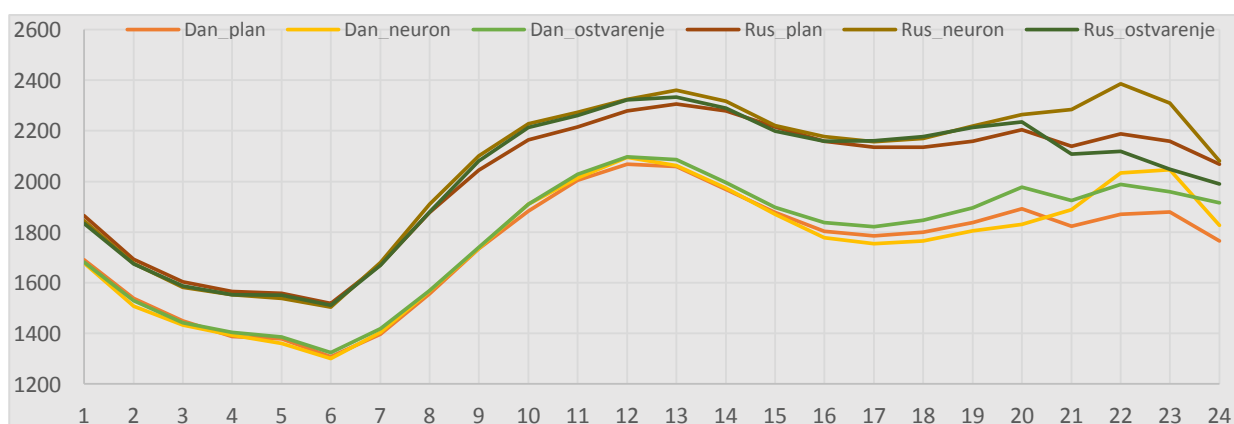


Figure 1. EES load diagrams of the Republic of Croatia for the days of football matches of the Croatian national football team against Denmark and Russia

Figure 1 shows load diagrams of the electric power system (EES) of the Republic of Croatia for the days when there were matches of the Croatian national football team against Denmark and Russia. Diagrams of the consumption plan created by the employees of HEP-Trgovina d.o.o. are shown in particular. and tools that use neural networks, as well as a diagram of realized electricity consumption. As is well known, the load diagrams differ for working days, holidays, weekends, half-working days, etc. Figure 1 also shows the difference in shape between Saturday and Sunday, that is, if the meteorological factors are similar, then, as a rule, the consumption of electricity higher on Saturday than on Sunday, and that is what happened here. What can be clearly seen is the difference in deviation between the plan of the employees of HEP-Trgovina d.o.o., the realization and the plan from the tool that uses neural networks. As Figure 1 shows, it can be seen that all the load diagrams are approximately the same until the start of the matches, but when the match starts, there is a significant deviation. Also, Figure 1 clearly shows that the employee plan of HEP-Trgovina d.o.o. took into account the influence of the match, while the neural network completely omitted such an influence in its plan. By this alone we can conclude that it is difficult for neural networks to predict extraordinary

events and how and in what form they will be reflected in the realization. From this we can conclude that neural networks are not yet sufficiently developed for such specific events and leave them to the planners when creating load diagrams.

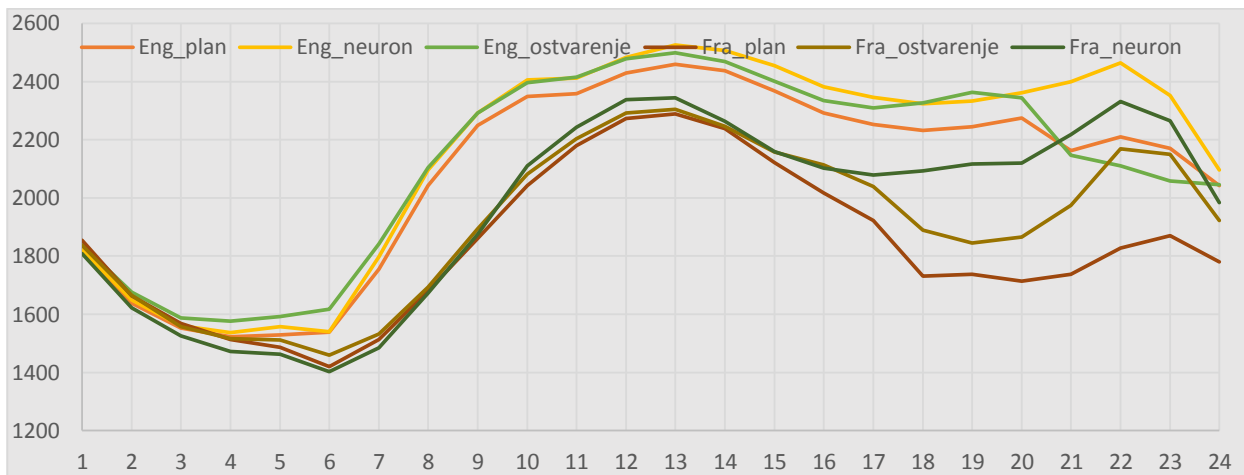


Figure 2. Load diagrams of the EES of the Republic of Croatia for the days of football matches of the Croatian national football team against England and France (WC finals)

Figure 2 shows the load diagrams of the HEP-Trgovina d.o.o. employee plan, realization and tool plan using neural networks for the matches against England and the World Cup final against France. In the given picture, it is possible to see the difference in the shape of the load diagram between a weekday (England) and a Sunday (France). Also in this example, it is noticeable that the load diagrams of the planner, realization and plan of the neural network are equal until the start of the match, but after that significant deviations begin. What is interesting is that on the day of the match against England, a few hours before the match, it started to rain in the Republic of Croatia, and as mentioned, given that it is summer, meteorological factors such as cloud cover and rain at that time of year affect the consumption diagram in such a way to put it down. As Figure 3 shows, a few hours before the start of the match, the load diagram did not drop, but the opposite effect occurred. The aforementioned jump in electricity consumption can be justified by the fact that before the start of the match, customers tried to do all the necessary activities in order to be able to watch the match in peace. If you take a closer look at the difference between the load diagram of the plan and the realization for the match against France, i.e. the final of the World Cup, you can see a big difference here. This difference can be justified by an extreme extraordinary moment. Namely, it is difficult to include everything that could happen in the load diagram plan, so for example when creating the load diagram for the day in advance (D-1), the planners cannot know during which time the match will take place, that is, whether the match will end in the regular part, overtime or penalty kicks, i.e. whether the Croatian national team will win or lose. Here it is possible to clearly see the difference between a match that ended in victory and a loss. If you take a closer look at Figure 2, it can be seen that after the match against England, the consumption diagram did not "recover", that is, its electricity consumption did not increase, which we can attribute to the celebration of a large number of fans. After the aforementioned match, many people came out to the streets, squares and parks to celebrate this historic moment together. When we look at the load diagram for the match against France, we can see that after the match the consumption diagram partially "recovered". In other words, there was an increase in electricity consumption during the late evening hours, even though after the match there were still people celebrating this historic day on the streets, squares and parks. Such situations further emphasize the importance of the start time of the match, i.e. how for the consumption diagram and deviation from the "usual form" it is not the same

whether the match starts in the afternoon or in the evening. In the end, we can conclude from the above examples that there is a much greater celebration, and thus the impact on the shape of the consumption diagram, when the Croatian national team wins, which is usually to be expected, and all of this is visible to us in the presented load diagrams.

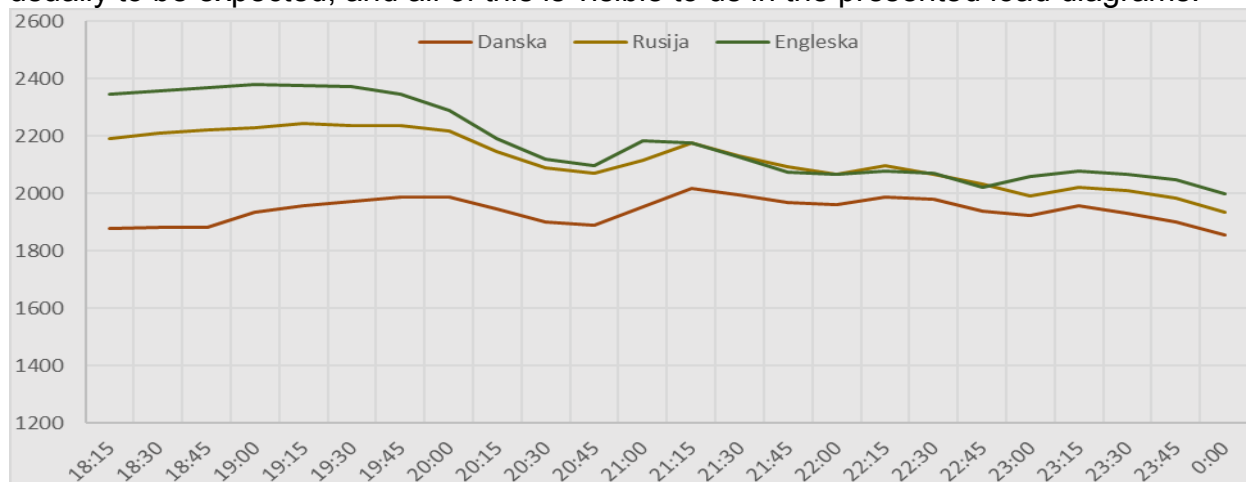


Figure 3. Display of consumption diagram in 15-minute resolution several hours before the start of the match, during the match and after the match

Figure 3 describes a 15-minute view of the realization of the load diagram for the matches of Croatia against Denmark, Russia and England. Considering that all the mentioned matches started at the same time, it is possible to see the similarity in the movement of the 15-minute performance. As it is known that the load diagram is not the same for every day, it is also possible to see here that the highest load diagram is for the match against England, but this is to be expected considering that the match was held on a weekday. What is interesting is that every time before the start of the match, a small increase in the load diagram is seen, followed by a collapse. The biggest drop in the load diagram occurred in the match between Croatia and England, but given the importance of the match, we can come to the conclusion that this was expected. At each half, sharp increases in consumption are visible, and this happened at the end of the regular part of the match and at the end of extra time. It is also interesting to note that the 15-minute performance clearly shows the difference in the end of the matches when we played against England, that is, Denmark or Russia. As is well known, the matches against Denmark and Russia ended in penalties, while the match against England ended in extra time, and this can be clearly seen on the load diagram. Namely, if you take a closer look at the realizations of the aforementioned load diagrams, it is possible to see that at the end of each match, an increase in electricity consumption was recorded. Such details are shown in Figure 3, which shows that the increase in spending in the match against England came 15 minutes earlier than in other matches.

Also, on this 15-minute presentation of the realization of the load diagram, it is also possible to clearly see the outcome of the match. If the load diagrams for the matches against Denmark, Russia and England are compared in more detail, it can be seen that the Croatian football team in the match against England was at a deficit in the first half. Namely, when you look at Figure 3, it is evident that at the aforementioned match, after the failure, there was an earlier jump in consumption for the first half, and therefore it is possible to assume that part of the audience did not watch the first half to the end, being dissatisfied with the football players' performance.

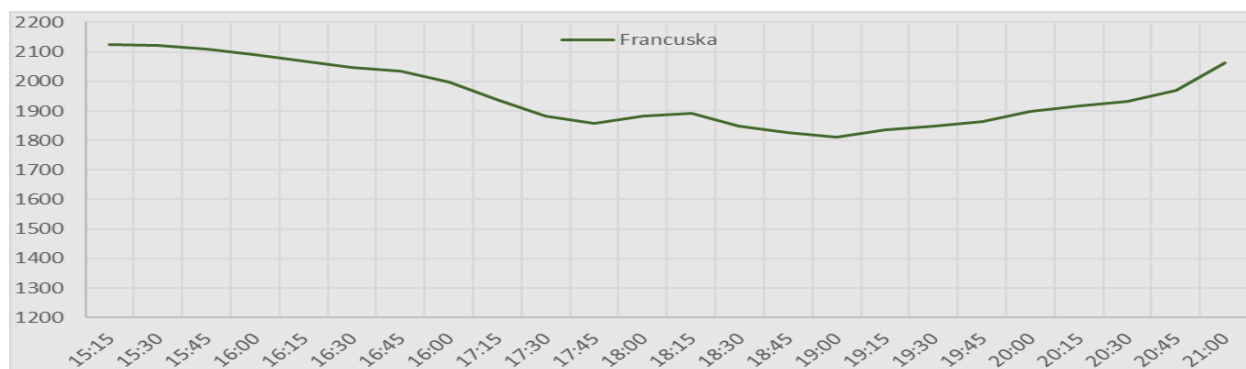


Figure 4. Display of consumption diagram in 15-minute resolution several hours before the start of the final match of the 2018 World Cup, during the match and after the match

Figure 4 shows a 15-minute realization of the electricity consumption diagram for the final match of the 2018 FIFA World Cup in Russia between Croatia and France. It is possible to see the course of the match from the picture. If you look carefully at Figure 3 and Figure 4, it is possible to conclude that in this case the match ended in the regular part. As Figure 4 shows, after the initial drop in consumption, i.e. the start of the match, there is only one recorded spike in consumption that was after the first part of the match (halftime). This is followed by a further decline in consumption. Figure 4 clearly shows that after 45 minutes (the second half of the match) consumption increases again, and we can conclude that the match is over. What is still possible to conclude by comparing Figure 3 and Figure 4 is that this match unfortunately ended with the defeat of the Croatian national team, because after the end of the match there was no additional drop in electricity consumption, but in this 15-minute presentation of the achievement, an increase in electricity consumption is clearly visible.

2.2. European football championship in 2021

Another major sports competition shown here is the 2021 European Football Championship in France. The next pictures show load diagrams for matches when the Croatian national team played in the relegation phase, i.e. only the match against Spain is shown.

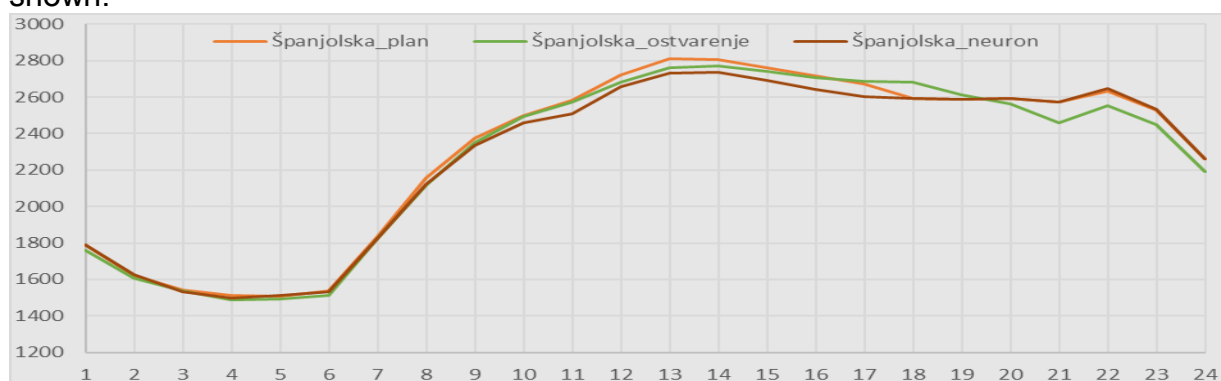


Figure 5. Electricity consumption diagram. energy of the Republic of Croatia on the day of the round of 16 match of the 2021 European Football Championship

Figure 5 shows the load diagrams of the HEP-Trgovina d.o.o. employee plan, the realization and the plan of the tool that uses neural networks for the round of 16 match of the European Football Championship against Spain. Also in this case, it is possible to clearly see that, as a rule, all the load diagrams match until the start of the match. It is also possible to see here that before the start of the match a small jump in electricity

consumption is seen, and after the match starts, a sudden drop in consumption follows. As was said for the match against France, here the Croatian national team was unfortunately defeated and there was no celebration after the end of the match, and this affected the recovery of the shape of the electricity consumption diagram, which took on its classic appearance for the evening rush hour in the summer period of the year.

2.3. World football championship in 2022

The third major sports competition presented in this work is the World Cup in Qatar in 2022. The images show the load diagrams for the matches when the Croatian national team played in the relegation phase, i.e. against Japan, Brazil, Argentina and the 3rd place match against Morocco.

Figure 6 shows the load diagrams of the HEP-Trgovina d.o.o. employee plan, the realization and the plan of the tool that uses neural networks for the matches against Japan and Brazil. The first thing that can be clearly observed are the different shapes of the load diagrams compared to the load diagrams that were shown at the past championships. The main reason for the different shape is the season in which the world championship was held in Qatar. Namely, all previous competitions were held in summer, so their load diagrams are similar, while this is the first competition that was held in winter. The biggest difference between the load diagram in summer and winter can be seen in the evening rush hour or in the morning hours. The main reason for the different shape of the load diagram in winter compared to summer is the time of sunrise and sunset. Due to less daily sunlight, consumers (customers) use lighting for longer, so consumption increases, which is manifested by a steeper shape of the load diagram in the morning hours and a longer evening peak.

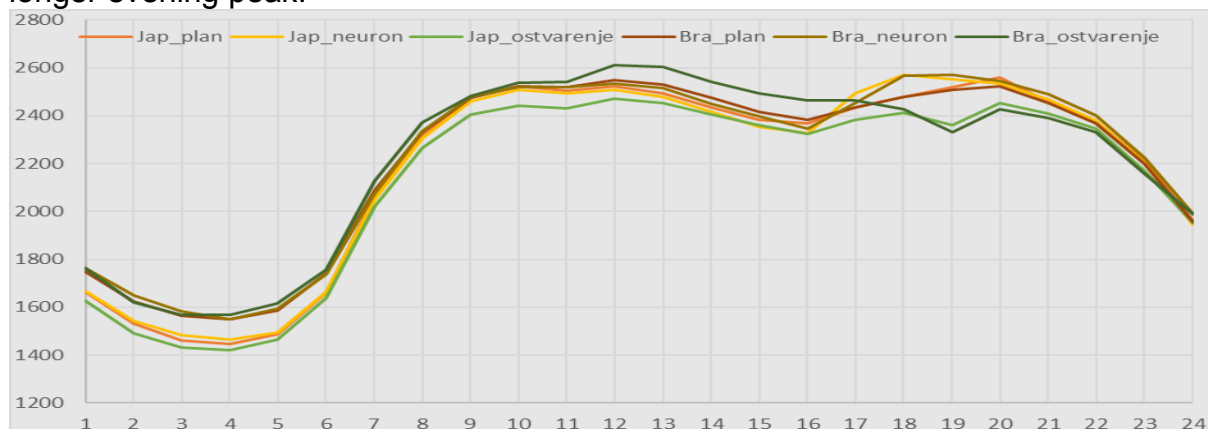


Figure 6. Electricity consumption diagram. energy of the Republic of Croatia on the day of the matches against Japan and Brazil during the 2022 FIFA World Cup

Figure 7 shows the load diagrams of the HEP-Trgovina d.o.o. employee plan, the realization and the plan of the tool using neural networks during the match against Argentina and the 3rd place match against Morocco. Also, here it is possible to see the difference between the load diagram during the weekday (match against Argentina) and during the weekend in this case Saturday (match for 3rd place against Morocco). As already stated earlier, the biggest deviations between the plan and the realization occur during extraordinary influences, that is, in this case, the match. Taking a closer look at the load charts for the World Cup in Qatar, it is possible to see that the smallest change in load chart performance occurred in the 3rd place match against Morocco. Namely, Figure 7 clearly shows that no major drop in electricity consumption occurred in the load diagram for the specified match. However, the drop in consumption is recorded and visible in Figure 7, which shows how the evening peak has fallen to the level of the afternoon peak. If you look at the consumption plan made by the planners, it is clearly visible that they

expected a significant drop in electricity consumption, so we can therefore conclude that the mentioned match was not attended like the previous three matches at this World Cup. Although our national team crowned this match with victory and 3rd place, there was no significant drop in electricity consumption after the match, even though a great sporting result was achieved. What is interesting and clearly shown in Figure 6 and Figure 7 is the fact that after the victory of our national team in the matches against Japan, Brazil and Morocco, there was no significant and long-lasting celebration in the streets, squares and parks, but it was mostly in closed spaces and households due to colder temperatures and worse weather. The consequence of the above is that after those matches, the consumption diagram returned to normal relatively quickly, and did not start with an additional drop, as in the case of the World Cup in Russia in 2018, when due to celebrations, but also much nicer and warmer weather, it continued with its prolonged decline.

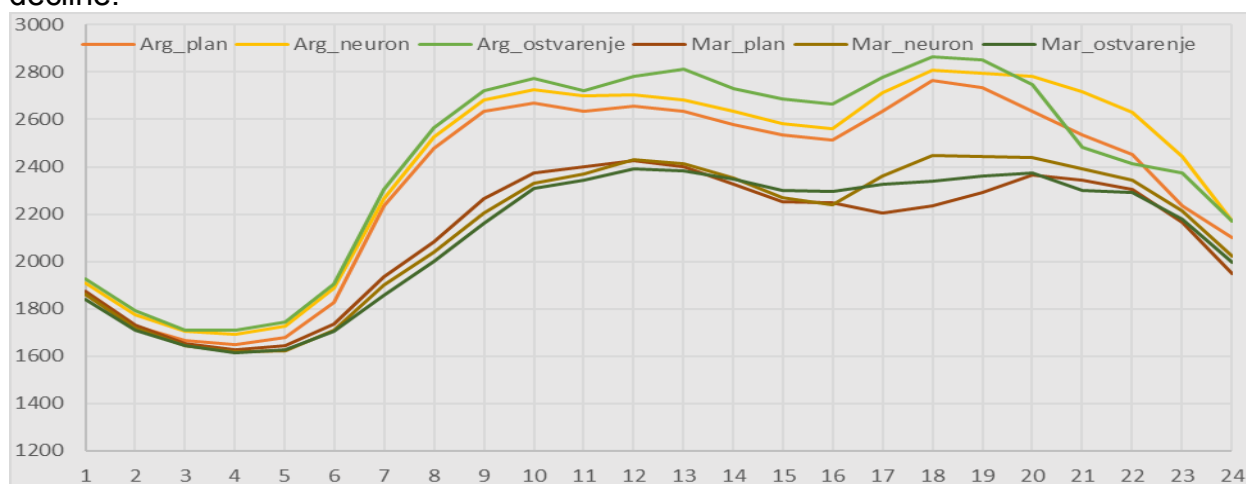


Figure 7. Electricity consumption diagram. energy of the Republic of Croatia on the day of the matches against Argentina and Morocco during the 2022 World Cup

3. CONCLUSION

In this paper, the short-term forecast of electricity consumption is briefly explained and all the problems associated with this area are partially presented. The short-term forecast of electricity consumption is important because it enables the optimization of production according to the technical requirements of production aggregates and all other elements in the power system (even operation as possible), but at the same time the need for greater flexibility due to increasing oscillations in the EES due to oscillations of distributed generation RES, the structure of electricity consumption in which households are mostly represented, and the ever-increasing oscillations in the hourly price diagram on the electricity market and all other energy sources. Due to the ever-increasing prices of balancing energy, it is necessary to make a daily load diagram as high-quality as possible at the day-ahead level (D-1), in order to minimize the deviation of the planned consumption from the actual consumption. As is well known, it is almost impossible to store electricity, and for all deviations at the daily level, as a rule, it is necessary to engage additional production units, which can result in an increase in total costs. All of the above is necessary to ensure the stability of the power system and secure supply to customers.

The aim of this paper was to observe the influence of meteorological factors and extraordinary events, or in this case significant sports competitions, on the electricity consumption diagram of the Republic of Croatia. As important as it is to recognize the dominant meteorological factor that will and to what extent affect the diagram of electricity consumption, it is just as important to recognize extraordinary events and their impact. It is logical to expect that during historical sporting events there will be a drop in consumption,

but to what extent and in what time, it is almost impossible to predict. Namely, just as it is almost impossible to predict the influence and duration of meteorological factors on the consumption diagram, it is also almost impossible to predict the course of the match itself and its influence on the consumption diagram. Whether the match will end in the regular part, overtime or in a series of penalties, this is a huge uncertainty for the planner and dispatcher and everyone else in the chain of planning and management of EES. All of the above gives a dose of specificity and interest to the work of planning the load diagram. Unfortunately, the auxiliary tools that use neural networks and artificial intelligence, from the above examples, have shown that they are not yet sufficiently developed for these specific cases, and that in such cases it is best to leave the creation of load diagrams to the human factor, i.e. planners. It is also very interesting that after the great sporting successes of the Croatian football team at the World Cup in Qatar in 2022. there was no prolonged celebration in open spaces, which can be attributed to worse weather conditions and lower temperatures compared to summer.

From all of the above, it is possible to come to a clear conclusion that the consumption diagram is highly subject to the influence of meteorological factors and the season, and in addition to them, the consumption diagram is also influenced by the habits of consumers, who in the observed cases, by their actions, clearly influenced its shape. The additional value of this work is that it connects the technical field of research with the meteorological and sociological, that is, it proves with concrete examples that in the case of the historical sports results of the Croatian national team, all the emotionality and synergistic action of all citizens of the Republic of Croatia come to the fore, as well as the fact that football and sport is generally the most important secondary thing in the world.

With their excellent results and emotions that captured the attention of all viewers around the world, this Croatian national football team has once again proven how much support they have in their homeland and how the superb spirit of sportsmanship connects people sometimes even "more than electricity 😊".

4. LITERATURE

- [1] George Gross, Francisco D. Galiana: Short-Term Load Forecasting
- [2] Chatum Sankalpa, Somsak Kittipiyakul, Seksan Laitrakun: Forecasting Short-Term Electricity Load Using Validated Ensemble Learning
- [3] Yusen Wang: Short-term Power Load Forecasting Based on Machine Learning, Stockholm, Sweden 2019
- [4] available at the link: <https://www.hops.hr/dijagram-opterecenja-dnevni>

G0411

Exploring the Potential of Quantum Computing for Electrical Power System Optimization

Zlatko Ofak (1), Dino Mileta (1), Tin Bobetko (1), Dario Jukić (2), Karlo Lelas (3), Hrvoje Buljan (4)

(1) Uprise d.o.o., Zagreb/Croatia;

(2) Faculty of Civil Engineering, University of Zagreb, Zagreb/Croatia;

(3) Faculty of Textile Technology, University of Zagreb, Zagreb/Croatia;

(4) Faculty of Science, University of Zagreb, Zagreb/Croatia;

Tel.: +385-98-442-502

zlatko.ofak@uprise.hr

Abstract

In order to achieve the goals of the European Green Plan on zero net greenhouse gas emissions by 2050 and achieve a resource-efficient and competitive economy, significant changes are expected in the electricity market and power system management in Europe. By increasing the share of variable energy sources and increasing the number of participants with different behavioral patterns, transmission system operators are faced with the challenge of ensuring security of supply to end customers. Given that building a network is an expensive and time-consuming process, optimizing the existing network maximizes the potential of the existing network while increasing security. The optimization process is an iterative, computationally demanding process based on linear algebra, i.e., multiplication of large sparse matrices and mixed integer linear optimization, which in the operational environment is time-limited to a few minutes. It is precisely the optimization execution time with high costs of the server system that is the main obstacle and challenge for further integration of optimization into operational processes.

Recent advancements in quantum computing indicate its potential for significantly faster execution times than conventional optimization algorithms, particularly due to its ability to explore multiple solutions simultaneously (which is the main issue when grid optimization is performed using topological measures due to their physical nature preventing superposition) and efficiently handle complex mathematical processes inherent in optimization problems. However, realizing these benefits requires addressing challenges such as developing tailored quantum algorithms, implementing error mitigation techniques, and achieving scalability for real-world applications.

This paper presents basic concepts of quantum computing and state-of-the-art quantum computers available, as well as mathematical concept of so-called sensitivity analysis, congestion management and optimization of electrical power system. Overview of existing quantum algorithms designed for the purpose of linear algebra is given, with special focus on Harrow-Hassidimi-Lloyd quantum algorithm. Finally, paper provides assessment of applicability of existing quantum algorithms and quantum computing (in terms of available qubits) on the problem of real-world electrical power system optimization for which authors developed a solution based on conventional algorithms and closed mathematical optimization.

Introduction

The global mission to significantly reduce carbon emissions has become one of the main change drivers within the energy sector and has put in place extremely challenging tasks in front of energy sector actors. In order to reach the European Green Deal targets of no net emissions of greenhouse gases by 2050, as well as to achieve a resource-efficient and competitive economy, significant changes can be expected within electricity market behavioral patterns and consequently in the premise of how the European electrical power system is operated.

Based on the legal requirements and incentives in place, one can expect following changes in terms of electrical power systems operation: a) significantly higher percentage of the intermittent (renewable) energy sources within the energy mix; b) significantly increased number of electricity market participants with different behavior patterns (electric vehicles, smaller production units, demand side response, prosumers, aggregation, multi energy networks), even on the lower voltage levels; c) significantly increased amount of data to be exchanged in a short time and on different levels; d) higher percentage amount of the transmission lines' capacity provided at disposal to the market in order to facilitate the overall energy trading as well as to bring the objective closer to the real time, thus allowing a more efficient grid operation and utilization.

All these requirements and operational uncertainties require stronger grid infrastructure (e.g. investing in smart physical assets, electrical grid expansion, installation of flexible assets that possess high balancing potential) and/or better utilization of the existing one. Given that building a network is an expensive and time-consuming process, optimizing the existing network presents an efficient solution which maximizes the potential of the existing infrastructure while increasing security. The optimization process involves a series of iterative, computation-intensive steps grounded in linear algebra, specifically involving the multiplication of large sparse matrices in order to compute factors needed for mathematical optimization. To be more specific, so-called remedial action optimization (RAO) problem is a problem of the complexity class non-deterministic polynomial time (NP-Hard) and no efficient algorithms exist to find the global optimum guaranteed in polynomial time.

Recent developments in quantum computing suggest it could greatly accelerate execution times compared to traditional optimization algorithms. This is largely because quantum computing can process multiple solutions at once - a major advantage when optimizing grids using topological measures, where the physical nature of the measure's limits superposition - and adeptly manage the complex mathematical tasks that optimization problems typically involve.

Many organizations are heavily investing in quantum computing bearing in mind the potential disruptiveness it can bring to the market. According to Precedence Research [1], the global quantum computing market size is projected to hit around USD 125 billion by 2030 and is poised to reach a CAGR of 36.89% from 2022 to 2030.

Chapter 1 of this paper will present in detail the business process and explain the problem of grid optimization. Additionally, it will explain principles behind quantum algorithms and what are competitive advantages of it compared to classical algorithms.

Chapter 2 discusses various quantum algorithms for linear algebra.

Chapter 3 provides main conclusions and predictions regarding future of quantum computing application on the problem of electrical power system optimization.

1. Requirements for Grid Services - Technical & Market Conditions

In order to ensure security of the energy supply, transmission system operators today rely much on the accuracy of predictions of the market positions, and at the same time cope with uncertainties mainly by contracting different production units that can offer flexibility when deviation is present. These flexibility options are ordered by the system operator either because of the market or due to an unplanned incident within the grid.

Aiming to allow optimal electrical power grid utilization on the European level in terms of available capacity and operation cost, optimization of electrical power grid was introduced, and was designed in order to meet the requirements related to coordinated use of remedial actions (RAs) among system operators in a cost-efficient way, all documented under existing EU legislation: a) Commission Regulation (EU) 2017/1485 [2] – The Guidelines on System Operation; b) Commission Regulation (EU) 2015/1222 [3] – The Guideline on Capacity Allocation and Congestion Management; c) Commission Regulation (EU) 2019/943 [4] – Regulation on the internal market for electricity. Main use of the RAO process is foreseen in scope of Coordinated security assessment (CSA/ROSC) and Coordinated capacity calculation (CCC) processes, which both present the main building blocks of the European power system design for the new era.

The existing process' designs foresee extremely challenging time limits (see Figure below for details) for the execution of the electrical power grid optimization process, which are expected to be shortened in the future due to increasing requirements linked to the design of European Intraday energy market. The mentioned time limits seem to be unreachable with the current setup, even for the limited computational problem, while real time optimization of electrical power grid, which can be considered as a holy grail of system operators and would allow redesign and implementation of new concepts in the European energy market, is not foreseen at all at this moment due to problem size and complexity. Overview of the current European energy market design is presented on the Figure below:

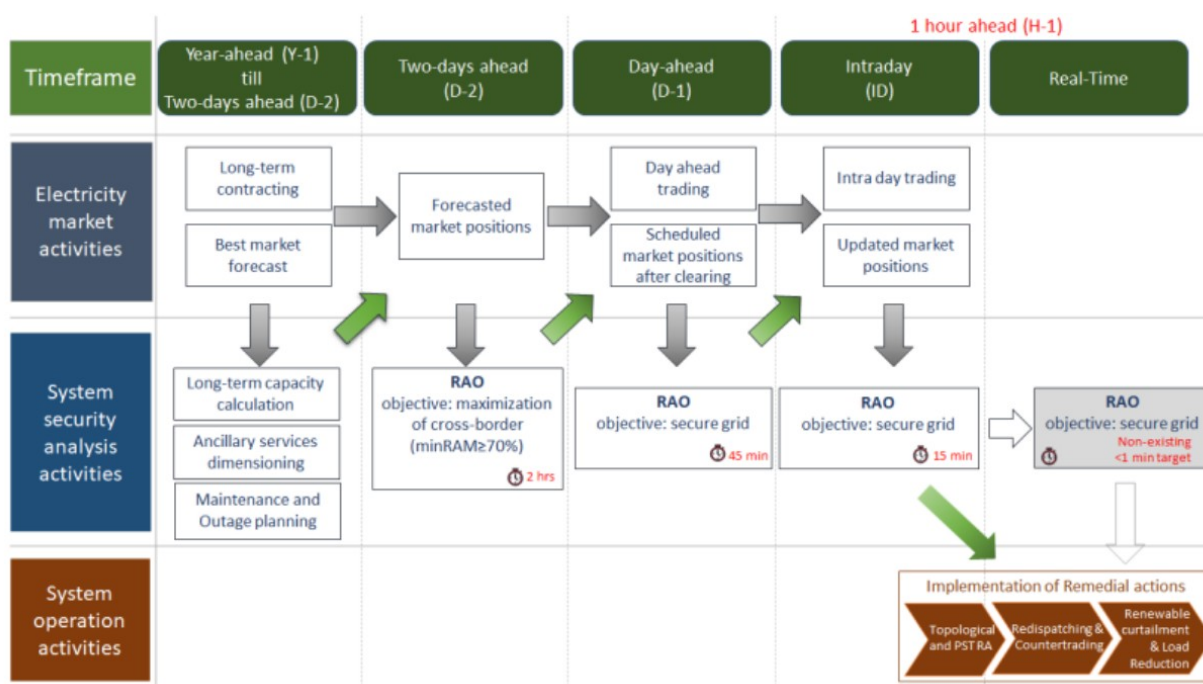


Figure 1 Overview of processes around European electrical power system operation

It is important to mention that once system operation reaches real time, the electrical power system operator is not focused anymore on the global optimum and cost of the

operation, but rather does his best to keep the system stable and ensure energy supply to all end users. In general, in case of security constraints identified in power system operation, three types of RAs are available to the power system operator: a) grid reconfiguration (topological RAs and PST tap changes) - non-costly; b) redispatching and countertrading – costly; c) Cross-border capacity and/or renewable generation curtailments and consumption reduction - last resort costly measure.

Additionally, one can easily conclude that with increased number of intermittent energy sources and number of market participants, forecasting of the market will become more complex and inaccurate, leading to: a) increased flexibility requirements – costly; b) increased number of redispatching and countertrading activations in real time - costly and not globally optimal; c) generation and load reductions – undesirable.

In the end, the following is going to reflect on the electricity prices for the end users, and likely to the unwanted usage of CO₂ emission units.

Considering that, depending on the process, minimal or no approximations can be applied to the optimization process, it is in principle divided into two main parts:

1. **Security analysis:** Main instrument to perform capacity calculation and analysis of the electrical power system stability in line with the forecasted and/or changed market positions, adjusted grid configuration due to unplanned unavailability of grid elements, etc. Within this step, load flow and sensitivity computations are performed for each outage, available remedial action (RA) and their combinations. The set of potential remedial actions, which system operators can apply to ensure stable grid operation, consist of the following: change of a control tap of power shifting transformer (PST), change of a topological status of a power grid element (e.g., switching on/off a high-voltage line, circuit breaker or busbar coupler), change of production and/or consumption at a certain node in the grid (e.g., redispatching). Sensitivities describe how much load flow/voltage will change on a certain element if some other condition is changed - nodal power injection, tap of the PST, element status. Calculation of these factors requires significant time that can easily increase with new outages/elements being observed and number of RAs to analyze.
2. **Combinatorial optimization:** combinatorial optimization of the RAs and their effects as calculated in step one. In general, optimization shall find optimal set of RAs activations in order to obtain a state in which the maximum value of element load flows is as small as possible, as well as associated system operation costs. To reach it, optimization algorithms favor usage of non-costly RAs (topological RAs and PST tap changes), ahead of costly RAs (changing of power plants production - redispatching). But the decision is not only based on the factors calculated in step 1, but also multiple external business constraints imposed by TSOs must be considered.

As discussed earlier, the calculation of factors integral to optimization involves iterative solving of nonlinear (e.g. Newton-Raphson method) or linear equations (e.g. DC load flow) using linear algebra techniques. Each modification in the system topology necessitates recomputation of the system. Notably, in an operational environment, these topology changes can amount to as many as 80,000 modifications leading to inadequately high computation times (it would take around 4 hours to solve this problem with present software and hardware used in European capacity calculation process, while for ROSC time and implementation feasibility assessment still does not exist for the full problem). To tackle it, current computation hardware is robust and complex, especially considering high security requirements.

The nature of quantum physics and consequently quantum computing represents a compelling solution for this problem. A primary benefit arises from the inherent nature of

quantum states, which allows that particles are in superposition of multiple states simultaneously. For example, an electron in a quantum system can simultaneously occupy multiple positions or energy states until it is measured. Consequently, opposite to classical computing where information is stored in bits which can be either in state 0 or 1, quantum computing stores information in quantum bits, or qubits, which can be in superposition of 0 and 1. Mathematically, quantum state is described as vector in Hilbert space. Using Dirac bra-ket notation, which is common when representing quantum algorithm, qubit can be defined as:

$$a|0\rangle + b|1\rangle,$$

where probability amplitudes a and b are complex numbers, with normalization:

$$|a|^2 + |b|^2 = 1.$$

In addition to the superposition principle, another important quantum physics property is the quantum entanglement. It enables to reach so called quantum supremacy for some of the algorithms already with 70 entangled qubits [5], meaning that quantum computer with such number of qubits will solve some problems that classical computer cannot solve. In this entangled state, measuring one qubit immediately affects the state of the other. If we measure the first qubit and find it in the state $|0\rangle$, the state of the second qubit is also determined by this measurement (for example, $|0\rangle$). If the first qubit is in the state $|1\rangle$ upon measurement, the second qubit will also be found in the specific state (for example, $|1\rangle$). This correlation holds no matter how far apart the qubits are, a phenomenon that Einstein famously referred to as "spooky action at a distance". The number of possible quantum states for 2 entangled qubits is $4 = 2^2$. It is straightforward to see that the number of possible quantum states for n entangled qubits is 2^n . This exponential growth, combined with the possibility of superposition, provides the superiority of quantum computers. When entangling quantum states, the mathematical tool we use is the tensor product, which underlies exponential growth. In classical systems, this is contrasted with the Cartesian product, where growth is linear.

This is evident from the quantum algorithm proposed by Shor [6,7] for factorization which is exponentially faster than any known classical algorithm, and Grover's quantum search algorithm [8] capable of searching a large database in time square root of its size.

The efficacy of quantum parallelism is notable; however, a significant limitation arises during the measurement of outputs. Upon measuring a quantum system, its quantum wave function collapses, transitioning the system from a state of superposition to a specific, determinate state. To resume computations, the system must be reinitialized to the appropriate initial state. Moreover, the management of measurements presents further challenges. Qubit quality, coherence times and error rates pose critical hurdles. In order to tackle such issues, multiple entities (including Google, IBM and various startups) employ various error correction algorithms, along with the development of quantum algorithms as such. Additionally, the challenges of scaling up the number of qubits are so great that some researchers think it will require totally different hardware from the microelectronics used by the likes of IBM and Google, where coherence time is typically around a millisecond at best, meaning that all quantum computation must happen within that time frame.

Most notable qubit types are: a) Superconducting qubits [9] - Operating in low-temperature environments, this is currently the most advanced technology; b) Trapped ions [10] - A technique that manipulates individual ions to realize qubits. Trapped ion qubits are

noteworthy for long coherence times as well as high-fidelity measurements; c) Topological quantum computing [11] - A research-stage technology known for stronger error resistance; d) Neutral atoms [12] – Using lasers, these atoms can be excited into a number of quantum states, any two of which can be used to create a qubit that is well suited for scaling up and performing operations (e.g., Aquila quantum computer); e) Photons [13] – By setting and measuring the directional spin states of individual light particles, photon qubits can be used to send quantum information across long distances through optical fiber cables and are currently being used in quantum communication and quantum cryptography.

In terms of the state-of-the-art quantum computer, at the end of last year, IBM announced a chip with 1121 qubits called the Condor [14] and the company Atom [15] released a chip with 1125 qubits, but error correction remains the main challenge.

2. Approach towards Flexibility and Business Experiences and success stories

As discussed in the previous two chapters, considering the intermittent nature of renewable energy sources, grid flexibility and better utilization of it will become increasingly important to maintain the security of supply in the future. Quantum computing as enabling technology could be one of the answers on how to efficiently optimize power system operation, even close to real time.

Having a tool that can provide optimal grid configuration and generation outputs should reduce flexibility requirements, and lead to more efficient wholesale markets and less curtailment needs.

Since current system optimization is based on the (iterative) solving of linear equations using DC load flow method, one of the quantum algorithms that could be used for this problem is Harrow-Hassidimi-Lloyd (HHL) quantum algorithm which theoretically provides exponential speedup [16]. HHL algorithm can be used to solve equation

$$A|x\rangle = |b\rangle,$$

where $A \in \mathbb{R}^{N \times N}$ is Hermitian matrix that is equal to admittance matrix vector $|x\rangle \in \mathbb{R}^{N \times 1}$ is the desired solution, i.e. the quantum state which encodes the power system nodal angles in its amplitudes, and vector $|b\rangle \in \mathbb{R}^{N \times 1}$ is the quantum state which encodes the known power system nodal balances in its amplitudes. The HHL algorithm run-time is theoretically equal to:

$$O\left(\frac{s^2 \kappa^2}{\varepsilon} \log(N_b)\right),$$

where N_b is number of linear equations, κ is (Hermitian matrix) system condition number, s is matrix sparsity and ε is accuracy of the solution.

The HHL algorithm has been experimentally implemented on various physical platforms, and it can now be performed on publicly accessible quantum computing platforms, such as the IBM Quantum Experience [17] using Qiskit software development kit, whose qubits are made from so-called superconducting transmons.

Main issues identified related to application of HHL algorithm for security analysis problem include: a) Need for quantum memory to perform iterative HHL-based quantum algorithms and achieve computational speedup; b) Need for more shallow-depth quantum circuits to mitigate noise impact and scalability issues; c) Need for a matrix preconditioning and/or filtering functions to address computational issues caused by ill-conditioned power systems; d) The process of extracting the values of nodal angles from the quantum state $|x\rangle$ reduces the speedup provided by quantum computers [18], therefore there is a need to formulate the problem in such a way that the quantities of interest are scalar products and

expectation values, which would reduce the number of measurements needed to obtain useful information from the solution provided by the HHL algorithm.

There are also other novel quantum algorithms being developed that can solve linear equations, such as algorithms based on adiabatic quantum computing (AQC) [19] or (variational) hybrid quantum-classical algorithms (VHQA) [20].

Briefly, in AQC we assume that the Hamiltonian of a certain quantum system depends on some parameter which changes in time, and that the system is initially in one of its non-degenerate eigenstates with an energy gap to other eigenstates. The adiabatic theorem ensures that such quantum system evolves in time in such a way that it remains the eigenstate of the current Hamiltonian, under the condition that the change of the Hamiltonian is sufficiently slow (adiabatic) and that there is always an energy gap. In other words, in the adiabatic process the eigenstate of the initial Hamiltonian continuously evolves into the eigenstate of the final Hamiltonian. In the context of quantum computing, we can imagine the final state of the system as a state which contains information about the requested the solution to the problem. In Ref. [19], the authors proposed two algorithms for solving the linear system, i.e., preparing the quantum state $|x\rangle$ which is proportional to the solution of $A|x\rangle = |b\rangle$. The advantage of such algorithms is that they do not use a phase estimation algorithm, nor an amplitude amplification algorithm, so a large number of ancillary (ancilla) qubits are not required.

VHQA algorithms are interesting in the context of reduced number of qubits requirements since optimization of variational parameters is performed on a classical computer. As a result, the number of required quantum gates, or the depth of the quantum circuit, is reduced, which leads to a reduction in noise. For example, the VHQA strategy has been applied in Ref. [20] where it has been demonstrated that even larger systems of linear equations (of dimensions 1024x1024) can be solved with such approach.

In addition to HHL, AQC, VHQA and other algorithms that would be used for sensitivity analysis which requires solving linear systems of equations, the optimization procedures for electric power systems generally need methods for solving nonlinear systems and can be defined with generic objective function $f(x)$ that has to be minimized. In this context, two important quantum optimization algorithms are quantum gradient descent method and the quantum Newton's method [21].

The gradient descent method seeks the point of minimum by starting from an arbitrary initial value x^0 and moving the argument of the target function in the direction of the negative gradient of the target function. The process continues in each subsequent step, according to the expression:

$$x^{t+1} = x^t - \eta \nabla f(x^t),$$

where $\eta > 0$ is parameter that can be adjusted during the iterative procedure.

In Newton's method, the iterative process also takes into account the curvature of the target function, namely the Hessian matrix H , whose elements are $H_{ij} = \frac{\partial^2 f}{\partial x_i \partial x_j}$, with a step:

$$x^{t+1} = x^t - \eta H^{-1} \nabla f(x^t),$$

where matrix element H_{ij} is calculated in point x^t .

The quantum version of these optimization algorithms described in [21] focus on sparse homogeneous polynomials, requiring the vector x to be normalized and utilizing qubit-based representations for efficiency. These algorithms, including quantum versions of gradient descent and Newton's methods, are designed to scale exponentially with the number of iterations yet poly-logarithmically with the vector dimension, suggesting they are effective for large systems where initial approximations are near true solutions. Challenges include their complexity and the need for additional quantum computational techniques like phase estimation and matrix operations, with their practical application and broader adoption dependent on future advances in quantum computing technology.

Note: We note that very recently several implementations of power-flow analysis in electric systems with quantum computing approaches have been reported (see Ref. [22] for the most recent one, and refs. therein). However, such calculations have been limited to small-scale test systems (for example, with up to 14-bus test system in [22]).

3. Added Values/Conclusion

This paper provides overview of the main challenges of power system operation where amount of the renewable energy sources in the energy mix is significant, where typical generation and load patterns do not exist anymore since more and more grid users act as prosumers and their number increases significantly. With the goal of better grid utilization and enhanced security, optimization of the grid operation has been introduced into multiple European grid and market operation processes. However, the optimization problem has been quite simplified due to the complexity of mathematical operations and consequently significant hardware requirements. Further advancements in this area are therefore slowed down or completely blocked.

Quantum algorithms and quantum computing become more and more advanced and stable, leading to the fact that they must be considered as enabling technology that could potentially bring breakthroughs to grid optimization.

This paper also discussed state-of-the-art quantum computers and quantum algorithms for linear algebra and linear optimization, with focus on HHL and Newton-Raphson quantum algorithms.

Main question to be answered though is how far is the point in time when quantum computing could be used for operational power system purposes. If the noise, i.e., errors in qubits, were small, computers with about 50 entangled qubits could compute the problem discussed using HHL algorithm in significantly reduced time [5]. However, since the noise (or random errors on qubits) is still significant, it is necessary to use what is known as the quantum error correction code, or schemes for error correction that require redundancy in the number of qubits needed for computation. Colloquially speaking, several entangled qubits are needed to record 1 qubit of information (redundancy), and a so-called quantum error correction scheme. Therefore, to perform the HHL algorithm for matrices of the order of size 100,000 squared, 50 entangled qubits need to be increased several times, and such computers do not exist today. As mentioned in the paper, just at the end of last year IBM released Condor with just over 1000 qubits, while their industry-defining roadmap for a decade of quantum innovation sets ambitious targets in terms of number of quantum gates and qubits developments until 2033.

Finally, Europe started to invest more in the quantum computing and IBM will complete a new EU quantum data center in Ehningen, Germany, in 2024, bringing local quantum resources to Europe [23].

The authors of this paper strongly believe that within the next 10 years there will be a quantum computer available able to solve the power grid optimization problem. Bearing in mind the importance of secure electricity supply and the complexity of grid optimization, there is a huge potential for application of quantum algorithms for RAO problem. Unfortunately, no one yet has been able to convincingly demonstrate a quantum advantage in solving large-scale power system problems mainly because of noisy intermediate-scale quantum (NISQ) era, where quantum devices are noisy and have limited quantum resources.

Therefore, the Authors strongly believe that development of scalable quantum algorithms which will be able to solve real size RAO problem must be put in focus now to be prepared once hardware is ready, especially considering disruptiveness it brings.

References

- [1] [Online]. Available: <https://www.precedenceresearch.com/quantum-computing-market>
- [2] [Online]. Available: <https://eur-lex.europa.eu/legal-content/EN/TXT/?uri=CELEX%3A32017R1485>
- [3] [Online]. Available: <https://eur-lex.europa.eu/legal-content/EN/TXT/?uri=CELEX%3A32015R1222>
- [4] [Online]. Available: <https://eur-lex.europa.eu/eli/reg/2019/943/oj>
- [5] D. Jukic, K. Lelas, H. Buljan, Feasibility and Design Study of Implementation Potential of Optimization Algorithm Currently Used in the Field of Power System Calculations in a Quantum Computing Environment, December 2020.
- [6] P. W. Shor, Algorithms for quantum computation: Discrete log and factoring. Proceedings of the 35th Annual Symposium on Foundations of Computer Science, pp. 124-134, November 1994.
- [7] P. W. Shor, Polynomial-time algorithms for prime factorization and discrete logarithms on a quantum computer, SIAM Journal on Computing 26, pp. 1484-1509, (1997).
- [8] L. K. Grover, A fast quantum mechanical algorithm for database search. Proceedings of the Twenty-Eighth Annual ACM Symposium on the Theory of Computing, Philadelphia, USA, pp. 212-219, May 1996.
- [9] M. Kjaergaard *et al.*, Superconducting Qubits: Current State of Play, Annu. Rev. Condens. Matter Phys. 11, pp. 369–95, (2020).
- [10] C. D. Bruzewicz, J. Chiaverini, R. McConnell, and J. M. Sage, Trapped-ion quantum computing: Progress and challenges, Appl. Phys. Rev. 6, 021314 (2019).
- [11] C. Nayak, S. H. Simon, A. Stern, M. Freedman, and S. Das Sarma, Non-Abelian anyons and topological quantum computation, Rev. Mod. Phys. 80, 1083 (2008).
- [12] L. Henriët *et al.*, Quantum computing with neutral atoms, Quantum 4, 327 (2020).
- [13] S. Slussarenko and G. J. Pryde, Photonic quantum information processing: A concise review, Appl. Phys. Rev. 6, 041303 (2019).
- [14] [Online]. Available: <https://www.ibm.com/quantum/blog/quantum-roadmap-2033>
- [15] [Online]. Available: <https://atom-computing.com/>
- [16] A. W. Harrow, A. Hassidim, and S. Lloyd, Quantum Algorithm for Linear Systems of Equations, Phys. Rev. Lett. 103, 150502 (2009).

- [17] [Online]. Available: <https://quantum.ibm.com/>
- [18] S. Aaronson, Read the fine print, Nat. Phys. 11, 291 (2015).
- [19] Y. Subasi, R. D. Somma, and D. Orsucci, Quantum Algorithms for Systems of Linear Equations Inspired by Adiabatic Quantum Computing, Phys. Rev. Lett. 122, 060504 (2019).
- [20] C. Bravo-Prieto, R. LaRose, M. Cerezo, Y. Subasi, L. Cincio, and P. J. Coles, Variational Quantum Linear Solver, Quantum 7, 1188 (2023).
- [21] P. Rebentrost, M. Schuld, L. Wossnig, F. Petruccione, and S. Lloyd, Quantum gradient descent and Newton's method for constrained polynomial optimization, New J. Phys. 21 073023 (2019).
- [22] Z. Kaseb, M. Moller, P. P. Vergara, and P. Palensky, Adiabatic Quantum Power Flow, <https://doi.org/10.21203/rs.3.rs-4368636/v1>
- [23] [Online]. Available: <https://newsroom.ibm.com/2023-06-06-IBM-to-Build-its-First-European-Quantum-Data-Center-to-Serve-Expanding-Ecosystem>

G05

International Projects for the Energy Transition

G0503

Market-based procurement of grid-friendly flexibility – the ENFLATE project

André S. Eggli (1), Sébastien Rolland (2), Christoph Imboden (1), Davide Orifici (2)

(1) Lucerne University of Applied Sciences and Arts, Lucerne/Switzerland;

(2) European Power Exchange EPEX SPOT, Paris/France;

Tel.: +41 41 349 33 53

andre.eggli@hslu.ch

Abstract

ENFALTE is an international research consortium funded within the Horizon Europe framework [1]. Aim is to support the electrification of the heat and mobility sector by developing tools for the streamlined integration of intermittent renewable energy sources at large scales. Thereby, flexibility procurement and coordination platforms are being developed and field tested. In total, six demonstration sites are deployed in Bulgaria, Greece, Spain, Sweden, and Switzerland. Among the consortium partners are prosumers, distribution system operators, transmission system operators, market operators, aggregators, regulatory bodies, flexibility service providers, and manufacturers.

This contribution outlines the intermediate results related to the eastern Switzerland demonstrator after one third of the overall project duration. Focus lies on the market design and its adaption into the EPEX SPOT “localflex” market platform. The platform covers the end-to-end journey for market-based flexibility procurement, from onboarding and asset registration, through trading, to calculating baselining and settlement results after flexibility events. A grid model within the platform represents the distribution substations where the local distribution operator requires flexibility. Assets are then associated with the correct substation and can be used to provide localized flexibility or aggregated to offer flexibility at higher voltage levels for the balancing group and TSO. Transactions on localflex are conducted by matching buy and sell orders via closed-gate, pay-as-clear auctions, after an accumulation period during which orders are submitted on the localflex platform.

The proposed market design will accelerate the coordination of TSOs, DSOs and consumers, by enabling the access of distribution grid-connected assets in flexibility markets, and thereby lower the barriers for the small-scale assets’ introduction in flexibility markets towards a robust pan-European electricity network that optimally operates with a 100% RES penetration rate while being economically viable for long-term operation.

Introduction

Today, only large assets participate in European flexibility markets, failing to address growing issues in local distribution networks and excluding the flexibility potential of a large portion of smaller installations. In Europe, demand side flexibility (DSF) is recognized as an instrument for the best utilization of current distribution grids and consequently to the best allocation of resources for grid investments. However, as of today, the number of local flexibility markets in the EU is limited to a small number of projects, most of which are in pilot stage.

This contribution outlines how a digital marketplace can lower the barriers for smaller assets to deliver flexible power at the distribution level. This will be achieved through standardization of the market process, digitization of the operation and harmonization into a local flexibility mechanism. Through the demonstration activities it is expected to diminish the costs associated with market-based procurement of flexibility in comparison to traditional approaches of flexibility activation (e.g. ripple control). At the same time, the hosting capacity of the grid shall be increased due to flexibility being used to avoid curtailment of renewable energy and the MV transformer lifespan will be improved due to improved utilization factor and reduced peak load.

1. Project Background and Implementation

This demonstration project achieves flexibility for grid resilience through consumer involvement and distributed energy resources integration via local flexibility markets. A centralized market platform facilitates the coordination of demand side flexibility contracting and activation. On the seller side of the market, flexibility offers from residential heat pumps, electric boilers and electric car charging are submitted to the market via an aggregator. On the buyer side, multiple actors purchase flexibility for a variety of use cases: (1.) The balancing group may purchase flexibility from the local market to optimize its day-ahead profile on the energy-only market. (2.) Closer to real time, demand side flexibility facilitates the avoidance of balancing group imbalance costs. (3.) The TSO procures short-term flexibility related to balancing services. In the pilot, this use case is facilitated via an aggregator. (4.) The local distribution system operator uses flexibility for peak shaving. The peak loading of grid components reduces, and costly grid expansion measures are postponed. During such hours of critically high energy flows, the physical grid limits are incorporated into the boundary conditions of the market clearing optimization algorithm.

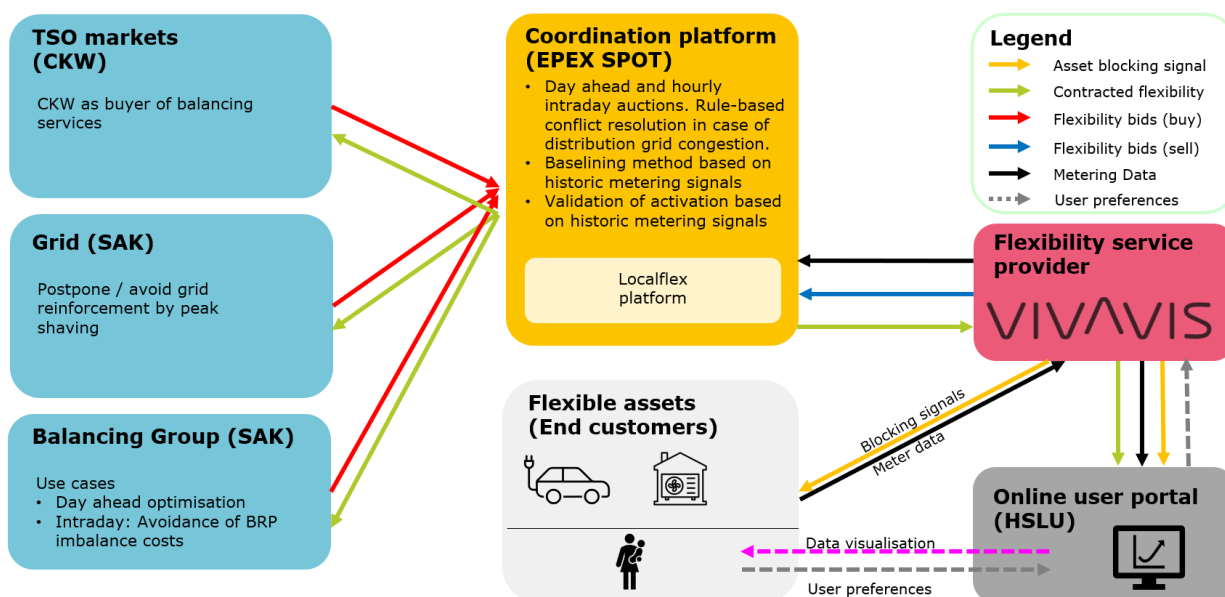


Figure 1: Market actors and their data interactions

For the trials, the platform has been configured to run utilization (activation) auctions at the day-ahead stage and then intraday on an hourly basis. Intraday auctions are scheduled to run 45 minutes before delivery to best facilitate the various use cases of flexibility procurement being demonstrated.

The pilot area spans the two neighboring villages “9243 Jonschwil” and “9247 Henau” in eastern Switzerland, which are part of the SAK distribution grid. It involves a grid area with 419 different end consumers, including a mix of industrial demand response, multi-family buildings, and single-family houses. The area selected is characterized by a high penetration of PV infeed, EV charging, and heat pumps. The whole pilot area is supplied by three MV/LW transformers, which operate close to their capacity limit in certain days of the year.

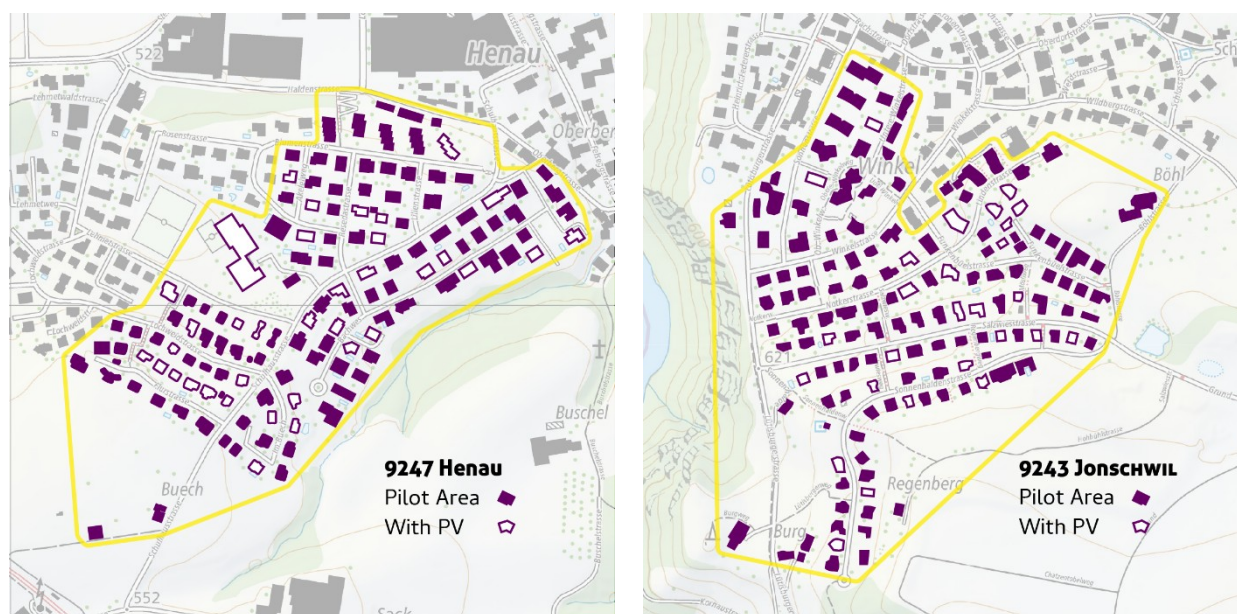


Figure 2: Perimeter of the pilot area in Henau (left) and Jonschwil (right).

3. Project Outcomes so far & Outlook

ENFLATE is a four-year project (September 2022 to August 2026). Starting from fall 2024, there will be one full year of pilot operation with live market operation and physical DSF activation in the pilot households.

The activities conducted so far focused on the market design and the necessary software upgrades. A screenshot of the localflex platform is shown in Figure 3.

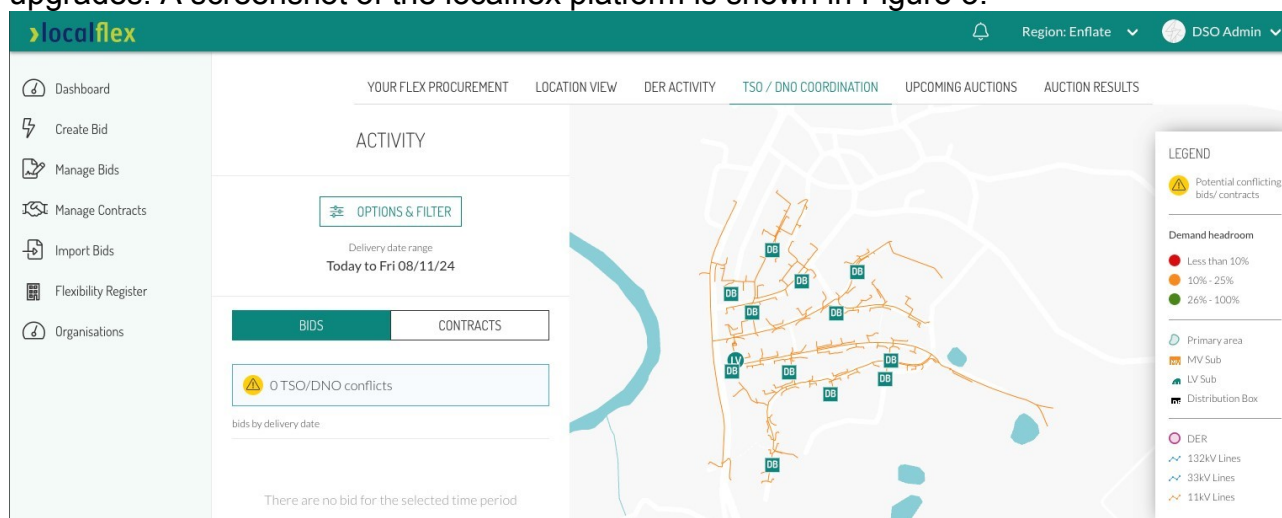


Figure 3: Screenshot of the localflex platform, zoomed in on the Jonschwil pilot area

Dedicated communication tools were developed to engage and onboard the pilot inhabitants. Hardware for metering and switching the residential heat pumps, electric boilers and electromobility charging stations was installed in all households.

Through the demonstration activities it is expected the diminishment of the costs associated with market-based procurement of flexibility in comparison to alternatives approaches of flexibility activation (ripple control, time of use tariffs), the hosting capacity of the grid will be increased due to flexibility being used to avoid curtailment of renewable energy and the MV transformer lifespan will be improved due to improved utilization factor and reduced peak load.

This demonstration aims to minimize the barriers for the establishment of new business models for stakeholders in the energy services, and thus increases both active consumers' willingness to invest in RES and their quality of life. The business models developed in the project enable households to combine the provision of energy services focused on flexibility with investments in assets at consumer level that contribute to long-term changes in electricity production or consumption, such as RES generation, deep renovations, new, more efficient and intelligent appliances that form a major part of household energy consumption (e.g., heating).

Beyond the ENFLATE project, it is envisioned that building upon the activities of the project more and more stakeholders in the European region will start creating new business models that combine services across different industries, with an explicit focus on the end-users' prosperity.

This project has received funding from the European Union's Horizon Europe program under the Grant Agreement No 101075783.

This work was supported by the Swiss State Secretariat for Education, Research and Innovation (SERI) under contract number 22.00283.

References

- [1] ENFLATE consortium website, <https://enflate.eu/>, Last accessed 2024-05-01.

G0504

A Case Study for Unveiling Flexibility Options in Achieving Swiss National Energy Goals

Olena Levon (1), André Eggli (2), Christoph Imboden (2)

(1) HSLU, Institute of Electrical Engineering, CC Digital Energy and Electric Power;

(2) HSLU, Institute of Innovation and Technology Management, FT Energy Economics,

Horw/Switzerland;

Tel.: +41-41-349-3034

olena.levon@hslu.com

Abstract

This paper examines the possibilities and crucial importance of leveraging flexibility within the Swiss electricity grid against the backdrop of the national energy targets for 2050. This case study focusses on an in-depth analysis around three low voltage transformers and corresponding 15min load/consumption measurements. The potential of flexibility as an imperative for ensuring a resilient and adaptive energy infrastructure is analysed.

The study focusses on opportunities for applying flexibility within the grid, emphasizing its pivotal role in mitigating challenges associated with the integration of renewable energy sources and the growing demand for electricity. The investigation delves into future energy flows based on Swiss Federal Office of Energy (SFOE) scenarios.

A detailed exploration of the historic 2023 metering data at the transformer level in the pilot area provides a foundation for the subsequent analysis, where multiple scenarios for the low voltage grid and the corresponding three transformers are outlined. The literature indicates that flexibility can be instrumental in addressing overloading risks and potential disruptions, especially during critical periods such as cold winter periods or sunny spring days. Our results reveal a concerning trajectory post-2030, indicating that without proactive measures, the transformers are susceptible to overloading – Although only for a few hours each year. This poses the question on whether a smart approach using demand side flexibility could avoid or delay costly grid extension measures.

This study seeks to not only contribute to the academic discourse on the topic but also serve as a practical guide for policymakers, grid operators, and energy providers. By illuminating the possibilities and opportunities for using flexibility, this contribution aims to inspire informed decisions in the pursuit of a secure, sustainable, and flexible energy supply for Switzerland's future.

Introduction

As the world transitions towards a low-carbon energy future and we stand at the crossroads of an energy evolution, characterised by a surging demand for electricity and an unprecedented transition towards sustainability, flexibility emerges as a pivotal factor in the resilience and adaptability of our power systems.

This paper explores the multifaceted importance of flexibility in addressing the challenges posed by the growing demand for electricity and the integration of intermittent renewable energy sources. Further, the feasibility of utilising flexibility in the ENFLATE project's pilot area will be analysed.

The Swiss national energy targets for 2050 aim to achieve a 90% reduction in greenhouse gas emissions and a shift to almost 100% renewable energy. A pivotal element of this strategy involves transitioning the electricity supply from large, centralised power plants to smaller, decentralised assets. Simultaneously, the heating and mobility sector is decarbonised by electrification. The growing integration of photovoltaics (PV), heat pumps, and electric vehicles (EVs) in Switzerland imposes various challenges on the country's electricity grid. The Swiss energy transformation assigns an entirely novel role to the electricity grids. Especially the low voltage levels are affected. Fortunately, at least some of these challenges posed to the existing grid infrastructure can be mitigated by deploying load-side flexibility in a smart way [1].

Flexibility in energy systems involves adjusting electricity supply or demand to match varying levels of renewable energy generation. This adjustment may be achieved through measures such as interconnection, demand response, storage, and flexible generation in power plants.

In 2022, the Swiss Federal Office of Energy (SFOE) developed the scenario framework 2030/2040 [2]. It is based on the Swiss national "Energy Perspectives 2050+". Currently, three scenarios are being considered, differing in the combination of technologies and the pace of transition to renewable energy sources in the electricity sector. These scenarios are:

- **"Reference" scenario 1:** This scenario prioritises a substantial electrification of the energy system and a rapid expansion of domestic renewable electricity production. Electric demand is expected to significantly increase as EVs and heat pumps become more common.
- **"Divergence" scenario 2:** This scenario foresees an even more substantial increase in electricity consumption combined with a delayed expansion of domestic production. This increase could lead to increased reliance on imported electricity and potentially higher electricity prices.
- **"Sector coupling" scenario 3:** This scenario assumes a more critical role for biogas and synthetic gases and a more rapid expansion of PV. These assumptions lead to a more decentralised energy system.

Table 1 below provides an overview of the most important indicators for the target years 2030 and 2040 at the national level. Substantial differences in electricity production and consumption will become genuinely apparent in 2040. Conventional electricity consumption will be reduced by around 15-18% in scenarios 1 and 3 and by around 8% in scenario 2 by 2040. This is attributed to efficiency measures in lighting, electrical appliances and building technology and by replacing direct electricity heating and electric boilers.

Table 1 - Overview of key indicators 2030/2040 for scenarios 1–3.

Source: SFOE Scenario framework for electricity network planning [2]

Year	2019	2030			2040		
Scenario		Sc. 1	Sc. 2	Sc. 3	Sc. 1	Sc. 2	Sc. 3
Electricity production							
PV installed capacity [MW]	2 520	9 770	7 650	12 210	24 070	10 100	30 090
Electrification							
EVs incl. plug-in hybrids*, number [thousand]	40	930	980	870	2 940	3 230	2 520
Heat pumps incl. large heat pumps*, [TWh]	2,44	6,81	7,15	5,53	9,79	10,77	6,96
Electricity consumption							
Household sector without heat pumps, energy volume [TWh]	17,25	14,60	15,33	14,66	12,99	14,28	13,08

The following sections aim to provide a visual understanding of the transformer loading in different scenarios, offering insights into the potential challenges and opportunities.

1. Characterisation of 2023 transformer loading based on historic smart meter data

This section investigates the implications of these scenarios for the Swiss electricity grid, focusing on the two neighbouring villages, "Henau" and "Jonschwil" in eastern Switzerland, which were chosen as pilot areas within the ENFLATE project [3].

There are three low-voltage transformers located within the pilot areas:

- One transformer in Henau with 400 kVA (which could potentially be upgraded to 630 kVA in the coming years)
- Two transformers are located in Jonschwil, each with 630 kVA nominal capacity.

The remainder of this section aims to analyse repercussions related to the growing integration of PV, heat pumps, and EVs in both pilot areas on the distribution grid throughout the period spanning the next two decades according to the SFOE Scenario framework. First, historic smart meter data is compiled as baseline. Second, the historic load is split into its individual components (PV, EVs, heat pumps, residual load). Third, these individual components are scaled to 2030 and 2040 according to the Swiss national energy transition goals.

The historic 2023 metering data is collected and aggregated at the transformer level. The PV generation data and the total load are directly measured by all 419 smart meters in the pilot areas. Availability of Heat pumps and EVs data until July 2023 allows to split the total demand side into components: (1.) Heat pumps, (2.) EVs, and (3.) the residual load as it can be seen at Figure 1.

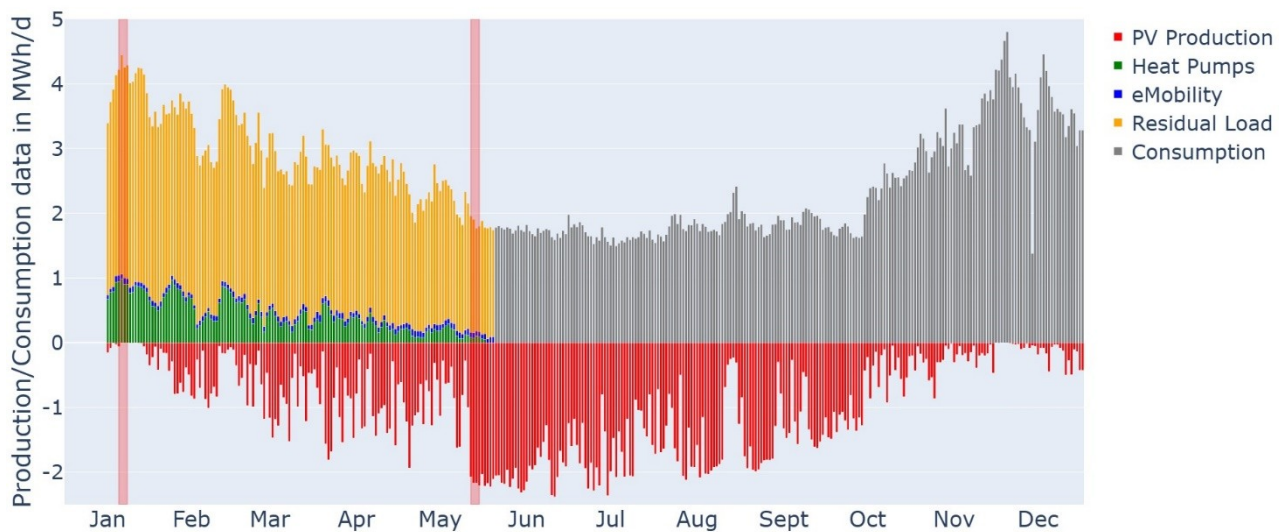


Figure 1 – 2023 smart meter data aggregated at the transformer in Henau

Figure 2 depicts the loading over a few critical days specific to the transformer in Henau that were indicated with red rectangles on Figure 1. The left-hand side of Figure 2 depicts cold winter days characterised by elevated energy consumption from EVs and heat pumps. The date range on the horizontal axis is chosen as the coldest three days in 2023, with the highest daily consumption measured. The right-hand side showcases three sunny spring days with increased PV production. The dates on the horizontal axis are chosen as the days with the highest irradiation values recorded in 2023.

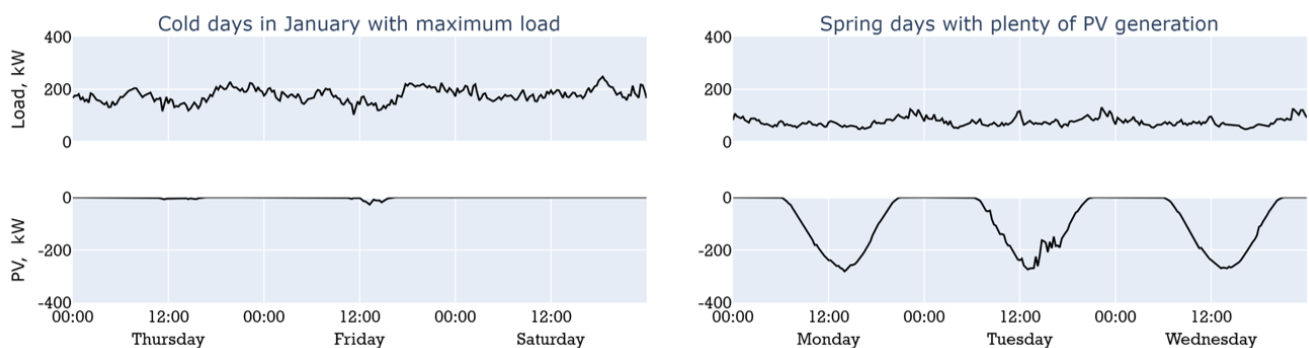


Figure 2 - 2023 smart meter data aggregated at the transformer in Henau for the two extreme periods: Cold winter days with high consumption (left), and sunny spring days with high PV infeed (right)

The data-extracting process for disaggregating the total demand side into components is shown in Figure 3. The heat pump component is estimated using non-intrusive load monitoring (NILM). A NILM algorithm from the DOMOs project [4] is deployed to extract the heat pump time-series load profiles from the total load.

Since the EV penetration today remains very close to zero, the time-series data for EVs is based on a dataset of 300+ cars from another measurement campaign outside the pilot area [5] and scaled to fit the pilot perimeters. The residual load is defined as the remaining load not assigned to heat pumps or EVs. Therefore, the residual load mainly consists of electric boilers, heating, kitchen equipment, lighting, etc.

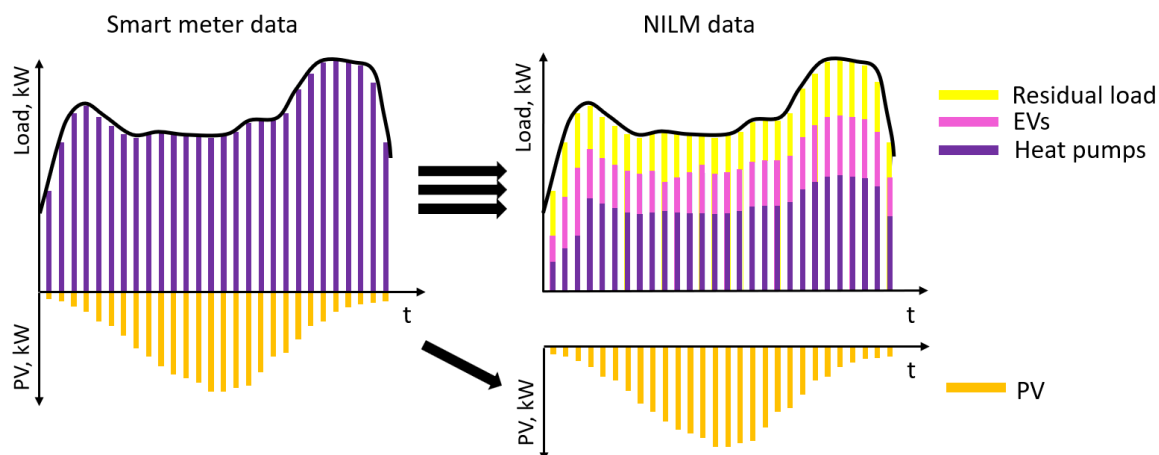


Figure 3 – Sketch of data extraction process from 15min smart meter data to its NILM components. Since PV is measured separately in the smart meter, only the consumption curve has to be split into three subcomponents using NILM

Figure 4 illustrates the status of the Henau transformer as of the year 2023, encompassing analysis of PV data, heat pumps, EVs, and residual load data, with the total summed at the transformer in kilowatts (kW). This transformer is operating well within its nominal operational limits as of 2023.

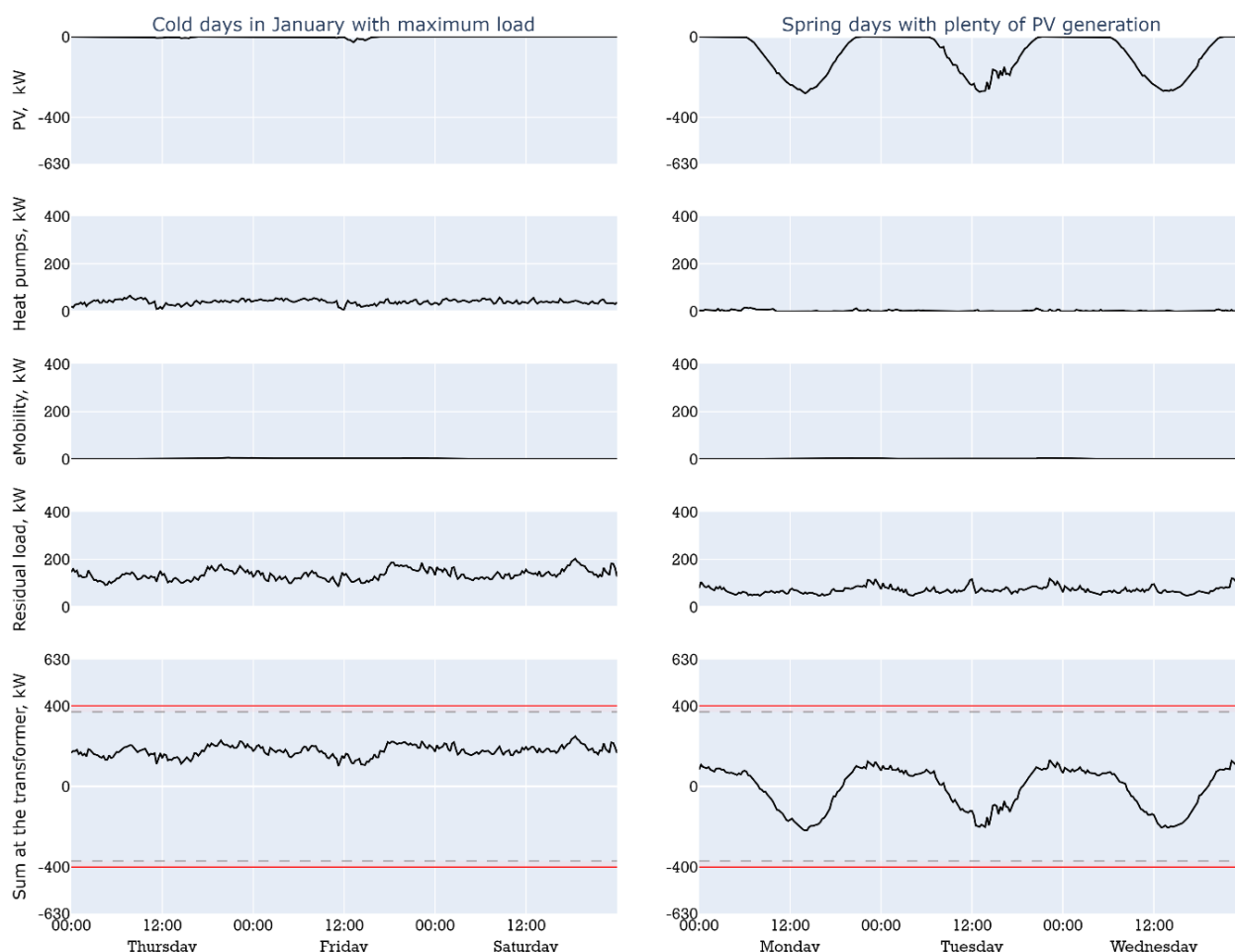


Figure 4 - Overview of 2023 situation at the transformer Henau based on historic metering value. Non-intrusive load monitoring algorithms are used to split the overall load into three components: heat pumps, electric vehicle charging, and the residual load.

2. Simulation of uptake scenarios

This section extrapolates the historic energy flows to 2030 and 2040 by scaling the historic metering data according to the SFOE scenarios. The purpose of the simulation is to examine how many years into the future grid reinforcement measures, or the use of flexibility will become critically important. It is assumed that the uptake of PV, EV, heat pumps, and residual load in the pilot area is directly proportional to the national uptake levels. The scenario interpolation process is shown in Figure by the example of heat pump uptake. The SFOE scenarios contain data points for 2019, 2030 and 2040. Therefore, coefficients for linear interpolation to 2019 are derived from data starting in 2023 (step 1). Steps 2 and 3 relate to the extrapolation towards the target years 2030 and 2040.

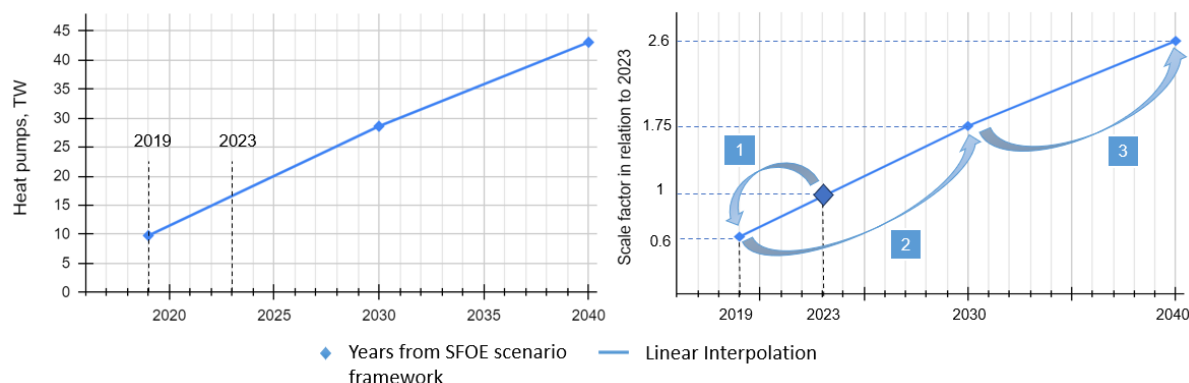


Figure 5 – Linear interpolation of heat pump uptake from 2023 to 2030 and 2040

In Figure 6, the results of all three SFOE scenarios for the transformer in Henau are presented for 2030. The linear scaling coefficient from Figure 5 is applied to all 2023 load curves. For each SFOE scenario [2], different coefficients apply, indicating the uncertainty interval. The lefthand column displays cold winter days with high energy consumption. The righthand column shows sunny spring days with lots of PV infeed and almost no load.

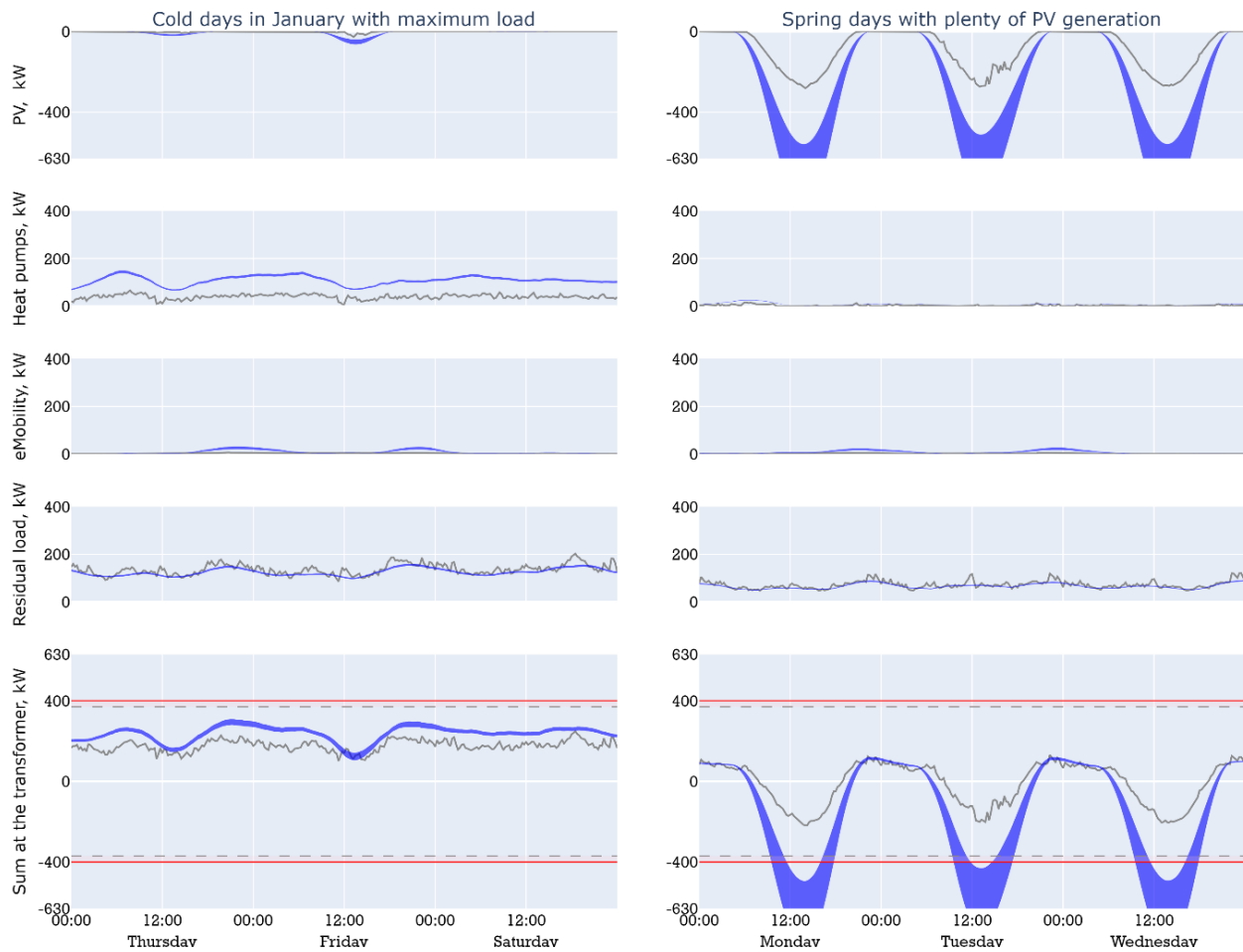


Figure 6 - Loading of the transformer Henau extrapolated to 2030. Gray lines correspond to historic 2023 measurement as baseline, while red lines indicate the transformer's current operational limits. The shaded blue area represents the range of SFOE scenarios 1 to 3.

Figure 7 shows the results for Henau extrapolated to 2040. Please note that the 400 kVA transformer has been upgraded to a 630 kVA unit.

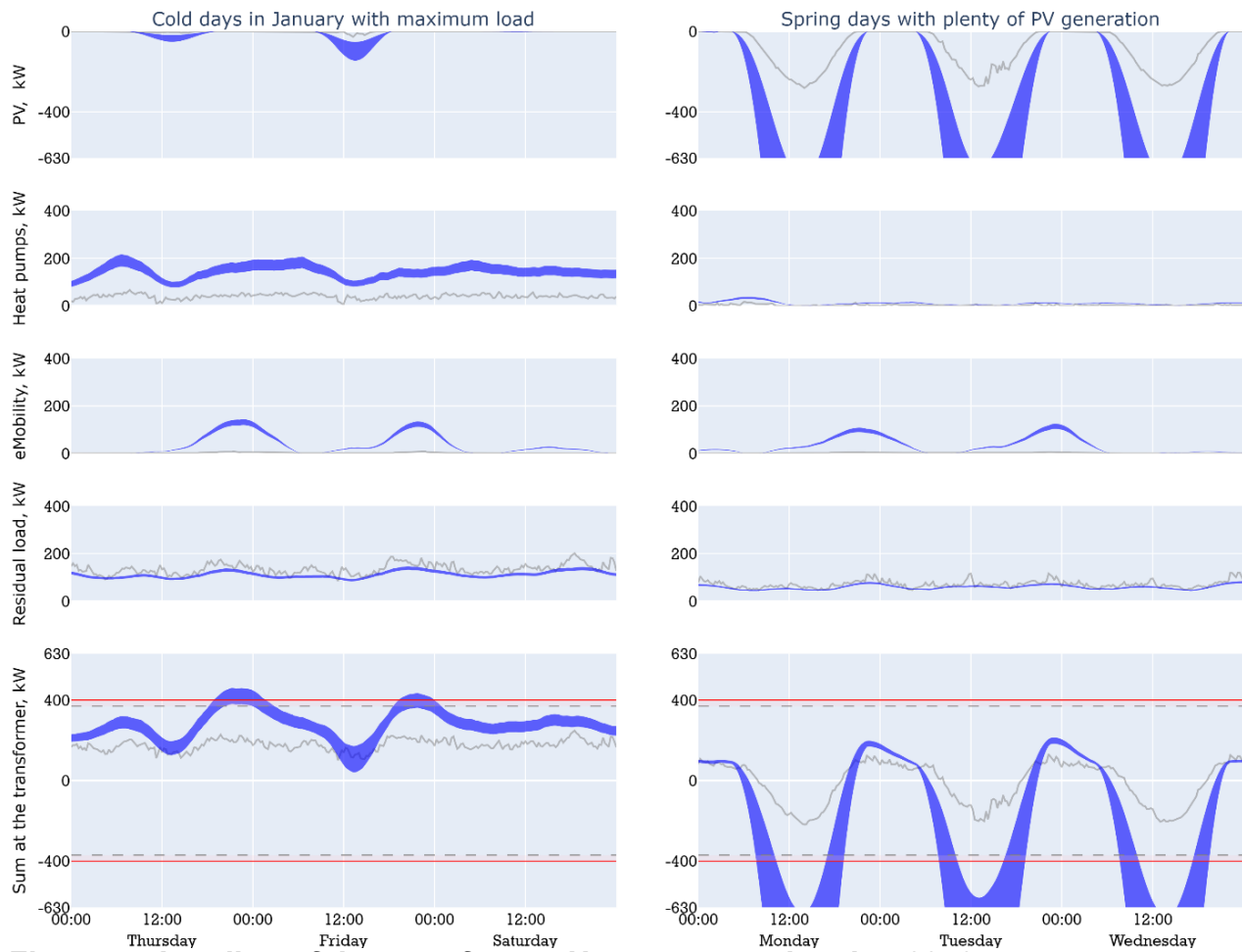


Figure 7 - Loading of the transformer Henau extrapolated to 2040

Figure 8 illustrates the 2040 scenario results for one transformer in Jonschwil. The data includes information on PV generation, heat pumps, EVs, and residual load, aggregated at transformer level.

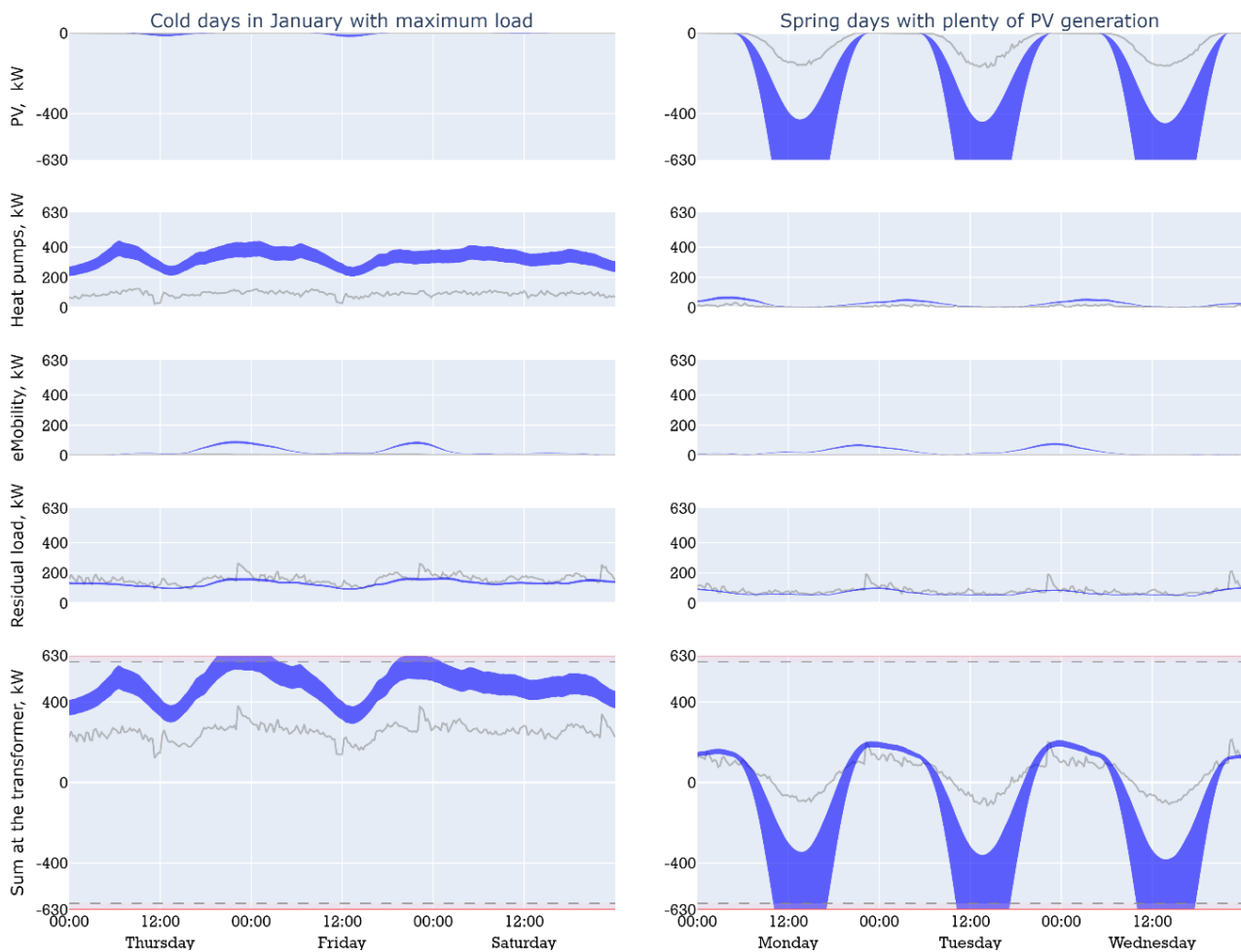


Figure 8: Loading of one transformer in Jonschwil extrapolated to 2040.

3. Flexibility in action

To investigate the potential of flexibility to postpone or avoid costly grid reinforcements, this chapter investigates a highly simplistic strategy for activating flexibility. Aim is to get a feeling for the effects on the grid loading by shifting the consumption of heat pumps and EV and curtailing PV infeed. The strategy is applied to the two critical time periods identified in Figure 1.

For heat pumps and EV, a maximum allowable power consumption limit is established. When this limit is reached, the excess energy consumption is shifted to later time periods. Specifically, when the consumption limit is reached during winter evening hours, EV charging is rescheduled to later hours. This redistribution considers the necessary time by which all EVs must be fully charged, ensuring that charging is completed within the required timeframe without exceeding transformer limits. For the solar energy generated by PV systems, production caps are implemented when generation levels exceed transformer limits. It is assumed that a centralised control entity at the transformer level dispatches each asset per asset group such that the maximum power limit is perfectly respected and perfectly tracked.

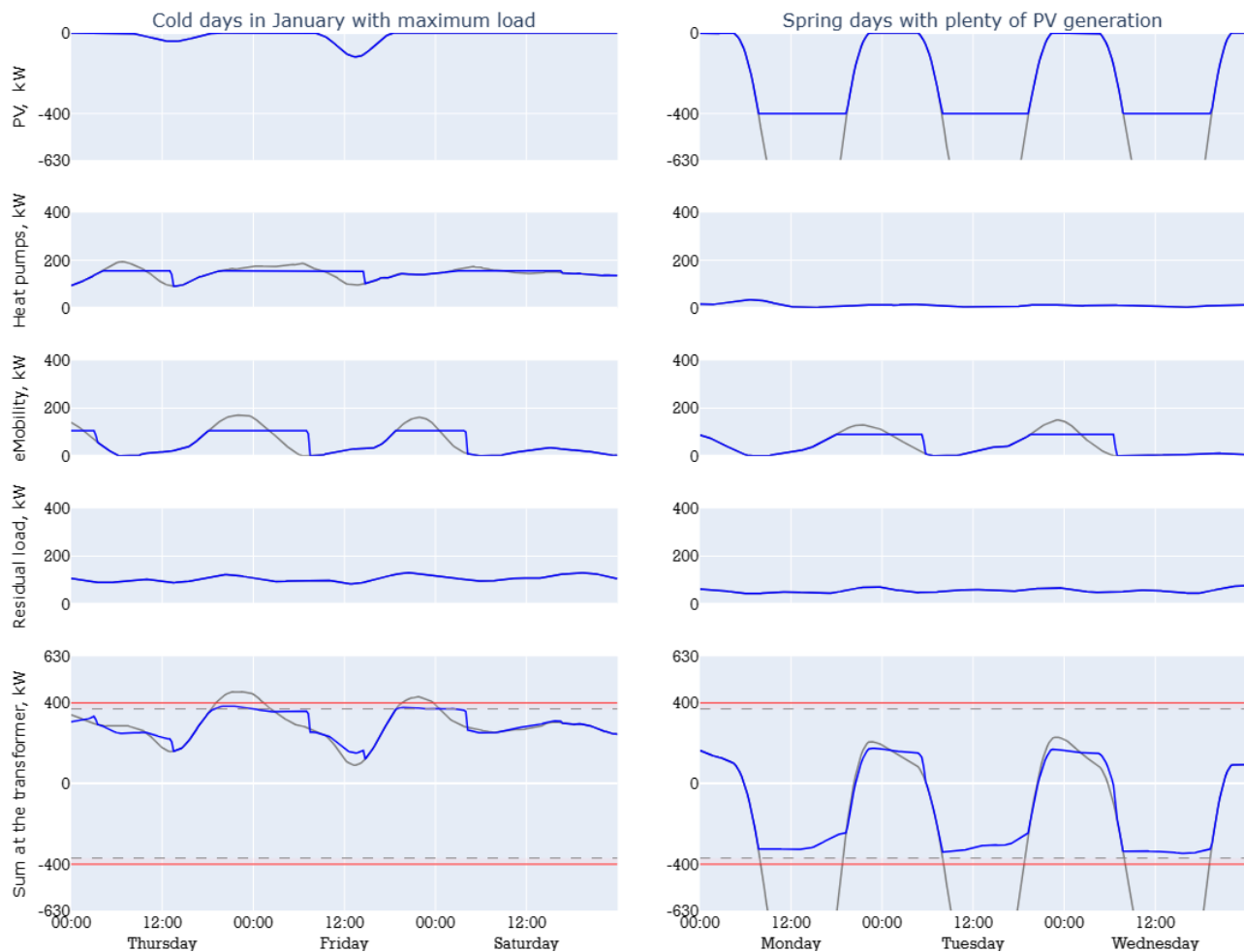


Figure 9: Resulting 2040 transformer loading for Henau when a combination of load shifting and PV curtailment is used to manage the transformer load during critical hours on critical days. Gray lines represent the SFOE scenario 1 for 2040 without flexibility measures. Blue lines show the load with curtailment implemented for heat pumps and EVs, and PV.

4. Analysis and interpretation of results

In the context of the scenario results for the year 2030 presented in Figure 6, the results indicate that without counteraction the transformer Henau will exceed its nominal operational limits around 2030. This underscores the critical importance of proactive measures and strategic planning to address potential challenges in ensuring the longevity and reliability of the grid infrastructure.

In Figure 7, the visual representation of the year 2040 scenario unveils a concerning situation at the transformer Henau. Particularly during cold winter days, overloading surpasses the transformer limits. Obviously, curtailing PV infeed alone will not help on critically cold winter days.

In the Jonschwil area, a situation like Henau is observed. An example of this is illustrated in Figure 8, focusing on one of the transformers in Jonschwil and depicting the predicted working conditions of the transformer in the year 2040. The findings indicate that by 2030, the transformer will be operating close to its normal limits. However, it is noteworthy that a few years after 2030, the transformer will undoubtedly exceed its operational limits.

An upgrade of the existing 400 kVA transformer in Henau with a 630 kVA unit is only a temporary solution, as this measure alone will not resolve all issues until 2040. This

emphasises the need to unlock demand response to ensure the resilience of the electrical infrastructure.

Figure 9 shows that, without flexibility measures, the transformer experiences up to four hours of minor overload during a cold winter day. During a sunny spring day, six hours of considerable overload is displayed. Results provide a preliminary assessment of the flexibility effect on the transformer loading.

Despite the high simplistic nature of the deployed load shifting and curtailment strategy, the number of hours with overloading is reduced to zero. Certainly, more advanced load shifting strategies could reduce the transformer loading further. It is worth noting that the PV curtailment yielded more substantial results than the load shifting.

Considering above findings, it becomes evident that the utilisation of flexibility is an appealing option to avoid renewable curtailment and delay costly grid reinforcement measures.

As we look ahead, the significance of flexibility becomes increasingly apparent, urging a comprehensive and forward-thinking approach to grid management. Solutions may involve harnessing flexibility, especially shifting energy consumption of EVs, heat pumps, and other loads.

References

- [1] Consentec GmbH, EBP Schweiz AG, Polynomics AG, 2022, <https://bfe.admin.ch/bfe/de/home/news-und-medien/medienmitteilungen/mm-test.msg-id-91974.html> (accessed 2024-02-02)
- [2] Swiss Federal Office of Energy (SFOE), 2022, <https://www.bfe.admin.ch/bfe/de/home/versorgung/stromversorgung/stromnetze/netz-entwicklung-strategie-stromnetze/szenariorahmen.html> (accessed 2024-02-01)
- [3] ENFLATE project, 2024, <https://www.hslu.ch/en/lucerne-university-of-applied-sciences-and-arts/research/projects/detail/?pid=6216> (accessed 2024-02-02)
- [4] DOMOS project, <https://www.domos-project.eu/> (accessed 2024-05-28)
- [5] Romano et al., 2024, Modelling charging behaviour of electric vehicles to estimate the potential flexibility income, to be published in the proceedings of the Grid Service Market Symposium 2024, Lucerne.

Acknowledgement of funding

This project has received funding from the European Union's Horizon Europe program under the Grant Agreement No 101075783.

This work was supported by the Swiss State Secretariat for Education, Research and Innovation (SERI) under contract number 22.00283.

G0505

Flexibility provision from local energy communities exemplified by the SUSTENANCE and SERENE H2020 projects

Birgitte Bak-Jensen (1), Rakesh Sinha (1), Sanjay Chaudhary (1), Hessam Golmohamadi (1), Gerwin Hoogsteen (2), Aditya Pappu (2), Bahman Ahmadi (2), Richard van Leeuwen (3), Javier F. Gonzales (3), Patryk Chaja (4), Weronika Radziszewska (4), Zakir Rather (5)

(1) Aalborg University, Denmark; (2) University of Twente, The Netherlands; (3) Saxion university of applied science, The Netherlands; (4) Institute of Fluid-Flow machinery, Poland; (5) Indian Institute of Technology Bombay/India;

Tel.: +45 21248501

bbj@energy.aau.dk

Abstract

When integrating a huge amount of fluctuating renewable energy, there is a need for mitigating the fluctuations by adapting the demand to the actual production. In the case of local production in households or a local energy community, the flexibility provision from the demand side should be optimized to ensure as much self-consumption as possible to minimize energy costs for the customer, but at the same time, the flexibility provision should also ensure needed hosting capacity of the nearby grid, by controlling the consumption and perform peak-shaving if possible. In the case of larger renewable power plants such as offshore wind farms, or large solar plants on land, the main flexibility provision has to be seen merely as a possibility to provide ancillary service to the electricity market as primary or secondary reserves. In several cases, prioritization is necessary in relation to whether the demand should be controlled according to the overall balancing or a local condition ensuring the hosting capacity.

The H2020 SERENE and SUSTENANCE projects look into flexibility provision from and scheduling of the energy consumption in local energy communities/areas at different demonstration sites in Denmark, The Netherlands, Poland, and India. In Europe, the local energy communities are grid-connected, and the optimization is mainly considering the control of heat pumps including their heat storage, EV-car charging, and in a few cases also the application of battery energy storage. The optimization is done in relation to cost optimization for the individual private costumers, which among others looks into enhancing the self-consumption of own produced energy – here mainly from PV power production, and at the same time, acts on the electricity market, buying energy when it is cheap, and selling in high price periods. Finally, the control also ensures that the local grid will not be overloaded, by also scheduling according to the local hosting capacity.

In India, there is also a grid-connected test site at the Indian Institute of Bombay, where the heat flow in a small house is controlled as well as car charging experiments. On the other hand, there are also two remote test sites in local villages, where there is no or only weak grid connection. Here the demonstration of flexibility provision is seen as a scheduling optimization on when to turn on the different demands, which include charging of electrical rickshaws, pumping of water, utilization of multi-purpose heat pumps for cooling and drying purposes as well as newly installed electric installations in the houses. Here the energy is generated by small wind turbines as well as PV panels, and battery energy storages are used to run the systems as microgrids.

In the paper we will show the different setup control methods, it will show how for instance the car charging facility at the University of Twente is optimized to ensure the grid hosting

capacity, how the heat-pump control is organized in the village of Voerladegaard in Denmark and how an overall set up energy system in the village of Przywidz is set up in Poland. Finally, the actual demonstration site ideas from Barubeda test site in India will be shown.

1. Introduction

In recent decades, the penetration of renewable energies, such as wind and solar, has increased in power systems worldwide. The primary challenge accompanying this high penetration of renewable energies is their volatility and intermittency. To mitigate the fluctuation in renewable power, demand flexibility can be integrated into power systems [1]. Demand flexibility is discussed across various sectors, including residential, industrial, agricultural, and commercial [2]. There are different power demands in the abovementioned sectors that can provide flexibility for power networks. Among them, electrical vehicles (EVs), Heat Pumps (HPs), Photovoltaic (PV) panels, and electrical batteries demonstrate particularly high potential.

In relation to EVs there has been a recent increase in the penetration, expected to become dominant in the next few years. Therefore, the flexibility potential of the mobility sector will play a crucial role in mitigating renewable power fluctuations [3]. EVs can be charged during periods of excess renewable power availability when electricity prices are low. Conversely, they can discharge power into the grid during periods of renewable power deficit corresponding to high electricity price hours.

The penetration of HPs is increasing in many areas, especially in regions without access to district heating or gas networks [4]. HPs can provide 3-5 times more heat energy than the electricity they consume. Their compressors can respond to demand response requests, adjusting power consumption in line with renewable power availability. In recent years, some research studies have focused on HP controllers to unlock heat-to-power flexibility. An Economic Model Predictive Controller (EMPC) has been designed for residential HPs to optimize flexibility in response to dynamic electricity prices [5]. This controller accounts for uncertainties related to weather forecasts from local weather stations. Additionally, a stochastic Model predictive control (MPC) is suggested to address electricity price uncertainties in various short-term electricity markets [6]. Many studies propose linking HPs with thermal storage to enhance flexibility potentials, with water tanks [7] and phase change material (PCM) storage [8].

When fossil fuel cars are phased out and replaced by EVs, power systems face several challenges such as voltage drops and power congestion due to the increased penetration of EVs [9]. However, if the charging and discharging operations of EVs are optimized, the power system can benefit from their substantial electrical storage capacity, effectively functioning as virtual power plants [10]. In the study [11], a bi-level coordination technique was applied to optimize the charging and discharging of EVs in residential areas to provide voltage regulation. Shared EVs and smart charging stations were suggested as practical solutions to mitigate congestion in distribution networks [12].

PV panels can supply portions of local power consumption, thereby reducing the burden on the local power grid and minimizing operational costs [13] and power losses [14] for the distribution network. Among these, rooftop photovoltaic sites play a key role in local demand supply [15]. Typically, PV panels meet demand during daytime hours. To address this limitation, PV panels are often connected to electrical batteries. In this way, a smart controller is proposed for the PV-battery system not only to fulfill local demand during nighttime hours but also to optimize the charging and discharging operations of the batteries based on distribution requirements [16]. Additionally, smart control is suggested to provide up and down voltage regulation [17].

2. Flexibility Provision from Demo Sites of H2020 Projects

In the paper, we will demonstrate various smart energy management systems including HPs, EVs, and PV-battery systems based on the two EU projects SERENE and SUSTENANCE, conducted across four demo sites in Denmark, the Netherlands, Poland, and India. Specifically, in the Netherlands, we address the EV smart charging facilities from the University of Twente to ensure grid hosting capacity. In Denmark, a flexible HP control is implemented in the village of Voerladegaard. In Poland, an overall flexible energy system setup is implemented in the village of Przywidz and in a housing association in Sopot. Finally, we will explain the actual flexibility provisions at the demonstration sites from the Barubeda, Borakhai, and Bombay test sites in India.

2.1. EV Flexibility in the Netherlands

The University of Twente Field Lab, commonly named *SlimPark*, meaning Smart Parking, is an EV charging station located at the University of Twente (UT). Figure 1 shows the actual *SlimPark* site at UT. It is a real-world laboratory of the Energy Management Research group of the UT, in which Energy Management algorithms are tested in practice with real users. It is therefore an essential bridge from theory to practice. It allows students and researchers to test and validate new concepts close to their office when theory is proven in simulation studies, but not yet ready for practice.



Figure 1. The EV charging station at the UT campus, i.e., SlimPark

The SlimPark Field Lab consists of the following components:

1. 9 3-phase 22kW (32A per phase) Mennekes Amtron Pro AC chargers.
2. 69 PV panels of 360W each, making in total 25 kW of rooftop solar panels.
3. 25kW PV inverter.
4. 30 kWh capacity with 20kW battery storage system.
5. All components are connected to a 3-phase grid connection with a 125 A per phase capacity.

All components are connected to a so called DEMKit system [18] for data gathering and for executing EV scheduling algorithms. DEMKit, short for Decentralized Energy Management toolkit, is a smart grid simulator and demo tool developed by the UT. It is used for thorough analysis and operational control of smart grids via simulations. With its agent-based design, it forecasts and plans energy use using local data.

Actual data from the charging stations, PV inverter, battery, and grid meter can be brought in via a Modbus TCP interface. The charging stations are managed through the open-source charge point operator back-end, SteVe which allows retrieval of precise arrival and departure times, energy charged, and user information. This data can then be utilized to

enhance control algorithms or experiment with various strategies within the DEMKit model. Figure 2 explains the schematic diagram of data and control flow in the SlimPark site.

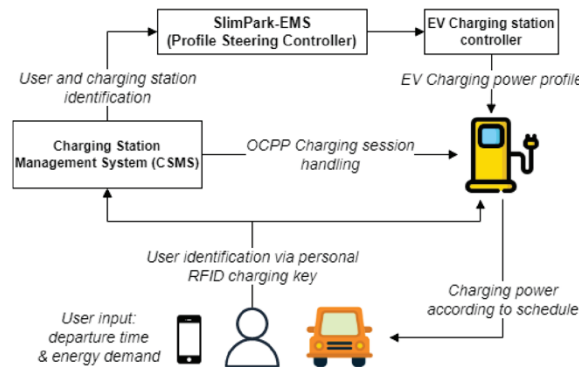


Figure 2. SlimPark demonstrator data and control flow schematic

Figure 3 investigates the added value of smart EV charging control and the implementation of a battery storage system in this demonstrator. Based on this simulation, spanning a work week, it is evident that there is significant potential for smart charging by synchronizing charging with local energy production through control. This will benefit the self-sufficiency of the parking lot, reduce carbon emissions, and significantly contribute to grid load minimization. The added value of a battery is very limited. However, the latter is included in the demonstrator for experimental purposes.

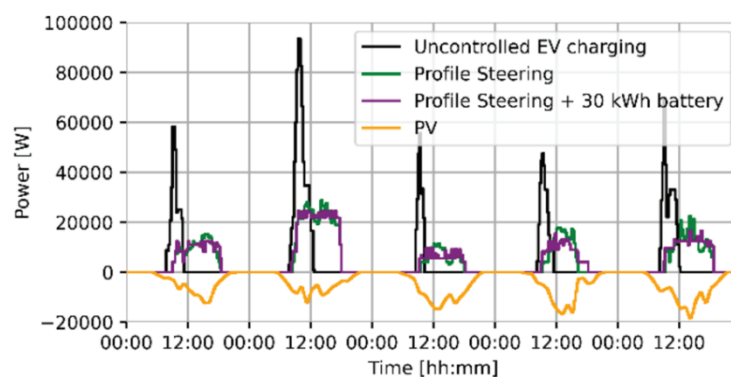


Figure 3. Example of simulation results for unlocking demand flexibility in the SlimPark site

2.2. HP Flexibility in Denmark

The Danish demo sites are located in Voerladegaard and Dorup villages, Skanderborg Municipality. The objectives of the demo sites are to remove the natural gas heating systems of individual residential buildings and replace them with HPs with smart salt PCM heat storage and PV systems. To achieve these aims, the following implementations are carried out on the demonstration sites.

• Demo Cases in Voerladegaard and Dorup Village

The Danish demonstration site for the SUSTENANCE project consists of 20 households with the following configurations:

- (1) 20 homes have HPs.
- (2) 6 different HP brands, sizes from 7 to 16kW.

(3) PCM storage capacities range from 200 – 1.500 liters.

(4) 10 homes have PV installed.

(5) 7 homes have an EV.

Figure 4 shows the HP and thermal storage in an individual houses of the demo site.



Figure 4. Installed HPs and thermal storage on the Danish demo site

Figure 5 illustrates a PI diagram of the HP controller in the Danish demo site. Based on the control diagram, the controller schedules the operation of the heating system in response to electricity prices. Assuming a strong correlation between electricity prices and renewable power availability, it optimizes the heat consumption to align with renewable power generation.

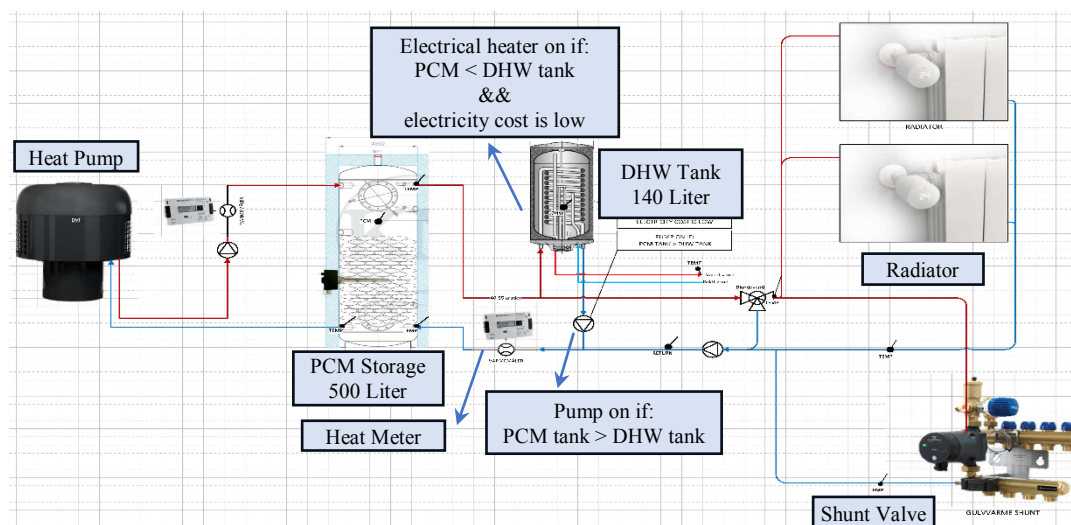


Figure 5. PI diagram of the HP controller in the Danish demonstration site

• Integration of RES Community Systems into Power Grids

At the same time, work is done to minimize bottleneck problems for the local power grid system caused by PV power production and power consumption for the HPs. In addition, cost-effective business models for heating individual residential buildings from integrated HPs with heat storage and PV systems are developed. The demonstration site can be called a *virtual smart PV micro-grid for energy communities*, where PV produced from individual PV systems in principal can be exchanged between individual residential buildings including *exporting* PV power to residential buildings with no PV system. Figure 6 illustrates the simulation results of the integration of the RES community systems into the power grid.

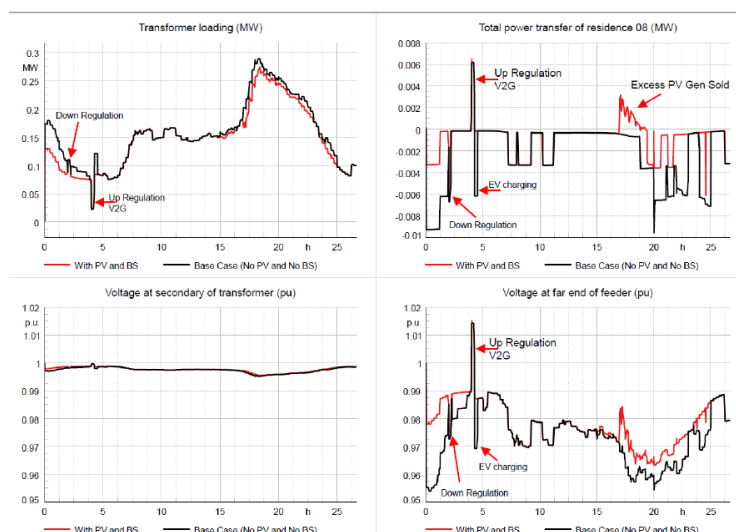


Figure 6. Simulation results on impacts from and integration of RES community systems into the power grid

2.3. Energy System Flexibility in Poland

The demonstration activities in Poland focus on the installation, demonstration, and testing of technologies for local electricity and heat production, EVs, energy storage and management for energy efficiency, and an increase in the share of local RES, visibility, and flexibility of the power grid. To achieve these aims, the following demonstrations are installed.

- **Smart Energy System in a Housing Association**

As the demonstration site for the SUSTENANCE project, in Poland, a residential building is chosen for the demonstration site in Sopot. The building has the utilities of water, gas, power, sewage, heat, and telecom. The energy consumption of the demo case is measured by installed meters for the living lab studies.

- **Local Energy Production, Storage and Management**

To unleash the heat-to-power flexibility, a GSJ 46EVI air HP is installed at the demo site in Sopot. Also, the main pipeline and water tanks were installed. Two tanks with a capacity of 150 m³ each will be used as thermal storage. Figure 7 shows the HP and the water tank in the Polish pilot site.



Figure 7. DHW (Domestic Hot Water) tanks and GSJ 46EVI HP in the Polish demonstration site

- **Energy storage and EV charging stations**

In the SERENE project, the Polish demo sites include Arena Przywidz and the primary school, Szkoła Podstawowa im. Unii Europejskiej w Przywidzu, located at the heart of Przywidz, which are equipped with 39.99 kWp and 26.04 kWp photovoltaic systems.

Within the SERENE project, the energy storage unit in fluid-flow technology was added to the Arena's power system. It is a storage of 20 kW of maximal power and 96 kWh of capacity, everything is located in the container standing near the building. Within the project also 3 chargers are installed – one DC charger of 25 kW and two AC ones of 22 kW each. The DC charger is used by the electric bus which is part of the electric rural bus line, with a bus terminal near Arena Przywidz. All those devices will be connected by the Energy Management System (EMS) that will manage the energy storage and the charging of the cars. The EMS will provide energy balancing with the aim of minimizing energy costs. Figure 8 shows the Arena Przywidz as the dome site and the electric bus that is used regularly around Przywidz.



Figure 8. Arena Przywidz as the Polish demo site with the electric bus for local citizens

In the demonstration sites, many simulation studies are conducted to examine the impacts of the sizable demands on the flexible operation of the power grids. As an example, Figure 9 explains that the application of ESS paired with PV can result in significant energy cost reduction.

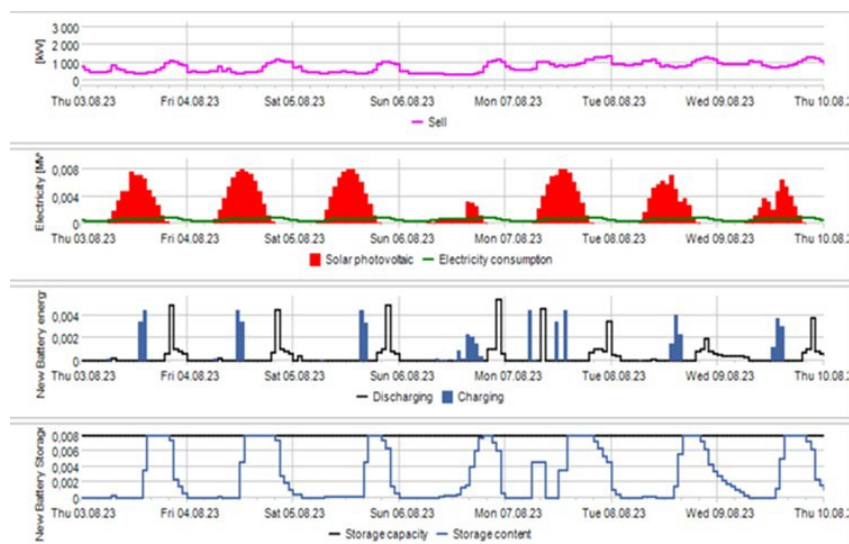


Figure 9. Example of Residential PV+ESS simulation

2.4. Energy System Flexibility in India

The main objective of the Indian demonstrations is to achieve customer-driven carbon-neutral local energy communities for remote off-grid villages, weak grid-connected remote communities, and district/suburban grid-connected communities. The goal of sustainable energy systems can be achieved by addressing critical verticals of energy, water, heating

and cooling, irrigation, cooking, and transportation through an optimized cross-coupled integrated energy carrier approach. As a part of the SUSTENANCE project, the above solutions will be deployed for demonstration at three uniquely different local energy systems focusing on the following pilots in India:

- (1) Barubeda Village, Jharkhand, as an off-grid local energy system.
- (2) Borakhai Village, Assam, as a weak grid-connected system.
- (3) IIT Bombay campus, Mumbai, Maharashtra, as a grid-connected integrated smart building system.

Figure 10 shows demand flexibility structure in one of the Indian demonstrators. As can be seen, in the grid-connected area, smart building provide flexibility for upstream networks. In the DC microgrids, PV panels, small wind turbines, domestic water supply, and EV charging stations are the key components of the demonstration sites.

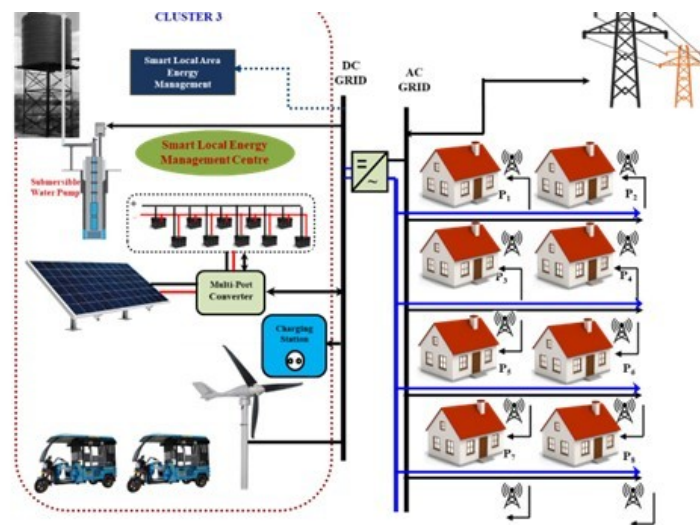


Figure 10. Key components of Indian demonstrations site for flexible energy management system

In the Indian demonstration sites several systems are initiated as prototypes which are detailed in the following.

- **Biogas-based Power Generator and Biogas-based Cooking**

The biogas plant has a 100 m³ capacity with a 12-kW generating facility with the primary product being biogas supply for cooking applications, and the secondary product being electricity generation. The raw material for the biogas plant will be sourced locally from the village and the same has been discussed and agreed with the local Village Energy Committee.

- **Low-Speed Hybrid Solar PV-Wind Power Plant**

Deployment of low-speed hybrid solar-PV wind is a part of generation deployment at the Borakhai site. The hybrid system will form part of the total generation system which includes 34 kW solar PV along with a battery storage system of around 290 kWhr. There are two sites physically apart from each other in Silchar, and the low-speed hybrid system is a part of the generation system at the 'off-grid' cluster.

- **Domestic Water Supply System**

Geoinformatics/GIS-based approaches were applied in the selection of optimized locations to install the PV water pumping system for cost-effective and energy-efficient operation. Water quality tests are initiated for the Borakhai site. Based on the groundwater level mapping conducted for Barubeda village, it is inferred that the exact groundwater level at

the preferred location for the installation set-up can be measured only through the actual borewell digging.

• Multi-Utility Heat Pump-Based Community Cooling, Heating and Drying

Design and analysis of the Multi-Utility Heat Pump (MUHP) are developed for milk chilling, water chilling for precooling of fruits and vegetables, and warm air for drying agro produce. Milk chilling from 36^{oC} to 6^{oC}, water chilling from 30^{oC} to 15^{oC}, and heating ambient air up to 45^{oC} and/or water heating from 25^{oC} to 55^{oC}. Figure 11 shows the installed MUHP in the pilot site.



Figure 11. Multi-utility heat pump unit at the Indian demonstration site

• Smart Electrical Building Systems

The smart electric building is developed at the campus of IIT Bombay. The building is equipped with a battery storage-enabled solar PV system. The net-zero electricity consumption of the building has been demonstrated in Figure 12 and further measurements are being taken from the building.

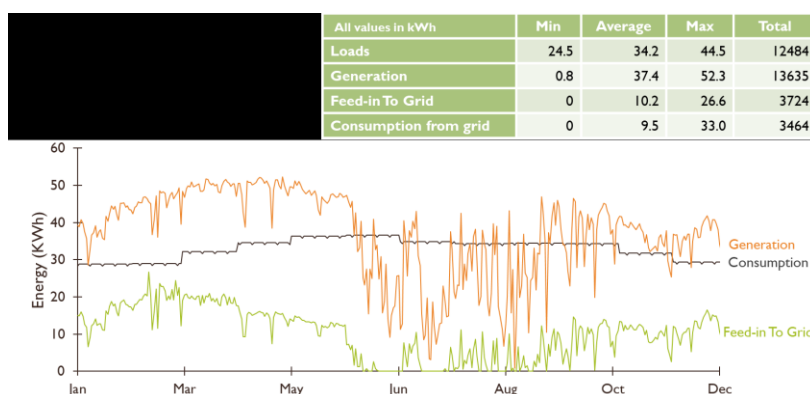


Figure 12. Net zero electricity of the smart electrical building on the campus of IIT Bombay

4. Conclusion

In this paper, we discussed different demonstration sites in EU countries, including the Netherlands, Denmark, Poland, and India as the Asian partner. The demonstration sites belong to two H2020 projects SUSTENANCE and SERENE which aim to integrate the flexibility of sizable demands, e.g., HP, EVs, and batteries into smart energy systems, alongside increasing the penetration of RES within energy systems.

The performance of demonstration sites shows that power and heat demand flexibility are workable solutions to provide support for local energy systems, e.g., voltage regulation and load balance. In addition, it can increase the penetration of renewable energy within local energy communities. The results are not standing only for interconnected grids but

also for off-grid remote areas. Herby, distributed energy systems benefit from cost-effective and reliable operation, while remote microgrids supply the local demands using locally available materials and resources.

Acknowledgment

This project has received funding from the European Union's Horizon 2020 research and innovation programme under grant agreement No. 957682 for SERENE and No.101022587 for the SUSTENANCE projects.



References

- [1] L. Hou, W. Li, K. Zhou, and Q. Jiang, "Integrating flexible demand response toward available transfer capability enhancement," *Appl Energy*, vol. 251, p. 113370, 2019, doi: <https://doi.org/10.1016/j.apenergy.2019.113370>.
- [2] H. Golmohamadi, "Demand-Side Flexibility in Power Systems: A Survey of Residential, Industrial, Commercial, and Agricultural Sectors," *Sustainability*, vol. 14, no. 13, 2022, doi: 10.3390/su14137916.
- [3] Z. Jiang *et al.*, "Charging station layout planning for electric vehicles based on power system flexibility requirements," *Energy*, vol. 283, p. 128983, 2023, doi: <https://doi.org/10.1016/j.energy.2023.128983>.
- [4] Global heat pump sales continue double-digit growth, <https://www.iea.org/commentaries/global-heat-pump-sales-continue-double-digit-growth>
- [5] M. A. A. Awadelrahman, Y. Zong, H. Li, and C. Agert, "Economic Model Predictive Control for Hot Water Based Heating Systems in Smart Buildings," *Energy Power Eng*, vol. 09, no. 04, pp. 112–119, 2017, doi: 10.4236/epe.2017.94B014.
- [6] H. Golmohamadi, K. G. Larsen, P. G. Jensen, and I. R. Hasrat, "Hierarchical flexibility potentials of residential buildings with responsive heat pumps: A case study of Denmark," *Journal of Building Engineering*, vol. 41, p. 102425, 2021, doi: <https://doi.org/10.1016/j.jobee.2021.102425>.
- [7] T. Péan, R. Costa-Castelló, E. Fuentes, and J. Salom, "Experimental Testing of Variable Speed Heat Pump Control Strategies for Enhancing Energy Flexibility in Buildings," *IEEE Access*, vol. 7, pp. 37071–37087, 2019, doi: 10.1109/ACCESS.2019.2903084.
- [8] M. Saffari, C. Roe, and D. P. Finn, "Improving the building energy flexibility using PCM-enhanced envelopes," *Appl Therm Eng*, vol. 217, p. 119092, 2022, doi: <https://doi.org/10.1016/j.applthermaleng.2022.119092>.
- [9] A. Ul-Haq, C. Cecati, K. Strunz, and E. Abbasi, "Impact of Electric Vehicle Charging on Voltage Unbalance in an Urban Distribution Network," *Intelligent Industrial Systems*, vol. 1, no. 1, pp. 51–60, 2015, doi: 10.1007/s40903-015-0005-x.
- [10] M. İnci, M. M. Savrun, and Ö. Çelik, "Integrating electric vehicles as virtual power plants: A comprehensive review on vehicle-to-grid (V2G) concepts, interface topologies, marketing and future prospects," *J Energy Storage*, vol. 55, p. 105579, 2022, doi: <https://doi.org/10.1016/j.est.2022.105579>.
- [11] Y. Wang, T. John, and B. Xiong, "A two-level coordinated voltage control scheme of electric vehicle chargers in low-voltage distribution networks," *Electric Power Systems Research*, vol. 168, pp. 218–227, 2019, doi: <https://doi.org/10.1016/j.epsr.2018.12.005>.
- [12] N. Brinkel, T. AlSkaif, and W. van Sark, "Grid congestion mitigation in the era of shared electric vehicles," *J Energy Storage*, vol. 48, p. 103806, 2022, doi: <https://doi.org/10.1016/j.est.2021.103806>.
- [13] L. E. S. e Silva *et al.*, "Probabilistic operational costs assessment of combined PV–PEV connections in LV distribution networks," *Electric Power Systems Research*, vol. 214, p. 108906, 2023, doi: <https://doi.org/10.1016/j.epsr.2022.108906>.
- [14] C. A. P. Pérez, L. G. Espinosa, and A. S. Fuentefria, "Reduction of energy losses through the integration of photovoltaic power plants in distribution networks," *IET Generation, Transmission & Distribution*, vol. 17, no. 16, pp. 3739–3750, Aug. 2023, doi: <https://doi.org/10.1049/gtd2.12930>.
- [15] B. Uzum, A. Onen, H. M. Hasanien, and S. M. Mueen, "Rooftop Solar PV Penetration Impacts on Distribution Network and Further Growth Factors—A Comprehensive Review," *Electronics (Basel)*, vol. 10, no. 1, 2021, doi: 10.3390/electronics10010055.
- [16] G. Kannayeram, N. B. Prakash, and R. Muniraj, "Intelligent hybrid controller for power flow management of PV/battery/FC/SC system in smart grid applications," *Int J Hydrogen Energy*, vol. 45, no. 41, pp. 21779–21795, 2020, doi: <https://doi.org/10.1016/j.ijhydene.2020.05.149>.
- [17] M. A. Shuvra and B. Chowdhury, "Reconfigurable and flexible voltage control strategy using smart PV inverters with integrated energy storage for advanced distribution systems," *IET Smart Grid*, vol. 3, no. 1, pp. 22–30, Feb. 2020, doi: <https://doi.org/10.1049/iet-stg.2019.0018>.
- [18] DEMKIT system control, <https://www.utwente.nl/en/eemcs/energy/demkit/>

G0507

VPP implementations: different types of services developed, experiences and platforms

Gary Howorth, Ivana Kockar
University of Strathclyde, Glasgow/UK;
Tel.: +44-141-444-7254
gary.howorth@strath.ac.uk.com

Abstract

Aggregation by Virtual Power Plants (VPP's) to provide flexibility to distribution and transmission networks is seen as an important element in the transition to Net-Zero. This paper presents work carried out in the SIES 2022 ERA-Net project, which is investigating in detail the possible provision of flexibility by different technologies. Thus, presented work will be based on real use cases.

One of the partners in the SIES 2022 ERA-Net consortium is the Engineering Technical Centre in Central Scotland (ETC), which has been set up to deliver a technology demonstrator system to manage energy pools using VPP software as well as to investigate how this VPP could operate using a variety of assets in a realistic setting. ETC has interests in two energy pools which are available for immediate deployment in the project:

- ETC's own premises and the wider Scottish Enterprise Technology Park energy infrastructure
- A test area at the Myres Hill wind turbine site

The sites include both electrical and thermal loads, battery storage that can be used for flexibility as well as other consumers in the area.

The VPP design includes the use of cloud-based third-party software for communication, hardware interfaces and an additional pilot VPP software platform providing enhanced services such as optimization scheduling and forecasting amongst other things. Devices from many manufacturers have been incorporated into the demonstrator plant.

The integration of these components and development of the VPP software has proceeded on a learning-by-doing approach. The paper will discuss the design, development of the VPP platform (hardware and software) including a review of the various other platforms that could have been used in the pilot. In particular, the paper will discuss the challenges with the implementation of the various components and present results on the performance of the design in the context of supplying flexibility services to a TSO/DSO. The VPP software has been running for over a year now and has allowed us to investigate issues with its operation such as reliability, forecasting (Machine learning), optimization (Stochastic and Deterministic) and its potential reuse and design for other

projects. Lessons learned and how such a design could be adapted to other potential types of users will also be discussed.

1. Introduction

Virtual Power Plants (VPP) will form an important element in the development of a future low carbon power market, as they will ease the interactions of system operators with thousands of potential customers. Exactly how these sources of flexibility will be managed and the economic impact on the players is still unclear. The challenge of employing flexibility in generation, consumption and storage in the context of a VPP depends on the appropriate optimization of market access, assets and an understanding of the constraints on the wider distribution system. The SIES 2022 project aimed to develop a digital energy utility management service (VPP) capable of managing local and regional energy systems and markets using a number of energy pools & use cases. Although flexibility markets it considered are mainly UK based, the approach can be extended for analysis in other countries.

The project (Fig. 1) focused on the technological and business related barriers and opportunities of how VPPs can function in flexibility markets to help local communities better manage their assets (power, heat, gas). Although it was focused on smaller locally based assets, the lessons learned from the project can be equally applied to larger and/or smaller projects. The majority of the assets were based at Engineering Technology Center (ETC) in East Kilbride, Scotland. Further details can be found at the project web site www.sies-project.com.

The VPP design includes the use of cloud-based third-party software for data storage, communication between certain assets, hardware interfaces and an additional pilot VPP software platform providing enhanced services such as optimization scheduling and forecasting amongst other things. Devices from various manufacturers have been incorporated into the demonstrator system, requiring appropriate integration procedures and settings. The integration of these components and development of the VPP software has proceeded on a learning by doing approach.

In summary the project consists of:

- Multiple Energy Pools (FindHorn, ETC demonstrator site (EK), Myres Hill) were used.
- Various technologies: Heat pumps, thermal stores, an auxiliary gas system, electrical load (up to 80kW), PV (12kW), wind (10kW+220kW) and different types of battery storage (178kWh) and an EV charger.
- Aimed to connect different types of assets, to maximize profits and provide support to an already congested grid.
- Was used for testing & developing algorithms/asset types and concepts

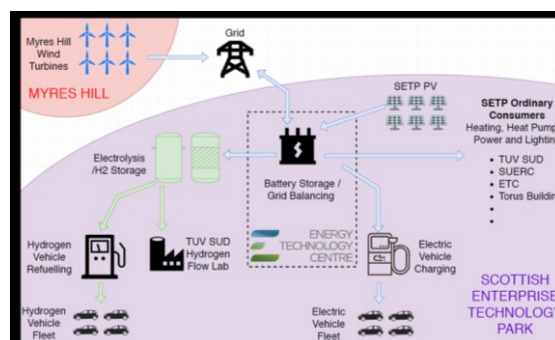


Figure 1: SIES Project Overview

The project also has access to data from the Findhorn Eco Village in Moray, Scotland which provides data from 3 wind turbines, a shared thermal store heat pump, domestic heat and hot water usage in several houses. Four community-owned wind turbines, which have a total capacity of 750kW, supply more than 100% of the community's electricity needs. The system is unusual in that the community owns its own private electricity grid. The electricity produced by the turbines is sent to a substation that meters the flows, alters the transmission voltages and acts as a switching station. Normally output is used on-site, but If production exceeds demand the surplus is exported to the grid and generates revenues. If there is no wind output the site imports from the grid. Overall Findhorn are net exporters of electricity.

Many lessons have been learnt during the development of the VPP platform in the SIES Project. These are summarized in Fig. 2 below.



Figure 2: VPP Challenges and Choices

In the remainder of the paper we will discuss each of the points shown in Fig. 2, highlighting experiences, success stories, and challenges. The paper will begin with an outline of the design, development of the VPP platform (Hardware and Software) including

an overview of existing suppliers and asset integration issues. This is followed by a discussion of Power markets, decision making algorithms and forecasting.

2. VPP Implementation

A VPP platform utilizing assets at a pilot plant and two other locations has been built and has been operating for over a year. Learning lessons have been extracted and a better view of how and why one would develop a VPP business has been developed.

The operation of the VPP can be thought of as a series of steps listed below:

- 1 (a) Obtain data from equipment
- 1 (b) Perform checks on data inputs
- 1 (c) Obtain weather
- 1 (d) Correct with local weather measurements if available
- 2 Forecast prices, power outputs and Demand for power heat etc.
- 3 Optimize make decision about dispatch of assets/flexibility to markets
- 4 Send control signals to assets
- 5 Review actions and analyse data

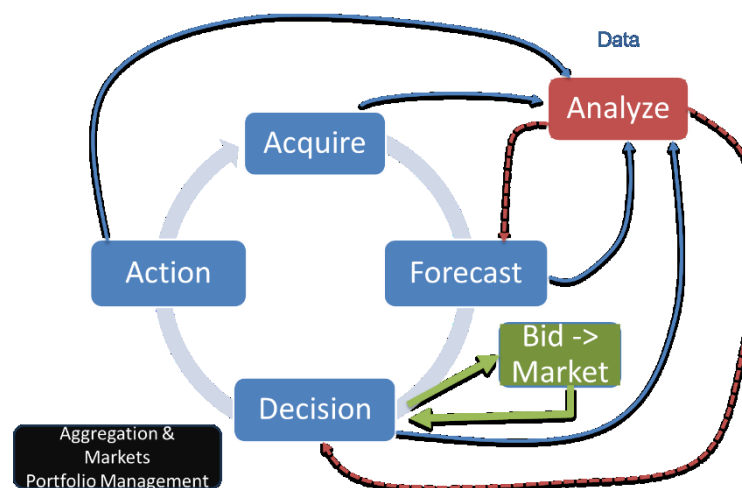


Figure 3: Actions Required by VPP

The VPP could be operated on a purely technical basis, without regard to markets, or as Commercial business, and our work focused on the commercial nature of a VPP.

This has important implications for the DSO as actions by a commercial VPP entity may not be in line with what a DSO wants.

Hardware Design

There are two key components to the design: (i) A VPP platform hosted on server on or off site (currently offsite); (ii) An Energy Management Control System (EMCS) that comprises of an Energy Asset Server, local asset network (Modbus RS485) and utilizes a cloud base AWS to store data from assets. The EMCS is used to provide a control and data logging interface between the Virtual Power Plant (VPP) application and the various energy assets and meters installed at the energy pools. The ECMS gathers operational

data from assets at the various energy pools and interfaces with AWS database & provides logging of instantaneous data from assets. Assets at the SIES project site are connected to a Modbus network which communicates with the ECMS.

AWS is used to host a cloud server which forms the central hub for EMCS data and interaction with separate VPP application. The VPP uses API's to send and retrieve data via a bounce server.

The Local assets uses VLAN over LAN (Energy Asset Network [EAN]), while EAN uses a Modbus Gateway and RTU's (TCP - RS485), and essentially forms a Modbus network. Modbus gateways are used to interface to the various existing Modbus RTU (RS485) devices to Modbus TCP, and to interface with the EMCS server.

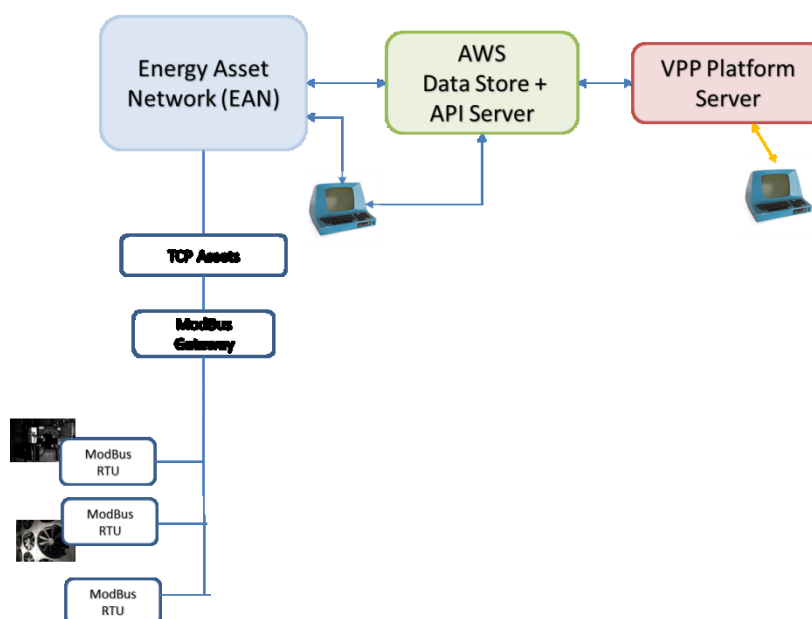


Figure 4: ECMS system

Software Design

Initially the project was to use a commercial version of VPP software, so an assessment at the time (circa 2021) was made of the potential suppliers shown here in Table 1 (for details see https://sies-project.com/fff02_files/existingproviders.html). At the time, few Vendors provided us with the appropriate decision making software that we required, although this has now become more prevalent. Some providers provided access to weather and forecasting services for a fee. Currently there are vendors that will provide users with AI/ML forecasting/decision models with their systems. We cannot comment on their accuracy or efficacy. There are many differences between VPP Software providers. Some provide software only with little support. Some focus only on one or two assets types, e.g. batteries only. In recent years some Open Source offerings have also become available (see [1]).

An Existing Framework PyEMLab-AGG [2] was developed as a Python object orientated simulator to model the interactions of aggregators (VPP owners and associated actions), domestic and industrial customers in a future flexibility market. The PyEMLab-AGG framework has been rebuilt to communicate in real time every half hour with assets at a number of locations including the SIES Project sites. The current architecture for the software framework is shown in Figure 5. Those modules marked with an asterisk* are for

future development. A key role of the model is to communicate with the assets in the field. This is achieved using API's, some of which have had to be developed for this project. Data is collected and stored for later use, but those that are needed for immediate use are also stored into in-memory storage in the repository object described earlier. The software uses a rolling time horizon to forecast prices and demand, and is used in the decision/Optimisation module. The optimiser, or decision model, looks to maximise revenues to the project and formulates schedules, which are then sent via the communication module to the various assets via AWS and the ECMS.

The original PyEMLab – Agg framework was designed as simulation software but this architecture has dual functionality (real time and simulation). This has proved invaluable for a number of reasons. Firstly, some of the assets have not been available to the project so the use of digital twins allows us to test software functionality and to try out new algorithms.

Elements	NEXT Kraftwerke	Smarter Grid Solutions	Moixa Grid Share	Limejump	Kiwi	gridIMP	Open Energi	Origami	Electric Imp	AutoGrid	AMPX
Individual Asset SCADA	Next Box	Integration Services?	yes	LI Smart Devices	Kiwi Fruit (Energy Imp supplied)	No?	No	No	Yes		
Decentralised Control Hub		Element Flex	yes			ImpHub			Yes		Yes
Centralised SCADA	N/A		?	N/A	N/A	N/A					
Cloud Optimisation Platform	NEMOCs	Cirrus Flex	?	"The Cloud"	Kiwi Core	N/A	Dynamic Demand 2.0	Flex, Storage	No	"AutoGrid Flex" uses "GridSight"	Yes including advanced AI and ML capability. Also Asset management
Market Trading	NEXTRA		?	'Ops and Trading Platform'		ImpHub				Yes; Under guise of Renewables Trading	?
EV charging Integration			yes incl VtoG							Yes	Yes
DSM/DSR Integration			yes							Yes	Yes
Features											
UK-based	No, Germany	Yes, Glasgow	Yes, Manchester	Yes, London	Yes, London	Yes, Somerset	Yes, London	Yes, Cambridge	UK office, US HQ	No, USA, India, Amsterdam, Japan	Yes Edinburgh Prauge and Toronto Affiliated with Amp energy which has offices in Spain Japan India -
Owner Direct Asset Control	Yes	Yes	Yes	Yes	Yes	Yes	?	?	N/A	?	?
Owner Generated Schedules	?	?	?	?	?	?	?	?	N/A	?	?
Suitable for kW and MW assets	Yes	Yes	Yes	kW?	kW?	MW?	Yes	?	Yes	Yes	Yes
Other comments	2nd in Gartner /Nexant Studies. Now Owned by Shell	Recently acquired by Mitsubishi	They started as Smart Battery Co but have platform to allow other assets to be utilised as battery type assets.	Limejump has been a wholly owned subsidiary of Shell since 2019, and is a part of Shell's Trading and Supply team.			BP acquired in 2021	Owned 14% by Aggreko. Power Rental company		Market leader according to Gartner and Nexant. Appears to have largest number of installations completed. Owned by Schneider	Grid Edge solution. AMP X was supported by Energy Catapult to develop said system https://es.catapult.org.uk/impact/projects/amp-x/
Web link	https://www.next-kraftwerke.com/	https://www.smartergrid.com/	https://moixa.com/business-services/	https://www.limejump.com/	https://www.kiwi-powered.com/	https://gridimp.com/	https://openenergi.com/	https://www.origami-energy.com/	https://www.electricimp.com/	www.auto-grid.com	www.ampx.energy
Testimonials	https://www.next-kraftwerke.com/vpp/case-studies	https://www.smartergrid.com/media-center/case-studies	https://moixa.com/case-studies/	https://www.limejump.com/knowledge-dge-hub/ssdc-opium-power-case-study/	https://www.youtube.com/watch?v=eUDBYjTYdU	https://gridimp.com/case-studies	https://openenergi.com/case-studies			https://www.auto-grid.com/case-studies/	https://www.youtube.com/watch?v=eSADLBf11o

Table 1: Overview of potential vendors

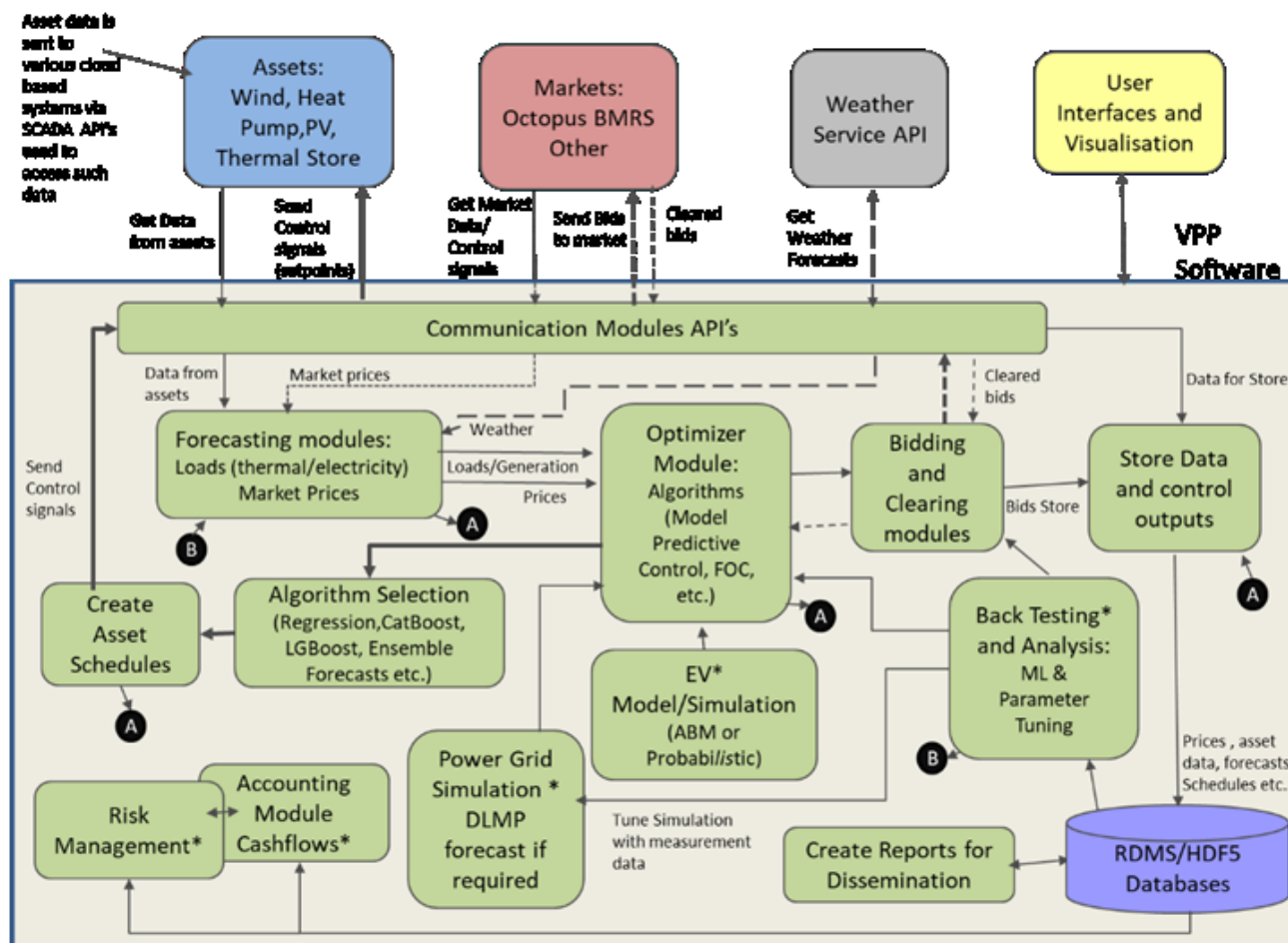


Figure 5: current VPP software architecture; block diagram

Secondly, the current demonstrator cannot gain access to some of the markets so a simulation environment allows to simulate these markets in the presence of real assets and their data. Using the experience gained from the VPP development we estimate that a fully blown commercial VPP platform is likely to cost in the region of £0.5 - £1 Million pounds to develop, and would include risk management, cyber security and accounting modules amongst other things.

3. Asset Challenges /Choice

The SIES project uses a mix of new and legacy assets from different manufacturers, some of which are over 10 years old. Integrating these assets into a VPP platform has proved to be time consuming process and more difficult than a simple plug and play. Defining communication channels and measurement specifications has also been challenging, especially as some of these measurements are not currently sourced.

The data captured during project operation has been used to value different business models for the pilot project [3]. The SIES project itself is relatively small (provision of ~ 70-80kW of flexibility). Scaling the values shown in [3] to 1 MW indicates that depending on routes/access to market, and asset combinations could provide a revenue benefit of up to ~£350,000 per year per MW of flexibility. An analysis using the tool presented at https://sies-project.com/fff02_files/evaluationtool.html, indicates that if the assets already exist, a Commercial VPP might make sense for assets sizes greater than about 0.3 MW.

Where asset investments are required, this figure rises to around 0.5 MW. Of course, this depends on the assumptions and costs assumed for the VPP service. Note that this tool assumes the use of one market i.e. Pico distribution flexibility but ability to participate in different markets and revenue stacking would be expected to increase this value.

4. Power Markets

A key element to any assessment for any commercial Virtual Power Plant (VPP) is the prices that one would expect to achieve in the various markets. There are a number of markets that a potential VPP can sell into or buy from and in the future would include:

- Longer term Storage/Flexibility Markets associated with Transmission (currently exists under the UK STOR” arrangements)
- Longer term Storage/Flexibility Markets associated with Distribution (Evolving trial systems set up – e.g. see Pico flex (<https://picoflex.com>))
- Day ahead and real time sales of Power between producers/consumers (wholesale EPEX and N2EX trading market places are currently available)
- Real time flexibility market at distribution or local level (future market)
- Frequency response services (e.g. FFR) and other ancillary services
- Bilateral markets between participants (current PPAs)
- Peer to Peer (P2P) markets (future markets)

The current markets are evolving at pace and regulators like the UK’s Ofgem are looking to make market access for flexibility services easier to access. Historically balancing markets have been focussed on providing flexibility or imbalance services via the transmission network. but Flexibility at the distribution market level is still evolving with several pilot markets such as Pico Flex being made available. Real time markets at the distribution level do not currently exist, but it is anticipated that they will.

Ultimately, a commercial VPP owner will be required to access these various markets to monetize its assets and generate revenues. This will require contractual arrangements as well as communication technologies to transfer data to the appropriate parties. VPP owners can communicate with the markets and the system operator (National Grid ESO in the UK). VPP owners can connect with these markets and system operator directly or indirectly (via Energy/Supplier/Retailers or Aggregators) through a variety of mechanisms.

Deciding how to sell, and selecting the right route to market, is essential to the success of any VPP product or service. Different routes to market will suit different kinds of assets producing different products/services. In the case of a Virtual Power Plant (VPP) it is not a simple case of picking one market over another, but to understand that having ability to switch between markets may be more valuable than any one market. There are costs (financial and other resources) to joining a marketplace and this needs an assessment of whether having access to additional markets is worth the cost of joining them. This can be likened to having an option. If the cost of the option far outweighs its value, then the market should not be accessed.

Assessment of the VPP value will take account of the value of these markets, the costs of access and will eventually enable us to determine the best setup for a particular use-case.

5. Forecasting

Forecasting is a key element of the VPP functionality and is described and discussed in reference [4]. The key take way from our work is the following:

- There are many algorithms one can use to forecast wind/solar output, including Machine learning algorithms such as CatBoost, LG Boost and stochastic models for price forecasting.
- Sometimes, (perhaps surprisingly) the simpler methods e.g. a simple logistic equation to estimate power output from renewables is more accurate than the more” sophisticated method
- Overall, operating errors of around 12% have been seen in operating the current VPP unit. This results in large discrepancies between expected and actual volumes exported to/from the grid for about 15% of the time!
- We believe that we can reduce this error to ~ 5% with the use of ensemble modelling techniques.
- We are developing ML algorithms to correct for the discrepancies in dispatch volumes. This has proved to be difficult, but are still working on this.

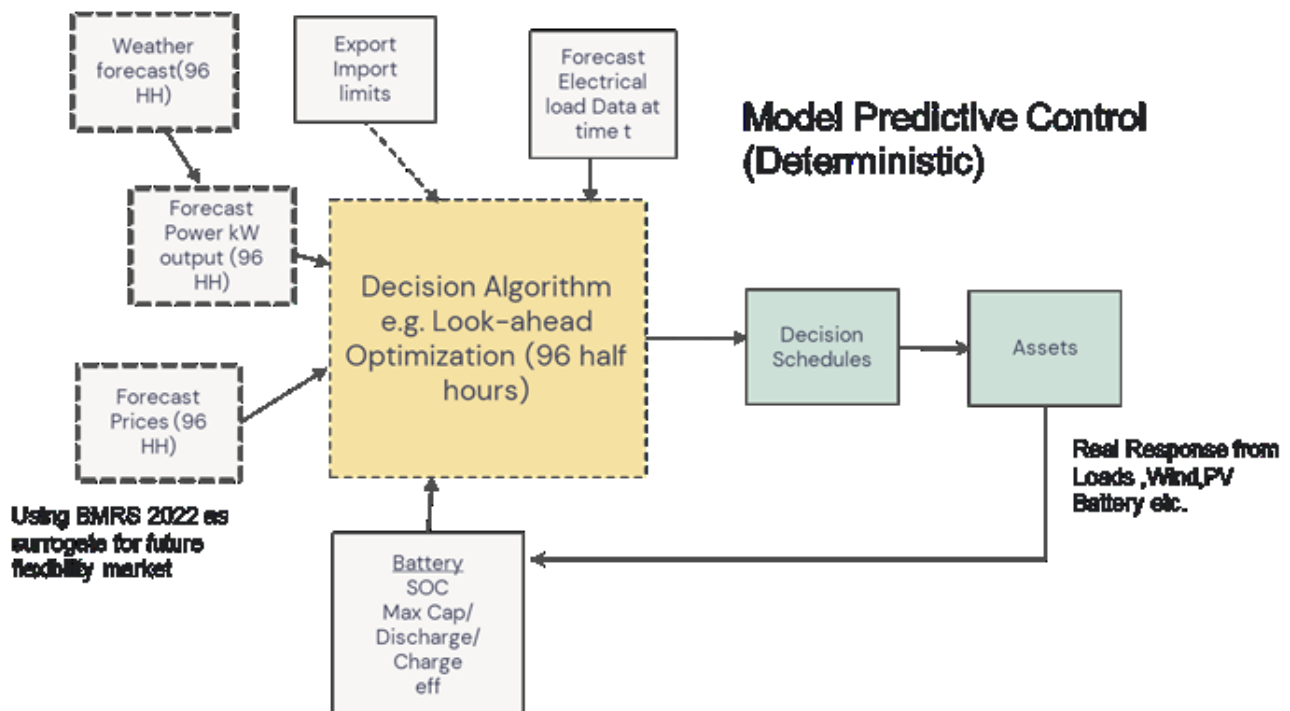


Figure 6: Forecasting modules and approach

6. Decision Making (Optimization)

A “deterministic” based decision optimization model, based on the work in reference [5] was originally included, but has been adapted to include battery degradation costs, import/export limits and carbon prices. It uses the Pyomo [6] modelling language and an open source GLPK MILP optimiser. This has been further adapted to include some elements of the current UK flexibility and wholesale markets, as well as contract structure selection, but this brings another level of complexity to the problem to be solved. Adding contract structure has increased solution times by a factor 150 – 1000. The optimizer, or

decision model, looks to maximize revenues to the VPP and formulates schedules which are then sent via the communication module to the various assets.

Discrete, Stochastic or Heuristics

An important part of the commercial VPP operation is to bring financial benefits to its operations. This essentially means the optimization of decisions, such as Discharge/Charge profiles on battery, thermal and other innovative storage technology, EV and Demand scheduling and market participation optimization with bidding. The inherent uncertainty associated with this problem in what is a complex system, and will become even more so with domestic customer involvement (added human behaviour dimension in future evolutions of the market). Experiments with stochastic solvers indicate that solution times for “relatively” simple problems can take many hours to solve. However, a future environment that could require bidding times of less than 5 minutes tends to suggest that other solutions need to be considered and/or found for this problem.

Linearizing and solving deterministically can help, but our recent experience on a problem which bids into real imbalance and flexibility markets shows the solution times can be excessive.

Our current incarnation of the assets uses a forward looking horizon deterministic optimization method. It solves relatively quickly, but does not account for the stochastic nature of the real problem. Essentially, we have a speed vs accuracy challenge, which is dependent upon the bidding timeframes e.g. potentially as short as 5 minute bid. Although AI/ML will prove to be a useful tool to forecast and, more generally operate VPP's, i.e. make decisions on asset dispatch, it is but one tool. AI is useful if data is stationary, as it can predict based on past patterns relatively fast. Unfortunately, markets are not stationary in the longer term and the addition of Human Behaviour (Domestic Consumers) into the flexibility mix will test their ability to forecast. Additionally, some form of heuristic might prove to be useful, albeit using a combination of models is thought to be a better approach and one that we have been pursuing.

7. Added Values/Conclusion

Although the development of a VPP pilot plant was meant to use commercially available software – it has turned out that for a variety of reasons that a “homegrown” development has occurred. This enabled us to learn more about the process of developing a VPP project from the ground up, and afforded us a better understanding of the benefits and challenges associated with such projects.

The integration of existing legacy hardware has proved to be a problem – lack of standardization, difficulty in obtaining manuals for older equipment and so on. Most importantly, the collection of, and use of, data to simulate future VPP configurations has proved to be a bonus. The software architecture can be used to run simulations, hardware in the loop or to operate as a real time VPP engine.

Thus, this development of the VPP software tool has provided a number of benefits:

1. Allowed us to use data in simulations for, asset combinations that we do not currently have access to
2. Enabled us to easily incorporate and try out new algorithms
3. Provided us with the ability to perform hardware in the loop simulations.

4. Provided opportunity to value alternative business models and, most importantly, to put a value of flexibility on those combinations.

References

- [1] Seita. (2024, 10 May). *The FlexMeasures platform*. Available: <https://seita.nl/core-technology/flexmeasures/>
- [2] G. Howorth and I. Kockar, "Understanding the Impact of Human & Corporate Behaviours on DSO Planning " in *Increasing Distribution Network Hosting Capacity 19 – 20 June 2024 CIRED 2024 Vienna, Austria, 2024*.
- [3] G. Howorth, I. Kockar, P. Tuohy, G. Flett, and J. Bingham, "Business models for virtual power plants and their impact on economic operation," in *27th International Conference on Electricity Distribution (CIRED 2023)*, 2023, p. 11346.
- [4] G. Howorth, I. Kockar, P. Tuohy, G. Flett, and J. Bingham, "The impact of forecasting accuracy on the economic performance of flexibility provision," 12-15 June, 2023.
- [5] B. L. S. Aigner, "System modeling and dispatch schedule optimization of combined PV battery system using linear optimization," Masters, University of Agder, 2021.
- [6] M. L. Bynum *et al.*, *Pyomo-optimization modeling in python*. Springer, 2021.

G0508

Empowering Prosumers in the Energy Transition: The REEFLEX Approach to Flexibility Markets and Improved Grid Management

**Gregorio Fernández (1), Asier Rueda (1), Lorena Elorza-Uriarte (1),
Marcos Remiro-Cinca (1), Georgios Skaltsis (2)**

(1) CIRCE Technology Centre, Zaragoza/Spain; (2) CERTH ITI, Thessaloniki/Greece;
Tel.: +34 699 350 921

gfernandez@fcirce.es, arueda@fcirce.es, lelorza@fcirce.es, mremiro@fcirce.es, gskaltsis@iti.gr

Abstract

In the dynamic environment of the electricity system, characterized by a notable influx of renewable energy sources and the electrification of loads, the significance of prosumers (consumers who possess the ability to both consume and produce, store and distribute their own energy) has grown increasingly crucial. The shift towards renewable energies, while advantageous for reducing carbon footprints and promoting sustainability, introduces a degree of variability and unpredictability into the grid. This variability presents challenges for grid operators who are responsible for maintaining the stability, balance and efficient functioning of the electrical system. To tackle these challenges, prosumers can assume a pivotal role by offering their flexibility in energy production and consumption (the ability to alter electric energy generation and demand patterns based on external signals) to support Distribution System Operators (DSOs) and even Transmission System Operators (TSOs) in managing the grid.

Flexibility markets have emerged as an innovative solution for harnessing the potential of prosumers in stabilizing the grid. Through engaging in these markets, prosumers have the ability to offer valuable flexibility services to grid operators. This not only assists in the management of the grid, but also presents an opportunity for prosumers to generate additional incomes, resulting in a mutually beneficial situation for both grid operators and prosumers. Nevertheless, navigating the intricacies of flexibility markets can prove to be overwhelming for many prosumers, as they must grapple with comprehending market mechanisms, regulations and the technical facets of effectively managing energy assets.

The objective of the REEFLEX project is to enhance the accessibility of flexibility markets, thereby facilitating the involvement and advantages for all types of prosumers. To achieve this, REEFLEX is dedicated to creating a collection of tools that streamline the management of electrical facilities and controllable assets for prosumers. These instruments are carefully designed to enable efficient management of energy resources and effortless participation in flexibility markets, thus overcoming a significant obstacle to prosumer engagement.

Within the REEFLEX project, a cloud platform is being developed, which is poised to incorporate a wide range of tools aimed at revolutionizing the landscape for prosumers within the flexibility markets as well as facilitating the participation of other actors such as aggregators or BRPs for example. These tools cover various functionalities across the entire flexibility management/operation/activation/valuation value chain: calculators that elucidate the possible flexibility options and their cost for different types of prosumers, mechanisms to determine the most advantageous flexibility market for each participant, calculating the flexibility requirements of the Distribution System Operator (DSO),

activation of P2P markets for energy trading between prosumers, NILM algorithms to gain in-depth knowledge of the consumption components of a prosumer, etc. These elements underscore the project's comprehensive approach to bolstering grid stability and efficiency. Among this suite of innovations, the algorithm for optimal management of microgrid assets of prosumers facilities emerges as a foundational component.

This specific algorithm serves as an illustration of the forward-thinking approach of REEFLEX, which is designed to meticulously examine the intricacies of energy production and consumption patterns among prosumers. Through the assessment of various manageable assets and careful consideration of factors such as energy prices, fluctuations in demand, the availability of renewable energy and storage capabilities, it develops personalized strategies for effectively operating prosumer grid systems and participating in flexibility markets. The design of this algorithm embodies the core mission of REEFLEX, which is to simplify the complexities surrounding energy asset management for prosumers, allowing them to make the most of their resources with minimal requirement for extensive market knowledge or direct manipulation of assets.

The entire suite of REEFLEX tools serves as evidence of the project's dedication to promoting a durable and effective energy ecosystem. Through equipping prosumers with the necessary resources to proficiently manage their energy assets, REEFLEX not only amplifies the stability and efficiency of the power grid, but also enables individuals and communities to actively contribute to the ongoing energy transition.

Introduction

The electric grid of the future is poised for transformation driven by the urgent needs of energy transition towards sustainable sources [1]. This transformation is catalysed by the proliferation of distributed energy resources (DERs) such as solar photovoltaics, wind turbines and energy storage systems, along with the increased digitization inherent in smart grid technologies. As the grid evolves from a centralized to a more distributed system, the roles and operations of Distribution System Operators (DSOs) are also undergoing significant changes to accommodate the dynamics of modern energy demands and the integration of renewable energy sources.

The transition to a smart grid is essential in addressing the critical challenges faced by DSOs, including the management of increased grid complexity, maintaining reliability. and ensuring efficiency in the face of fluctuating energy supplies and demands. Smart grid technologies empower DSOs thanks to the development of Information and Communication Technologies with advanced monitoring, control capabilities and enhanced automation facilitated by real-time data communications and IoT technologies [2]. These advancements are vital in managing the intermittent nature of renewable energy sources which, while beneficial for reducing carbon footprints and promoting sustainability, introduce variability and unpredictability into the grid and are key to involve prosumers in the management of the grid since it allows prosumers to help solving grid needs in a decentralized manner that few years ago was impossible to achieve.

One of the principal challenges in this evolving grid landscape is maintaining balance and stability. As traditional baseload power generation is progressively replaced or supplemented by variable renewable energy (VRE), the importance of flexibility in energy use becomes paramount. Flexibility in this context refers to the ability of grid participants—increasingly prosumers [3] —to modify their energy generation or consumption patterns in response to grid needs or (through) economic signals. This flexibility can manifest through

peak shaving, load shifting and participation in demand response programs [4], which are critical for smoothing out the variability caused by high penetrations of VRE.

It is also important to consider that the energy transition towards decarbonization of society involve electrification of loads that previously relied on fossil fuels such as domestic heating or car mobility. This electrification process put extra stress on the grid as increase in consumption and grids may not be prepared to deal with this new scenario, generating congestions and power quality problems such as voltage deviation. In this context, flexibility from prosumers assets also helps to organize efficiently electric consumption without having to rely on grid expansion and other infrastructure investments.

However, the participation of prosumers, particularly small and medium-sized entities, in flexibility markets is not without constraints. These participants often face significant barriers, including a lack of technical expertise to manage and optimize energy assets, insufficient understanding of market mechanisms and the regulatory and economic challenges of interfacing with traditional grid operations. Small-scale prosumers, in particular, may find the initial technological investment and the complexities of regulatory compliance daunting. Also, flexibility markets may set a minimum power threshold as an entry requirement and the vast majority of small-scale prosumers are not able to reach it without participating in broader flexibility schemes through other agents such as aggregators or retail electric companies.

1. REEFLEX approach to empower prosumers in flexibility markets

The REEFLEX project [5] stands at transforming how prosumers interact with Local Flexibility Markets (LFM). By empowering and facilitating the participation of all types of prosumers, REEFLEX addresses the growing need for flexibility within the energy grid, which is increasingly characterized by the variable nature of renewable energy sources.

The primary objective of REEFLEX is to establish a range of feasible interoperable solutions and services which enhance the engagement of energy consumers in demand side flexibility (DSF) markets. These tools and services are constructed upon the establishment of a centralized interoperable platform, linking various stakeholders in the multi-sector energy framework, facilitating their entry into diverse flexibility markets (local, national, European) and offering a selection of tailored interactions and services from the catalogue to meet their energy requirements.

The tools under development in the REEFLEX project are grouped into three pillars:

- P1, Interoperability and data exchange platform. Development of a central platform, enabling the connection and interoperability of all devices, accounting for synergetic, cross-sectoral networks, improving data secure and privacy exchange through these assets.
- P2, Optimal management and flexibility potential. Mobilizing demand response and new services thanks to the standardization of smart assets connected through IoT and the development of a set of solutions aiming at achieving optimal management of microgrids in accordance to end users' demands.
- P3, Connection and interactions with flexibility markets. Establishing easy connections to any flexibility markets, reducing entry barriers and transaction costs.

Pillar 1: Interoperability and data exchange platform	I1.1) Data exchange, handling and interoperability I1.2) VERIFY: Web-based platform enabling LCA/LCC of projects I1.3) USE: Platform enabling uniform evaluation of projects I1.4) Flexibility potential classification for any given asset
Pillar 2: Optimal management and flexibility potential	I2.1) Second-life batteries as flexibility assets I2.2) Predictive flexibility potential and operation of distributed devices I2.3) NILM techniques for large consumers' load disaggregation I2.4) Innovative inverters for storage systems and electric vehicles (V2G) I2.5) Optimal management of the grid
Pillar 3: Connection and interactions with flexibility markets	I3.1) End-users' potential flexibility calculation and aggregation I3.2) Calculation of DSO flexibility needs I3.3) Optimal market selection I3.4) P2P and bilateral energy exchange trading

In order to develop these tools and achieve the project objectives, a consortium has been formed comprising all actors involved in the flexibility value chain, from flexibility providers to flexibility buyers for a better operation of their electricity grids. Technical partners with extensive experience in this type of projects are also involved. A list of REEFELX project partners is given below [6]:

- Prosumers who are going to provide flexibility from their premises:
 - Sociedad Municipal Zaragoza Vivienda SL, ZAVI
 - Holbæk Kommune, Holbæk
 - Cnet Centre For New Energy Technologies SA, EDP-NEW
 - Smart Energy Lab – Association, SEL
 - Abilix Soft LTD, ABILIX
 - Temsa Skoda Sabanci Ulasim Araclarlanonim Sirketi, TEMSA
- Developers of technology, of manageable systems:
 - Betteries Amps GMBH, BETT
 - Arcelik A.S., ARC
 - Enerbrain SRL, ENERB
- Aggregators and ESCOs that will take small prosumers by the hand and bring them to the market:
 - Sistemas Urbanos De Energias Renovables SL, URBE
 - Watt And Volt Anonimi Etairia Ekmetalleysis Enallaktikon Morfon Energeias, WVT
 - Hive Power SA, HIVE
 - Que Technologies Kefalaioushiki Etaireia, QUE
 - Kainotomia Idiotiki Kefalaioushiki Etaireia, INNO
- Regulatory experts:
 - Yugoiztochnoevropayska Tehnologichna Kompania Ood, SETECH
 - Lietuvos Energetikos Institutas, LEI
 - University Of Piraeus Research Center, UPRC
- Market operators:
 - OMI-Polo Espanol SA, OMIE
- DSO:
 - Azienda Elettrica Di Massagno SA, AEM

- Research centres:
 - Fundacion Circe Centro De Investigacion De Recursos Y Consumos Energeticos, CIRCE
 - Ethniko Kentro Erevnas Kai Technologikis Anaptyxis, CERTH
 - Ubitech Limited, UBI
 - Suite5 Data Intelligence Solutions Limited, SUITE5
 - Scuola Universitaria Professionale Della Svizzera Italiana, SUPSI
 - Fundacion CARTIF, CARTIF
- Communication and exploitation experts:
 - Rina Consulting SPA, RINA-C
 - Smart Innovation Norway AS, SIN

REEFLEX places significant focus on showcasing and replicating these solutions in seven distinct countries with varying energy constraints to guarantee interoperability [7]: Spain, Greece, Switzerland, Bulgaria, Portugal, Denmark and Turkey.

2. REEFLEX framework

The REEFLEX platform is designed with a multi-layered approach to streamline flexibility management in modern energy systems. The platform comprises three distinct layers: the local operation layer, the data layer and the business layer. The local operation layer focuses on the optimal operation of microgrids, connecting directly to flexibility assets and utilizing AI techniques to enhance automation and efficiency. This layer integrates key innovations to manage flexibility assets locally while minimizing transaction costs. The data layer serves as the central backbone, providing high-quality data to support analytics and business optimization functions. It includes AI-driven intelligence services, privacy and cybersecurity measures, and mechanisms to enhance data quality, ensuring robust and secure data management.

The business layer of the REEFLEX platform is dedicated to interfacing with flexibility markets, forecasting flexibility needs, and suggesting optimal market selections. It facilitates the trading of flexibility assets by identifying the best bids and offers based on current market prices, thereby optimizing economic returns. Additionally, the platform includes a comprehensive consumer engagement framework aimed at informing and training all stakeholders, from residential consumers to industry managers and regulators. This engagement process ensures that technological solutions are user-centric and widely accepted, enhancing the overall impact of the REEFLEX project in advancing grid flexibility and efficiency.



3. Optimal microgrid management

Optimization algorithms are critical in the realm of microgrid management as they provide a systematic approach to manage the local energy production, storage and consumption of energy within a microgrid. These algorithms take into account various factors including energy demand forecasts, renewable energy generation, energy prices and the physical and technical constraints of the microgrid's components. The primary goal is to obtain the most appropriate management strategy in order to minimize operational costs, maximize energy efficiency and maintain grid stability.

The optimization algorithms for the management of the assets in microgrids has been implemented in several applications. The specific algorithm discussed in FLEXICIENCY [8], [9] project and EV-OPIMNANGER project [10], which are also representative of those used in the REEFLEX project, illustrates a general optimization framework that is adaptable to various microgrid configurations, whether residential, commercial, or industrial environments. The advantages of this management methods are the key where the algorithms management effectively different assets, from traditional and flexible loads to advanced battery storage and renewable generation technologies.

Main challenges Addressed by Optimization Algorithms

Optimization algorithms play a crucial role in demand response management. Energy consumption and production is adjusted in real time through metering instantaneous parameters and predictive scheduling of incoming energy consumption and demand. As a result, the system is able to respond to grid demands or economic signals by modifying the predictive baseline power schedule. This flexibility can help in balancing the supply-demand equation, thus stabilizing the grid and preventing outages.

The increase of renewable energy has carried out a new problem of irregular energy flow regarding when the energy is obtained and when is it used. Energy storage is the solution to this problem but, with the integration of systems like BESS and EV charging stations, managing the storage and timely release of energy becomes essential. Optimization algorithms ensure that energy storage systems operate within their optimal parameters, reducing wear and tear and extending their lifespan. They manage charge and discharge cycles based on energy availability and demand, optimizing the use of stored energy and reducing reliance on external power supplies.

The intermittent nature of renewable energy sources like solar and wind can pose challenges to grid stability. Optimization algorithms help in effectively integrating these sources by predicting energy generation and adjusting the microgrid operations

accordingly. This includes minimizing curtailing generation when necessary to prevent overloading the grid and maximizing the use of generated energy when production peaks.

Optimization Algorithm flexibility

The optimization applications under development have several factors that make them very attractive to the management of smart grids. The development of the algorithm implemented in CIRCE, to be used in REEFLEX project, has shown several flexibilities in different aspects:

- Flexibility in microgrid configurations. Thanks to the mathematical equations that defines the real electrical microgrid circuit, the developed algorithm can be implemented in several circuits, whether they are grid-connected, isolated, connected in DC, AC both.
- Independence in the number and technology of the circuit components. The structure of the algorithm allows the configuration of different technologies for energy generation, storage and consumption. The system can have photovoltaic power generation, battery energy storage, hydrogen generation and EV chargers, among others. It is also possible not to connect all elements or, on the other hand, to connect more than one of the same technologies. In conclusion, the algorithm is independent of the number and technologies of the circuit, configurable by an input file.
- Multiple users connected to the grid. The system can have both several users and a single user. That will define the final destiny of the energy generated and it can be distributed with different criteria. However, the algorithm itself calculates the optimal energy distribution for all the users and all the loads connected regardless of the final number of users.

In addition to the physical flexibility in terms of available system devices, one of the main advantages of the flexibility of the algorithm is the availability to run it in different environments. It can be used remotely in the cloud by uploading the necessary calculations and connecting it to other devices in the system. At the same time, it is possible to use it in local gateways where the calculations are performed on the devices themselves. Despite the limitations that these scenarios may have, due to the limited number of resources available, with limited memory capacity, this algorithm has no problem operating on these platforms.

Example of an Operational Strategy

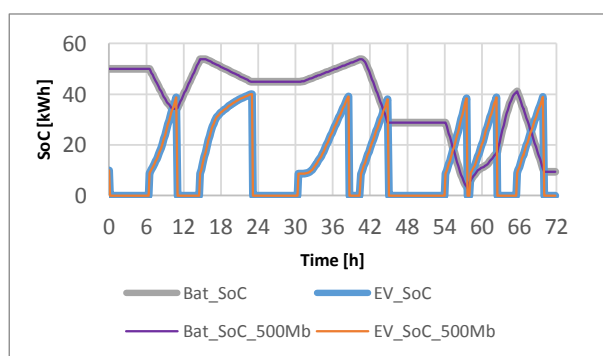
One of the scenarios tested with the optimization algorithm corresponds to an isolated petrol station with a solar generation system, battery energy storage, electric vehicle charging and a hydrogen system with electrolyze and fuel cell. The optimization algorithm developed uses a comprehensive model that includes:

- PV System Constraints: Prioritizes the use of solar energy by minimizing associated operational and maintenance costs. The possibility of curtailment is included.
- Battery Storage Constraints: Manages battery operations to extend life and efficiency, incorporating limits on charging and discharging.
- EV Charging Constraints: Balances the need for rapid charging with grid capacity and stability. It depends in EV time availability and the power limits of the charger.
- Hydrogen System Constraints: Manages hydrogen production, storage and usage, ensuring efficient operation of electrolyzers and fuel cells.
- Grid Connection Constraints: Controls the interaction with the main grid, managing energy import and export based on contracted power and variable energy costs.

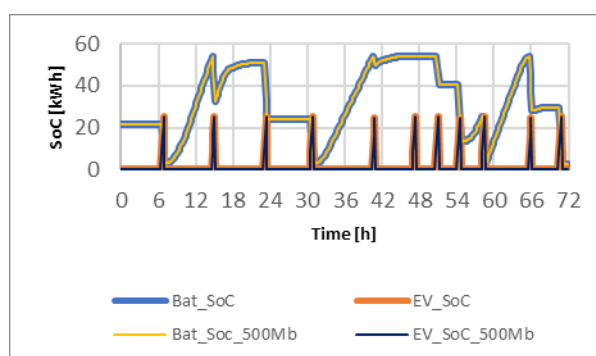
These constraints are part of a mathematical model that also incorporates flexibility options, allowing the algorithm to adjust operations based on variable energy prices and demand signals from flexibility markets. The initial case under examination corresponds to an isolated grid instance with a battery State of Charge (SoC) exceeding 80% and a limited quantity of charging vehicles. The second case has an initial battery SoC below 40% and the number of electric vehicle charges is double that of the previous case.

The results obtained within the test demonstrated the flexibility and stability of the implemented algorithm. The data presented in the following table indicates that both the duration of the simulation and the results of the objective function remain consistent regardless of the location where the algorithm is deployed, even when the calculation capacity is restricted by a memory constraint. Moreover, the predictions for the charge of the vehicles and the use of batteries generate the same forecasts, as the graphs below demonstrate.

		Objective function	Simulation Time
Case 1 SoC_init = 80 % EV_charged = 6	Memory limit, 500 Mb	-103.84 €	14.38 s
	No limit	-103.84 €	10.36 s
Case 2 SoC_init = 40 % EV_charged = 12	Memory limit, 500 Mb	-90.98 €	29.88 s
	No limit	-90.98 €	20.69 s



Case 1



Case 2

4. Conclusions

In the dynamic electricity system, prosumers play a crucial role in the face of increasing renewable energy sources and electrification of loads. The renewable energy shift benefits sustainability but adds variability, posing challenges for grid operators. Prosumers can help by offering flexibility in energy production and consumption to assist in grid management. Flexibility markets enable prosumers to provide valuable services to grid by participating, benefiting both parties. Prosumers can generate additional income by engaging in flexibility markets. Understanding market mechanisms, regulations and technical aspects can be challenging for some prosumers, mainly smaller ones.

The aim of the REEFLEX Project is to improve the availability of flexibility markets, which in turn facilitates the engagement and benefits for all categories of prosumers. In order to realize this goal, REEFLEX is committed to developing a set of resources that simplify the supervision of electrical infrastructures and controllable assets for prosumers. These tools are meticulously crafted to enable effective management of energy assets and customer

involvement in flexibility markets, thereby surmounting a significant hurdle to prosumer participation.

One of the most important algorithms to be developed in the framework of the REEFLEX project is the optimal operation of microgrids, as it allows maximum use of the flexible, manageable resources of each prosumer. The optimization algorithm shown in this article, one of several being developed in the project, will be tested in the project on various execution platforms, in the cloud and on physical platforms or gateways. For this reason, in these initial phases of the project, the stability of the solution is being tested by emulating different execution environments with positive results.

References

- [1] Ma W, Xue X, Liu G. Techno-economic evaluation for hybrid renewable energy system: application and merit. *Energy*, Volume 159, 2018, Pages 385-409, ISSN 0360-5442, <https://doi.org/10.1016/j.energy.2018.06.101>.
- [2] S. Golshannavaz, S. Afsharnia and F. Aminifar, "Smart Distribution Grid: Optimal Day-Ahead Scheduling With Reconfigurable Topology," in *IEEE Transactions on Smart Grid*, vol. 5, no. 5, pp. 2402-2411, Sept. 2014, doi: 10.1109/TSG.2014.2335815
- [3] Zhang C, Wu J, Zhou Y, Cheng M, Long C. Peer-to-Peer energy trading in a Microgrid. *Appl Energy* 2018;220:1–12. <https://doi.org/10.1016/j.apenergy.2018.03.010>
- [4] Eid C, Codani P, Perez Y, Reneses J, Hakvoort R. Managing electric flexibility from Distributed Energy Resources: a review of incentives for market design. *Renew Sustain Energy Rev* 2016;64:237–47. <https://doi.org/10.1016/j.rser.2016.06.008>
- [5] <https://reeflexhe.eu/>, May 2024
- [6] <https://reeflexhe.eu/partners/>, May 2024
- [7] <https://reeflexhe.eu/demo-site/>, May 2024
- [8] G. Fernández, M. A. Oliván, J. Sediles, J. Sanz, J. Almajano, J. Bruna, A. Muñoz, "Performance monitoring and optimization of an electric vehicle charging station" in 32nd Electric Vehicle symposium (EVS32), Lyon, France, May 2019
- [9] G. Fernández, M. A. Oliván, J. Sediles, A. Muñoz, J. Bruna, H. Bludszuweit, I. Prieto, "Transformation of a microgrid into a distribution grid support asset" 2019 25th International Conference on Electricity Distribution, Madrid, Spain
- [10] G. Fernández, J. Almajano, E. García, H. Bludszuweit, S. Machín and J. F. Sanz, "Control structure for optimal demand-side management with a multi-technology battery storage system," 2019 24th IEEE International Conference on Emerging Technologies and Factory Automation (ETFA), Zaragoza, Spain, 2019

G07 Enabling Technologies II & Operation & Regional Conditions

G0701

Sector Coupling for Renewable Energy Sources Integration – A Case Study for the German Gas Transmission Network

**Luisa Di Francesco (1), Marco Cavana (1), Yifei Lu (2,3), Pierluigi Leone (1),
Andrea Benigni (2,3,4)**

(1) Department of Energy “Galileo Ferraris”, Politecnico di Torino, Torino/Italy;

(2) IEK-10: Energy Systems Engineering, Forschungszentrum Jülich, 52428
Jülich/Germany;

(3) RWTH Aachen University, 52056 Aachen/Germany;

(4) JARA-Energy, 52425 Jülich/Germany;

luisa.difrancesco@polito.it

Abstract

Sector coupling is a possible way to increase the flexibility of the energy system enabling surplus power generated by renewables to be converted through electrolysis into a fuel, typically hydrogen, that can be transported and dispatched through blending in the natural gas grid or pure in a dedicated backbone. This integration of the electricity and gas sectors aids in stabilising the power grid, mitigating imbalances caused by unforeseen volatilities and excessive renewable power production. However, it is necessary to understand the impacts of transporting and distributing hydrogen on gas networks from multiple perspectives, as explored in this research.

The aim of this work is the assessment of the hydrogen receiving capacity of the gas network under coupling with the power network, in case of a hydrogen blending limit of 20%vol. The addressed case study consists of the simulation of the German gas transmission network with direct green hydrogen injection coming from renewable electricity surplus. Germany, being one of the biggest gas markets, having expressed a strong interest in the development of a hydrogen market and with its highly meshed gas infrastructure is an interesting playground for this case study. The topology, demand and hydrogen data are collected from open-source datasets, while the fluid-dynamic model is an own development in MATLAB.

The regional surplus of electricity produced by renewable energy sources is converted into hydrogen through electrolysis; this fuel is then injected into the gas grid, in the same region where the electricity surplus occurs.

For the day of the highest hydrogen production, an hourly simulation is run: the amount of curtailed hydrogen and its location is obtained, as well as the amount of energy that has been successfully integrated into the gas grid.

The final aim is to quantify the additional flexibility that sector coupling provides while ensuring gas quality requirements.

Introduction

In order to decarbonise the energy sector, renewable energy sources play an important role. In Europe, renewable power generation is steadily increasing, reporting in 2022 a share of 41.2% of the total EU gross electricity consumption [1]. During the same period, Germany witnessed renewable energy sources contributing to 44.1% of gross electricity production, with wind power alone comprising 21.6% [2]. The primary challenge associated with renewable energy sources lies in their intermittency, stemming from the volatility of the available energy from sunlight and wind. Consequently, achieving electrical flexibility becomes imperative for electricity systems with significant penetration of renewable energy, enabling the maintenance of balance between power generation and demand.

Power-to-gas emerges as a promising technology, involving the conversion of excess electricity generated by renewable energy sources, primarily into hydrogen that can be transported via pipeline as a pure gas or in a mixture with natural gas [3]. Such sector coupling between electricity and gas not only supports the operation of the power grid but also addresses issues arising from the unpredictability of power injections from wind parks, which can disrupt the balance between generated and required electric power [4].

Moreover, the production of hydrogen with renewable electricity gains importance when considering the fact that, in Germany, in 2023, 19 TWh of RES has been curtailed, resulting in 3.1 billion euros of congestion management, which represents a consistent loss of money and energy [5]. This problem is not restricted to a specific country, rather it is a common issue among all the power systems with a large share of intermittent renewable generation.

The acceptability of hydrogen into the natural gas pipeline infrastructure is a frequent source of debate in the EU. A recent European Directive [6] established a cap of 2% volume of hydrogen that can be blended for cross-border transport.

Germany, as one of the largest natural gas markets in the EU, has always expressed a strong interest in the further development of its hydrogen infrastructure. In 1938, the Ruhr region saw the construction of its inaugural long-distance hydrogen pipeline spanning 215 kilometres [7]. In November 2023 the country's government unveiled a plan for hydrogen transport via pipelines to the major ports, industries, power plants and storage facilities of the country [8][9]. As well as pure hydrogen transport, the country is also enhancing blending with natural gas, in fact, it reports the regulatory framework with the highest concentration limit at the transmission level (10%) in the EU; furthermore, there are several pilot projects blending even higher hydrogen concentrations [10].

Thus, it can be asserted that the gas network incorporating hydrogen injection constitutes a complex system necessitating safe and predictable operation. Consequently, meticulous monitoring and thorough examination of any alterations to this infrastructure are imperative.

Although some examples of gas network simulation with hydrogen blending and sector coupling can be found in the literature, it is clear that there is a need to fill an important gap: in fact, the requirements of the natural gas network concerning hydrogen blending are not taken into account, even though it is important to understand how much, with respect to the total green hydrogen produced with power-to-gas, can actually be accepted by the network and how much must be curtailed in order to comply with the current regulations.

On the other hand, a quantitative estimation of extra renewable energy integrated within the system by means of sector coupling is necessary as a proxy of the degree of flexibility that power-to-gas options can unlock.

Therefore, the objective of this paper is to present, by using a gas network model, an assessment of the curtailment of hydrogen with the aim of quantifying the actual acceptance of the natural gas network and estimating the potential of sector coupling. The proposed simulation method is calibrated on the German gas transmission network: the data regarding network topology, domestic consumption, cross-border flow and green hydrogen production are collected from open-source datasets, while the fluid-dynamic model alongside quality tracking and curtailment is developed in MATLAB. Besides the baseline scenario, an additional simulation is conducted wherein hydrogen is blended at different points within the grid to reduce its curtailment as an enhanced operational strategy in sector-coupling scenarios. The concluding section of this study provides a summary of the findings and draws the key conclusions.

1. Model of the German gas transmission network

1.1 Open-Source Input Data

The data needed to run the simulations are mainly of two types: topology data and consumption data.

Topology data is sourced from the SciGRID_gas project, specifically, the dataset labelled SciGRID_gas IGGIELGN [11]. This dataset is compiled from various open-source data outlets, encompassing information about the European gas network.

The processed network dataset comprises 658 nodes and 1019 pipelines, representing the German gas transmission network, as depicted in Figure 1. Each node within the network requires an assignment of natural gas demand, a process detailed in subsequent sections.

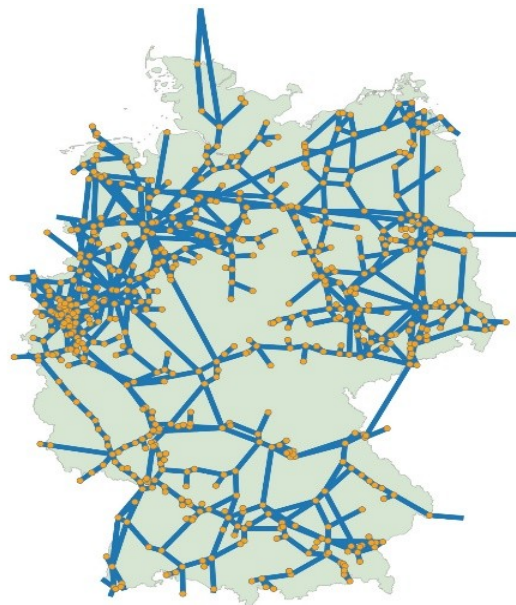


Figure 5 – Network model of the German gas transmission network used in this work

The domestic demand for natural gas is provided by DemandRegio [12], where data and tools for the spatial and temporal breakdown of German electricity and gas demand are provided. The outcomes include three demand time series, each corresponding to an analysed sector (industrial, residential and services). These results are available at a

NUTS-3 resolution, with a temporal resolution of 15 minutes for the industrial sector and one hour for households and commercial, trade and services (CTS) sectors.

To accurately simulate the network behaviour, it is crucial to consider the gas import and export into and out of the country. Specifically, regarding gas exchanged between Germany and neighbouring countries, data from the German Network Agency (Bundesnetzagentur) are employed. These records are based on calculations from the data provided by German transmission system operators for natural gas and they are available at [13].

Lastly, the data concerning hydrogen injection is derived based on the Open Power Systems Data dataset, which provides weather data as well as data about the location and the electrical capacity of the renewable (PV and wind) power plants in Germany [14][15]. These data enable the calculation of renewable energy production: the electricity generated by renewable plants is deducted from the electricity demand in order to calculate the renewable electricity surplus. It is important to point out that this deduction is made on a regional balance: Because in this work the power generation dispatch and the German power transmission system are not modelled, the transmission of the surplus of electricity in a region is not considered, instead, it is fed to electrolyzers for hydrogen production.

To dampen this simplification, which leads to an overestimation of the renewable electricity surplus, the maximum domestic electrolyser capacity has been set to 10 GW, according to the German power network development plan for 2030 [16]. If this threshold is overcome, the regional surplus is proportionally redistributed to match the country's total of 10 GW, i.e. regions with higher renewable surplus will be allocated a larger share of electrolyser capacity.

This regional renewable electricity surplus is subsequently introduced into the gas grid as hydrogen. As stated by SRIA Key Performance Indicators [17] for an alkaline electrolyser, the full stack efficiency in 2024 is 68% (LHV based). From this value, another 5% is deducted to take into account the Balance of Plant (BoP) and the fact that the electrolyser will not always operate at its nominal power.

According to the calculations, for 2015, the renewable electricity generated amounts to approximately 192 TWh, aligning with the data presented in [18] for the same year. Wind farms provide the largest share, accounting for 147 TWh, while 46 TWh is obtained from PV plants.

Conversely, the curtailment of this electricity (utilised as surplus for hydrogen conversion) stands at about 38 TWh which accounts for roughly 19.8% of the total renewable energy production. According to [5], the actual curtailment in 2023 amounted to 19 TWh, so the initial hypothesis leads to an overestimation of the curtailed renewable power generation.

The total gas consumption in Germany, as provided by DemandRegio, amounts to 659 TWh in terms of energy. Therefore, hydrogen could potentially meet 4.3% of this demand, with the hypotheses specified above.

1.2 Scenarios definition for sector coupling

The generated dataset comprises data of the German gas transmission grid and hourly demand data at each network node for a year. To illustrate the most unfavourable scenario regarding sector coupling, a one-day hourly simulation is conducted during the peak green hydrogen production day.

To make significant comparisons, several case studies are run:

- 1 Base-case scenario without hydrogen injection: this is a hourly time-series simulation of the German gas transmission network with natural gas.
- 2 Full hydrogen injection scenario (no curtailment): here, the whole amount of green hydrogen produced by the renewable energy sources is blended in the natural gas

- grid and compliance with technical standards (i.e. DVGW G 260 (A) Technical rule, Gas quality) is not taken into account.
- 3 Technical standard compliant scenario with hydrogen injection and curtailment: compliance with gas network technical standard with hydrogen cap set to 20%. Even if the current injection limit in the country is set to 10%, the authorities report the existence or the planning of projects aiming to increase the hydrogen acceptance limit of their networks [10].
 - 4 Enhanced sector coupling scenario with localization of hydrogen injection points: in the previous cases, hydrogen is injected near the PV plant or wind farm responsible for the electricity surplus employed for its production, regardless of the characteristics of the site. In some cases, the injection was performed in small pipelines located in regions with low consumption and this led to higher curtailments. To highlight the importance of the injection point and to enable a higher blending of hydrogen, the curtailment analysis is performed on a new configuration in which the electrolyser positions are chosen more carefully. The importance of this choice is highlighted in [19], here the authors accentuate the fact that electrolyzers will have a significant impact on both the gas and power grid and that their positioning deserves proper TSO attention. In this new scenario, hydrogen is injected in pipelines that are able to bear higher flow rates but, at the same time, they are not too far from the production site (100 km at maximum).

In the subsequent section, the main results of the simulation of the previously described scenarios are summarized and commented on.

2. Results

Figure 2 shows the hydrogen that is accepted and the gas demand at every hour of the day according to the technical standard compliant scenario (scenario 3). It can be observed that the maximum hydrogen acceptance occurs in the early morning, between 5 and 7 a.m., at the same time, the gas demand peaks as well, in accordance with [20], and when the demand is higher it is possible to mix more hydrogen in the natural gas flow.

The minimum hydrogen acceptance occurs at night, between 11 p.m. and 1 a.m., even if the renewable surplus is high (see Figure 3), the acceptance of hydrogen is low simply because there is low gas demand, so the grid is not accepting blending.

In the middle of the day, gas demand is not as high as in the morning or evening, furthermore, electricity surplus is at its minimum, therefore the network does not experience a high hydrogen concentration.

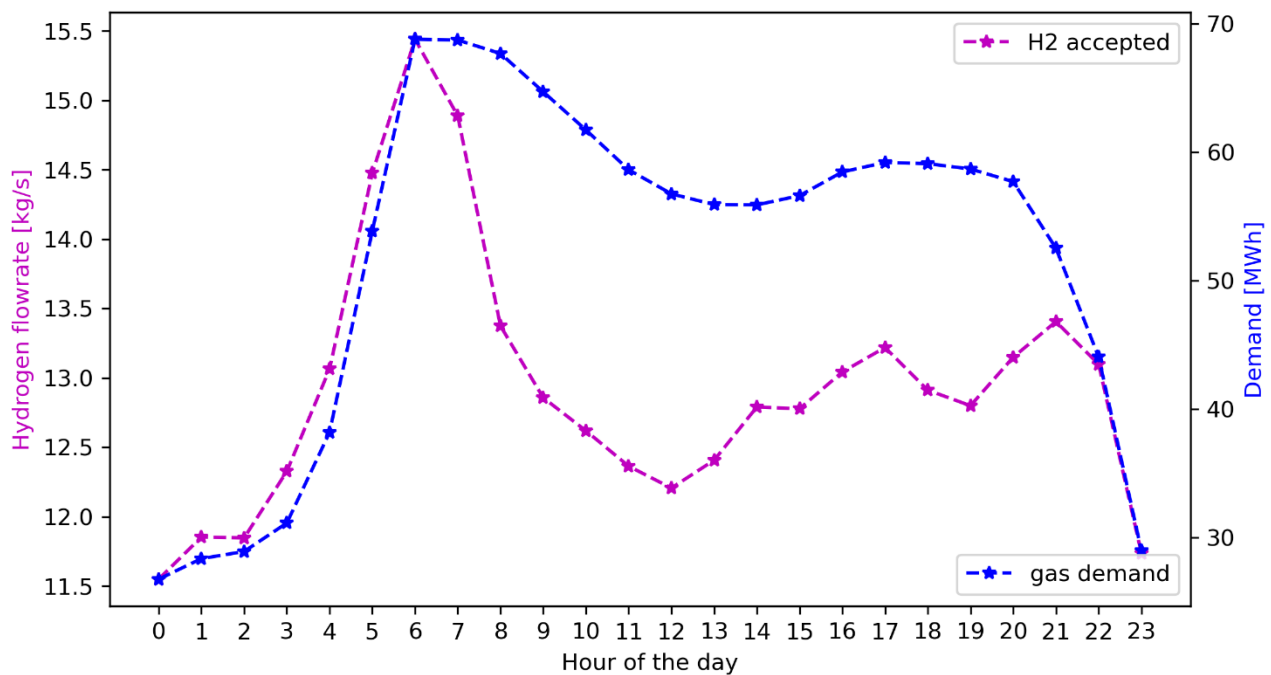


Figure 2 - Hourly hydrogen acceptance and natural gas demand

Figure 4 shows the location of the hydrogen injection nodes and their corresponding curtailment; Figure 5 shows the renewable electricity surplus for the German NUTS-2 regions. It is possible to notice that the highest curtailment corresponds to the zones with the highest renewable plant concentration: in the northern part of Germany, the wind farms are very common, while in the south-east the PV plants are more common [21][22]. Notably, on the considered day of simulation, the areas with surplus are close to each other making difficult and less attractive other flexibility options such as increasing power network interconnections and transmission capacity.

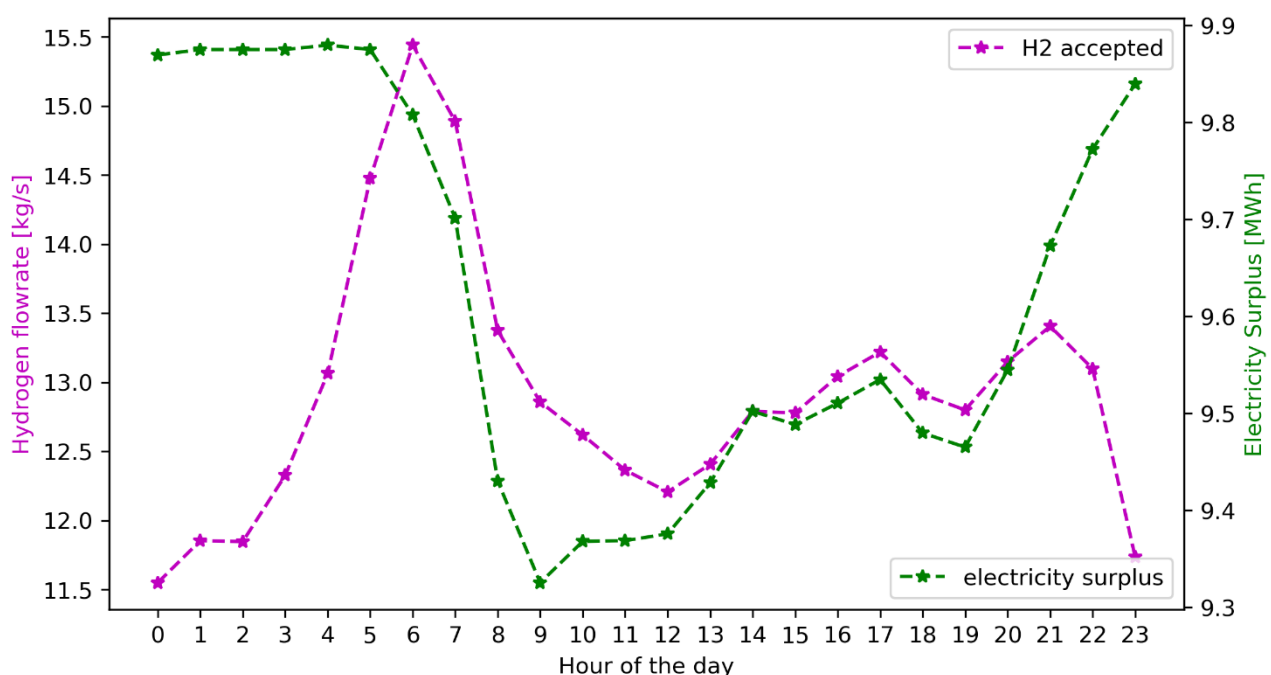


Figure 3 - Hourly hydrogen acceptance versus electricity surplus

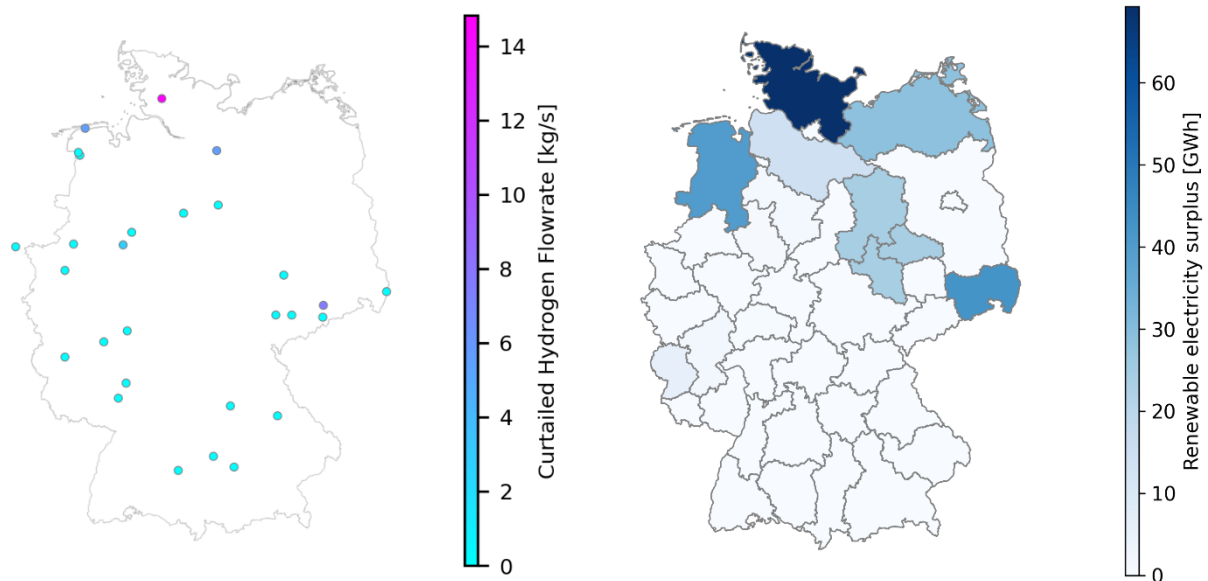


Figure 4 - Hydrogen curtailed from the hydrogen injection pipelines at 6 a.m.

Figure 5 – Renewable electricity surplus for the day in which it is maximum

Figure 6 shows the concentration of hydrogen in all the nodes of the network, without and with curtailment (left and right respectively). It is possible to notice that the most stressed parts of the grid, in terms of hydrogen concentration, are the same in the two cases. However, in the latter case, hydrogen concentration does not overcome the user-specified limit of 20% and, in general, remains lower than 10%, as per the regulatory framework [10].

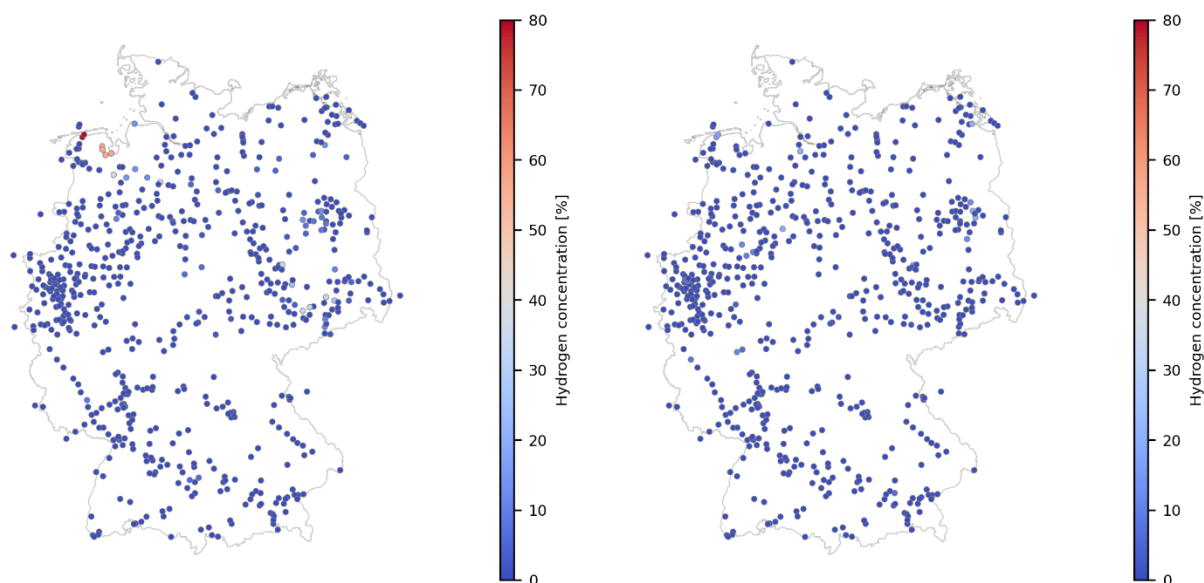


Figure 6 - Hydrogen concentration in the nodes of the network before (left) and after (right) curtailment at 6 a.m.

The hydrogen acceptance depends on the amount of natural gas flowing in the pipelines. In order to increase the acceptance, it is possible to explore some strategies for the localisation of the hydrogen injection points; notably, hydrogen can be injected where the gas flow rate is high, so that a higher amount can be blended. However, it is also important to inject the fuel at a point that is sufficiently near to the production site, in order to reduce transportation costs. Therefore, new injection points are chosen relaxing from the requirements about the distance from the production site (from 20 to 100 km), but enabling injection in bigger pipelines that can bear higher flow rates. As a result, the hydrogen acceptance is increased, as displayed in Table 1.

	Technical standard compliant	Enhanced sector coupling
Total hydrogen available [kg/s]	51.9	51.9
Accepted hydrogen [kg/s]	15.4	21.4
Curtailed hydrogen [kg/s]	36.5	30.5
Curtailed percentage [%]	70.3	58.7

Table 1 - Comparison with different hydrogen injection points

The controlled hydrogen blending i.e. curtailment, can enable hydrogen usage in the natural gas network, thereby lowering CO₂ emissions, while maintaining the physical properties of the mixture near to the case with conventional natural gas transport. It can, therefore, be a way of utilising hydrogen without disrupting the natural gas grid reliability. As per German regulations, the heating value of the gas mixture circulating in the network has to be in the range of 30.2 – 47.2 MJ/m³ [23]. In the case of curtailment, the heating value is compliant with the regulations, reaching a minimum value of 32.2 MJ/m³.

The findings indicate that approximately 230 GWh of renewable energy would be curtailed during the day. By converting it into hydrogen, with the efficiency specified in section 1, the potential renewable energy integrated by sector coupling (e.g., therefore switching from electricity energy carrier to hydrogen energy carrier) amounts to about 173 GWh. With hydrogen injection, it becomes feasible to utilize 44 GWh, thereby enabling the utilization of 29% of the renewable energy that would otherwise be curtailed. The remaining 129 GWh are not directly injected into the natural gas network in the form of hydrogen to be compliant with the gas network requirements. However, this amount of hydrogen can still be stored or used for other purposes than blending, enabling different business models.

3. Added Values/Conclusion

Examining the integration of hydrogen into the high-pressure natural gas transmission system holds significant importance, as it is a means for renewable electricity integration and CO₂ emission reduction. However, as hydrogen possesses markedly different properties compared to natural gas, it is imperative to thoroughly investigate the implications of power and gas sector coupling from the point of view of the natural gas infrastructure, since operators of the natural gas transmission system are keen on preserving the existing operational conditions of the network while increasing the hydrogen content in the gas mixture.

Besides the fluid dynamic simulation, this paper models as well the curtailment of green hydrogen, which is crucial to control the composition of the mixture flowing in the grid. This model is then applied to the German gas transmission network and two main conclusions are drawn:

- The hydrogen curtailment depends on natural gas demand, a low demand leads to a high curtailment. Therefore, it would be possible to schedule the **hydrogen injection operation** based on the hourly gas demand.
- The careful **localization of injection points** is crucial since it can enable a higher acceptance rate of hydrogen as shown in this work.
- Sector coupling possesses the capacity to utilise renewable electricity that might otherwise go unused.
- Sector coupling and, more in general, integration of renewable gases within the gas network requires careful monitoring and availability of real-time operational data for safe operation.

Although this study has some major limitations, including the fact that the power system is not analysed and a simplified analysis of the surplus potential/profile, it gives some quantitative insights about opportunities of sector coupling, the need to introduce operational strategies of gas networks for optimal hydrogen injection schedule and of guidelines for site-selection of injection points. Further study is needed, especially about business case analysis exploring the feasibility of pure sector coupling upon potential low capacity factors of electrolyzers; more complex dispatch strategies could be explored by looking at gas network integration and other uses of hydrogen in pure form. Finally, similar simulations could be explored in the view of exploring sector coupling between power network and future hydrogen backbone where relaxation of gas quality constraints may be beneficial.

References

- [1] European Union, "Electricity from renewable sources up to 41% in 2022," 2024. [Online]. Available: [https://ec.europa.eu/eurostat/web/products-eurostat-news/w/ddn-20240221-1#:~:text=In%202022%2C%20renewable%20energy%20sources,coal%20\(less%20than%2017%25\).](https://ec.europa.eu/eurostat/web/products-eurostat-news/w/ddn-20240221-1#:~:text=In%202022%2C%20renewable%20energy%20sources,coal%20(less%20than%2017%25).) [Accessed 03 05 2024].
- [2] F. S. O. o. Germany, "Gross electricity production in Germany," 05 4 2023. [Online]. Available: <https://www.destatis.de/EN/Themes/Economic-Sectors-Enterprises/Energy/Production/Tables/gross-electricity-production.html> [Accessed 10 05 2024].
- [3] L. G. S. H. C. Bin Miao, "Long-distance renewable hydrogen transmission via cables and pipelines," *International Journal of Hydrogen Energy*, vol. 36, pp. 18699-18718, 2021.
- [4] S. C. M. C. R. Giulio Guandalini, "Power-to-gas plants and gas turbines for improved wind energy dispatchability: Energy and economic assessment," *Applied Energy*, vol. 147, pp. 117-130, 2015.
- [5] B. Wehrmann, "Curtailing of renewable power increases in Germany in 2023 as re-dispatch costs recede", Clean Energy Wire, Available: <https://www.cleanenergywire.org/news/curtailing-renewable-power-increases-germany-2023-re-dispatch-costs-recede>
- [6] D. ST-16522-2023, "Proposal for a REGULATION OF THE EUROPEAN PARLIAMENT AND OF THE COUNCIL on the internal markets for renewable and natural gases and for hydrogen (recast)," 2023.
- [7] Z. T. G. Z. C. Z. e. a. Hantong Wang, "Research and demonstration on hydrogen compatibility of pipelines: a review of current status and challenges," *International Journal of Hydrogen Energy*, 2022.

- [8] Hydrogeninsight, “German hydrogen pipeline network will begin transporting H2 in 2025, with 9,700km in place by 2032, says government,” 2023. [Online]. Available: <https://www.hydrogeninsight.com/policy/german-hydrogen-pipeline-network-will-begin-transporting-h2-in-2025-with-9-700km-in-place-by-2032-says-government/2-1-1554455>.
- [9] Reuters, “Germany presents hydrogen core network plan in bid for 2045 climate neutrality,” 2023. [Online]. Available: <https://www.reuters.com/business/energy/germanys-core-network-hydrogen-fuel-cost-20-bltn-euros-by-2032-fnb-gas-chairman-2023-11-14/>.
- [10] A. f. t. C. o. E. Regulators, “ACER Report on NRAs Survey -Hydrogen, Biomethane, and Related Network Adaptations,” 2020.
- [11] A. P. a. W. M. Jan Diettrich, “SciGRID_gas IGGIELGN,” 17 05 2021. [Online].
- [12] F. Gotzens, B. Dr.-Ing. Gillesen, S. Burges, W. Hennings, J. Prof. Dr.-Ing. Müller-Kirchenbauer, S. Seim, P. Verwiebe, T. Dr.-Ing. Schmid, F. Jetter and T. Limmer, “DemandRegio – Harmonisierung und Entwicklung von Verfahren zur regionalen und zeitlichen Auflösung von Energienachfragen – Abschlussbericht,” *Forschungszentrum Jülich GmbH, Jülich; Technische Universität Berlin, Berlin; Forschungsstelle für Energiewirtschaft e. V., München*.
- [13] Bundesnetzagentur, “Daily data,” [Online]. Available: https://www.bundesnetzagentur.de/DE/Gasversorgung/aktuelle_gasversorgung/start.html. [Accessed 04 03 2024].
- [14] Stefan Pfenninger and Iain Staffell. *Open Power System Data*. Version 2020-09-16. Data Package Weather Data, 2020. doi: 10.25832/weather_data/2020-09-16. url: https://doi.org/10.25832/weather_data/2020-09-16
- [15] Ingmar Schlecht and Milos Simic. *Open Power System Data*. Version 2020-05-20. Data Package Renewable power plants, 2020. doi: 10.25832/renewable_power_plants/2020-05-20. url: https://doi.org/10.25832/renewable_power_plants/2020-05-20
- [16] Bundesministerium für Wirtschaft und Klimaschutz, Fortschreibung der Nationalen Wasserstoffstrategie: NWS 2023, 2023/07
- [17] EU Commission, Clean Hydrogen JU – SRIA Key Performance Indicators (KPIs). url: https://www.clean-hydrogen.europa.eu/knowledge-management/strategy-map-and-key-performance-indicators/clean-hydrogen-ju-sria-key-performance-indicators-kpis_en
- [18] U.S. Energy Information Administration. Germany’s renewables electricity generation grows in 2015, but coal still dominant. url: <https://www.eia.gov/todayinenergy/detail.php?id=26372#:~:text=Renewable%20electricity%20generation%20in%20Germany,the%20country%27s%20gross%20electricity%20generation>
- [19] A. a. S. N. a. S. e. S. N. a. I. A. European Commission and Directorate-General for Energy and Lliceto, “Hydrogen’s impact on grids – Impact of hydrogen integration on power grids and energy systems,” Publications Office of the European Union, 2023.
- [20] M. P. et al., “Capturing variation in daily energy demand profiles over time with cluster analysis in British homes (September 2019 – August 2022),” *Applied Energy*, vol. 360, 2024.

- [21] L. Holm, "Wind power Germany 2016 fact sheet: electricity generation, development, investments, capacity, employment and the public opinion. Data: Strom-Report, BWE, BmWi, Dt. WindGuard, Fraunhofer, AEE, EWEA (WindEurope)," 2016.
- [22] L. Holm, " Solar power Germany 2016 fact sheet: electricity generation, development, investments, capacity, employment and the public opinion.," 2017.
- [23] bayernwerk, "Gasfamilien nach DVGW-Arbeitsblatt G 260 (Gasbeschaffenheit)," [Online]. Available: <https://www.bayernwerk-netz.de/content/dam/revu-global/bayernwerk-netz/files/kommunen/installateure/bayernwerk-gasfamilien-erdgase-gasgeraetekategorien.pdf>.

G0702

UrbanTwin: Development of a Local Energy Strategy and Grid Infrastructure 2050

**Pål Forr Austnes (1), Riccardo Saporiti (2), Catarina G. Braz (3), Bingqian Liu (3),
Luc Girardin (3), Mario Paolone (1), Fabio Nobile (2), François Maréchal (3),
Max Chevron (4)**

(1) Distributed Electrical Systems Laboratory, EPFL Lausanne, ELL 136 Station 11,
1015 Lausanne/Switzerland;

(2) Scientific Computing and Uncertainty Quantification – CSQI Chair, EPFL Lausanne,
Bâtiment MA, Station 8, 1015 Lausanne/Switzerland;

(3) Industrial Process and Energy Systems Engineering Group, EPFL Valais Wallis,
Rue de l'Industrie 17, 1951 Sion/Switzerland;

(4) Services Industriels de Lausanne, Lausanne/Switzerland;

+41 21 693 46 70

pal.austnes@epfl.ch

Abstract

The Swiss Energy Strategy 2050 aims at steering the energy supply system towards a net zero-emission target by 2050 while ensuring an efficient, renewable and secure energy supply. Achieving such an objective requires a substantial increase in electricity generation through binding targets for decentralized renewable generation. In this respect, the Swiss parliament recently increased the target of photovoltaic (PV) production for 2035 from 11.5 to 35 TWh, representing a growth of 2.2 TWh per year, compared with the yearly 6 TWh produced in 2022. At the same time, the decarbonization of districts and buildings' heating/cooling, as well as private mobility will increase the electricity demand by around 12 %, according to the Swiss Energy Outlook 2050+. This implies a large deployment of distributed PV in districts' low-voltage (LV) distribution networks, as large-scale PV plants are constrained by space needs. The combination of increased end-user consumption and distributed PV requires large investments in new assets, but also in infrastructure. In particular, the characteristics of the power flows in LV-grids will change significantly, possibly leading to overloading on lines and reduced power quality.

In this work, we propose a decision-support framework for sustainable urban energy system planning considering investment costs, operation costs and accurate modelling of boundary-conditions. Our framework integrates large datasets from in-field sensors and infrastructure in a multi-objective planning tool targeting municipalities and other governmental entities.

Introduction

Switzerland is committed to a rapid reduction of greenhouse gas emissions. Following the referendum of June 18, 2023, the approval of the “Climate and Innovation Act” means that Switzerland has legislated a reduction to net-zero emissions by 2050. The long-term climate strategy lays the foundation for emissions reduction through 10 principles, based on the “Energy Perspectives 2050+” plan from 2020 [1]. Net-zero emissions include negative emissive technologies; however, the ambition is to reduce current greenhouse gas emissions by 90%. Emission reduction is thus required across all sectors and relies heavily on electrification. Sectors with large emissions, such as buildings and mobility, should transition to renewable energy, e.g. using heat pumps for heating/cooling and battery electric vehicles (BEV). Although the Swiss electricity grid is largely decarbonized today, due to the use of nuclear and hydropower generation, the significant expected demand increase along with the progressive phase-out of nuclear power generation means additional renewable energy resources need to be added. Rosser et al. [2] estimates an additional need of 9 TWh of electricity for cars and buses in 2035, and 17 TWh in 2050. The government's response has been to promote modern renewable energies such as solar PV and wind power. The large increase in demand and intermittent supply requires investment in infrastructure. In particular, the use of distributed energy resources (DERs), such as solar rooftop PV requires careful modelling of physical flows in the LV-grid as it can become congested.

The development of sustainable and resilient energy systems is a critical challenge facing urban areas worldwide, particularly as cities strive to meet ambitious climate goals and accommodate growing populations. In this context, urban digital twins have emerged as powerful tools to aid city planners and decision-makers. These models combine big data, edge-sensing and multi-step multi-objective optimization models to build a digital replica of a city's critical infrastructure enabling real-time observability, simulation of scenarios and planning exercises for optimal asset-utilization, cost-minimization and user satisfaction. Digital twin models spanning multiple sectors allow for sector-coupling, i.e. combining sectors such as energy, water, buildings, mobility and waste in a holistic framework to allow coordinated operation and planning. They have been enabled by the large expansion of edge-sensing devices (e.g. Internet-of-Things), large databases of in-field measurements, increased computing capacities, development of complex machine learning and statistical tools and homogenization of standards and protocols for data exchange.

To increase the utilization factor, reduce the need for costly grid expansion and minimize PV curtailment, maximum LV-grid hosting capacities must be estimated. These capacities should include grid constraints and uncertainty in production and consumption to reflect the actual grid loads. Currently, real-time monitoring of LV-grids is limited, rendering their state practically unobservable. This requires accurate planning of the network design and expansion to ensure constraints are respected during operation. The relevant grid constraints are nodal voltages, lines and transformers loading. In this respect, the legislative framework for power quality in European grids is formalized in the EN 50160 standard [3]. According to EN 50160, voltage variations in LV-grids should not exceed $\pm 10\%$ of the nominal voltage. Under normal operation, 95% of the 10-minute average voltage in a weekly period shall lie within the 10% limit. Line loading constraints are specified by the manufacturer and typically consist of a long-term, short-term, and emergency current-carrying limit.

LV-grids are traditionally designed with a radial topology and power-flows were historically uni-directional, i.e. from the MV/LV-transformer to the loads. However, with the increasing adoption of DER, particularly rooftop solar PV, reverse power flows can occur. The transition of LV-nodes from simple consumers to prosumers means that operational constraints might occur more often. Indeed, reverse power flows might lead to voltage constraints at certain nodes, increased lines and transformers loadings and generally larger uncertainty of the actual power flows. Furthermore, the increased complexity of the LV-grid is highly problematic because of the lack of observability and controllability of DER. Additionally, DER curtailment, for example, if nodal voltage constraints exceed the permissible values of the grid-connected inverters, leads to loss of revenue for end-consumers, often without compensation. A better understanding of the integration of DER in LV-feeders is needed to optimize the hosting capacity of DER and guarantee the whole system's safe operation.

On the path to net zero in urban areas, buildings can play a pivotal role, by operating as *renewable energy hubs*, a concept introduced by Middelhave, 2022 [4].

Renewable energy hubs (Figure 1) maximize the use of energy from renewable sources to meet their self-demand through the optimal management of renewable energy sources and operation of energy conversion and storage technologies.

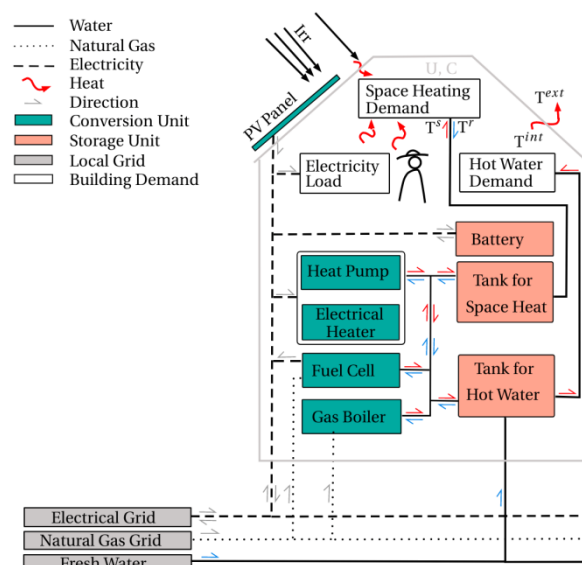


Figure 1: Representation of a renewable energy hub at the building level [4]

This work proposes a framework to integrate DERs into LV grids, aiming to maximize the use of renewable energy sources and support the transition to net-zero emission urban areas. It addresses the technical challenges and infrastructure limitations associated with this integration to ensure grid stability and reliability, support legislative and regulatory compliance, and minimize the risk of operational constraints and loss of revenue for end consumers. The framework optimizes both investment, operational and environmental costs and creates scenarios intended to support municipalities' decision-making.

2. Methodology

The integration of DERs into LV grids is a complex problem involving a wide variety of input data types and a large-scale multi-objective optimization problem, and the workflow of the framework needs to be designed carefully. The developed model jointly combines

data and sub-models from different sources to allow a multi-objective optimization problem to be solved. The different components of the model are detailed in the following sub-sections and highlighted in Figure 2. The pillar of the framework is the UrbanTwin database, which synthesizes data from different sectors to provide a unified, detailed repository of urban information. From the database, different data products are extracted, such as building information, weather data and electricity grid data and used in individual models developed within the framework. The different models communicate boundary conditions to connected models which allows them to refine constraints. The principal optimisation routine is based on the REHO tool. To find the optimal PV-hosting capacity, theoretical PV-hosting capacities based on available surfaces are generated by the REHO tool. Subsequently, the probabilistic load flow model evaluates the feasibility of the installed PV and communicates the theoretical PV hosting capacities per node back to the REHO model. This process continues iteratively until grid constraints are respected for all REHO scenarios.

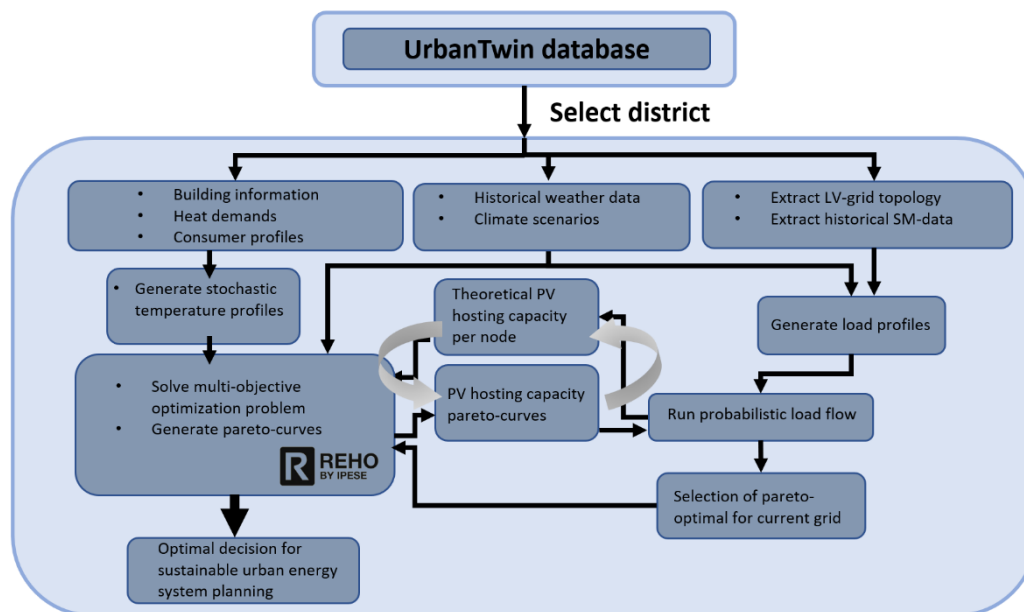


Figure 2: Overview of the model framework

2.1 REHO – multi-objective energy planning tool

REHO (Renewable Energy Hub Optimizer - <https://REHO.readthedocs.io/en/main/>) is an open-source decision support tool for the optimal planning of energy, considering buildings or districts as renewable energy hubs [5].

Buildings are energetically characterized by their affectation, year of construction, renovation state, and size in terms of ERA (energy reference area). Table 1 shows the characteristics of the buildings used in this study. The model considers three types of energy demands: space heating (SH), domestic hot water (DHW), and electricity for lighting and appliances. These demands are met by either importing energy from the electrical grid and natural gas grid or using available resources, such as solar energy. Load profiles for DHW and electricity of lighting and appliances are parameters of the model, which can be generated from the standardized national norm SIA 2024:2015 [6]. SH demands are modelled using a model predictive control strategy within the energy management system (EMS), ensuring the optimal operation of heat supply and storage technologies. SH demands represent the necessary heating energy to maintain the desired comfort temperature, considering both heat loss and heat gain. Heat loss in the

building comes from conduction and air renewal, which are determined by the building insulation level and the external temperature. Heat gain primarily comes from electric appliances, building occupancy, and solar irradiation.

The heating demands of a building can be satisfied by an air-water heat pump, an electrical heater or a gas boiler. Energy storage is possible using a stationary battery, domestic hot water and buffer storage or the building envelope. Photovoltaic panels can be installed on both roofs and facades, while at the same time shading from neighboring surfaces and roofs is considered, influencing the actual potential for local solar generation. This energy system is also connected to the natural gas and electricity networks, being able to import and export electricity from the grid.

The sizing of different technologies installed in a building and their operation is optimized with a mixed integer linear programming formulation considering not only the investment cost of the equipment but also the operational cost over several years. However, a detailed yearly operational analysis of the energy system in a building requires 8760 timesteps if we investigate the operation problem with an hourly resolution. This leads to a large-scale optimization problem which is intractable for current commercial mathematical solvers. Therefore, a k-medoids method is used to cluster the days into 10 typical days based on the weather data, assuming that weather conditions are periodic over the years. Multiple-objective optimization (or Pareto optimization) was applied to capital costs (CAPEX) and operation costs (OPEX) minimizing the objective function:

$$Objective = \varepsilon \cdot CAPEX + (1 - \varepsilon)OPEX$$

Multiple energy unit configuration scenarios are obtained by varying ε in steps of 0.1 from 0 to 1.

Table 1: Parameters of the buildings in the case study

	B1	B2	B3	B4	B5
Category ¹	V/II	I	I/II/IV/V	I	I
Year of construction/ renovation	1981-1990/ 1961-1970	1919-1945	1919-1945/ 1961-1970	<1919	1919-1945
ERA (m ²)	34261	1507	5047	651	541
Solar roof area (m ²)	9952	518	1125	317	205
Solar facade area (m ²)	20059	1126	15022	814	731
Overall heat transfer factor (kW/Km ²)	0.0017	0.0020	0.0020	0.0018	0.0020
Heat capacity (kW/Km ²)	117	120	120	120	120
Indoor temperature (°C)	20	20	20	20	20

2.2 Generation of stochastic heat-pump demand profiles

The heat-pump demand profiles are obtained by REHO, which assumes a deterministic behaviour of the variables that affect it. This results in an unrealistic trend. In this research, we suppose that the values of the external temperature and solar irradiance obtained after clustering are the ground truth, however, we model random fluctuations around these data by Stochastic Differential Equation (SDE).

This approach is motivated by the uncertain nature of temperature and solar irradiance and the propagation of the uncertainty induced by the clustering process.

We report the stochastic model used for the temperature; a similar one is used for solar irradiance.

We suppose that the normalized value of the temperature follows the SDE:

$$dT(t) = \left(\frac{dT_{ref}(t)}{dt} - \gamma(T(t) - T_{ref}(t)) \right) dt + \sqrt{2\sigma T(t)(1 - T(t))} dW(t),$$

where $T_{ref}(t)$ is a reference temperature profile, in our case, to achieve differentiability, we use a trigonometric approximation of the true profile. γ, σ are two positive parameters estimated from the correlogram and the quadratic variation of the process respectively. For more details about the properties of this model, we refer, e.g., to [7].

We use the same SDE model for each typical day, however, different values of the parameter γ are inferred for each of these days. A fixed value of σ is instead estimated from the complete time-history. With this model at our disposal, we can run MC simulation to create several possible scenarios of temperature and irradiance for each typical day.

In Figure 3 we report the temperature of the first typical day (red line) and confidence intervals obtained by simulating the SDE trajectory 10000 times. These trajectories can then be used in REHO to represent a sample of the real temperature value for a given day.

¹ (I to XII) based on SIA 2024:2015 [6]

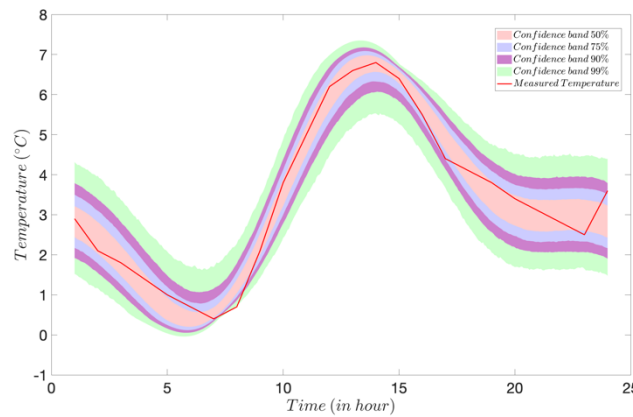


Figure 3: Measured temperature and associated confidence intervals for 10000 simulations.

2.3 Electrical distribution grid

Modelling of the electricity grid is done by combining measured values, real grid topology and associated electrical models along with scenario-based optimization. The Lausanne distribution grid consists of more than 700 MV/LV (11/0.4 kV) transformer stations. A digital version of the network has already been implemented in NEPLAN, specifying voltage levels, transformer and line parameters and topology. In the proposed framework, the user can either select an MV/LV transformer, a district or a household. Then, the associated LV-feeder specifications are extracted for the study in question. The MV/LV transformer along with the LV-feeder used in the case study is shown in Figure 4.

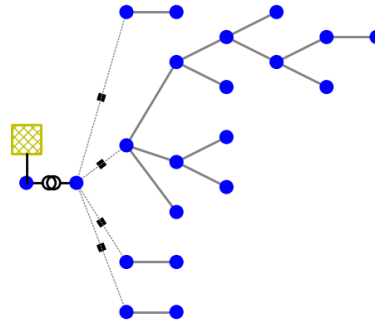


Figure 4: LV-feeder topology in the case study.

Measured values of electricity consumption per 15-minutes are obtained from Smart Meters (SMs) located at every end-consumer and aggregated at building-level to address privacy concerns. The associated loads are a mix of residential and commercial (see Table 1).

2.4 Modelling uncertainty in the LV-grid

Since both residential loads, DER-production, and heating profiles are uncertain, the resulting impact on the grid is uncertain. To assess the adequacy of the LV-feeder for different scenarios, we run stochastic power flow studies using the Monte-Carlo approach and verify probabilistically that grid constraints are respected. To this end, simulations are run hourly for a typical day in each of the 4 seasons. The uncertainties considered are listed in Table 2 and Figure 5 highlight the Monte-Carlo algorithm. In the initialization, an LV-feeder is selected along with its corresponding MV/LV transformer, the admittance matrix Y_{BUS} , base power S_N and base voltage V_N as well as the parameters of the simulation. Iterating over all the 10 REHO Pareto-curves, we solve the load flow problem for different realizations of the random variables. For every iteration of the MC-simulation, we draw a realization of the random variables for a specific REHO-pareto curve, season and hour in the day. The stopping criteria for the Monte-Carlo simulations is the Gaussian stopping rule [8] with a confidence level of $p=0.95$ for a tolerance of $1e-3$.

Table 2: Overview of random variables in the Monte-Carlo simulations

Random variable	Probabilistic description
Slack node voltage magnitude: V_0	Truncated Gaussian
Residential electricity demand: P_{res}, Q_{res}	Gaussian kernel density estimation on SM data clustered by hour-of-day
Heat Pump electricity demand: P_{HP}, Q_{HP}	Scenario from REHO
Global Horizontal Irradiance: GHI	Gaussian kernel density estimation on historic data clustered by season and hour-of-day

2.4.1 Modeling of random variables

The nodal voltage at the slack bus (primary side of MV/LV transformer) is influenced by the state of the higher-level grid. This is taken into account by modelling it as a truncated Gaussian distribution centred at 1.02 p.u. with a standard deviation $4e-3$ p.u. and truncation at 0.97 and 1.06 p.u.

Residential load profiles are generated by clustering historical load profiles by hour of the day and assessing the cross-correlation between buildings. Nodes that have a significant cross-correlation are grouped and modelled with a multivariate kernel density estimation based on Gaussian kernels. This ensures that the correlation-structure present in historical data is reflected when scenarios are drawn for the Monte-Carlo simulations.

The REHO model generates 10 heating demand profiles per building, for every pareto-curve. The 10 profiles reflect typical days in a year. Finally, the REHO model also generates a list of installed PV-panels per building, for every Pareto-curve. This list includes the tilt angle, the orientation (azimuth) and the rated power of the PV panels. To estimate the AC-power output of the PV-panels given the GHI, we estimate the plane-of-array irradiance using the PVLIB library [9]. Plane-of-array irradiance is converted into AC-power considering the standard panel efficiency, temperature coefficient of power and inverter losses.

```
Pseudo-code: Stochastic power flow
initialize:
    grid ← (YBUS, SN, UN)
    params ← (max_iter, season, hour_of_day)
for REHO_scenario=1:10:
    for it=1:max_iter:
        [V0, Pres, PHP, GHI] ← sample(REHO_scenario, season, hour_of_day)
        PV injections ← GHI_to_power(GHI, REHO_scenario, season, hour_of_day)
        Nodal residential loads ← Pres
        Nodal HP loads ← PHP
        result[REHO_scenario, it] = solve_LF(V0, Pc, Qc, Pg, Vg)
        stop_condition = evaluate_stopping_condition(result, it)
        if stop_condition==True:
            it ← max_iter
    return result
```

Figure 5: Stochastic power-flow algorithm using Monte-Carlo sampling.

2.5 Case study

In the case study, we showcase the results of applying the UrbanTwin framework to a neighbourhood in Lausanne. The neighborhood consists of 5 buildings and their parameters are given in Table 1. The buildings are supplied by a low-voltage feeder of the Lausanne electricity grid (see Figure 4) and in the case study, we consider the feasibility of replacing the current heating system, which is a combination of gas and fuel oil, with HPs, as well as the maximum PV hosting capacity.

3. Results

We first assess the PV hosting capacity of the grid and through the iterative process, we reduce PV capacities allocated by REHO until all Pareto curves are feasible for the grid. The stochastic temperature profiles are used by REHO to generate heat demand profiles. In this instance, we examine a scenario where all buildings install HPs to cover their heating demands. We also verify that the additional loads do not violate the constraints of the LV-feeder.

3.1 Grid constraints violation

We assess the feasibility of REHO's Pareto curves by calculating probabilistic nodal voltage deviations and line and transformer loadings in the LV-feeder. We report the results from typical summer days and typical winter days, reflecting constraints related to PV-injections and HP-loads, respectively.

3.1.1 Summer Day

In the summer, HP-loads are minimal, and the grid constraints are related to PV-injections. This typically leads to the largest *reverse* power flows in a LV-feeder. Figure 6 shows the resulting impact on nodal voltage deviations and lines and transformer loadings after the optimisation routine to select the maximum PV hosting capacity. Initially, line loadings exceeded 300% using the available surface area for installing PV panels. The iterative process of our framework reduces PV hosting capacity until grid constraints are respected for all REHO scenarios. The grid operator now has a holistic view of the grid planning exercise; on the one hand, they can accurately quantify the PV hosting capacity with the current grid, allowing to limit costly grid expansions. On the other hand, they can visually map grid elements which are operating close to their capacity and therefore plan expansions or reinforcements accordingly.

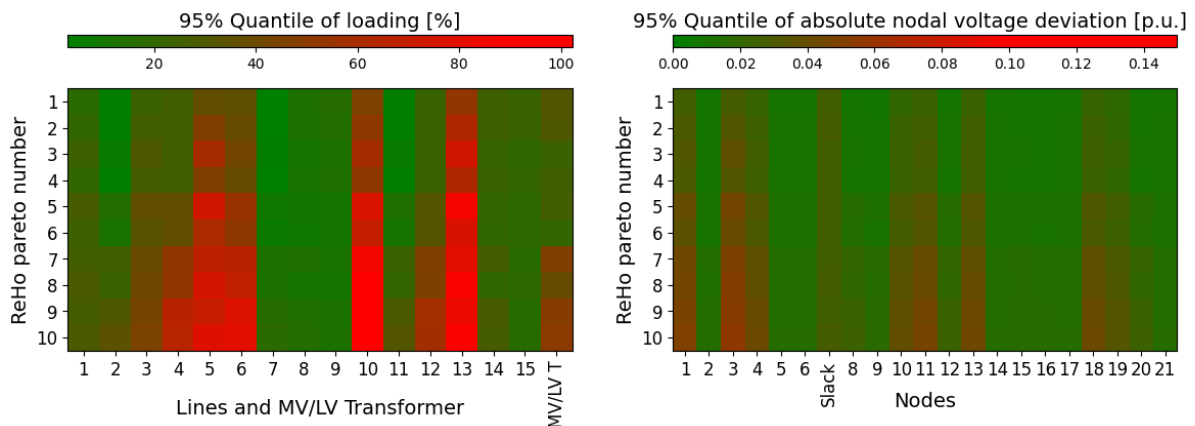


Figure 6: Grid constraint results for the REHO pareto results *after* limiting the PV boundary conditions. **Left:** 95% quantile of loading for all the lines and the MV/LV transformer. **Right:** the 95% quantile of absolute deviations from the per-unit reference voltage. We only report the worst-case values overall 24 hours of a day. As seen, there are no violations of line or transformer loadings or nodal voltages for all REHO scenarios.

3.1.2 Winter Day

In the winter, HP demand is at its highest while PV production is at its lowest. This typically leads to the highest power flows in a LV-feeder. Figure 7 shows the resulting grid loadings in a scenario where all heating demands are covered by HPs.

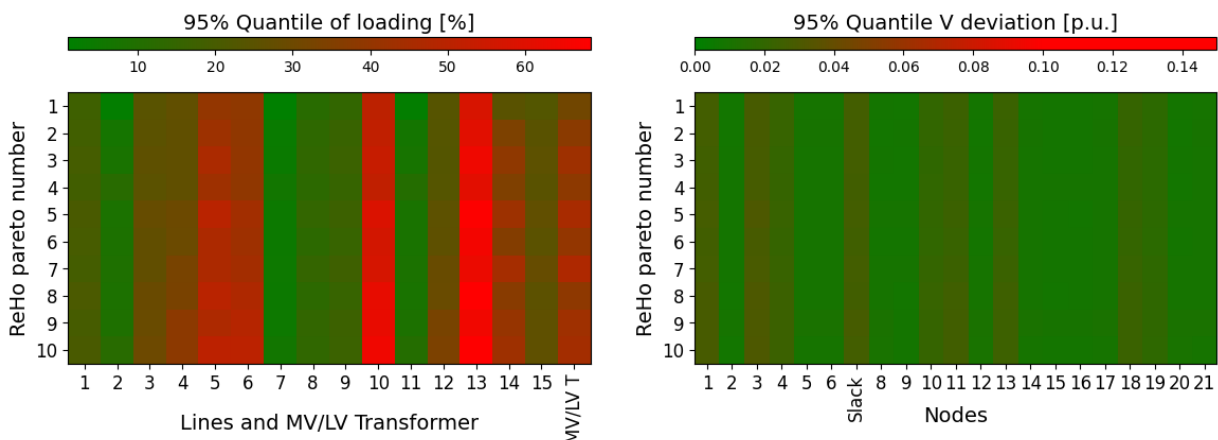


Figure 7: Grid constraint results for the REHO pareto results of a typical winter day. **Left:** 95% quantile of loading for all the lines and the MV/LV transformer. **Right:** the 95% quantile of absolute deviations from the per-unit reference voltage. We only report the worst-case values overall 24 hours of a day. We observe that grid loadings only increase mildly for all REHO-scenarios.

3.2 REHO Results

Figures 8 (a) and (b) present the results from the multi-objective optimization after applying the constraint on maximum PV hosting capacity, and their impact on some performance indicators.

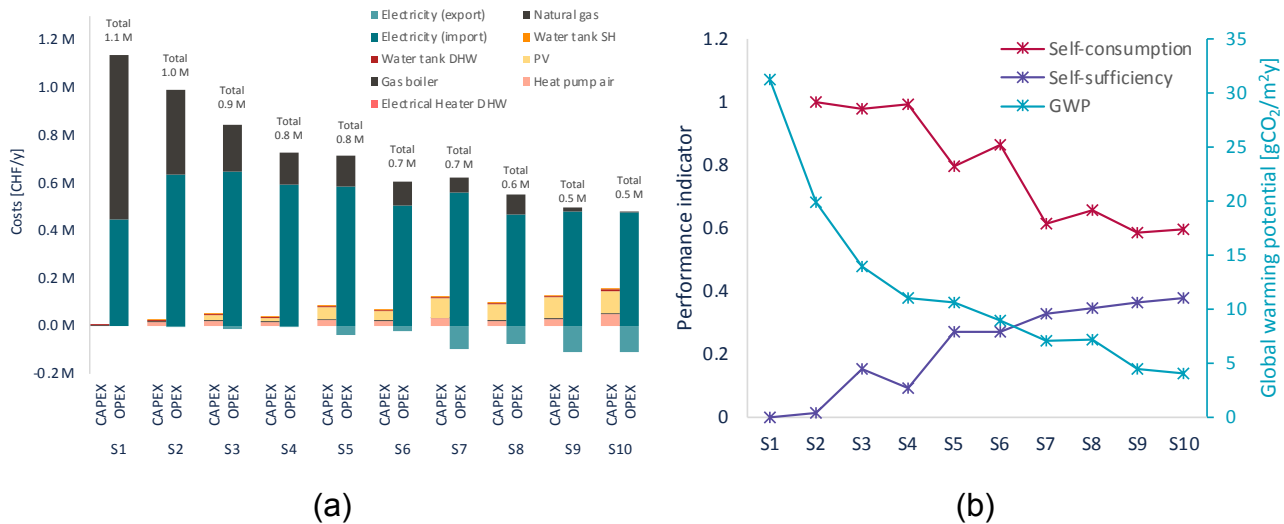


Figure 8: REHO results of the multi-objective optimization after the implementation of the constraint on the maximum PV hosting capacity. (a) Detail on the costs. (b) Performance indicators.

The introduction of epsilon constraints (ϵ), enables the decision-maker to explore a broader range of solutions and analyze the trade-offs between different energy system configurations. As greater emphasis is given to capital expenditures, the system increasingly depends on the district grid (lower levels of self-sufficiency), resulting in significantly higher operational and total costs, as well as higher environmental impacts. In contrast, the adoption of decentralized energy systems proves to be advantageous for reducing the total cost of the energy system, and the emissions of CO₂.

Conclusion

In this paper, we present a decision-support framework for sustainable urban energy system planning based on a digital twin. The framework consists of a comprehensive database, multiple individual models that share boundary conditions between them, and a central multi-objective energy infrastructure optimization tool to optimally design an energy system. The utility of the framework is showcased in a case study to optimally plan the expansion of rooftop PV in a LV-feeder and verify the adequacy of current grid infrastructure to support the build-out of HPs to cover heating needs in Lausanne, Switzerland. The combination of an accurate model of the electricity grid, considering uncertainties on production, consumption and slack nodal voltage, and the multi-objective optimization planning tool REHO gives utilities the freedom to explore different scenarios and trade-offs between CAPEX and OPEX costs. In the future, we seek to expand the model by including climate scenarios, EV-charging demand and flexible resources such as community energy storage systems.

Acknowledgement

The authors extend their gratitude to Services Industriels de Lausanne for providing access to the data and for their invaluable support in this work.

References

- [1] Energy perspectives 2050+. Zusammenfassung der wichtigsten Ergebnisse. Swiss Federal Office of Energy (SFOE) 2020.
- [2] Rosser et al. Conception Infrastructure de recharge 2050. Suisseenergie.ch May 2023
- [3] European Committee for Electrotechnical Standardization. EN 50160: Voltage Characteristics of Electricity Supplied by Public Distribution Networks. Brussels: CENELEC, 2022.
- [4] Luise Middelhauve, On the role of districts as renewable energy hubs. PhD thesis, EPFL, Lausanne, Switzerland, April 2022
- [5] Lepour, Dorsan & Terrier, Cédric & Loustau, Joseph & Maréchal, François, Renewable Energy Hub Optimizer (REHO) – A Comprehensive Decision Support Tool for Sustainable Energy System Planning. 33rd European Symposium on Computer-Aided Process Engineering, Florence, Italy, 2024
- [6] Norme SIA 2024, Données d'utilisation des locaux pour l'énergie et les installations du bâtiment, Zurich, Switzerland, 2015
- [7] Renzo Caballero, Ahmed Kebaier, Marco Scavino, and Raúl Tempone. Quantifying uncertainty with a derivative tracking sde model and application to wind power forecast data. Statistics and Computing, 31(5):64, Aug 2021.
- [8] Bicher, Martin & Wastian, Matthias & Brunmeir, Dominik & Popper, Niki. (2022). Review on Monte Carlo Simulation Stopping Rules: How Many Samples Are Really Enough? SNE Simulation Notes Europe. 32. 1-8. 10.11128/sne.32.on.10591.
- [9] Holmgren, W., Hansen, C., and Mikofski, M. "pvlib python: a python package for modeling solar energy systems." Journal of Open Source Software, 3(29), 884, 2018

G0703

Managing and Optimizing a Set of PV Installations at the Low-Voltage Grid Level: A Data-Driven Concept through Machine Learning Techniques

Thibaud Alt (1), Beat Wolf (2), Jean-Philippe Bacher (3), Frédéric Montet (4)

(1) Groupe E SA, Route de Morat 135, 1763 Granges-Paccot/Switzerland;

Tel.: +41 26 352 52 52

thibaud.alt@groupe-e.ch

(2,4) iCoSys institute, HEIA-FR, HES-SO University of Applied Sciences and Arts, Western Switzerland, Bld de Pérolles 80, 1700 Fribourg/Switzerland;

beat.wolf@hefr.ch, frederic.montet@hefr.ch

(3) ENERGY institute, HEIA-FR, HES-SO University of Applied Sciences and Arts, Western Switzerland, Bld de Pérolles 80, 1700 Fribourg/Switzerland;

jean-philippe.bacher@hefr.ch

Abstract

This paper proposes a data-driven approach to managing and optimizing a set of photovoltaic (PV) installations by exploiting the possibilities of spatio-temporal modeling and machine learning techniques. Given the variable nature of solar energy production, optimizing PV installations for maximum output and efficiency is crucial. The aim is to identify trends, patterns, challenges, and opportunities for improvement in the operation of multi-site PV systems as well as to provide information for optimal management of the low-voltage network. A diverse array of methods are compared to forecast energy production, detect declines in system performance and refine maintenance scheduling. This study contributes to the growing field of renewable energy management by showcasing the effectiveness of ML models in optimizing a set of PV systems. It sets the stage for future progress in incorporating renewable energy sources into the electrical grid.

Introduction

The global energy transition, marked by a shift towards sustainability, highlights the urgent and significant challenges facing many countries in their current energy strategies. Among these, Switzerland, which aims to deactivate all its nuclear power plants by 2050 [1], has ambitious targets that require it to rapidly compensate for lost energy production and increase the integration of renewable energies. Against this backdrop, this paper proposes a data-driven approach to managing and optimizing a set of PV installations by exploiting the possibilities of spatio-temporal modeling and Machine Learning (ML) techniques. Given the fluctuating of solar energy production, optimizing PV installations for maximum output and efficiency is crucial. Integrating PV systems into the existing grid improves flexibility through self-consumption but brings with it a number of challenges related to grid stability and sizing. The aim is to identify trends, patterns, challenges, and opportunities for improvement in the operation of multi-site PV systems as well as to provide information for optimal management of the low-voltage network.

Using historical information on energy production, weather conditions, and PV systems specifications, solar production estimates derived from these models are compared with actual measurements to proactively detect underperforming installations. By analyzing this data, ML models are designed to map out standard operational patterns of PV plants, thereby identifying deviations indicative of potential issues. This methodology not only refines the accuracy of solar output forecasts but also offers an efficient way for the maintenance and optimization of PV installations, ensuring cost-effective and impactful interventions. A diverse array of methods ranging from conventional statistical methods, through Machine Learning (ML) algorithms, to advanced Deep Learning (DL) architectures are compared to forecast energy production, detect declines in system performance and refine maintenance scheduling. These methods were rigorously tested on a dataset, comprising multiple heterogeneous data from over 400 PV installations over a minimum historical period of two years, all situated within Western Switzerland.

This document is organized into several key sections. *Section 1: Context* provides an overview of the general context, outlines known issues, and reviews related works. *Section 2: Dataset* details the consolidated dataset that has been utilized. *Section 3: Methods* elucidates the techniques employed to identify declines in system performance. *Section 4: Results* showcases the findings from the study. *Section 5: Discussion* examines the results and proposes potential future directions. The final section, *Conclusion*, offers a comprehensive summary of the paper.

1. Context

Switzerland is currently facing several major challenges in its energy transition. The Federal Council has drawn up an energy strategy for 2050 [1], the main aim of which is to decommission the five existing nuclear power stations by then. In 2023 the total electricity consumed in Switzerland was 56.1TWh, marking a decrease of -1.7% compared to the previous year [2]. In the meantime, the Swiss have to find various ways to compensate for this 25 TWh production deficit, induced by the shutdown of these five power plants and the projected increase in consumption due to the decarbonization of mobility and housing sector. This transition requires coordinated measures and effective implementation to promote energy efficiency, increase the share of renewable energies, modernize electricity grids, and speed up administrative procedures. One of the building blocks of this transition is the use of renewable energies, and in particular the optimization and maintenance of existing PV installations. There are a number of areas where improvements can be made to maximize the contribution of existing PV installations to this energy transition. Firstly, it is essential to improve the performance of existing solar installations by using more

advanced technologies and carrying out regular maintenance and cleaning of the solar panels. This will ensure maximum solar electricity production. In addition, the integration of energy storage systems, such as batteries, means that the electricity generated can be stored for later use, guaranteeing continuous availability even when there is no sun. In addition, the integration of solar installations into smart grid systems offers more efficient management of the park and possible synergy options. Finally, raising awareness and training the owners and managers of solar installations in best maintenance and operating practices are crucial to maximizing their return.

The canton of Fribourg is aiming to significantly increase its production of PV solar energy by 2050 [3]. By September 2023, PV installations were already producing 200 GWh a year, and the aim is to reach 600 GWh by 2035 and 1,300 GWh by 2050. To achieve this, the canton is focusing on developing solar PV, making it an essential part of its future energy supply. Groupe E, the western Switzerland Distribution System Operators (DSO), connected the first PV installation to its grid twenty years ago. Since then, the pace has continuously accelerated, increasing from 500 installations per year a decade ago to over 5000 in the sole year of 2023. The number of connected PV systems has doubled since the end of 2020, reaching more than 20,000 installations by the end of 2023 [4]. Together, they represent a total installed capacity of 360 MW and an annual production of 360 GWh. In September 2023, Groupe E commissioned the largest solar farm in Switzerland, covering an area of 47,000 m² including 19,000 panels. Operating this growing solar park presents a number of crucial challenges, particularly in terms of maintenance and servicing, performance monitoring and management, and grid integration. In addition, managing and exploiting the data generated by this fleet of installations, combined with in-depth analysis, offers the possibility of identifying trends and opportunities for improvement.

The main aim of this study is to make full use of the data produced by PV installations in order to optimize their contribution to solar energy production. This approach focuses on two main areas: firstly, the creation of a high-quality reference dataset to establish a solid and reusable basis for building models, and secondly, the implementation of a maintenance and in-depth analysis strategy.

2. Dataset

The first objective of this study is to provide a set of reference data. To achieve this, various data sources have been identified and collected. Thanks to the consolidation operations carried out on these data and the creation of a reference dataset, several PV installations are now available in the created dataset. This new dataset is structured in the form of tabular data made up of three tables presented in chapter 2.1. The total number of PV installations available for this analysis is 417, as shown in Figure 6.

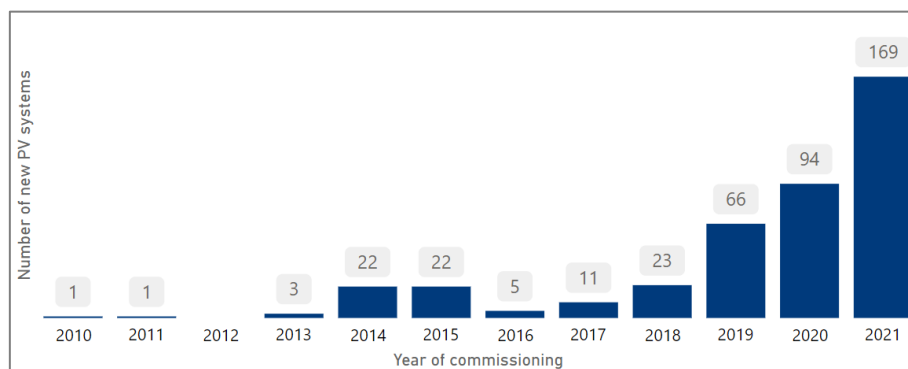


Figure 6 : Number of collected PV systems data grouped by commissioning year

These installations are grouped by year of commissioning. Installations commissioned after 01.01.2022 are deliberately not included in the analysis. This decision is explained by the need to have consistent historical data to reliably assess changes in performance and characteristics over time. These 417 PV installations are spread across Western Switzerland in a geographically diverse manner, encompassing all the French-speaking regions and Bern. This balanced distribution ensures significant representation of diverse weather conditions and terrain. Each different environmental zone will allow a significant representation of specific climatic and topographical conditions. The geographical diversity of the sites means that potential variations in sunshine and altitude can be taken into account.

The various data sources collected and integrated into the reference dataset contain several dimensions. These dimensions have been divided into three tables detailed in the chapter 2.1. These tables will provide a structured framework for organizing and analyzing the data, facilitating a deeper understanding of the various dimensions and their interrelationships within the dataset.

2.1 Tables dimensions

The used dataset is structured in the form of tabular data made up of three tables: *pv_systems*, *telemetry* and *maintenance_cases*. Each table is interconnected via a distinct and shared unique identifier (UID), making it easier to identify the specific data associated with each PV site.

pv_systems — This table is the heart of the reference dataset. It serves as a repository for a wealth of detailed information relating to PV systems. This information includes data on the installation, such as the date of installation, the type of installation and the technical specifications. In addition, precise geographical information allows each PV system to be located. The solar production capacity of each site is also documented, providing valuable insights into the energy potential of each installation. Information on the life cycle of each PV system is available, providing an overview of the sustainability and efficiency of these systems over time. The various components of PV systems, such as solar panels, inverters, and energy storage systems, are detailed. Finally, relevant administrative information, such as customer details, current system status and management information, is also stored in this main table.

telemetry — The second table in the reference dataset encompasses a full spectrum of telemetry data. This table is a valuable resource that provides a detailed historical overview of energy production, consumption, and storage system status. Each record in this table is time-stamped, allowing rigorous chronological tracking of data for each installation. This makes it easy to analyze trends and patterns over time, providing valuable information for future system optimization. In addition, the table also incorporates meteorological data, including temperature, humidity, and wind speed. Together, these data form a comprehensive resource for the analysis and continuous improvement of energy performance.

maintenance_cases — The third table in the reference dataset is a comprehensive compilation of recorded maintenance cases. This table includes details of the customer, the address of the installation, the specifics of the maintenance contract, the nature of the problem encountered, and the interventions carried out. Each entry in this table has time fields, enabling the duration of the interventions to be tracked. In addition, the table contains detailed information on the components replaced and the actions carried out during each intervention.

3. Methods

This section describes the diverse methods employed for several purposes: forecasting energy production, identifying decreases in system performance, and optimizing maintenance scheduling [5]. A range of techniques are explored and compared, from conventional statistical methods, through ML algorithms, to advanced DL architectures. By leveraging diverse methods and meticulously isolating system characteristics in different manners, the aim is to compare the results obtained through these techniques. It is conceivable that certain installations demonstrating insufficient performance across multiple techniques can be identified simultaneously. Subsequently, these identified underperforming installations be the subject of a more detailed analysis to pinpoint anomalies and facilitate predictive maintenance. For each method, the technique used, any ML models employed, and the data extracted from the reference dataset will be presented. The combination of results from different methods is presented in Chapter 4.

3.1 Statistical methods

This chapter presents the statistical techniques used, such as the calculation of the production index discrepancy analysis and the comparison of produced energy per installed surface.

3.1.1 Production Index Discrepancy Analysis

The first approach is a simple statistical method based on the use of a specific tool. For each PV installation, a production index is calculated using dedicated software. This index, which is fixed, is based on specific characteristics such as solar irradiation, the year's weather conditions, the PV technology used, the installed power, and the orientation and inclination of the panels. With each additional year of operation of the installation, the production index decreases by 0.8%, as shown by trending line on Figure 7. Then, for each installation, the delta between actual production and the index is calculated and consolidated as a percentage in a table. The facilities are then classified into 4 categories according to the following thresholds: above/corresponding to expectations (greater or equal to 100%), slightly below expectations (100% to 95%), below expectations (95% to 90%), and significantly below expectations (lower than 90%). The main drawback of this method is its assumption that the production index decreases by a fixed percentage with each additional year of operation.

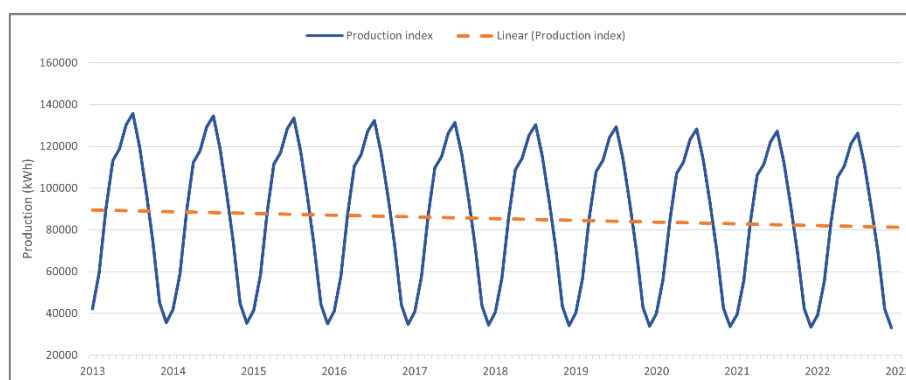


Figure 7 : Estimated production index over the years and decreasing trend line

3.1.2 Produced energy per installed surface

This second method involves calculating the amount of energy produced by a PV system over a defined period normalized by the surface area of the PV panels. This normalization allows for a fair comparison between different installations, regardless of their size. The method initiates by calculating the cumulative energy output of each PV system throughout its operational lifespan, measured in kilowatt-hours (kWh). Next, the total energy production is divided by the surface area of the PV panels to obtain the energy produced per unit of the surface area, measured in square meters (m²). Once the energy production per surface area is calculated for each PV system, these values are compared with the average value calculated across all sites or installations under consideration. The performance of each PV system can be categorized into different groups or classifications according to the comparison results. An alternative approach would involve normalizing the data not based on the surface area, but rather by the stated peak power. However, this method was not selected due to the less reliable nature of peak power data. This approach has the advantage that the only necessary data are the sum of the energy produced over a given period of time and the installed surface area. One potential disadvantage of this method is that it may not fully account for variations in panel efficiency or environmental factors across different installations. Since it normalizes energy production solely by the surface area, it might overlook differences in panel quality, orientation, shading, or other factors that could affect performance. Additionally, it does not consider fluctuations in energy production due to factors such as weather conditions or maintenance issues, which could impact the accuracy of performance comparisons. Another disadvantage arises from the reliance on the average value calculated across all sites or installations in the dataset. If the dataset changes, this value will also change.

3.2 Clustering based methods

In this section, clustering, the first ML based method is introduced. Clustering techniques aim to partition a dataset into subsets. This is particularly useful for identifying inherent patterns and grouping data points based on similarity. In the context of energy production analysis, clustering algorithms can help uncover distinct clusters of PV installations with similar characteristics or production profiles [6]. Manual, k-means, and Density-Based Spatial Clustering of Applications with Noise (DBSCAN), the three clustering methods, focus solely on PV system specifications. These methods aim to group PV installations according to inherent similarities in their characteristics. The produced energy is normalized by the surface area to account for differences in the size of the PV panels. This normalization process reduces the available PV systems in the main dataset from 417 to 99 for which information on the surface area is available. Once the PV systems are distributed into clusters, the analysis continues by calculating the production average for each group. This average represents the typical production of installations within that particular group. Subsequently, each installation is compared to the production average of its corresponding group. This comparison allows for the assessment of each installation's relative performance compared to its peers. A delta is calculated by subtracting the actual production of each installation from the production average of its group. This delta represents the difference between the individual performance of each installation and the average performance of its group.

3.2.1 Manual clustering

This approach involves the manual categorization of PV systems based on specific attributes. While it lacks the automation of algorithmic clustering, manual clustering allows for expert domain knowledge to guide the grouping process, potentially uncovering nuanced patterns not captured by automated methods. The features selected for manual

clustering are main panels orientation and main panels inclination. Only two features have been chosen for manual clustering because they are deemed to have the most significant impact. This configuration results in the formation of 15 clusters.

3.2.2 k-means clustering

The k-means algorithm is a popular clustering method that partitions a dataset into a predetermined number of clusters by minimizing the sum of squared distances within each cluster. In this study, k-means was used to group installations with to groups of features. The first set (A) includes: main orientation degree, main inclination, latitude, longitude, altitude, category, and type. The second set (B) incorporates the features from the first set as well as the roof type, the roof slope, the panel manufacturer, and the inverter manufacturer. The optimal result with k-means is achieved using the second set (B) with 29 clusters.

3.2.3 DBSCAN clustering

Unlike k-means, DBSCAN does not require specifying the number of clusters beforehand. Instead, it identifies clusters based on density connectivity, grouping together data points that are closely packed while labeling outliers as noise. DBSCAN is particularly useful for identifying irregularly shaped clusters and handling noise effectively, making it suitable for clustering PV installations with varying densities and spatial distributions. In this study, DBSCAN was used to group installations with the same feature sets as k-means (sets A & B). Once clustered, each site is labeled with a specific group number. By comparing the members of each group, it is possible to identify potential correlations between the different characteristics of PV systems, thereby gaining a better understanding of their respective performances. The optimal result with DBSCAN is achieved using the second set (B) with 10 clusters.

3.3 Produced energy predictions

In this section, the first DL techniques are introduced. The core aim of this approach is to harness the power of ML and DL methods to generate precise forecasts of energy production for individual PV systems on a daily basis. By using ML and DL techniques to forecast the energy production of individual PV systems, and then comparing this with the actual output, it is then possible to obtain a performance score. Three distinct methods have been developed to anticipate energy production. The first, detailed in chapter 3.3.1, relies only on the analysis of historical telemetry data collected from each PV installation. It aims to predict daily time series of production. The second approach, detailed in chapter 3.3.2, integrates specific installation characteristics, in addition to incorporating aggregated data on annual production. The third and final method, detailed in chapter 3.3.3, uses only a few of the technical characteristics of PV installations and therefore allows a prediction based on a restricted set of data. The second and third methods aim to predict energy production on an annual basis.

3.3.1 DeepAR model

For this prediction approach, production data is collected and summarized by daily produced energy (kWh). With this daily basis, the *DeepAREstimator* class from the *GluonTS* framework is used to train a DeepAR prediction model. *GluonTS* is a Python package for probabilistic time series modeling, focusing on DL-based models, that includes *DeepAR* model. The DeepAR model is a supervised learning algorithm specified for forecasting time series by using Recurrent Neural Networks (RNN) [7]. Once all predictions are completed, the results are aggregated for each PV system by week, and the delta with the real production of the year is calculated. This delta provides a performance index as detailed in Chapter 4.

3.3.2 Fast and Lightweight AutoML (FLAML)

For this second prediction approach, the FLAML Python library has been chosen. FLAML library can find accurate ML models automatically, efficiently, and economically from a defined set of settings [8]. The used set of features used to predict the produced energy includes installation year, surface, main orientation degree, main inclination, latitude, longitude, altitude, category, type, roof type, roof slope, panel power and the total energy produced for the years 2018 to 2022, if the data are available. After multiple training sessions, the best-found model is an XGBoost with 13 estimators, which provides a good balance between performance and efficiency. These estimators correspond to the number of trees boosted by the gradient. Once the best-performing model has been trained, predictions are made on the test set, and the delta between the predicted and actual values is calculated.

3.3.3 XGBoost with limited depth model

This third prediction approach has the advantage of using only a small fraction of the characteristics of PV systems. These characteristics are the date of commissioning, the peak power, the orientation and inclination of the panels, the type (residential or commercial) and a geographical area determined by the location of the PV system. Several ML models were tested, including Light Gradient-Boosting Machine, Random Forests, XGBoost and CatBoost [9]. The most promising results were achieved with the XGBoost with limited depth model, employing 10 estimators and a maximum depth of 6.

4. Results

In this chapter, the results of applying the various methods outlined in Chapter 3 are showcased, and a comparative analysis of the outcomes yielded by these techniques is conducted. The goal here is to compare the results of the various methods used and to identify the PV systems that show lower performance according to several of these methods. Thanks to the Production Index Discrepancy Analysis method, five installations with problematic production for at least three years were identified. These installations, referred as witnesses, can be used as a baseline for other methods.

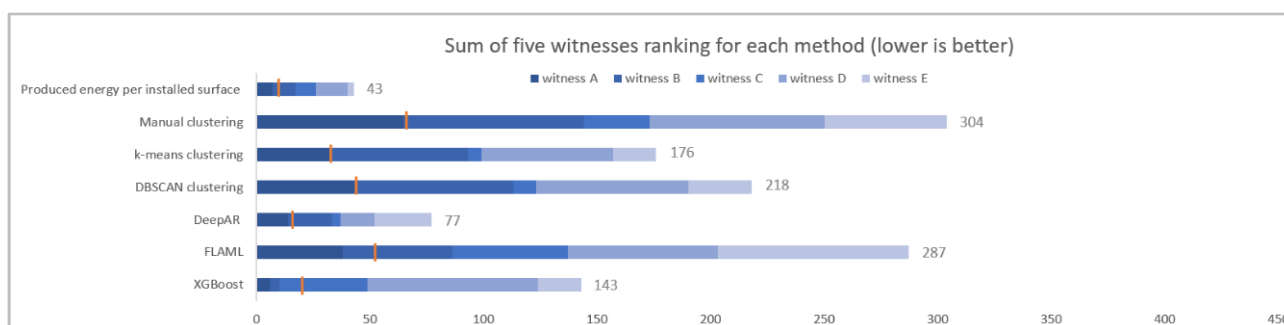


Figure 8: the sum of ranking of each witness by method, the bestvalue is the lowest

As shown on Figure 8, methods are compared by the total ranking of the five witnesses. The scale ranges from 15 (the baseline score) to 485 (the worst score). The number in gray indicates the sum of the ranking, while the orange line shows the median. Produced energy per installed surface and DeepAR methods rank below 100. The rank of the highest witness for produced energy per installed surface method is 14, while the median rank is 9. For the DeepAR method, the highest ranking is 25, while the median rank is 15. Clustering-based methods achieved the highest rankings of 79 for manual, 61 for k-means, and 70 for DBSCAN, with median rankings of 65 for manual, 32 for k-means, and

43 for DBSCAN. FLAML method obtains the highest ranking of 84 and a median of 51. Finally, XGBoost with limited depth method obtains a last witness ranked at position 75 and a median ranking of 19.

On Figure 9, the performance breakdown of PV systems is grouped into 25% intervals. The number of for each interval is displayed in white, while the red line indicates the baseline of well-functioning systems. Systems that underperform are those that repeatedly appear in intervals below 75%.

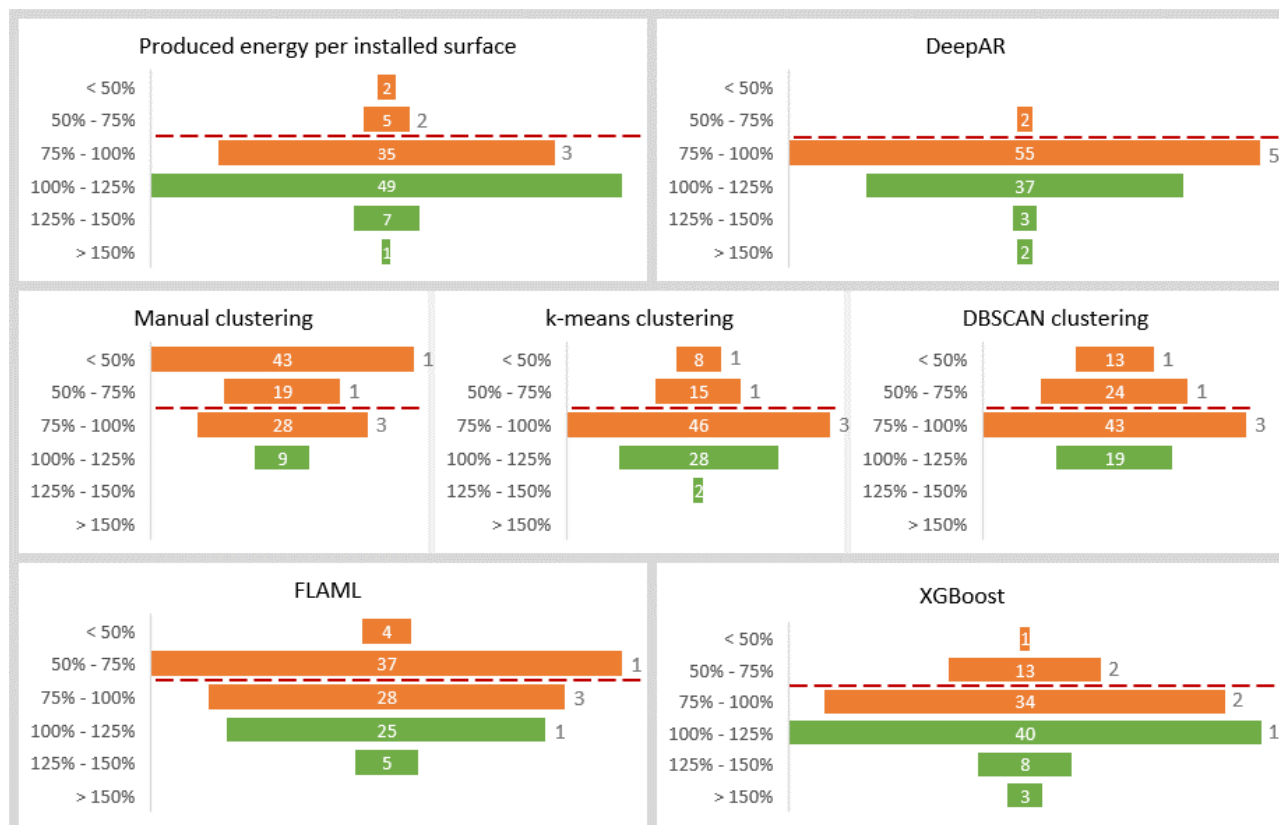


Figure 9: comparison of the performance breakdown of PV systems for each method, number of witnesses in gray

Produced energy per installed surface method identifies a total of 7 underperforming PV systems, including 2 of the 5 benchmark systems. The tree clustering-based methods categorize 1 PV system in the first interval, 1 in the second interval, and 3 in the 75%-100% interval. Manual clustering indicates that 62 PV systems are underperforming, while k-means identifies 23 underperforming systems, and DBSCAN identifies 37. Surprisingly, DeepAR model includes more than half of the dataset within the 75%-100% interval, including the 5 witnesses. Only two systems are considered significantly underperforming. Lastly, the FLAML and the XGBoost methods are the only ones that classified witnesses in an interval greater than 100%, which suggests that the results may not be reliable. However, these methods still indicate 41 and respectively 14 under-performing PV systems.

5. Discussion

The *produced energy per installed surface method* achieves the best results in ranking the witnesses. However, it requires precise production data and a significant common denominator, such as surface area or peak power. Unfortunately, these essential elements

are unavailable for more than 75% of actual PV systems. *Clustering based methods* achieve mixed results in ranking the witnesses. However, their primary advantage is that they do not require production information and are only based on technical characteristics. The accuracy of their ranking could be enhanced by carefully selecting features that are essential and available on most of the PV systems currently in service. The *DeepAR model*, like statistical methods, requires production data, which shares the same disadvantages. However, this data can be aggregated, requiring less precision. It achieves accurate results for the ranking of witnesses. It obtains accurate results for the ranking of witnesses. The *FLAML method* has the advantage of only requiring some technical data and an annual estimation of the produced energy, but it falls short in terms of witness detection. The *XGBoost with limited depth model* produces encouraging results and has the immense advantage of requiring a limited number of features. All methods have a recall of 1 (every witness is included in intervals below 100%), except for the FLAML and the XGBoost methods, which have a recall of 0.8.

With the results established in Chapter 4, and considering only results below 75% from each method (excluding witnesses), it is observed that 12 PV systems are deemed underperforming by four or more methods. Among these, ten installations are considered poorly performing according to four methods, one according to five, and another according to six. This discovery is a significant outcome of the study, signaling potential areas for intervention and optimization. However, formally confirming the status of these installations would require on-site verification, introducing logistical challenges. Future research directions would focus on detecting anomalies in specific sites that have been identified as abnormal or underperforming, starting with the first group identified. Additionally, the aim is to explore other methods as presented in Chapter 3 like a fourth clustering method, called Time Series-Based Clustering, leveraging production time series data [10]. Another way would be to use advanced DL architectures like Graph Neural Networks (GNNs) and Transformers [11], Transfer Learning (TL) [12], or zero-shot forecasting [13] to enhance detection of PV systems that show abnormal performance without needing the energy data produced.

Conclusion

In this paper, an innovative data-driven approach to find underperforming PV installations is proposed. At a time when the global energy transition demands increased integration of renewable energies, the proposed approach aims to leverage historical data of energy production, weather conditions, and PV system specifications to optimize their performance and efficiency. By analyzing this data, a comparison of a range of methods has been conducted, spanning from conventional statistical methods to advanced clustering and DL techniques. There is no single method: the choice depends on the data available. Depending on the data available, one method or another may be more appropriate. The results show that several installations are performing below expectations and require special attention. However, it is acknowledged that challenges persist, including on-site verification of identified underperforming installations and more specific anomaly detections.

In conclusion, this study marks a significant milestone in the management and optimization of PV installations at the low-voltage grid level, providing data-driven solutions to address the challenges of the energy transition towards a more sustainable future. The findings emphasize the importance of continuous innovation and adaptation in renewable energy management, setting the stage for further advancements in incorporating renewable energy sources into the electrical grid. Future research will focus on enhancing clustering methods and integrating more sophisticated ML models to achieve even greater accuracy and reliability in PV system performance optimization.

References

- [1] T. E. a. C. Federal Department of the Environment, "Principles of energy policy," [Online]. Available: <https://www.uvek.admin.ch/uvek/en/home/energy/energy-strategy-2050.html>. [Accessed 02 05 2024].
- [2] S. F. O. o. Energy, "Electricity consumption down by 1.7% in 2023," 18 04 2024. [Online]. Available: <https://www.admin.ch/gov/en/start/documentation/media-releases.msg-id-100748.html>. [Accessed 02 05 2024].
- [3] S. d. I. d. I. d. Fribourg, "Le Conseil d'Etat adopte une stratégie solaire photovoltaïque ambitieuse," 01 09 2023. [Online]. Available: <https://www.fr.ch/deef/sde/actualites/le-conseil-detat-adopte-une-strategie-solaire-photovoltaique-ambitieuse>. [Accessed 02 05 2024].
- [4] G. E. SA, "Le réseau électrique de Groupe E a accueilli sa 20'000e installation photovoltaïque," 21 12 2023. [Online]. Available: <https://www.groupe-e.ch/fr/decouvrir-groupe-e/medias/communiques-de-presse/20000-installations-photovoltaiques>. [Accessed 02 05 2024].
- [5] U. K. Das, K. S. Tey, M. Seyedmahmoudian, S. Mekhilef and M. Y. I. Idris, "Forecasting of photovoltaic power generation and model optimization: A review," *Renewable and Sustainable Energy Reviews*, 01 2018.
- [6] Z. a. K. I. a. R. M. Wang, "Clustering Based Methods for Solar Power Forecasting," *International Joint Conference on Neural Networks (IJCNN)At*, 07 2016.
- [7] D. Salinas, V. Flunkert, J. Gasthaus and T. Januschowski, "DeepAR: Probabilistic forecasting with autoregressive recurrent networks," *International Journal of Forecasting*, 07 2020.
- [8] D. P. Kumar, N. Kaur and S. S. Kushana, "Efficient Time Series Photovoltaic Production Forecasting using FLAML with Traditional Machine Learning Algorithms," *2023 7th International Conference on Intelligent Computing and Control Systems (ICICCS)*, 17 05 2023.
- [9] D. Adhya, S. Chatterjee and A. K. Chakraborty, "Performance assessment of selective machine learning techniques for improved PV array fault diagnosis," *Sustainable Energy, Grids and Networks*, 03 2022.
- [10] Z. Zhang, J. Wang, Y. Xia, D. Wei and N. Yunbo, "Solar-Mixer: An Efficient End-to-End Model for Long-Sequence Photovoltaic Power Generation Time Series Forecasting," *IEEE Transactions on Sustainable Energy*, 10 2023.
- [11] J. Simeunović, B. Schubnel, P.-J. Alet, R. E. Carrillo and P. Frossard, "Interpretable temporal-spatial graph attention network for multi-site PV power forecasting," *Applied Energy*, 12 2022.
- [12] S. M. Miraftebzadeh, C. G. Colombo, M. Longo and F. Foiadelli, "A Day-Ahead Photovoltaic Power Prediction via Transfer Learning and Deep Neural Networks," *Forecasting*, 17 02 2023.
- [13] V. Ekambaram, A. Jati, N. H. Nguyen, P. Dayama, C. Reddy, W. M. Gifford and J. Kalagnanam, "Tiny Time Mixers (TTMs): Fast Pre-trained Models for Enhanced Zero/Few-Shot Forecasting of Multivariate Time Series," 09 04 2024.

G0704

Interoperability by Sovereign and Secure Data Exchange in Trustworthy Data Spaces

Andreas Rumsch, Eugen Rodel, Christoph Imboden

Lucerne University of Applied Sciences and Arts, Horw/Switzerland;

Tel.: +41-41-349-3391

andreas.rumsch@hslu.ch

Abstract

More and more services need data from different sources. An example is a grid service aggregating distributed loads in a pool. Such a pool could consist of a large number of different loads, each from different manufacturers. The grid service then needs access to the data of all these devices. To keep costs low and to avoid the installation of gateways in the field, already existing infrastructure and data connections shall be used. This is where Data Spaces come into play. A Data Space builds a trustworthy platform to exchange data under full control of data owners. Open questions regarding the implementation of a Data Space are: Are software components available? How to ensure trustworthiness through governance? How to integrate existing standards? How can business cases benefit from Data Spaces?

Data Spaces set the concept and define the required elements, covering technical aspects as well as governance and legal topics. The authors have implemented a demonstrator of a Data Space, which shows the challenges one is facing when implementing or when connecting to a Data Space via so called connectors. Business cases have been developed in a series of workshops with representatives from industry.

The demonstrator is built based on a software framework provided by the International Data Spaces Association (IDSA). This framework shows good maturity compared to others. Based on the fundamentals of IDSA, it is possible to build a trustworthy Data Space, although the effort to integrate the connectors is still high and must be reduced. Many different ontologies representing standards already exist with very specific applications. The concept of Data Spaces eases the integration of ontologies via a vocabulary hub. Beside technical aspects, implementing Data Spaces also involves complying with data laws. The framework takes these into account and provides support.

Data Spaces can be seen as an open infrastructure for secure and sovereign data exchange, based on agreements, rules and standards. This is crucial for innovative business models. A common governance is crucial for gaining stakeholders' trust and willingness to participate in a Data Space that enable a future data economy. This necessitates a neutral and trustworthy non-profit organization to establish and operate the Data Space and the required infrastructure.

Further projects to implement Data Spaces have been initiated where grid services or a web-based HEMS will be realized to show the benefits of using Data Spaces.

Introduction

The expansion of PV systems in Europe is progressing. Since 2021 alone, installed capacity in the EU has risen from 164 GW to 260 GW in 2023 [1], and in Switzerland from 3.4 GW to 5.2 GW in the same period [2]. This is leading to an increasing decentralisation of electricity generation, as smaller and therefore more plants are producing this energy. Measures to stabilise the electricity grid must adapt to this change. One approach is to decentralise stabilisation by having many electrical loads such as charging stations, heat pumps, boilers, washing machines or dishwashers form a pool in which the individual appliances are switched on or off as required. Further, PV systems, batteries in houses and cars, or smart meters must be monitored. This requires a high degree of interoperability, which is an increasingly important requirement for stabilising the grid. In the example given, interoperability means that the operator of the pool can access data from different devices from different manufacturers and can also control these devices.

A classic approach to achieving interoperability is the use of gateways (fig. 1). The pool operator has access to the data of the devices via the gateways and can also control them in this way. The main task of the gateway is to standardise the protocols used by the various device manufacturers to provide a unified interface for the pool operators.

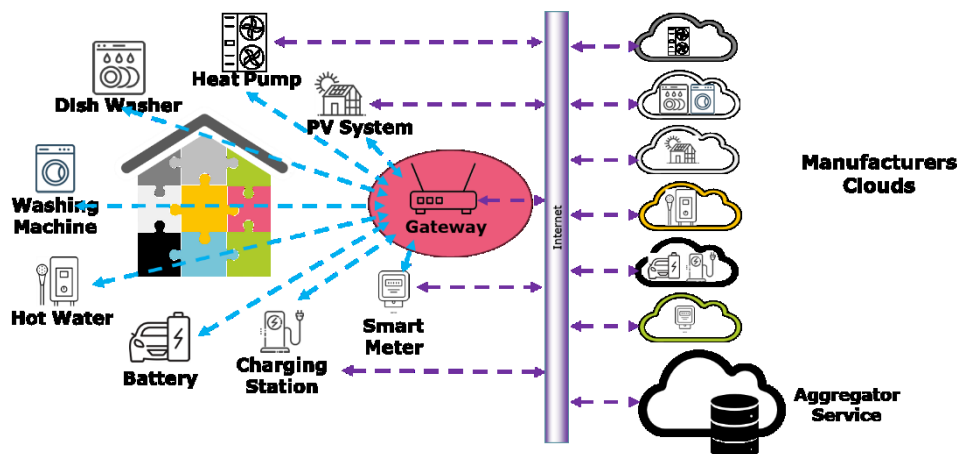


Fig. 1:
Classic approach to achieving interoperability with gateways.

A major disadvantage of the gateway approach is that a gateway must be installed in every household participating in the pool. In addition to the material costs for the gateway, the costs for installation and configuration are particularly significant. In our test area in Switzerland, we account for several hundred CHF per installation. These costs can make it impossible to roll out a good technical solution profitably on the market. Solutions that can do without the gateway would therefore have a clear advantage.

There are solutions without a gateway since modern devices are already equipped with an interface to the manufacturer's cloud. A pool operator could save costs by accessing the manufacturers' clouds directly (fig. 2). This is possible if the manufacturers grant access to the information stored in their cloud via an API.

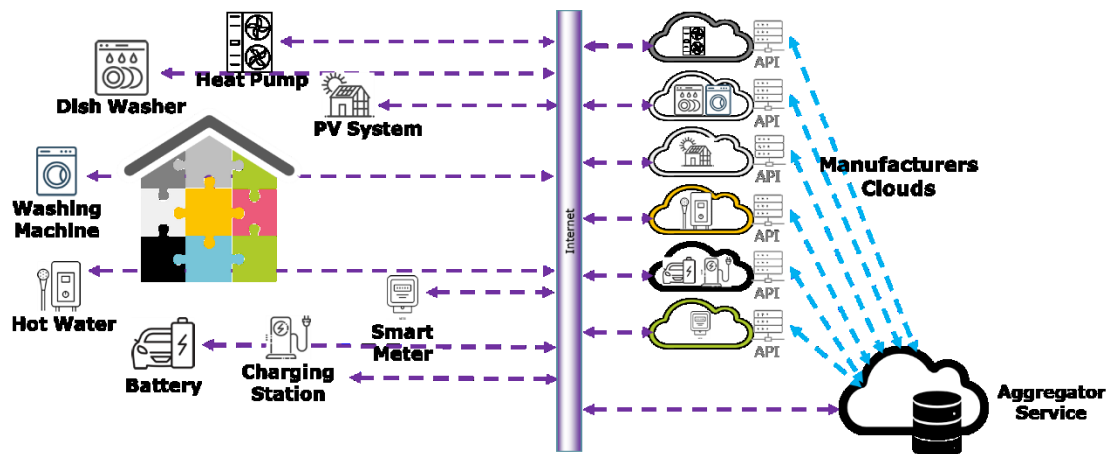


Fig. 2:

A pool operator can access the information stored in the manufacturers' clouds via APIs.

The approach of accessing the data via an API entails some disadvantages in terms of potential security risks. The manufacturers of the devices and the pool operator are responsible for ensuring that data security is maintained. And because a pool operator must agree with several manufacturers how he can access the data, the pool operator must implement appropriate security measures with all manufacturers, which in turn entails a high time and financial outlay. One of the questions for manufacturers is to what extent they can trust the pool operator to use the data in accordance with the agreement.

Another aspect is the extent to which the owners of the data (i.e. the users of the devices) have control over how their data is used. An agreement would have to be reached between the three parties of user, manufacturer and pool operator, which in turn can involve a great deal of effort.

This is where Data Spaces come into play. Only known and authorised organisations or individuals can participate in a Data Space. The Data Space thus represents a trustworthy infrastructure in which all participants can securely exchange data in accordance with the data owner's specifications. In addition to software components, a Data Space also includes a set of governance rules that cover processes at an organisational and legal level. Data exchange does not take place directly between providing and consuming participants, but rather the Data Space serves as an intermediary (fig. 3). The rules for data exchange are defined in the Data Space, which also eliminates the need for participants to reach a bilateral agreement.

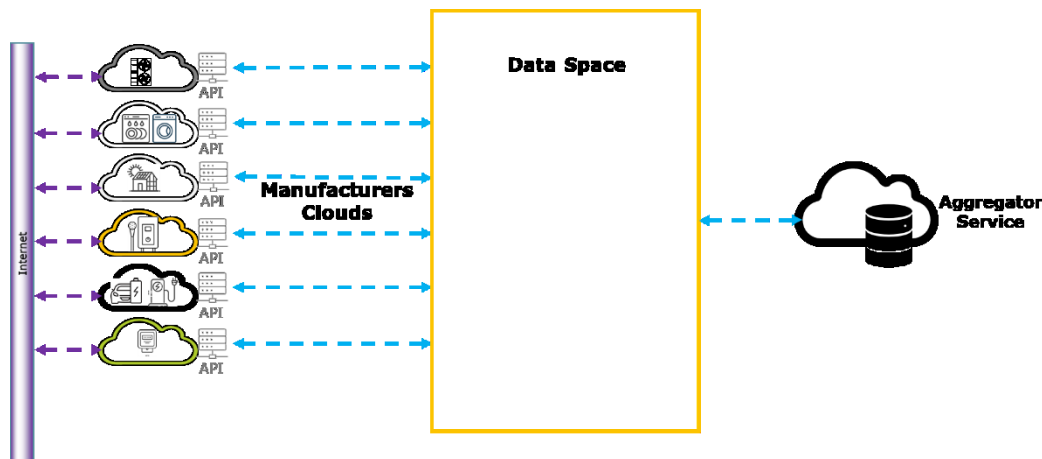


Fig. 3:

Data exchange takes place with the Data Space as an intermediary, controlled by a set of rules defined in the Data Space.

This paper describes what Data Spaces are, and how they are used in real world scenarios. Chapter 1 describes the concept of Data Spaces, chapter 2 shows in more detail how the example of pooling loads for flexibility is realized using the technology of Data Spaces. Chapter 3 dives into the realization of a Data Space and the challenges encountered. The benefits and the potential of using Data Spaces are discussed in chapter 4.

1. Concept of Data Spaces

This chapter delves into a general architecture overview, and a specific description of the software components utilized. Integral to Data Spaces are specific requirements:

- Data is not redundantly stored; it remains in its original location.
- Data owners retain control over determining access permissions for their data.
- Participants can trust the identity authenticity of others.
- No centralized entity manages data.

A Data Space is a data integration concept based on four pillars [3]:

- Data is left where it is created or managed, which results in a distributed data architecture and a distributed data infrastructure.
- There is no common database schema (data integration on the semantic level) required; therefore, vocabularies are needed to achieve semantic interoperability between the distributed data.
- Data Spaces allow for data redundancies and «co-existence» of data.
- Data Spaces can be nested, i.e., several Data Spaces can overlap but do not have to be disjoint and participants can be part of multiple Data Spaces.

In addition, the concept of Data Spaces comprises data sovereignty and data traceability. Data providers want to determine who can do what with their data, and they want transparency about what happens to their data when they share it. Further, data recipients must be able to trust that the data providers are who they say they are. A trust anchor is needed and is achieved through a certification process. A digital certificate is required to document this trust anchor.

The foundation of Data Spaces lies in a distributed software architecture. Connectors play a pivotal role in facilitating the provision and utilization of data while upholding data sovereignty. These connectors serve as the distributed data endpoints. Additional components are essential to enable these endpoints to discover each other and engage effectively. Broker services act as intermediaries, connecting data providers with data consumers and facilitating with the help of a vocabulary hub data exchange, ensuring a harmonious match between data supply and demand. Clearinghouse services oversee the successful execution of data transactions without delving into the data itself. To ensure trust, the identity provider only grants access to the data space to participants with a valid certificate. The components mentioned here are described in fig. 4.

In summary, Data Spaces unlock the potential for innovative business models by bridging the gap between data integration and application-driven value creation. Through a distributed software architecture and the careful orchestration of connectors, broker services, and clearinghouse services, Data Spaces empower organizations to harness data while respecting the sovereignty of its providers, thus catalysing a new era of data-driven innovation.

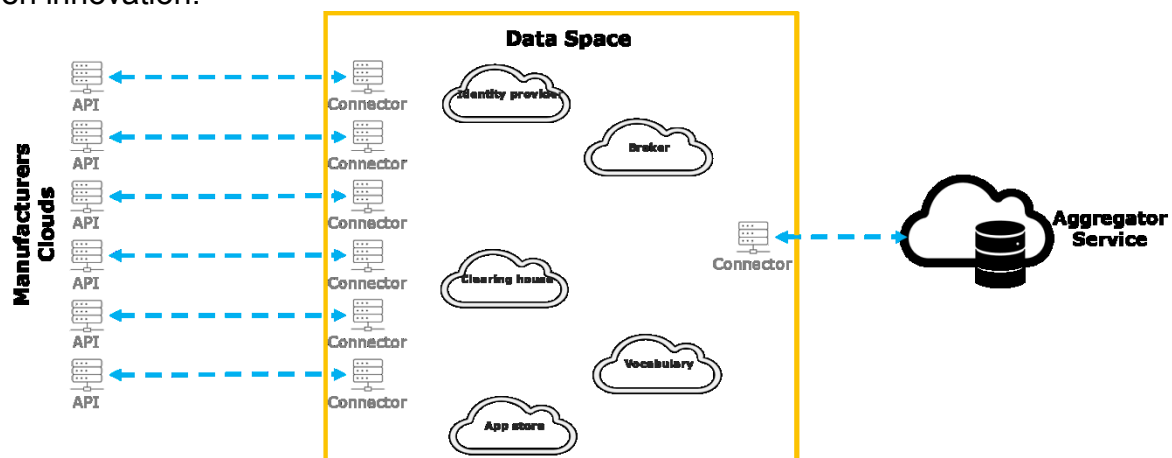


Fig. 4:
Components needed for a Data Space

1.1 Reference architecture model

The International Data Spaces Association (IDSA) offers a software architecture for Data Spaces with the abovementioned characteristics. IDSA created a Reference Architecture Model (RAM) (fig. 5) describing five levels and three perspectives.

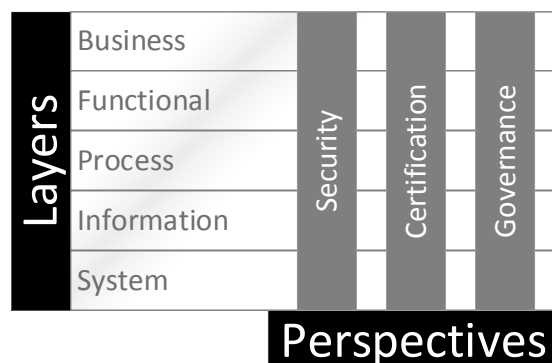


Fig. 5:

The five layers and three perspectives of the reference architecture model from International Data Spaces Association

Business Layer

In the business layer, the RAM defines the roles of the participants in the Data Space and categorizes them. It also specifies basic patterns of interaction between the roles and thus contributes to the development of innovative business models by the participants providing digital, data-driven services.

The business layer summarizes the roles into the four categories core participants, intermediaries, software developers, and Governance Bodies.

Functional Layer

The functional layer specifies the functional requirements for Data Spaces and the resulting functionalities to be implemented. The functional architecture is divided into six areas, each of which comprises a group of functionalities of the software.

Trust: Functional requirements must be met to achieve trust.

Security and Data Sovereignty: The functionalities regarding security and data sovereignty are fundamental in International Data Spaces.

Ecosystem of Data: A Data Space needs data source descriptions, meta data brokering and vocabularies.

Standardized Interoperability: This comprises functionalities for a standardized exchange of data between participants, which is the fundamental functionality in a Data Space.

Data Markets: To generate value, a Data Space must include concepts for clearing, billing and governance.

Information Layer

The information layer specifies the information model, the domain-independent, common language, i.e. the vocabulary used in the Data Space. The information model is an essential agreement that is shared by the participants and components of the IDS and facilitates compatibility and interoperability.

The main purpose of this formal model is to enable the (semi-)automatic exchange of digital resources within a trusted ecosystem of distributed parties while preserving the data sovereignty of the data owners. The information model supports the description, publication and identification of data products and reusable data processing software. Once the corresponding resources are identified, they can be exchanged and consumed via easily discoverable services. Apart from these core assets, the Information Model describes key elements of the International Data Space, its participants, its infrastructure components, and its processes.

Process Layer

The process layer specifies the interactions between the various components of the International Data Spaces. The most important processes are:

Onboarding: Onboarding describes what needs to be done to gain access to the Data Spaces

Data Offering: For the data offering a complete description of the data is an important prerequisite so that others can take advantage of the data.

Contract Negotiation: Connectors must negotiate the contract, i.e. accept data offers by negotiating the usage guidelines, which range from simple access restrictions to complex obligations before and after data exchange.

Exchanging Data: Connectors can only exchange data with each other once all previous process steps have been successfully completed. A connector calls up the data operation that relates to the contract agreement.

Publishing and Using Data Apps: Another relevant process is the publication and use of data apps. The apps are used to transform or process the data and are published by app providers in an app store and certified by the certification body if required. A connector can search for apps in the app store, download the appropriate app. The app is executed in the context of the connector.

System Layer

At the system level, the Data Space represents a distributed system in which the participating parties host the different Data Space components on their infrastructure. The connector initiates the exchange of data to and from the internal data resources of the participating organizations' enterprise systems and the Data Space. The connector provides metadata to the Metadata Broker as specified in the connector's self-description. This de-scription may include information about the technical interface, authentication mechanisms, and associated data usage policies. Usage agreements are transmitted by the connector to the Clearing House to establish trust. The Clearing House logs information about transactions to establish trust and transparency or to enable billing. The Vocabulary Hub provides vocabularies that specify the semantics of the exchanged data. Connectors can load applications from the App Store that run in the context of the connector and process data according to usage policies.

The System Layer maps the roles from the Business Layer and the processes from the Process Layer to a concrete data and service architecture. This represents the technical core of the Data Space (fig. 6).

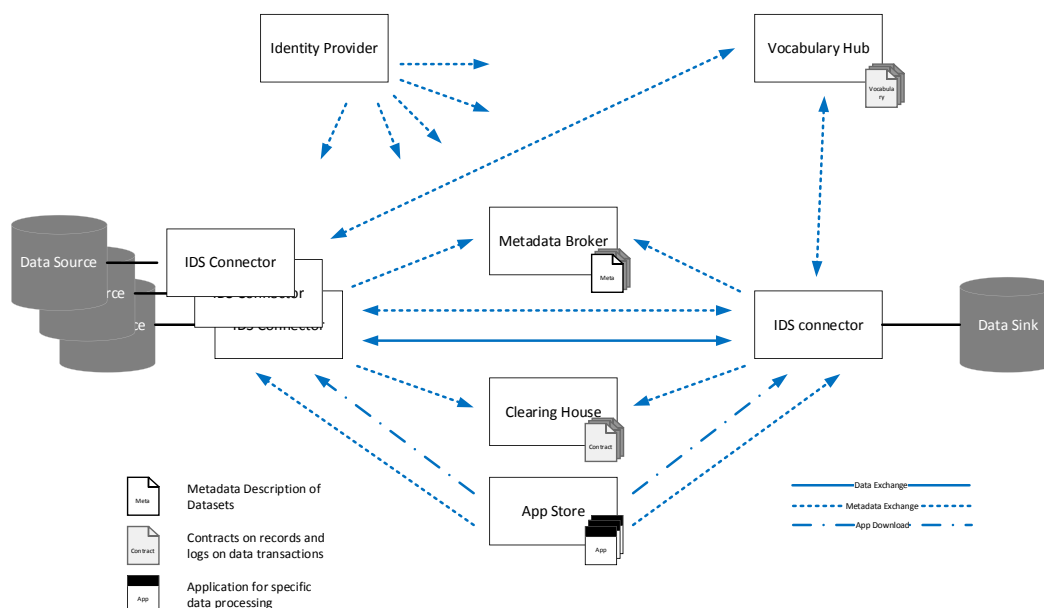


Fig. 6:

The system layer shows the interaction between the components of a Data Space and maps roles and processes to a data and service architecture.

Certification Perspective

To guarantee data security and data sovereignty, the Data Space relies on consistent certification of all components. In this way, the Data Space ensures that all players and components adhere to the rules of the Data Space. Certification applies to all levels of the architecture model.

The certification scheme outlines required levels and focuses for each role. At the functional level, core components must meet core security requirements for compliance certification. Conformity assessment includes the information level, functionality, protocols, and information model compatibility. Relevant processes are evaluated for compliance. At the system layer, certification focuses on security requirements, ensuring components are suitable for a trustworthy Data Space.

In addition to the Trust Levels, three Assurance Levels are applied as part of the certification process, ranging from self-assessment to external assessment.

To ensure the high quality and transparency of the certification process, all evaluation facilities must first be approved by the impartial certification body. This process comprises a compilation of all relevant information and documents and a check whether the evaluation facility complies with all the requirements of the Data Space and can be approved as an evaluation facility.

Security Perspective

A strategic requirement for Data Spaces is to provide secure data exchange. This is imperative to build and maintain trust between the components and organizations participating in the Data Space. A Data Space's security architecture must include measures to identify components in the Data Space, protect communication and data exchange, and control the use of the exchanged data. Connectors ensure that the specifications and requirements of the security architecture are applied to the interactions and operations in the Data Space.

Implementation of security depends on the layer, ranging from a security architecture on business level to technically implementing security specific hardware components on system level. For each level the measures to guarantee security must be adapted accordingly.

Which of the requirements are to be implemented depends on the required trust level. In the Data Space, a distinction is made between three trust levels: 1) interoperability in the Data Space, 2) complete function for controlling data usage, and 3) additional protection against internal attacks.

Governance Perspective

In the reference architecture model, the governance perspective defines the roles, functions and processes of the Data Spaces from the perspective of governance and compliance. A key point here is to describe the requirements to be fulfilled by the business ecosystem, which are necessary for secure and reliable interoperability between the companies. The architecture of Data Spaces does not impose any restrictions on cooperation between organizations and does not require compliance with predefined rules. The participating organizations determine the rules to be followed. The architecture as a functional framework enables the rules to be implemented.

The management of data-related resources through decision-making rights, responsibilities, roles, and ownership makes data governance a fundamental element in the Data Space ecosystem. Data governance makes it possible to successfully engage in a collaborative ecosystem. It is therefore important to create organizational structures and processes that clearly describe who can make what kind of decisions and what responsibilities are associated with these decisions.

From a governance perspective, data is an economic asset. Governance therefore focuses its activities on enabling new digital business models through the exchange of data. However, this considers the demands of data owners. This data ownership is another issue that must be respected by governance. In the legal sense, there is no ownership of data, as it is an intangible asset. Data sovereignty expresses the fact that the data owner always retains control over the use of their data.

2. Pooling Loads Using a Data Space

This chapter shows how aggregators can use a Data Space for the pooling of electrical loads to offer balancing energy on the market. In the context of Data Spaces, it is primarily the exchange of data that is of interest; the description does not go into the details of the provision of balancing energy.

The example describes the pooling of household appliances such as heat pumps, boilers, washing machines or charging stations for electric cars [4]. An aggregator requires data of a static (type, connected load, ...) or dynamic (status, availability, current power consumption, ...) nature for its service. To be able to provide the necessary power for balancing energy, many such devices with a low power consumption compared to classic balancing energy suppliers are required. The aggregator must be able to access this data to be able to offer the balancing energy at all. As the devices come from different manufacturers, the aggregator is faced with the challenge of being able to exchange data with devices from all manufacturers.

The solution approach using a Data Space envisages that each manufacturer's cloud is connected to the Data Space via a connector (fig. 7). These manufacturers are, in the sense of a Data Space, the data providers, providing the data coming from the devices. A service provider, such as the aggregator described above, is also connected to the Data Space via a connector. The aggregator is a data consumer. The onboarding procedure in the Data Space ensures the authenticity of the participating parties and provides a trustworthy framework in which the data can be exchanged by issuing certificates.

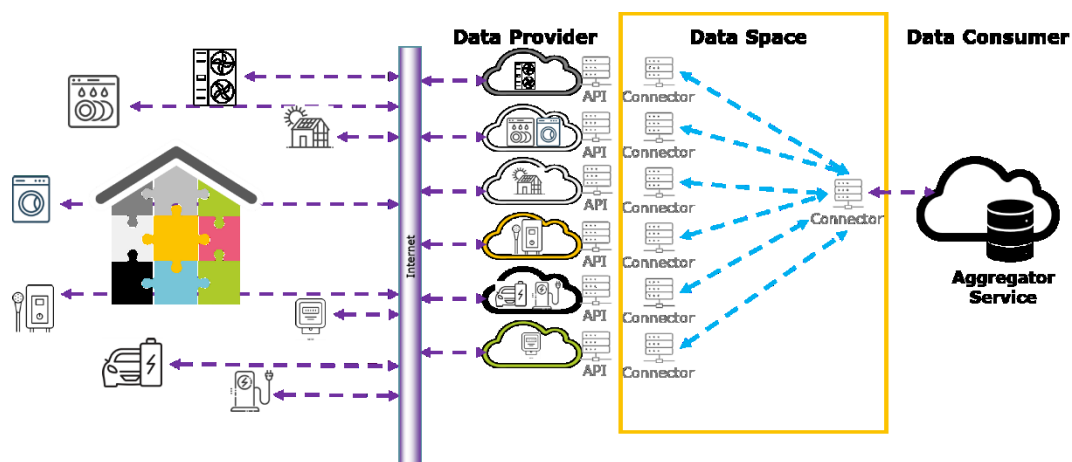


Fig. 7:
Solution approach for an aggregator using a Data Space.

The manufacturers of the devices (data providers) can make any of their data available in the Data Space, provided that the data owner declares his consent. To enable the aggregator (data consumer) to assess whether this data is useful for them, they can query the metadata provided by the manufacturers. In addition, the producers provide a description of their data (ontologies or vocabularies) so that the aggregator knows the meaning of the data. The aggregator then concludes a contract with the owners of the devices for the use of the data. In the case of pooling, the contract also stipulates that the owners also make their devices available as flexibilities. Such a contract not only includes that the aggregator may use the data, but the data owners also define how the aggregator may use the data using a data usage policy. These processes are shown in fig. 6.

Not all data has to be transferred to the aggregator. For example, it is conceivable that a consumption forecast for individual appliances could be calculated close to the manufacturer. In Data Spaces, an app running in the context of the connector can perform these calculations. This approach has the advantage that the aggregator does not need to receive the raw data in the first place and can therefore minimise the amount of data to be transmitted. The advantage for data owners is that the raw data does not even leave a

controllable space, the Data Space, so privacy can be preserved as much as possible. The app store in the Data Space provides the apps.

The clearing house registers all transactions in the Data Space to be able to settle fees or costs. The information about the transactions only store what type of data was transferred and when, but not the data itself. The data owners thus always retain full transparency as to who requested which data from them and when. For the aggregator, the transactions serve to compensate the owners of the devices according to the use of the electrical loads.

To be able to use the devices in the pool for balancing energy applications, the aggregator must also be able to control them. A Data Space makes it possible not only to retrieve data from the manufacturer's clouds, but also to write data back to them. In this way, the aggregator can send information to the devices, which informs the devices about grid-friendly operation. It should remain under the control of the devices as to how they implement the information. In other words, whether they interrupt or resume operation immediately or whether they first complete a process that is currently running. The aggregator can then retrieve data on the current operating status via the Data Space.

3. Realization of a Data Space and Challenges

The authors have implemented a Data Space as a demonstrator as part of a project for the Swiss Federal Office of Energy (SFOE). They evaluated suitable software for this purpose. The International Data Spaces Association (IDSA) provides well-developed software with good documentation as open-source software. With the software components of the IDSA, it is possible to set up a Data Space in such a way that it fulfils all the requirements of the reference architecture model and thus represents a trustworthy space for exchanging data.

When implementing a Data Space, it has become clear that an extremely important requirement is the correct handling of certificates for all components involved in the Data Space. The certificates must be signed by a recognised, trustworthy authority. This is because only components certified in this way contribute to trustworthiness.

The process for exchanging data is highly complex, which leads to high implementation costs. The process consists of several steps from the negotiation of the data offer to the exchange of data, whereby security and sovereignty must be always guaranteed. The project team plans to provide a reference implementation so that the connection of data sources to the Data Space can be realized with less effort.

Challenges in the implementation of Data Spaces can also be expected at an organisational level. For example, ontologies are often difficult to understand and are not always available in a digitally processable form. This is the case if the ontology is available as a document from which the structure of the data model cannot be read automatically.

Although Data Spaces realize their full potential if the aggregated data sources can be used for many applications, many European projects are currently creating their own Data Spaces [5]. However, the European Data Strategy recommends realizing a Data Space for different domains (e.g. energy or mobility) [6]. However, these so-called Common Data Spaces are not yet sufficiently developed and do not represent a viable alternative in the projects.

4. Benefits and Potentials of Data Spaces

As already mentioned in the previous section, Data Spaces unfold their potential above all when a Data Space can be used for multiple use cases. A Data Space with many connected clouds represents a valuable source of data that service providers can use for their products. A Data Space can also make data available for research projects.

A major benefit of using a Data Space is that new business models can be realised without having to set up a complex infrastructure [7]. This requires the existence of a Data Space that provides the data required for the business model. If this condition is met, the service provider only needs to create a connector and have it certified. This represents a one-off effort, which is comparatively low when compared with the alternative of installing gateways at the customer's premises.

The concept of Data Spaces is based on trustworthiness by design. On the one hand, this can lead to many manufacturers participating in a Data Space as data providers. On the other hand, trustworthiness should also lead to data owners making their data available for the provision of services. In addition, the owners of the data retain their data sovereignty and can determine who is authorised to use the data and for what purposes.

5. Conclusion

The concept of Data Spaces is one way in which future digital applications can exchange data. Data Spaces are designed from the outset to be trustworthy, secure and sovereign. Data Spaces utilise an existing infrastructure that device manufacturers have already set up for data exchange. Data exchange does not result in data being stored multiple times. It remains at the data source and is only exchanged on request when required.

Certificates for participants in the Data Space and for components ensure trustworthiness. Authentication and encryption ensure security, while data usage policies together with the clearing house guarantee sovereignty.

Several challenges still need to be overcome before Data Space technology can be widely used. For example, it must be possible to reduce the effort required to implement a connector and connect to proprietary data sources. This can be done, for example, with a reference implementation that is made available to potential participants in the Data Space. For a smooth exchange of data, data providers and data consumers must agree on ontologies that are to apply in the Data Space. However, this requires digitally analysable representations of the ontologies, which currently applies in only a few cases.

With Data Spaces, new business models can be implemented in a new data economy without complex installations. The availability of a variety of different data sources enables the development of innovative or even disruptive business ideas. This potential must be utilised through the consistent further development and dissemination of Data Spaces.

References

- [1] „Solar Energy“. Accessed 10. Mai 2024.
https://energy.ec.europa.eu/topics/renewable-energy/solar-energy_en.
- [2] BFE, Bundesamt für Energie. „Elektrizitätsproduktionsanlagen in der Schweiz“. Accessed 10. Mai 2024.
https://www.uvek-gis.admin.ch/BFE/storymaps/EE_Elektrizitaetsproduktionsanlagen/.
- [3] Otto, Boris, Michael ten Hompel, und Stefan Wrobel, Hrsg. Designing Data Spaces: The Ecosystem Approach to Competitive Advantage. Cham: Springer International Publishing, 2022. <https://doi.org/10.1007/978-3-030-93975-5>.
- [4] „Equigy – Crowd Balancing Platform“. Accessed 21. Mai 2024.
<https://www.swissgrid.ch/de/home/newsroom/dossiers/crowd-balancing-platform.html>.
- [5] International Data Spaces. „Data Spaces Radar“. Accessed 21. Mai 2024.
<https://internationaldataspaces.org/adopt/data-spaces-radar/>.
- [6] „European Data Strategy - European Commission“. Accessed 21. Mai 2024.
https://commission.europa.eu/strategy-and-policy/priorities-2019-2024/europe-fit-digital-age/european-data-strategy_en.
- [7] International Data Spaces. „Data Spaces“. Accessed 21. Mai 2024.
<https://internationaldataspaces.org/why/data-spaces/>.

G08

Enabling Technologies

G0802

Data-driven predictive control for demand side management: Theoretical and experimental results

Mingzhou Yin (1), Hanmin Cai (2), Andrea Gattiglio (2), Fazel Khayatian (2), Roy S. Smith (1), Philipp Heer (2)

(1) Automatic Control Laboratory, Swiss Federal Institute of Technology in Zürich, Zürich/Switzerland;

(2) Urban Energy Systems Laboratory, Swiss Federal Laboratories for Material Science and Technology (Empa), Dübendorf/Switzerland;
hanmin.cai@empa.ch

Abstract

Demand side management is vital for secure and efficient operations in energy systems with increasing renewable energy use. Current modeling and control methods lack scalability for widespread application. This paper introduces a new signal matrix model predictive control (SMM-PC) algorithm. This method offers stochastic forecasts that account for both disturbances and measurement inaccuracies with minimal parameter adjustments, thus enhancing reliability through likely constraint fulfillment. Its efficacy is thoroughly benchmarked against three advanced algorithms in a space heating scenario using a precise simulator. These findings are corroborated by real-world tests on the system replicated by the simulator. To test versatility, the algorithm is also applied to varied systems such as a residential water heater and a stationary battery. Simulations indicate that the SMM-PC algorithm can increase constraint adherence and energy savings by up to 90% and 8%, respectively, when compared to other data-driven strategies. Experimental outcomes further verify its adaptability across different demand side management tasks, with consistently solid control performance in all cases.

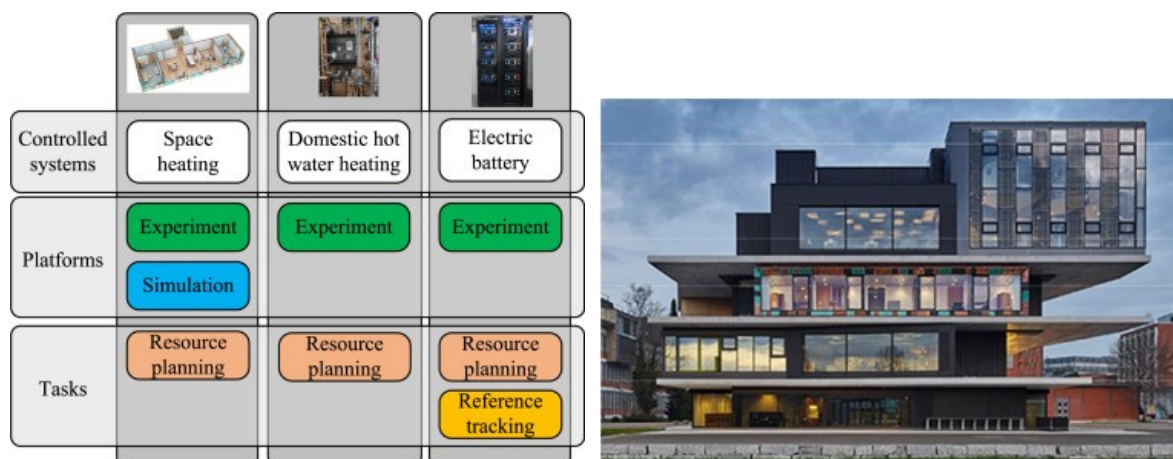


Figure 1. Overview of case studies (left) and physical facility for experimental verification (right).

Introduction

While the increasing penetration of renewable energy resources contributes to mitigating climate change, the intermittency in their production is expected to significantly challenge the energy system operation. Meanwhile, the International Energy Agency estimates that one billion households and eleven billion smart appliances could actively participate in demand response programs globally by 2040 [1], which can be seen as a subcategory of demand side management (DSM). This opens up the possibility of applying active DSM on a large scale to cope with the surge of renewable energy, as well as facilitating energy conservation and improving the occupants' comfort. In the existing literature, model predictive control (MPC) has been viewed as a promising control strategy to enable DSM. For example, MPC is used to provide distributed coordination of buildings to support flexible energy infrastructure operation. However, due to the large number of heterogeneous controlled systems, first-principles modeling approaches cannot ensure timely and cost-effective implementation. In fact, modeling often takes up the majority of the budget in applying model-based control, in terms of both time and cost. Therefore, data-driven control methods have recently received considerable attention. This work addresses this challenge by developing a novel data-driven control algorithm and systematically assessing its performance across heterogeneous components in simulation and experimental studies.

In this work, a novel indirect data-driven predictive control framework, dubbed signal matrix model predictive control (SMM-PC), is presented. SMM-PC is first proposed with maximum likelihood prediction. Reliable stochastic prediction under noise is later provided, which is very difficult to obtain in other data-driven methods. On the other hand, stochastic MPC approaches have been widely studied in the literature and applied in the building sector, and guarantee high-probability constraint satisfaction by enforcing chance constraints. Similar techniques can be applied to stochastic data-driven predictors.

The contributions of this work are threefold. Firstly, the existing SMM-PC algorithm is extended to explicitly account for disturbances and measurement noise by incorporating the stochastic control framework with chance constraints. This algorithm provides a disciplined yet easy-to-implement approach to achieve reliable operation with data-driven methods under various uncertainties. Secondly, the performance is extensively analyzed by comparing multiple state-of-the-art data-driven algorithms using a high-fidelity simulator for space heating (SH) control. Results demonstrate that the proposed stochastic SMM-PC algorithm not only satisfies operating constraints more reliably than competing methods, but it also reduces energy consumption at the same time. In addition, experiments have been carried out to validate the controller's performance on the same facility on which the simulator has been built. Lastly, the transferability is experimentally evaluated across different types of controlled systems, including a domestic hot water (DHW) heating system and a stationary electric battery. It is demonstrated that the SMM-PC algorithm is easily transferable to different types of controlled systems with satisfactory performance since there are very few tuning parameters involved. An extended version of this manuscript can be found in [2].

1. Approach towards Flexibility and Business Experiences and success stories

A series of numerical and experimental case studies have been carried out to evaluate the performance and transferability of the stochastic SMM-PC algorithm. The studies, summarized in Figure 1, consider transferability across heterogeneous controlled systems, transferability from simulation to experiment, and the impacts of certain control tasks.

Three controlled systems were investigated: a space heating system, a DHW heating system, and a stationary Lithium-ion electric battery, representing typical demand-side resources. All the system configurations and data presented in the rest of the paper are based on the NEST building located at Empa in Switzerland, shown in Figure 1. Typical control tasks include constrained resource planning and trajectory tracking. In the building sector, constrained resource planning is prevalent and aims to minimize total energy consumption while ensuring constraint satisfaction. Reference tracking tasks can also be formulated for the stationary electric battery, as it is considered to be a promising candidate for ancillary service provision through tracking reference signals set by system operators.

Space heating The system considered in this study is a three-room apartment, hereafter referred to as the UMAR unit. Each room was treated as one thermal zone and heating power was dissipated into the zones through constant volume radiant ceiling panels. The continuous power setpoint, determined by the controller, was realized by regulating the valve opening, which was converted into discrete opening and closing sequences using pulse-width modulation logic. Additionally, the control of space heating was subject to constraints imposed by occupants' perception of comfort. Although other indoor conditions also influence occupants' comfort, temperature sensors are the most commonly available for assessment, so thermal comfort bounds were expressed as temperature limits in this study. As the unit is residential, the thermal comfort bounds were predefined, considering the unit to be unoccupied during the day and occupied during the night. The definition led to relaxed temperature constraints during unoccupied hours. Specifically, the constraints were set to be between 20°C and 26°C from 08:00 to 16:59 and between 22°C and 24°C from 17:00 to 07:59 of the second day.

Various approaches have been proposed in the literature to compare control algorithms for space heating, ranging from a simulation-only approach using a hypothetical physics-based model to an experiment-only approach with a placebo comparison. The latter requires two identical physical systems running different control algorithms in identical conditions, which is rarely possible in reality. Other studies employ a degree-day metric, in which average boundary condition (e.g., ambient temperature) is considered, neglecting other factors such as heat gains. In this work, we first benchmarked control algorithms on a high-fidelity white-box model of the physical system. The model was based on detailed knowledge of the system layout and the heat storage and transfer characteristics of the construction materials. Additionally, the model was calibrated with three-year field measurements at a 1-minute temporal resolution, capturing both the dynamics of the physical system and the heat gains due to occupants. Due to the high model fidelity, a high level of confidence in the expected control performance can be ensured. The transparency and reproducibility of the results are ensured by providing the model in an open repository. An experimental study was then conducted to evaluate constraint satisfaction with Algorithm 1 using the signal matrix model.

Domestic hot water heating Energy consumption of DHW is taking an increasing share of the total energy consumption, especially for newly-constructed and renovated buildings with better-insulated envelopes. DHW is often equipped with a water buffer tank for hydraulic decoupling and reducing the load diversity factor. Energy scheduling needs to guarantee sufficient hot water storage within the tank and a minimum temperature constraint of 45°C was considered. Additional periodic temperature boosting to the level of 60°C is necessary to avoid Legionella contamination. In this work, temperature boosting once per week was considered by introducing a step change in the lower temperature limit. The water tank has three temperature sensors vertically distributed along the tank wall, and the measurements differ due to stratification. In the experiment, the average measurement was considered. Lastly, due to high uncertainties associated with individual occupants' water draw activities, a persistence forecast of water draw was implemented using the most recent weekly water draw patterns.

Stationary electric battery Stationary electric batteries are increasingly popular in the residential sector due to the large mismatch between rooftop solar production and the residential load pattern. Such electricity storage can be used for arbitrage in the electricity market through constrained energy scheduling and for stabilizing power system frequency through reference tracking. Since no standard evaluation metric and use case can be found in the literature, two simple artificial case studies were considered. In the first case study, the amplitudes of battery charging and discharging power were minimized while guaranteeing that the state-of-charge was maintained within the predefined dynamic limits. Since the limits varied over time, knowledge of the future system response was necessary. In the second case study, the battery's charging and discharging powers were controlled such that its SOC followed a reference signal. Although classical PID control schemes also excel at reference tracking and the future system response is not crucial to consider, this case study was carried out to cover all possible applications.



Figure 1. Overview of case studies (left) and physical facility for experimental verification (right).

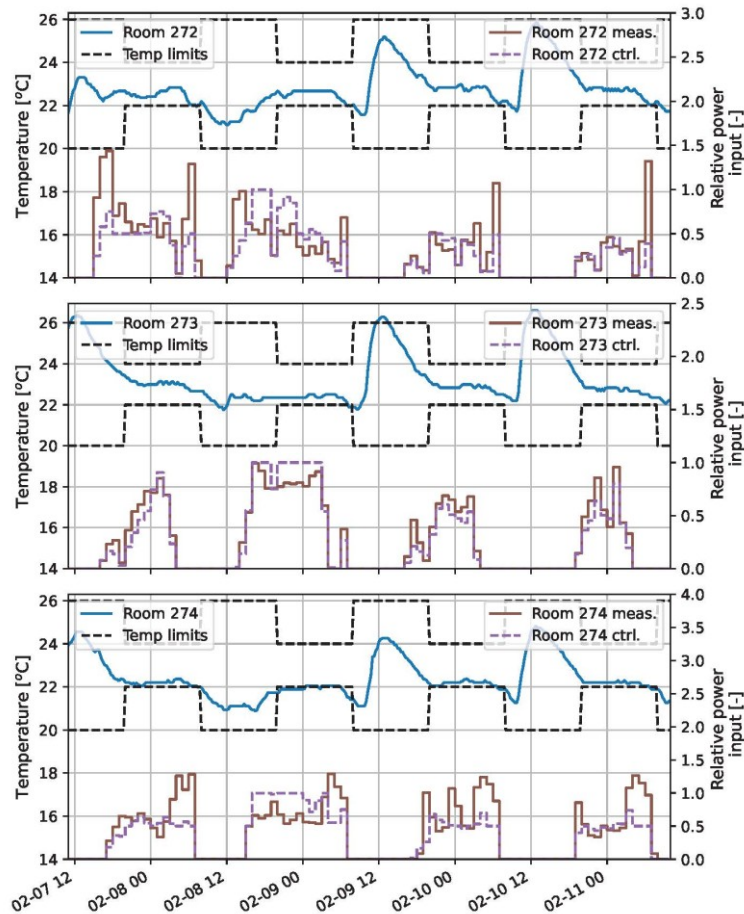


Figure 2. Experimental results of space heating control. Top plot: results for Room 272. Middle plot: results for Room 273. Bottom plot: results for Room 274. The dashed black curves show temperature limits. The solid blue curves show temperature trajectories. The dashed purple curves show controller decisions (scale at left). The solid olive curves show realized thermal power inputs into the rooms in relative terms by normalizing using thermal power capacities (scale at right).

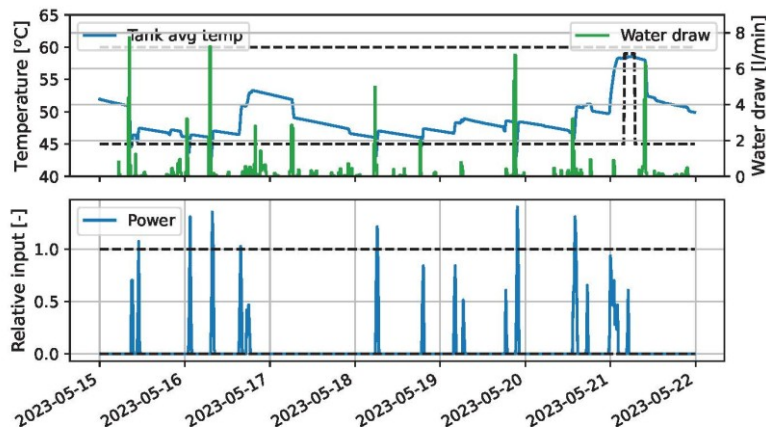


Figure 3. Experimental results of controlling domestic hot water heating. Top plot: the solid blue curve shows the average tank temperature trajectory and the dashed black lines indicate temperature limits (scale at left). The solid green curve shows the actual water draw profile (scale at right). Bottom plot: the solid blue curve shows the measured thermal power into the tank and the dashed black lines indicate expected thermal power limits. The maximum power varies depending on supply temperature.

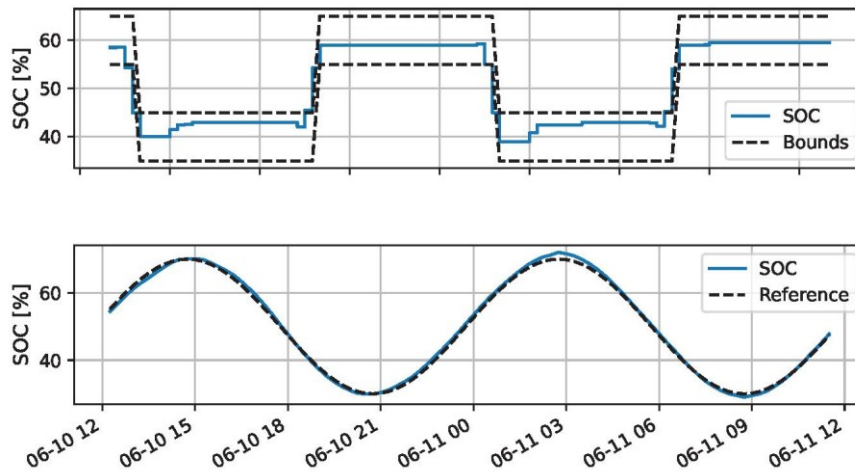


Figure 4. Experimental results for the control of an electric battery. Top plot: resource planning task. Bottom plot: reference tracking task. The solid blue curves show the actual SOC. The dashed black lines indicate temperature limits for the top plot and the reference trajectory for the bottom plot.

2. Added Values/Conclusion

Space heating The experiment was carried out between February 7 and February 11 of 2023. During the experiment, the prediction horizon and the confidence level of constraint satisfaction were set to be 15 (3.75 h) and 0.7, respectively. They were the same as the values used in the simulation study. The experimental results summarized in Figure 2 include temperature measurements, control decisions, and realized power inputs into each temperature zone. Different from the numerical study, the actuation of control decisions is subject to errors in practice, leading to mismatches between control decisions and realized power inputs in Figure 2. It can be observed that the temperature in each room was maintained within the predefined comfort zone most of the time. The accumulated constraint violations in Rooms 272, 273, and 274 are 0.025 °Ch, 2.159 °Ch, and 1.518 °Ch, respectively. Additionally, in all rooms, preheating decisions can be observed once the step increase of the lower temperature limits was within the horizon of the controller. The results validated the hypothesis that SMM-PC is able to ensure constraint satisfaction within the technical capability of the underlying physical system.

Domestic hot water heating The experimental results of DHW heating control are summarized in Figure 3, where both water draw and average tank temperature time series are shown together with predefined temperature limits. It can be observed that average tank temperatures were mostly maintained within the predefined limits. The accumulated constraint violation over one week was observed to be 3.9 °Ch. Since the control task was to minimize energy consumption, the tank temperature was kept close to the lower limit leaving only necessary hot water, which contributed to reducing heat loss through the tank wall. A large constraint violation was observed when the step change of the lower temperature limit occurred due to decontamination. This was due to the large uncertainty level in the water draw activities and the narrow feasible bound during decontamination, which resulted in the infeasibility of the tightened constraints. In other words, the data-driven algorithm was not able to guarantee high-probability constraint satisfaction with the available data. In this case, it is recommended to relax the output constraints and/or to include more data on the water draw activities to provide data-driven load forecasts.

Stationary electric battery The experimental results of the electric battery control are shown in Figure 4 for both the resource planning task and the reference tracking task. The resource planning results show that the SOC of the battery was maintained within the limits, verifying the constraint satisfaction hypothesis. The accumulated constraint violation was 15.95 %h. Since the SOC limits were artificially designed, the accumulated constraint satisfaction value was not a crucial performance indicator. In this experiment, a high confidence level of 0.95 was used, so the actual SOC profile appeared to be conservative, and the trajectory stayed in the middle of the predefined zone to actively avoid constraint violation. The results of the reference tracking experiment show remarkable precision; in fact, the root mean square error between the reference signal and the actual SOC is only 0.79 %. To put it in context, the measurement quantization error is 0.5 %. Both experiments confirm the applicability of SMM-PC to typical control tasks for electric batteries.

Scalable modeling and control frameworks can facilitate demand side management, a critical tool for the reliable and efficient operation of future energy systems. To address current limitations, this work proposes a novel data-driven predictive control algorithm using the signal matrix model. By using a stochastic control framework, this algorithm is designed to be reliable against noise and disturbances. The performance of the methodology is comprehensively evaluated in high-fidelity simulations by comparing it against other data-driven predictive control approaches, and its transferability is validated in multiple experimental studies. Two main conclusions can be drawn from the quantitative results. Firstly, compared to the state-of-the-art data-driven predictive control algorithms, the proposed algorithm can improve occupants' thermal comfort and energy savings by up to 90% and 8%, respectively. Secondly, the algorithm effectively ensures constraint satisfaction, and its performance can be transferred to other systems with minimal tuning effort. Therefore, the proposed algorithm can facilitate large-scale deployment of demand side management to support energy system operation. To conclude, several limitations must be noted. First, while data-driven approaches provide scalability, the interpretability of the decisions still needs to be assessed. Poor interpretability could potentially compromise the security of a system comprising many automated and distributed devices, which are aggregated to support secure grid operation in the first place. Second, while the transferability across different controlled systems was evaluated, it remains to be assessed for the same type of controlled systems with different characteristics. For example, the proposed algorithm needs to be tested on a large group of heterogeneous buildings with different heating input systems.

References

- [1] International Energy Agency, "Digitalization and Energy." 2017. [Online]. Available: <https://www.iea.org/reports/digitalisation-and-energy>
- [2] M. Yin, H. Cai, A. Gattiglio, F. Khayatian, R. S. Smith, and P. Heer, "Data-driven predictive control for demand side management: Theoretical and experimental results," *Applied Energy*, vol. 353, p. 122101, Jan. 2024, doi: 10.1016/j.apenergy.2023.122101.

G0803

Assessment of Economic Surplus of the European Balancing Platforms

Ulf Kasper (1), Andreas Kindsmüller (1), David Steber (1), Simon Remppis (2), Dominik Schlipf (2), Alexander Warsewa (2)

(1) Ampriion GmbH, System Operation, Pulheim/Germany;

(2) Transnet BW GmbH, System Operation, Wendlingen/Germany;

ulf.kasper@ampriion.net; d.schlipf@transnetbw.de

Abstract

The implementation of the Electricity Balancing Regulation marks the beginning of a transformative process aiming at establishing a single European internal market for balancing energy, which will significantly change existing practices in the field of system balancing. Therefore, this paper describes the fundamentals of balancing in a broader context as well as the specifics of European balancing platforms and highlights various facets of economic surplus relevant to the exchange of balancing energy. It introduces the phenomenon of exceeding demand since there are periods in which the participating TSOs request activation of more volume of balancing energy than they have submitted to the balancing platforms themselves and different pricing strategies of balancing service providers (BSPs) across Member States. By examining consumer rent, producer rent and congestion income, the methodology outlined in this paper will provide a detailed assessment of the economic surplus associated with the exchange of balancing energy, following up on a previous academic contribution.¹

Neglecting additional surplus due to unsatisfied demand, the economic surplus attributed to the Platform for the International Coordination of Automated Frequency Restoration and Stable System Operation (PICASSO) amounts to €73.2 million in its first year of operation. Similarly, the Manually Activated Reserves Initiative (MARI) platform yields an economic surplus of €8.3 million in the first 12 months after go-live. While acknowledging the different operational strategies of the countries connected to MARI and PICASSO during the considered period, the observed difference in economic surplus across platforms is in line with expectations: Automatic frequency restoration reserves (aFRR) are activated around ten times more frequently than manual frequency restoration reserves (mFRR) resulting in a similar ratio of the economic surpluses. The benefit of balancing platforms is expected to significantly increase as more countries become operationally integrated into the balancing platforms in the next years.

However, it is crucial to note that the increasing economic surplus is partly accounted to increasing cost for balancing energy, resulting from both market design changes (e. g. the transition from pay-as-cleared to pay-as-bid mechanisms) and more expensive wholesale market conditions.

Following the introduction of European balancing platforms, the cross-border procurement of balancing capacity emerges as a plausible next step to foster competition at European balancing markets. Although some collaborations, such as the Grid Coordination Cooperation (GCC) and the Austro-German aFRR balancing capacity collaboration are already in operation, further harmonization is expected based on European regulatory initiatives. Given the scarcity of Cross-Zonal Capacity (CZC), additional analysis is required to identify whether CZC should be allocated within the day-ahead market for scheduled energy or within the balancing capacity markets, recognizing potential differences in market competitiveness across jurisdictions.

1 ee-public-nc-downloads.azureedge.net/strapi-test-assets/strapi-assets/2022_ENTSO_E_Balancing_Report_Web_2bddb9ad4f.pdf

Introduction

European regulation aims at establishing a Europe-wide domestic market for balancing energy. For this purpose, European balancing platforms have been set up to link the so far national balancing markets. In 2022, the last two balancing platforms MARI⁴ and PICASSO⁵ have gone live. Therefore, this paper aims at assessing their economic and environmental impacts.

As Amprion GmbH and TransnetBW GmbH have been designated as common service providers operating the balancing platforms for Frequency Restoration Reserves (and Imbalance Netting - IN), both transmission system operators (TSOs) are also responsible for calculating the economic surplus resulting from the actual balancing platform operation which is subject to several reporting obligations on European level [1]. The principles of the determination of economic surplus and a first in depth analysis for the first year of operation were elaborated in [2]. The results indicate that this distribution of the different rents may vary in the future when more TSOs join the European balancing platforms or depending on the monetary value attributed to additionally satisfied demand. This paper provides the economic surplus of the balancing platforms for the calendar year 2023 and presents a methodology to assess, as a first indicative, their environmental impact. The latter is approached by analyzing CO₂ emission prevented or retained due to PICASSO and IN.

Section II provides an overview on the relevant field of observation (i. e. electricity balancing in general, European balancing platforms and elements of economic surplus). Subsequently, section III describes the methodology applied to assess the balancing platforms' economic impact as well as approaches to estimate CO₂ emission reduction potential. Finally, section IV provides sums up the results of the calculations. An outlook in section V concludes the paper.

European Balancing Platforms

In EB Regulation, standard products for balancing energy were defined on European level for the first time. Balancing services can, amongst other possibilities, be classified by the time required for a full activation (full activation time, FAT) into

- Frequency Containment Reserve (FCR),
- automatic Frequency Restoration Reserve (aFRR),
- manual Frequency Restoration Reserve (mFRR) and
- Replacement Reserve (RR).

While FCR only contains a frequency deviation due to an imbalance between generation and consumption of electrical energy (proportional controller) in the whole synchronous area, FRR restores the system frequency to its original target value by providing additional energy in the responsible LFC area to the system (proportional-integral controller). In general, balancing services must be procured market-based in Europe.

EB Regulation also introduced the concept of European balancing platforms to which all European TSOs will connect to extend the Europe-wide cross-border exchange of aFRR, mFRR and RR balancing energy as well as IN. These European balancing

⁴ Manually Activated Reserves Initiative

⁵ Platform for the International Coordination of Automatic Frequency Restoration and Stable System Operation

platforms are balancing service specific optimization systems enabling the exchange of standard products for balancing energy across Europe or allowing to avoid counter-activation of balancing energy. This results in cost-efficient activation of balancing energy respecting available CZC. While IN facilitates netting of aFRR demands before activating balancing energy, PICASSO, MARI and TERRE⁶ enable the cross-border cost-minimal activation of balancing energy for each balancing service. This publication focuses on MARI and PICASSO, which were both launched in 2022. In the emission study, the contribution of IN is also considered. For more details about the European balancing platforms, we refer to [2].

Methodological approach

Economic Surplus

Economic surplus is the change in social welfare when comparing a scenario with exchange of balancing energy (coupled scenario) with a reference scenario without such an exchange (decoupled scenario). For each European balancing platform, economic surplus of an LFC area consists of the producer rent gain, the consumer rent gain and the congestion income resulting from exchange of balancing energy with other LFC areas.

The actual results of the area optimization function (AOF) are considered in the coupled scenario, i. e. TSOs of the considered countries activate balancing energy from a common merit order list, if there is an imbalance to be covered and sufficient CZC is available. In the decoupled scenario, TSOs in each country cover their imbalances only by activating balancing energy bids from the respective local merit order list. In this hypothetical situation, no balancing energy can be exchanged, resulting in balancing costs which would have occurred if the European balancing platforms had not been in place at all. As the validity period of standard products for balancing energy is 15 minutes, each scenario consists of 35,040 optimization runs p.a. for MARI. For PICASSO, a calculation must be performed for each optimization cycle of 4 seconds resulting in 7,884,000 runs p.a. For more details about the economic surplus related to European balancing platforms, refer to [2].

To assess the economic surplus generated at the balancing platforms, the coupled and decoupled scenarios are considered as different configurations for MARI and PICASSO. For both balancing platforms, the calendar year of 2023 is considered. In 2023, Austria (AT), Czechia (CZ) and Germany (DE) have participated continuously in PICASSO. Italy (IT) joined the PICASSO platform in July 2023. During first half of 2023, only CZ and DE participated in MARI operationally. AT started participating in the mFRR platform in the end of June 2023.

CO₂ emission impact of IN and PICASSO

Besides the analysis of the economic surplus, the impact of PICASSO and the IN on CO₂ emission is also assessed. The contribution of MARI is not investigated in detail, since the effect is small in comparison.

Compared to the monetary bid information taken as a basis to calculate the economic surplus, the actual AOF has no information about CO₂ emission and is therefore not able to take it into account in the optimization cycles. Thus, only the impact of the optimization on CO₂ emission can be assessed, which is approached by analyzing the influence of avoided aFRR activation of IN and PICASSO.

⁶ Trans European Replacement Reserve Exchange

To avoid misinterpretation of the results and to enable a detailed analysis, the effect of the optimization is analyzed separately for avoided aFRR activation in positive and negative direction. Activation of aFRR can be avoided through netting of imbalances and redistributed between participating LFC areas by the AOF. When aFRR demand of a LFC area is covered by activating (cheaper) bids in another via PICASSO, this is also regarded as avoided activation in the first LFC area. In the other area, it results in additional activation.

Balancing services are provided by prequalified units which comprise (amongst others) steam turbines, hydro turbines and hydro pumps as well as load. Avoiding positive aFRR activation mainly prevents increased energy generation via (steam or water) turbines and marginally impedes a decrease in load. In negative direction, reducing aFRR activation causes turbine generation to be maintained and prevents the increase of load from active pumps (and to a minor extent other loads). On top of that, avoiding aFRR activation in either direction also reduces energy conversion losses. The above best reflects the actual aFRR generation mix in Europe [3].

As a proclaimer - calculating the precise effect on CO₂ emission is not possible since the required data is not available. For starters, one would need to know the (time-varying) emission coefficients of aFRR activation and electricity generation for each control area (and country). It is also debatable whether emission factors found in literature account for e.g. methane slip correctly [4]. We attempt to get as close as possible given the information at hand. Emission balance of positive aFRR for a country i in each time step is calculated as follows:

$$E_{aFRR^+}^i = -e_{aFRR^+}^i (c_{IN,i}^- + c_{AOF,i}^-).$$

Here, $e_{aFRR^+}^i$ is the emission factor of positive aFRR, $c_{IN,i}^-$ the downward correction factor (i. e. avoided activation of positive aFRR) resulting from imbalance netting and $c_{AOF,i}^-$ the downward correction factor determined by the AOF. It is assumed that $e_{aFRR^+}^i$ is constant and identical to the emission factor of power generation of country i . Neglecting load reduction, $E_{aFRR^+}^i$ is always negative (reduction of emissions).

Similarly, the emission balance of negative aFRR is obtained as

$$E_{aFRR^-}^i = p_{gen}^i e_{aFRR^-}^i (c_{IN,i}^+ + c_{AOF,i}^+),$$

where $e_{aFRR^-}^i$ is the emission factor of negative aFRR and $c_{IN,i}^+$ and $c_{AOF,i}^+$ the upward correction factors (avoided activation of negative aFRR) from imbalance netting and the AOF, respectively. If at least a certain percentage of negative aFRR is provided by increasing load, p_{gen}^i reflects the share of generators in the mix that lower energy production when activated. Thus, $E_{aFRR^-}^i$ is always positive and reflects emissions retained due to cross zonal coordination. We assume that $e_{aFRR^-}^i = e_{aFRR^+}^i$ and $p_{gen}^i = p_{gen}$ for each country.

Emission factors of electricity generation for 2023 are taken from [5] and are listed in TABLE III. They are expected to deviate significantly from the actual values and can only be used for exemplary and qualitative assessment of emission balances.

TABLE III. **Emission factors of electricity generation in 2023 for each participating country in in gCO₂eq/kWh [5]**

country	e_{aFRR}^i	country	e_{aFRR}^i	country	e_{aFRR}^i	country	e_{aFRR}^i	country	e_{aFRR}^i
AT	111	CR	205	ES	174	IT	331	RO	241

BE	138	CZ	381	FR	56	NL	268	RS	636
BG	335	DE	450	GR	337	PL	662	SI	231
CH	35	DK	152	HU	204	PT	166	SK	116

Results

Economic Surplus

According to the methodological approach described in previous section, the economic surplus generated by PICASSO and MARI can be calculated for a whole calendar year. Results will be discussed in this section followed by those of the emission analysis with data of 2023.

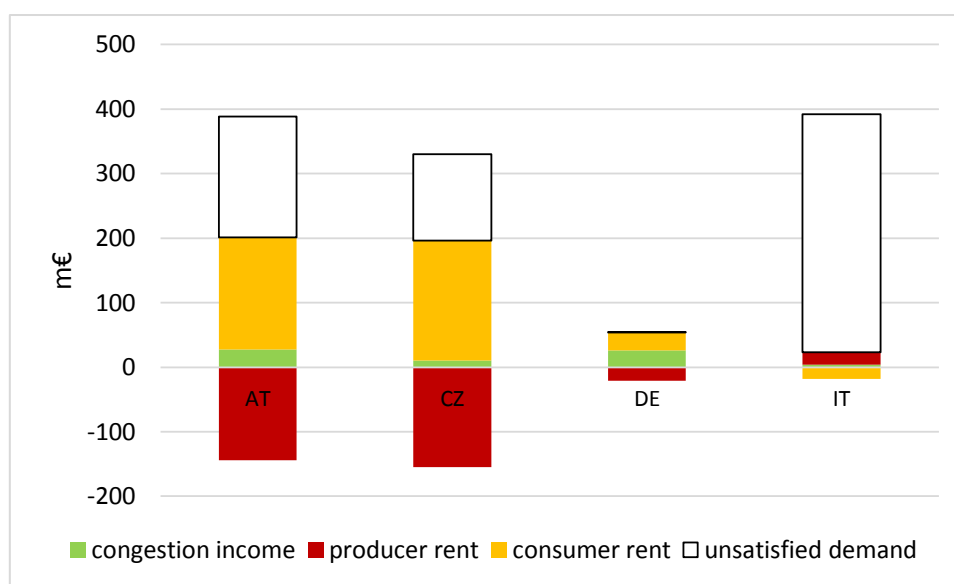


Figure 10 – Economic surplus of PICASSO in 2023 for each participating country

decomposed into congestion income, producer and consumer rent as well as the upper limit of value assignable to additionally satisfied demand (unsatisfied demand).

Results of the economic surplus calculation for the PICASSO platform in 2023 are depicted in Figure 10. It shows the total economic surplus for each participating country composed of congestion income, producer and consumer rent as well as the maximum monetary value of demand that would have been unsatisfied without the platform. This assumes that each TSO would pay the maximum price of $\bar{P} = 15,000$ €/MWh for unsatisfied demand. For a more detailed discussion of additionally satisfied demand, refer to [2].

In 2023, AT benefitted most from the PICASSO platform. Without considering additionally satisfied demand, AT's economic surplus sums up to 56.8 m€. Rewarding additionally satisfied demand with \bar{P} , the surplus would increase to 244.5 m€. In the same time interval, CZ's economic surplus amounts to 41 m€ plus 134.1 m€ with maximally priced unsatisfied demand. In DE, the basic economic surplus is 33 m€ while the maximum savings due to unsatisfied demand are 0.4 m€ (as there is hardly exceeding demand). The Italian TSO TERNA operationally joined PICASSO on July 19th, 2023, which is why the economic surplus of IT of 4.8 m€ (excluding additionally satisfied demand) is small in

comparison. Two peculiarities are noted when looking at the result for IT in Figure 1. Firstly, avoided unsatisfied demand is more than twice as high as that of any other participating country. This can be accounted to comparably high imbalances commonly occurring in IT, which makes IT the country benefitting most from PICASSO with respect to the coverage of aFRR demand. However, this does not imply that IT also benefits most economically – which leads to the second point. Unlike the other countries, IT has a negative consumer rent and a positive producer rent. This implies that TERN paid higher prices for aFRR than in a scenario without PICASSO.

The economic surplus of PICASSO in 2023 is about 30 m€ lower than the economic surplus reported in [2] for the first operational year, even though another country joined the platform. This can mostly be attributed to generally lower price levels at the wholesale energy markets. Note that the contribution of additionally satisfied demand is not included and is also neglected in the remainder of this paragraph. While the economic surplus of AT in 2023 is still significantly higher than that of other countries, the difference is reduced compared to the first operational year. CZ and DE were almost equal in the first operational year. In 2023, the difference is more pronounced. Economic surplus generated by the sum of consumer rent and producer rent is again almost equal to the surplus due to congestion income. This indicates that there is still not enough cross zonal capacity available to always activate bids jointly, which was also previously observed in [2] and [6].

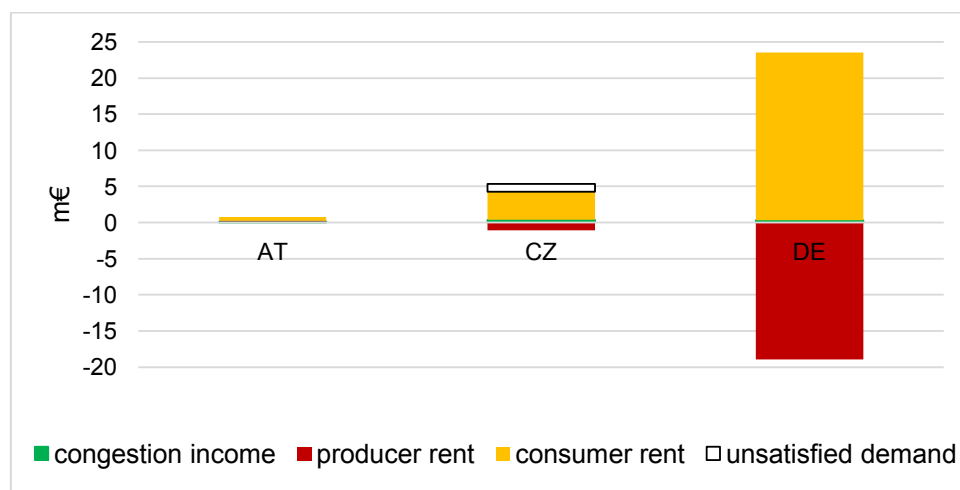


Figure 11: MARI economic surplus in 2023 for each participating country decomposed into congestion income, producer and consumer rent as well as the upper limit of value assignable to additionally satisfied demand (unsatisfied demand).

Like to PICASSO results, Figure 11 shows the results of the economic surplus calculation for the MARI platform in 2023 for each participating country. Due to the non-automated decision process to activate mFRR, unsatisfied demand hardly occurs for this balancing service at the moment. Applying $\bar{P}=15,000$ €/MWh results in a total economic surplus of 9.6 m€. It is to be noted that the likelihood of additional satisfied demand to occur might increase in MARI after more TSOs joined the platform.

In 2023, CZ and DE have an almost equal benefit from MARI while the economic surplus generated for AT is comparatively low as AT has only participated in the platform operationally half a year. Without considering savings due to unsatisfied demand, the

overall economic surplus generated in MARI operation sums up to 8.5 m€. Depending on the weighting of unsatisfied demand, the surplus increases by up to 1.1 m€. In the same period, CZ's economic surplus consists of 3.2 m€ plus additionally up to 1.1 m€ based on the chosen approach for considering unsatisfied demands. In DE, the economic surplus is 4.6 m€. AT has realized an economic surplus of 0.8 m€ in 2023. In general, the extra surplus from additional satisfied demand in CZ tends to be higher than in AT or DE as the local TSO tends to submit (price-elastic) mFRR demands to the MARI platform, which cannot be covered in the decoupled scenario as there are not sufficient (relatively) cheap bids available to satisfied the demand at the given maximum price in CZ.

Most TSOs currently being connected to MARI and PICASSO apply a more reactive approach to balance the system: Imbalances are not covered by proactive activation of mFRR but (automatic) activation of aFRR. Thus, the overall economic surplus generated by MARI is about ten times smaller than the economic surplus generated by PICASSO. This matches the observation that the overall activation probability for aFRR is about ten times higher than for mFRR [3].

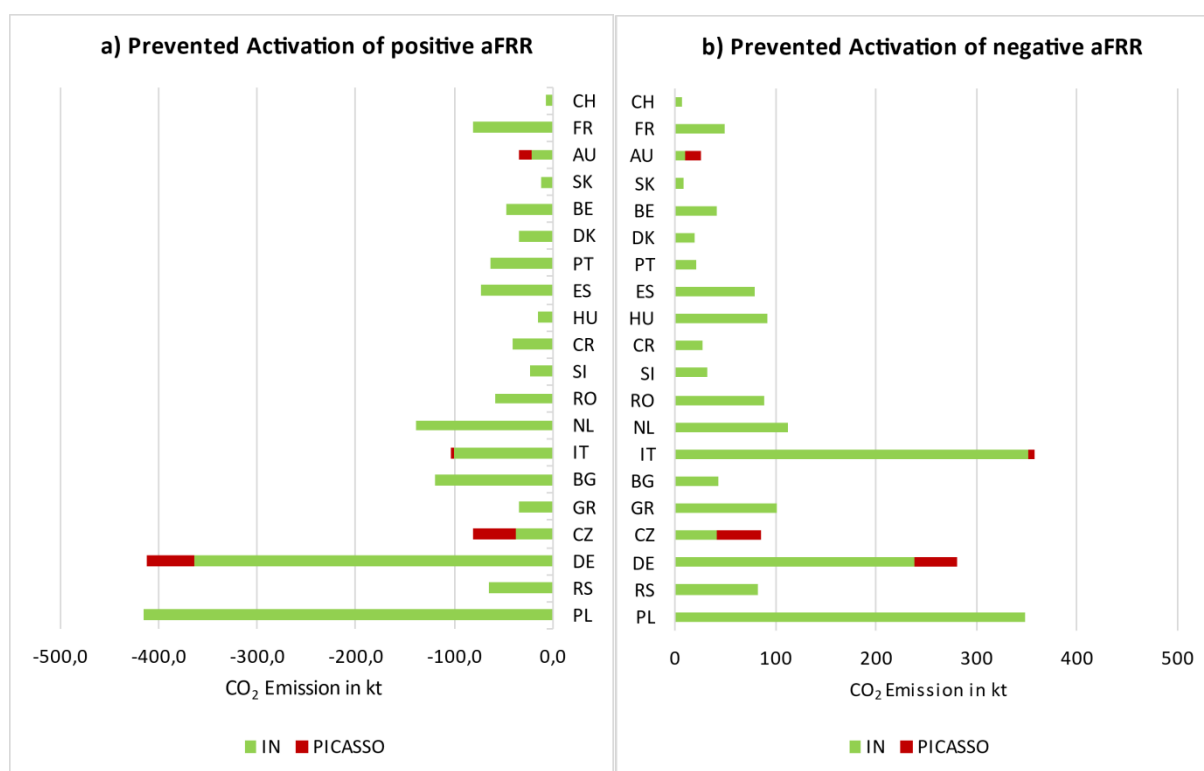


Figure 12 – Impact of imbalance netting and the AOF on the CO₂ emission of a) positive aFRR b) negative aFRR

CO₂ emission impact of IN and PICASSO

Results for the estimation of the prevented amount of emissions in kilo tons (kt) of CO₂ equivalents in 2023 due to avoiding activation of positive aFRR are shown in Figure 12a. Countries are sorted according to their emission factor of electricity generation starting with the lowest (CH) on top and ending with the highest (PL) at the bottom. It is distinguished between the contribution of IN and PICASSO respectively. The highest reduction of emissions is observed for countries with high emission factors, such as DE and PL, which imported positive aFRR in 2023. Even though FR imported more than twice the amount of positive balancing energy than PL, emissions reduction is insignificant

compared to PL because of the prevalence of nuclear power plants. Compared to imbalance netting, the AOF mostly contributes significantly less to emission reduction, except for CZ, where more than half of the avoided emissions are attributed to PICASSO.

Large errors are made in this calculation in case the energy mix of positive aFRR in a country differs significantly from that of the general electricity generation mix. This is e. g. the case for DE, where most positive aFRR is provided by pumped-storage hydroelectricity units with considerably lower lifecycle emissions than the electricity generation mix in DE. Better approximations can be achieved by estimating emission factors based on the amount prequalified for positive aFRR by technology. However, this would have to be done for all European countries included in this study that are not necessarily harmonized in the way they procure aFRR or collect and provide required data.

Another major source of error is the assumption that upward correction factors have an immediate effect on generation, which neglects the dynamics acting in between (e. g. of controllers and effectors). Assuming $p_{gen} = 0.95$ for the generator share in the negative aFRR mix of each country and thereby ignoring the remaining 5 % of load in terms of its impact on CO₂ emission, we arrive at the results depicted in Figure 12b for 2023. Again, it is observed that countries with a higher emission factor of electricity generation (such as IT, DE and PL) contribute more to retained emissions than those with lower emission factors. IT is especially noticeable as the country that exported the most energy via IN in 2023 and therefore contributed most to generating additional emissions, whereas net CO₂ reduction results for DE and PL when comparing Figure 12a and Figure 12b.

Regarding inaccuracies, the same as discussed above for positive aFRR also holds for negative aFRR. An additional source of error is the assumed share of generators providing negative aFRR. With the assumed 95 %, a net additional CO₂ emission of 42.7 kt is generated by IN and PICASSO in 2023. When reducing the percentage to $p_{gen} = 0.8$, a net reduction of CO₂ emission by 258.1 kt results. Given the high impact the discussed sources of error on the net emission balance, we would like to point out that none of these numbers shall be used to make claims about the emission impact of European balancing cooperations without further discussing and mitigating the inaccuracies.

Conclusions and Outlook

Implementation of EB regulation has started the process of creating a European domestic market for balancing energy significantly changing existing processes in the field of system balancing. Therefore, this paper not only introduced balancing in general as well as the European balancing platforms specifically but also the different elements of economic surplus for the exchange of balancing energy. Since there are periods in which some TSOs submit more demand to the balancing platforms than bids, the concept of exceeding demand has been highlighted including different pricing options.

Considering consumer rent, producer rent and congestion income, the approach described in this paper allows a more precise assessment of economic surplus for the exchange of balancing energy than previous publications [3]. Without additional surplus due to unsatisfied demand, the economic surplus of PICASSO sums up to 135.6 m€ in 2023. Applying the same assumptions, MARI provides an economic surplus of 8.5 m€ in the comparable period. Although not each country has been connected operationally to MARI and PICASSO for the same duration in the considered periods, the relation between the economic surplus per platform matches the expectations: As aFRR is roughly activated ten times more often than mFRR, it seems plausible that also the economic surplus is about

ten times higher. Anyway, a significant increase is to be expected, as other countries will join the balancing platforms operationally in the future. However, it has to be noted that the economic surplus is partially also caused by the increasing costs for balancing energy resulting from both, changes in market design (e. g. applying pay-as-cleared instead of pay-as-bid and introducing quarter-hourly products for balancing energy which both also may facilitate enacting market power in markets with already limited competition such as the balancing markets) and general situation at the wholesale markets [7], [8].

An approach to estimate the impact of balancing platforms on CO₂ emission was also presented in this paper. The aim of this analysis was not to accurately quantify the impact on emissions. Rather, it is supposed to provide guidance and stress the different factors involved in an estimation of the emission balance. In addition, we pointed out problems and sources of errors. The more reliable data is available in the future, the closer we can get to an accurate approximation of reality.

References

- [1] European Network of Transmission System Operators for Electricity (ENTSO-E); „Market Report 2023,“ Brussels, 2024.
- [2] U. Kasper, A. Kindsmüller, D. Steber, S. Remppis, D. Schipf and A. Warsewa, “Assessment of Economic Surplus Generated at the European Balancing Platforms,” *IEEE Transactions on Energy Markets, Policy and Regulation*, pp. 1-10, 2024.
- [3] European Network of Transmission System Operators for Electricity (ENTSO-E), „Balancing report 2022,“ Brussels, 2022.
- [4] E. A. Bouman, A. Ramirez und E. G. H. , „Multiregional environmental comparison of fossil fuel power generation - Assessment of the contribution of fugitive emissions from conventional and unconventional fossil resources,“ *International Journal of Greenhouse Gas Control*, Nr. 33, pp. 1-9, 2015.
- [5] EMBER, „Yearly electricity data,“ [Online]. Available: <https://ember-climate.org/data-catalogue/yearly-electricity-data/>. [Zugriff am 05 June 2024].
- [6] European Network of Transmission System Operators for Electricity (ENTSO-E), „Quarterly Pricing Reporting,“ [Online]. Available: https://www.entsoe.eu/network_codes/eb/quarterly-pricing-reporting/. [Zugriff am 05 June 2024].
- [7] K.-M. Ehrhart, M. Ott und R. Wang, „Justification and Specification of Maximum and Minimum Balancing Energy Prices,“ Karlsruhe Institute for Technology (KIT), Takon GmbH, and Leibniz Centre for European Economic Research (ZEW), Karlsruhe, Germany, 2021.
- [8] H. Haghigha, H. S. and A. R. Kian, “Pay-as-bid versus marginal pricing: The role of suppliers strategic behavior,” *International Journal of Electrical Power & Energy Systems*, vol. 42, no. 1, pp. 350-358, 2012.